THE STRENGTH AND STIFFNESS OF SLABS TO COLUMN JOINTS

ISAM MAJED SHAKER

BSc

A Thesis submitted for the Degree

of

Master of Philosophy

DEPARTMENT OF CIVIL ENGINEERING

The University of Aston in Birmingham

April 1981

SUMMARY

The Stremgth and Stiffness of Slabs
to Column Joints.

Isam Majed Shaker

MPhil. in Civil Engineering
1981

The strength and behaviour of the edge column-slab connection of a flat plate under different loading conditions, taking account of the column shape in calculation of the shearing capacity of the slab, was studied.

The programme was to obtain data to be used for establishing a method for analysis of this connection.

A test programme was undertaken to obtain information about the behaviour and strength of such connections. A total number of 15 specimens were tested under loads gradually increasing to failure.

A method for the prediction of the ultimate capacity of edge slab-column connections is developed.

This theoretical analysis is applied to other available slab tests and compared with the experimental findings. Good agreement is obtained between the test and calculated loads. A number of conclusions are drawn from these comparisons as well as from the experimental observations. Some suggestions are also made for further research on the subject.

Key words: columns (structural); concrete slabs;
flat plates (concrete); punching shear.

ACKNOWLEDGEMENTS

The author wishes to express his gratitude to his supervisor, Mr A W Astill, for his help, guidance and encouragement throughout this research project.

The author would also like to express his gratitude to Professor M Holmes, Head of the Department of Civil Engineering at the University of Aston, for the opportunity to carry out this work.

Thanks are due to Mr W Parsons and all the technical staff who helped during the experimental work.

Thanks are also due to Mrs B J Tennant for her excellent typing of the script.

NOTATION

A_c = shear area of slab at d/2 from the periphery of the column.

b_0 = length of critical shear section at d/2 from the periphery of the column.

b_1 = $r_1 + d/2$

b_2 = $r_2 + d$

d = effective depth of slab

e = eccentricity in load applied to column

f'_c = ultimate compressive strength of concrete

k = coefficient used in defining external moment carried by vertical shearing stresses acting at the critical section

M''_{CD} = bending moment at section $\overset{''}{CD}$

M_0 = moment capacity for V = 0

M^t_{AD}, M^t_{BC} = torsional moment at sections $\overset{''}{AD}$ and $\overset{''}{BC}$

M_u = ultimate moment

P = ratio of area of tension steel to area of concrete

r_1 = side dimension of the column perpendicular to free edge

r_2 = side dimension of the column parallel to free edge

t = thickness of slab

V = vertical shear force

V_{calc} = shear force at predicted ultimate load

V_{flex} = shear force at which flexural failure takes place

V_0 = shear capacity for zero eccentricity

V_{test} = measured shear force at failure

v = shear stress

v_{max} = maximum shear stress

v_m = shear stress from bending moment

v_s = shear stress from vertical shear force

v_u = ultimate shear stress

CONTENTS

LIST OF TABLES

Page No.

CHAPTER VI

LIST OF FIGURES

Page No.

CHAPTER VI

CHAPTER 1

INTRODUCTION

1.1 General

Reinforced concrete floor construction can be divided into two categories:

1 - slabs supported on beams spanning between columns

2 - slabs supported only at the columns which are called flat slabs or flat plates.

The joint between the slab and the column in reinforced concrete flat plate floors is often the most critical section. From strength considerations a joint must be strong enough to resist the forces from the members framing into it. For the individual members, knowledge of the internal forces developed due to the external forces and deformations imposed on the structure could be sufficient for an efficient design layout, but the situation at the interaction of these members is quite different. This region is subjected to a complex stress distribution due to the effect of multi-directional forces, such as axial load, bending moment, torsion and shear transferred by the members as a result of the external loads. The situation is further complicated by the effect of the forces arising from creep, shrinkage and temperature change. In the light of these considerations the necessity for investigating the strength and behaviour of the slab-column joints under the influence of various design variables is evident.

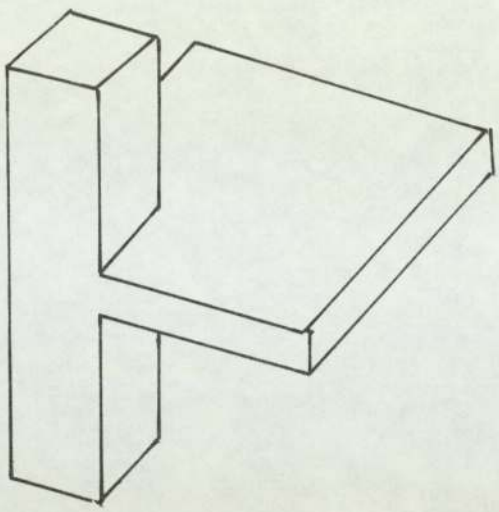

(a) Corner joint

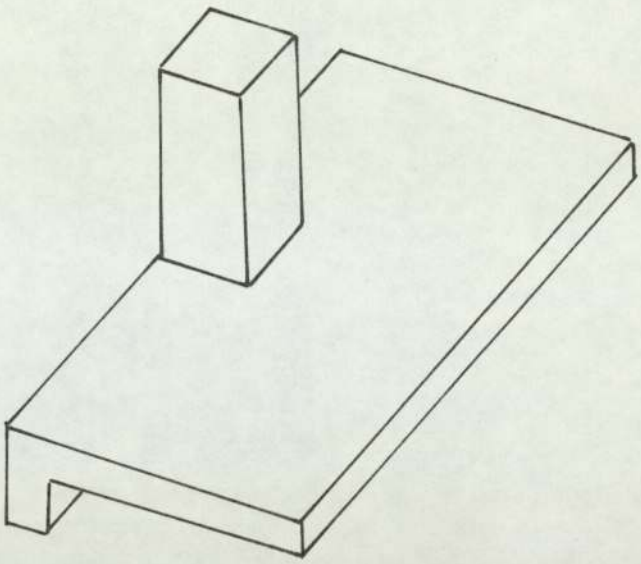

(b) Edge joint with spandrel beam

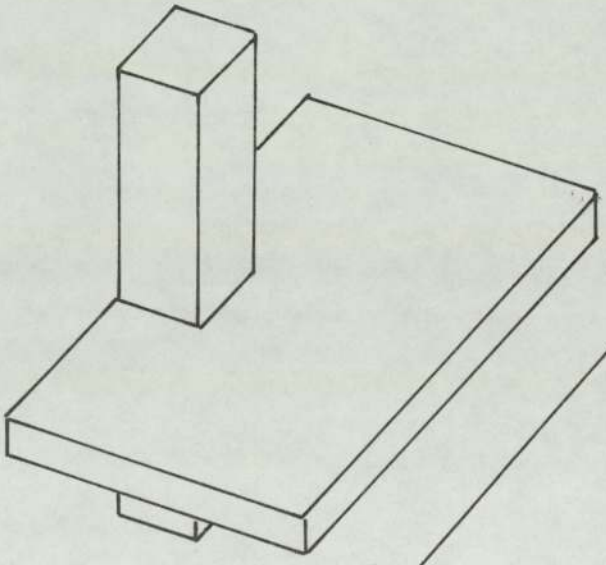

(c) Edge joint without spandrel beam

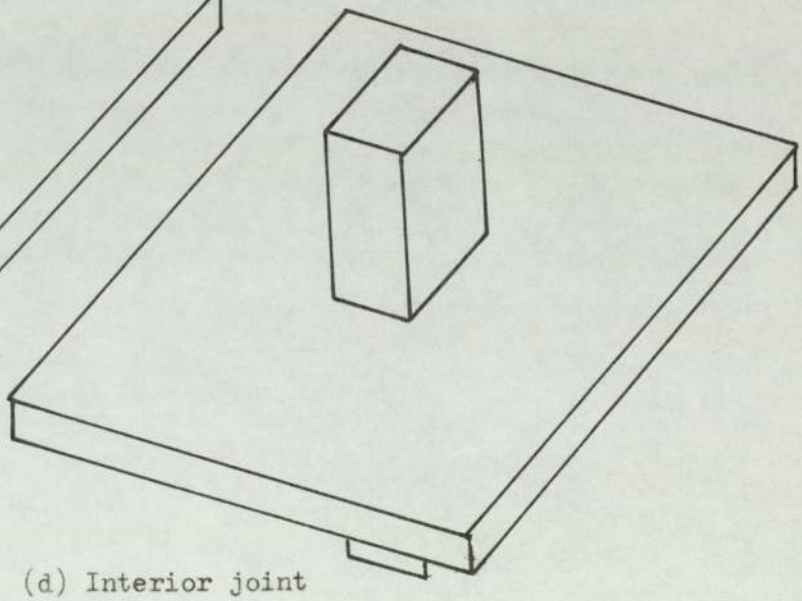

(d) Interior joint

Fig. 1.1 Different types of slab-column joints

The slab-column joint in a reinforced concrete flat plate usually occupies one of the four situations shown in Figure 1.1, viz.,

(a) corner joint with or without beams

(b) edge column with spandrel beam

(c) edge column without spandrel beam

(d) interior joint.

Edge and corner column connections tend to be the most critical as far as the moment and shear transfer are concerned.

The economy of the entire structure is, to a large extent, governed by the degree to which the ultimate strength of the connection between the slab and the column can be predicted and utilized.

Most studies on the strength of flat plate structures at their connections with columns were carried out on square and circular slabs simply supported at the edges and loaded through concentric square or circular column stubs. These specimens were designed to simulate the parts of flat plate in the actual structure bounded by lines of contraflexure in the vicinity of an interior column. Little information is available regarding the shear strength of these slabs near columns when both axial load and significant moment are to be transferred, as is specially the case with exterior column-slab connections.

1.2 Object and Scope of the Investigation

The object of this investigation was to study experimentally the strength and behaviour of the edge column-slab connection of a flat plate under different loading conditions, taking account of the column shape in calculations of the shearing capacity of the slab. The programme was to obtain data to be used for establishing a method for analysis of this connection. For this purpose a test programme was undertaken to obtain information about the behaviour and strength of such connections, and to investigate the shear and moment behaviour of edge connections of a flat plate structure.

The type of test specimen shown in Fig. 3.1 was chosen for the following reasons:-

(1) There was not enough test data available on this type of connection concerning the column shape.

(2) This type of connection is simple in detail of construction while it gives valuable information concerning the major problem.

In all, 15 specimens were tested under loads gradually increasing to failure. All specimens were supported and loaded as shown in Fig. 3.1.

The parameters which are believed to have the greatest influence on the moment-shear strength of an edge connection in flat plate structure are tabulated in Table 3.1.

The following parameters were kept constant in all the specimens during the tests:

(1) Concrete strength f'_c.

(2) The tensile steel ratio, P, kept constant at 2.5 per cent.

(3) The thickness of slab, t, which was kept constant at 75 mm.

(4) The column perimeter (three sides only) was kept constant at 540 mm.

1.3 Method of analysis

In Chapter VI a method for the prediction of the ultimate capacity of edge column-slab connections is developed. The method is capable of predicting the ultimate capacity of this type of connection in the following cases:

(1) Edge connection subjected to bending moment in plane perpendicular to the free edge of the slab.

(2) Edge connection subjected to axial load and bending moment in a plane perpendicular to the free edge of the slab.

The various approximations were compared with experimental results when available. In the same chapter (Chapter VI) the test results of the writer and those found elsewhere were compared with the theoretical predictions.

CHAPTER II

REVIEW OF LITERATURE

2.1 General

The problem of shear strength of slabs at their connections with columns was recognised as early as 1913[1] and has been extensively investigated by several researchers in the last two decades due to the increased development and use of flat plate structures and the inclination towards the use of small column sizes. A primary practical need, therefore, is the development of improved reinforcing details and design criteria for transfer of loads from the plate into the supporting column.

A brief summary of the work on the problem of shear strength of flat plate slabs prior to 1961 has been reported by Moe[2]. The European Commiteee on concrete republished, in 1965 and 1966, many of the more recent investigations.[3,4] Comprehensive test[5] data and reliable design criteria[6,7] exist to estimate shear strength at interior columns carrying reasonably concentric loads. Design procedures have also been developed for shearhead reinforcement made from rolled steel structural sections.[6,7,8]

In contrast, limited experimental work is available regarding shear and moment transfer at exterior columns[9,10] and other cases of interior columns especially for taking

into account the column shape in calculations of the shearing capacity of the slab.

Design procedures have so far been formulated by assuming that a fraction of the bending moment causes non-uniform distribution of vertical shear stresses.[2,7,11,12]

The review of the literature in this article will be divided into two parts: the first part will deal briefly with the strength of a column-slab connection subjected to concentric load, and the second part of the review will deal with studies carried out to investigate the problem of combined moment and shear transfer.

2.2 Shear strength near the column of symmetrically loaded slabs (concentric loading).

The earliest study of the shear strength of slabs is that of Talbot[1] who in 1913 presented his well-known investigation on reinforced concrete footings. Altogether 114 wall footings and 83 column footings were tested to failure. Of the latter, approximately 20 specimens failed in shear. On this basis Talbot proposed the following formula for calculating the nominal shear stresses at an assumed critical section located at a distance from the column faces equal to the effective depth of the slab

$$v = \frac{V}{4(r + 2d)jd} \qquad (2.1)$$

Table 2.1 Location of the critical section governing the ultimate shearing strength as proposed by different researchers and codes.

Name of the researcher or code	Distance of critical section from column periphery
Talbot 1913	d
ACI Code (318-56)	d
Forsell and Holmberg 1946	t/2
Whitney 1957	d/2
ACI Code (318-63)	d/2
ACI Code (318-71)	d/2
ACI Code (318-77)	d/2
B.S. Code CP 114-57	d/2
B.S. Code CP 110-72	1.5h
Hognestad 1953	0
Elstner and Hognestad 1953	0
Di Stasio and Van Buren 1960	d-1½" (diagonal tension) 0 (punching shear)
Moe 1961	0

where,

v = the shear stress

V = the shearing force

r = the side dimension of square column

d = the effective depth of slab

jd = the internal moment arm of slab.

He found that relatively high values of shear strength were obtained when large percentages of tensile reinforcement were used. This study has formed the basis of design practice for reinforced concrete footings in many countries throughout the world.

Many improvements have been made in the design methods, especially in adjusting the magnitudes of the allowable stresses.[5,13,14,15,17]

Researchers and designers have differed considerably in their proposals for the position of the critical section. Table 2.1 shows some of the proposals, and the differences can be seen.

A second experimental investigation of 24 wall footings and 140 column footings were tested to failure in 1944 by F E Richart, who concluded that shearing stresses are frequently a critical feature of the design of a footing despite high bond stresses. The shearing stresses at failure, calculated at a distance "d" from the face of the column (by equation (2.1)) varied generally from less than

$0.05f'_c$ to $0.09f'_c$. With respect to shearing strength Richart observed:

> "The use of the critical section at less than the distance "d" outside the column faces seems well worth considering in interpreting the test results, as does also the allowance of a portion of the maximum shear for the doweling effect of the reinforcing bars. These features are considered here as possible explanations of footing action, not at this time as suggested design methods."

Hognestad[19] in 1953 presented the results of an extensive re-evaluation of the shear failures of footings which were reported by Richart.[18] Hognestad recognised the effect of superimposed flexure on the ultimate shearing strength and introduced the ratio $\phi_0 = \frac{V_{test}}{V_{flex}}$ as one of the parameters in the statistical study of the results. He suggested that the shearing stresses could be computed at zero distance around the loaded area since this seemed to give the best measure of shearing strength.

Hognestad found that the ultimate shearing strength could be calculated within the range of variation in parameters covered by Richart's tests, by using the following equation.

$$v = \frac{V}{\frac{7}{8}b'd} = \left(0.035 + \frac{0.07}{\phi_0} \right) f'_c + 130 \text{ psi} \qquad (2.2)$$

where b' = perimeter of critical section taken at the periphery of the column.

Elstner and Hognestad[20] reported shear tests on 24, 6 ft square and 6 inch thick reinforced concrete slabs. The majority of these slabs were supported along all four edges. The results of these tests, as well as those reported by Forsell and Holmberg[17] and by Richart and Kluge were analysed and compared favourably to the strengths predicted by Equation (2.2).

Keefe[21] in 1954 investigated the effectiveness of a special type of shear reinforcement known as a "shearhead". The slabs with the shear heads had an ultimate shear capacity nearly 40% higher than those without.

Elstner and Hognestad[20] in 1956 reported on tests of 38, 6 ft square slabs; 24 of these tests were reported in Reference 20. The following equation was found to predict the shear strength of all the slabs tested by the authors with good accuracy

$$v = \frac{V}{\frac{7}{8}b'd} = 333 \text{ psi} + 0.046 \frac{f'c}{\phi_0} \qquad (2.3)$$

Whitney[22] in 1957, presented an ultimate strength theory for shear strength based on a re-evaluation of previously reported test results.[18, 23] The major assumption made was that the shear strength was primarily a function of the ultimate resisting moment of the slab per unit width inside the "Pyramid of Rupture", which he defined as a frustum of a cone or pyramid with a surface sloping out in all directions from the column at an angle of 45°.

Scordelis, Lin and May[24] in 1958 investigated the shearing strength of prestressed lift slabs by testing 6 ft square slab specimens. Final failure of all slabs occurred when the steel collar punched through the slab. A variable amount of flexural cracking was visible just prior to failure and was generally smaller in the thicker slabs which had column recesses. On the basis of their study the following were some of the conclusions advanced:

(1) The ultimate punching shear stress as computed by $\frac{v}{f'_c} = \frac{V_{test}}{\frac{7}{8}b'd f'_c}$ varied between 0.101 and 0.211 at the edge of the collar, between 0.079 and 0.157 at a distance d/2 from the edge of the collar, and between 0.058 and 0.127 at a distance d from the edge of the collar. Therefore it cannot be considered to be constant at any one of these locations

(2) The test data agreed quite well with results obtained using the ultimate shearing strength formula proposed by Elstner and Hognestad[20] and by Whitney.[22]

They concluded also that these formulas would yield sufficient accuracy for prestressed concrete slabs provided a suitable method is used to calculate the ultimate flexural capacity.

(3) Adequate provision should be made in the design so that ultimate flexural capacity will govern failure rather than ultimate shear capacity,

since a shear failure may be sudden and without warning.

Base in 1959 reported on small scale tests of centrally loaded reinforced concrete slabs supported on four edges. One of the important conclusions was that

> "the amount of tensile reinforcement in the slabs and the resulting amount of flexural cracking seemed to affect the punching failure significantly."

Kinnunen and Nylander[26] in 1960 reported on a number of tests carried out on circular concrete slabs, approximately 6 ft in diameter and 6 in thick, reinforced with top mesh only. The slabs were supported by tie-rods along the circumference and an upward vertical load was applied at the centrally placed column stub. The principal parameters were, the type and the amount of slab reinforcement (ring, ring and radial, and two way), and the column size (approximately 6 in and 12 in diameter). Two expressions were proposed for calculating punching strength, derived from the equilibrium at failure of a segment of the slab, and are given in terms of the properties of the concrete and reinforcement, and of the slab and column dimensions. The calculation of the strength is a trial and error process and was restricted to slabs with radial or circular reinforcement. In 1963 Kinnunen[27] extended the theory to cover slabs with two way reinforcement, but the method was still rather time-consuming. Also in 1963, Anderson presented a study on slabs with shear reinforcement. His

assumptions were not different from Kinnunen and Nylander's[26] assumptions for slabs without shear reinforcement.

Moe[2], in 1961, reported tests of 43, 6 ft square slabs which were very similar to the test specimens of Elstner and Hognestad. Moe's major variables were effect of openings near the face of the column, effect of column size, effect of eccentricity in the applied load and effectiveness of a special type of shear reinforcement. He also included a statistical study of 140 footings and 120 slabs tested by earlier investigators. Some of the more important conclusions arrived at in Moe's study are:

(1) The critical section governing the ultimate shear strength of the slabs and footings should be measured along the perimeter of the loaded area.

(2) The shear strength of slabs and footings is to some extent dependent upon the flexural strength.

(3) The unit shearing strength is highest when the column size is small compared to the slab thickness.

(4) The ultimate shearing strength of slabs and footings, as determined in the short time tests, can be predicted with good accuracy by

$$v_u \text{ (psi)} = \frac{V}{b'd} = \left[\frac{15\left(1 - 0.075\frac{r}{d}\right)}{1 + 5.25\frac{b'd\sqrt{f'_c}}{V_{flex}}} \right] \sqrt{f'_c} \qquad (2.4)$$

(5) Inclined cracks in the slabs developed at loads as low as 50% of the ultimate strength.

(6) In cases of moment transfer between square columns and slabs, test results indicate that it is safe to assume that the portion of the moment transferred through vertical shearing stresses is distributed along the perimeter of the column as shown in Fig. 2.3. Maximum shearing stresses due to combined action of vertical load and moment should not exceed the values expressed by Equation (2.4).

(7) Since shear failure is undesirable in a concrete structure, slabs and footings should be designed so that flexural strength governs. This is accomplished by placing a limitation on shearing stresses as expressed by

$$v = \left(9.23 - 1.12\frac{r}{d}\right)\sqrt{f'_c} \quad \text{for } r/d < 3$$

$$v = \left(2.50 + 10\frac{d}{r}\right)\sqrt{f'_c} \quad \text{for } f/d > 3$$

Yitzhaki,[29] in 1966, reported results of tests on circular slabs. He proposed the following expression for calculating vertical punching strength of an interior column

$$V_u = 8(1 - q/2)d^2(149.3 + 0.164pf_y)(1 + 0.5\, r/d) \quad \text{(psi)} \qquad \ldots (2.5)$$

where p = percentage of slab reinforcement

fg = yield stress of the steel

$q = p \frac{f_y}{f'_c}$ (is the reinforcement index).

The three terms in Equation (2.5) express the effect of concrete strength $(1 - q/2)$, slab reinforcement strength $(p f_y)$ and of the r/d ratio. The numerical constants in the middle bracket were evaluated by trial and error from the available test data.

The above expression can be written in terms of a nominal ultimate shear stress on a critical section at a distance "d" from the column perimeter

$$v_u = \frac{Vu}{(4r + 8d)d} = (149.3 + 0.164\, pf_y)(1 - q/2) \quad \text{(psi)} \qquad \ldots (2.6)$$

Since in the practical design the value of "q" varies between 0.15 and 0.25, the effect of concrete strength given by the term $(1 - q/2)$ is relatively small. The ultimate shear strength, therefore, largely depends on the effect of slab reinforcement strength (pf_y). The stress v_u is (according to Equation (2.6)) independent of r/d.

The 1963 ACI Building Code referred to nominal

ultimate shear stress in case of square interior column

$$v_u = \frac{V_u}{(4r + 4d)d} < 4\phi\sqrt{f'_c}$$

where ϕ is a reduction factor assumed by the code[6] as 0.85. When v_u exceeds the specified value the strength may be augmented by shear reinforcement, but the design steel stresses are only 50% of the recommended yield stresses, so the maximum value of v_u should not exceed $6\phi\sqrt{f'_c}$. For slabs less than 10 in thick, shear reinforcement is considered ineffective. The code also requires that the shear stresses be checked for the slab acting as a wide beam.

CP 114 (1957)[30] refers to nominal shear stresses which may be calculated from the following formula:

$$v = \frac{V_w}{4(r + d)d} < v_{perm} \qquad (2.7)$$

$$v_{perm} = 40 + \frac{u}{50} \quad \text{for } u > 3{,}000 \text{ psi}$$

where

V_w = shear force at working load

v_{perm} = permissible shear stress.

The effect of r/d ratio and slab reinforcement are not considered in Equations (2.6) and (2.7).

Long and Bond,[31] in 1967, presented a theoretical method

of analysis for the calculation of the punching load of an interior column and flat slab structure with two-way slab reinforcement. The method is based on elastic thin-plate theory from which the stresses in the compression zone were derived, assuming a linear distribution of stress. They also reported results of tests on four $\frac{1}{4}$ scale slabs and columns. Long [32] in 1968 extended the theory to predict the ultimate capacity of slabs under combined normal loads and bending moments.

In a progress report presented to ACI committee 426, Shear and Diagonal Tension, March 31, 1968, Zaidi, Sabnis and Roll [33] presented an extension to Moe's [2] work on punching strength of slabs with openings in the column vicinity. They extended the scope of their work beyond that of Moe's by considering different shaped holes and various hole configurations.

Based on statical analysis of their 125 test specimens on small scale slab specimens (test specimens were modelled after Moe's slabs with a geometrical scale factor of 2.5) the following relation (Equation 2.8) was proposed to replace Equation (2.4) for slabs with openings in the column vicinity.

$$v_u \text{ (psi)} = \frac{V_u}{b' d \sqrt{f'_c}} = \frac{14(1 + 0.15 r/d - 0.425 e/d)}{1 + 10 \frac{b' d \sqrt{f'_c}}{V_{flex}}} \qquad (2.8)$$

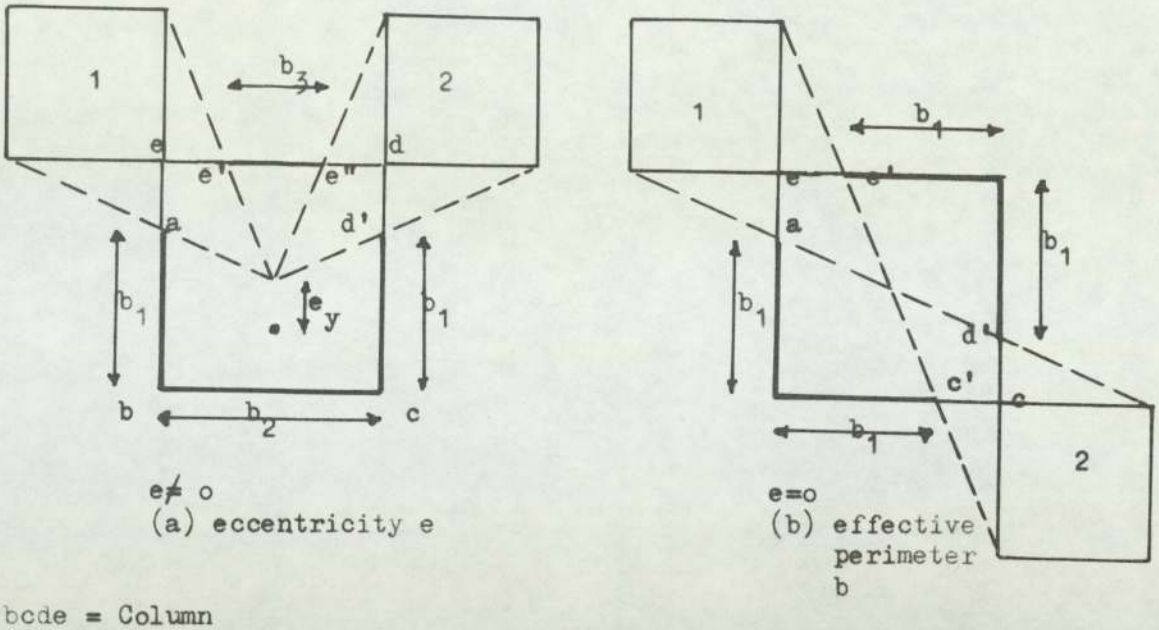

bcde = Column

1 and 2 = Openings

b' = Perimeter of the column excluding the portion within the radial projections from the centre of the column to the corners or edges of holes.

=abcd' + e"e' =2b1 + b2 +b3 (Fig.(a))

= abc' + d'de'

= 4b1

e = $e_x + e_y$ = Sum of eccentricities of the centre of gravity of the effective perimeter with respect to the centre of the column.

Note: The different eccentricities in two cases although b' is the same for both

Fig. 2.1 Concepts of effective perimeter and eccentricity.

It may be noted that Equation (2.8) resembles that of Moe's Equation (2.4) to a large extent, except for the presence of the extra parameter e/d which allows for including the effect of unsymmetrically located holes (Fig. 2.1). For the analysis of their test results, Zaidi, Sabnis and Roll obtained one concrete compressive strength, f'c, from test cylinders in Moe's tests. An increase of 20 percent in the compressive concrete strength f'c was found for smaller cylinders.

The effect of columns elongated in plan on the behaviour of flat plate structures was later considered by Smith and Simmonds,[34] and Simmonds.[35] A reinforced concrete flat plate test structure consisting of nine panels was tested. Column elongation in long direction was 0.4 of span. Moments and deflections in one of the interior panels were determined by elastic analysis. The results were compared with the empirical method of ACI 318-63. Although no specific results were reported regarding the ultimate capacity of a column slab connection, the crack pattern of the exterior connections confirmed the observations reported in the present investigation.

Hawkins[36] in 1970 studied the effect of column rectangularity on the strength and behaviour of 9 slab column specimens. The test specimens were made to simulate an interior column-slab connection in a flat plate structure. All slabs were 7 ft. square, 6 in. thick and supported on a

centrally located rectangular column. The variables included in this study were the aspect ratio for the column, the loading pattern and the reinforcement pattern. For 8 of the specimens the length of the column perimeter was kept constant at 48 in. and the aspect ratio varied between 1 and 4.3.

The load was applied concentrically to the connections by means of rods at 24 in. centres along two opposite edges or along the four edges of the slab.

He concluded that the nominal shear stress decreases markedly as the aspect ratio increases. The shear capacities were consistent with those calculated from the 1971 ACI Building Code for specimens with columns having long-to-short side ratio less than 2.0. For larger ratios the ultimate shear stress dropped to $3.2\sqrt{f'_c}$ at a ratio of 4.3. Based on the results for the nine specimens, a design provision was proposed for the nominal shear stress in slabs having rectangular columns:

$$\underset{(psi)}{v_u} = \frac{V_u}{b' d \sqrt{f'_c}} = (2.5 + 3.0 r_2/r_1) \text{ but not greater than } 40 \quad \ldots \quad (2.9)$$

where r_2 = width of smaller column face

r_1 = width of larger column face.

2.3 Shear strength of slabs in moment and shear transfer: (eccentric column loading).

Only limited information is available regarding the shear strength of flat plate floor slabs near their connections with columns when both axial load, V, and bending moment, M, are to be transferred.

In 1959 Rosenthal[37] reported the results of tests on simply supported circular reinforced concrete slabs. The tests included eleven specimens, three of which were loaded eccentrically through a centrally located circular column stub. For concentrically loaded connections he concluded that Hognestad's[19] empirical equation which considers the combined effect of shear and flexure in a centrally loaded slab when used for slabs containing tension reinforcement only, resulted in satisfactory agreement with the test data. For the three eccentrically loaded specimens, only one of them showed a clear eccentric failure (punching and unsymmetrical crack pattern). This showed, nevertheless, that if an eccentric load is applied there can be a decrease in ultimate strength of the slab, and in this case the reduction was about 15%.

In 1960, Tsuboi and Kawaguchi[38] reported nine tests on mortar slabs 3 ft. 4 in. square, and 1 3/16 in. thick, simply supported along two opposite edges. Three of these slabs were made of plain mortar. Moments were applied to the slabs in a plane parallel to the free edges through

concentric square stubs 8 in. square. The slabs were assumed to represent one interior panel of a flat plate floor. The variable in the six reinforced slabs was the distribution of the reinforcement in the direction parallel to the plane of the applied moment although they all contained the same amount of reinforcement. The reinforcement in the perpendicular direction was kept the same.

The latter test slabs were grouped into three identical pairs. In the first pair, seventy percent of the reinforcement parallel to the plane of the applied moment was distributed in the column strip and the rest uniformly distributed in the middle strip. In the second pair the reinforcement was uniformly distributed over the entire width of the panel. In the third pair, thirty percent of the reinforcement was uniformly distributed in the middle strip.

One slab of each of the identical pairs was subjected to gradually increasing moment, while the other was subjected to reciprocally repeated moment. In the latter case, loading was reversed at three stages; first a little outside the elastic range, then in an elastoplastic state and finally near the ultimate strength. Two trends were observed with respect to the ultimate strength of test slabs:

(1) Higher failure moments occurred in slabs with greater ratio of reinforcement in the column strip for both types of loading.

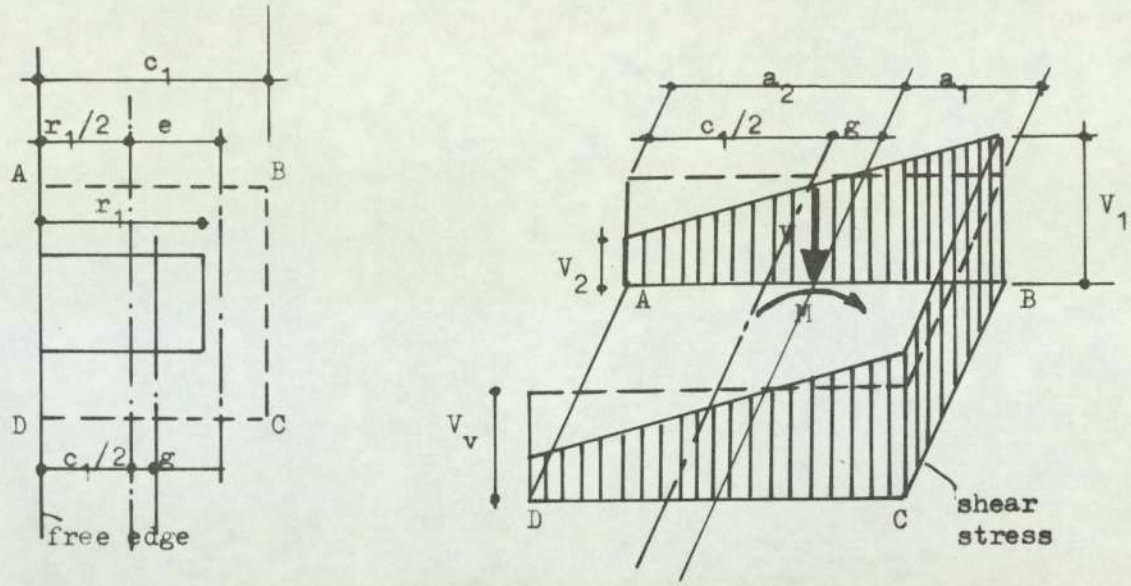

(a) Edge connection

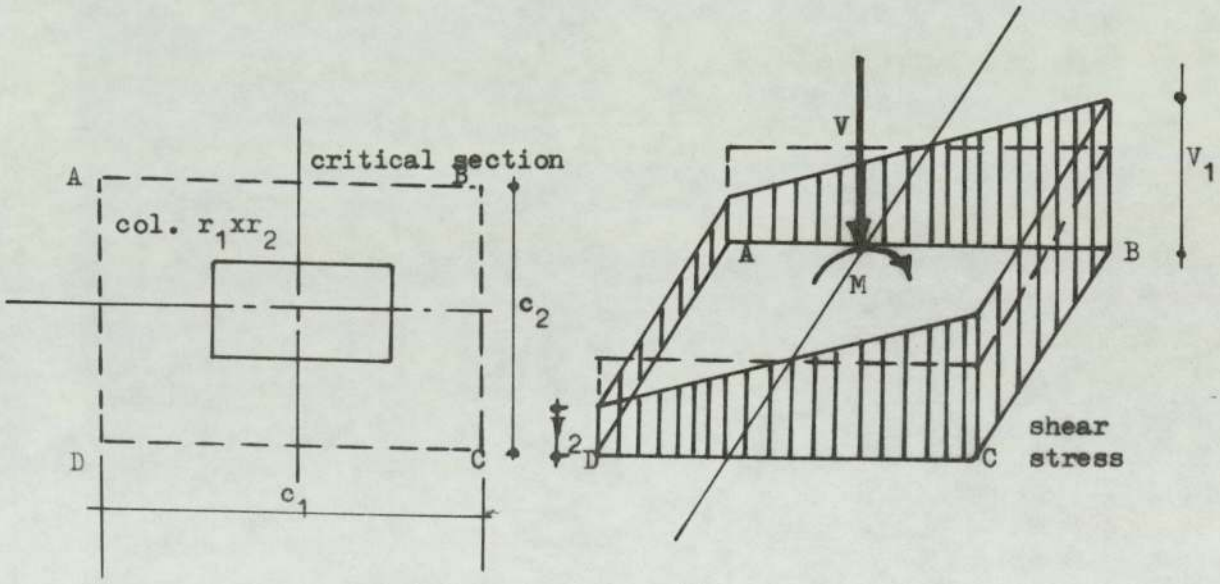

(b) Interior connection

Fig. 2.2 Critical section for diagonal tention and assumed distribution of shear stress.

(2) Static reversal of loading reduced the ultimate capacity of the connections, especially after load reached the ultimate in the previous half of the cycle.

Di Stasio and Van Buren,[11] in 1960, presented a working stress method of analysis for calculating the maximum unit shearing stresses, determining both diagonal tension and punching shear due to combined shear and bending moment loading at exterior and interior connections. The major criterion of this method is the limitation on the vertical shear stress on a critical section located at a specified distance from the face of the column. According to their suggestions, two critical sections of the slab in the vicinity of the column have to be checked, namely:
(1) a critical section for diagonal tension following a periphery parallel to the column faces at a distance t-1½ in. therefrom; (2) a critical section for punching shear at the column-slab intersection. The applied shear, V, and moment, M, were assumed to cause the shear stresses shown in Fig. 2.2. The maximum and minimum unit shears were calculated by equations of the form:

(1) <u>For exterior edge connection (Fig. 2.2 (a))</u>

$$v_1 = \frac{8t}{7d}\left[\frac{V}{A_c} + \frac{(M - M_{BC} - V_e)a_1}{J_c}\right] C \qquad (2.10(a))$$

$$v_2 = \frac{8t}{7d}\left[\frac{V}{A_c} - \frac{(M - M_{BC} - V_e)a_2}{J_c}\right] C \qquad (2.10(b))$$

where

$A_c = (2C_1 + C_2)t$

C_1 = Length of critical section parallel to the plane of the bending moment.

C_2 = Length of critical section perpendicular to the plane of the bending moment.

e = Distance of the centroid of the section being sheared from the column centroid.

$a_1 = \frac{C_1}{2} - g$

$a_2 = \frac{C_1}{2} + g$

t = slab thickness

d = effective depth of slab

$C = \frac{1}{1 + (m - 1)P}$

m = modular ratio $\left(\frac{E_s}{E_c} \right)$

P = ratio of total (top and bottom) steel slab

M_{BC} = flexural moment resisted by the slab section BC

J_c = property of the assumed critical section analogous to polar moment of inertia

$$= \frac{2tC_1^3}{12} + \frac{2C_1t^3}{12} + 2C_1tg^2 + C_2t\left(\frac{C_1}{2} - g \right)^2$$

(2) For interior connection (Fig. 2.2 (b))

$$v_1 = \frac{8t}{7d}\left[\frac{V}{A_c} + \frac{(M - M_{AD} - M_{BC})C_1}{2J_c}\right]C \qquad (2.11(a))$$

$$v_2 = \frac{8t}{7d}\left[\frac{V}{A_c} - \frac{(M - M_{AD} - M_{BC})C_1}{2J_c}\right]C \qquad (2.11(b))$$

where in this case

$$A_c = 2(C_1 + C_2)t$$

$$J_c = \frac{2tC_1^3}{12} + \frac{2C_1t^3}{12} + 2C_2t\left(\frac{C_1}{2}\right)2$$

The above formulae are for the critical section of diagonal tension. For the critical section for punching shear, the same formulae are applied with the substitution of the proper values for M_{BC}, M_{AD} and the dimensions to conform with the smaller periphery.

Di Stasio and Van Buren limited the maximum shear stress to 0.0625 f'_c, on a critical section directly at the column periphery (critical section for punching shear). With respect to permissible stresses on the critical section for diagonal tension the recommendations of the 1956 ACI Building Code,[39] which was applicable at that time, were followed, namely:

$$v_u = 0.3\ f'_c \neq 100 \text{ psi}$$

when at least 50% of the required column strip steel crosses the section, or

$$v_u = 0.025 f'_c \not> 85 \text{ psi}$$

when at least 25% of the required column strip steel crosses the section.

In 1961 Kreps and Rees[40] reported the results of six tests carried out by Fredrick and Pollauf[41] on square flat plate specimens, simply supported along two opposite edges and free along the other two edges. The specimens were loaded through concentrically located 6 in. square column stubs by axial loads and bending moments in a plane parallel to the free edges. Depth of the slab and the distribution of the reinforcement were included as important variables. No significant results concerning the shear problem were given by the authors, since their programme was primarily conducted to determine the effective width, in relation to slab depth, of the column strip available to transmit a column moment into the slab for a flat plate of reinforced concrete exposed to lateral (seismic or wind) loads.

Also in 1961, Moe[2] reported twelve tests on 6 ft. square, 6 in. thick slabs. The slabs were simply supported along all four edges in such a way that no negative reactions could be taken at the supports, and corners were free to lift. Load was applied at different eccentricities through a centrally located square column stub. The eccentricity of the applied load varied from 0 to 24 in.

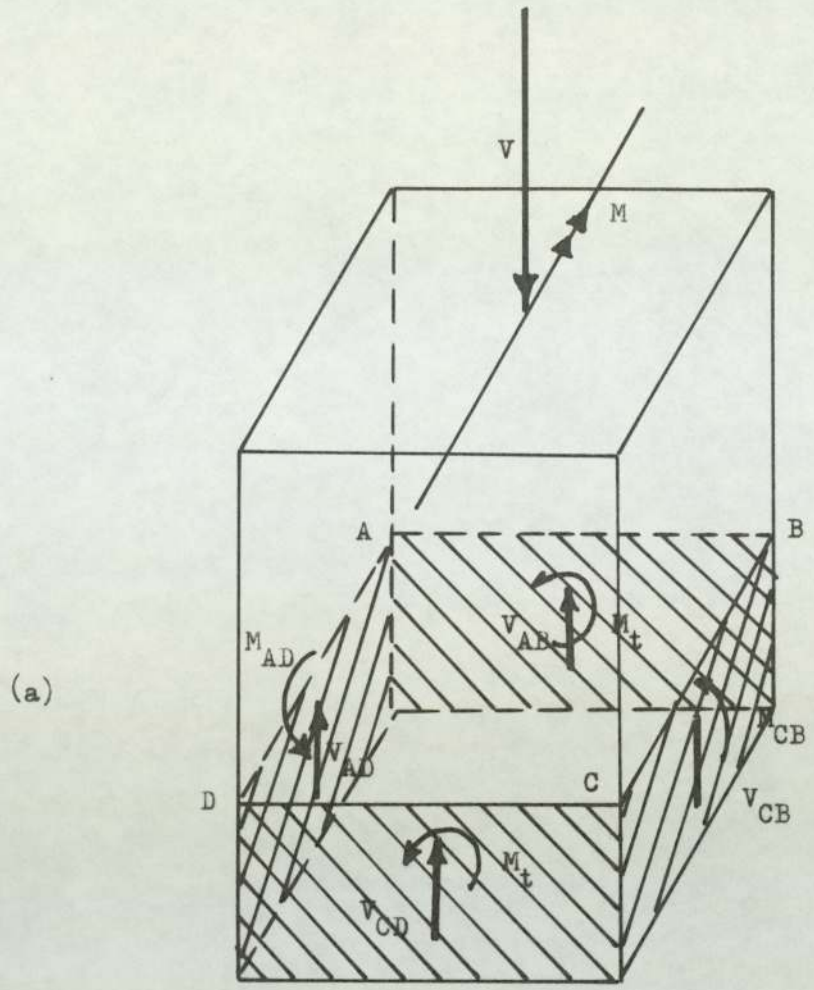

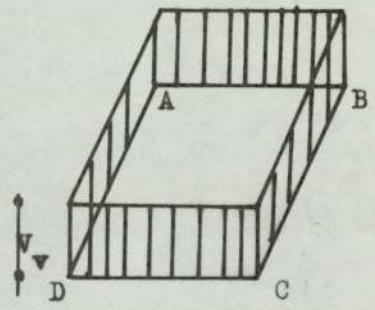

(b) Distribution of shear stresses due to load V .

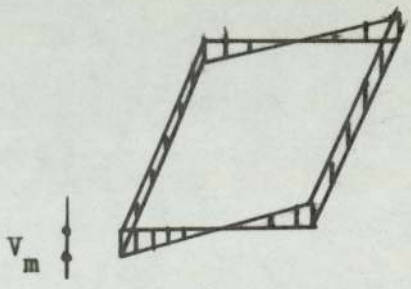

(c) Distribution of shear stresses due to moment M .

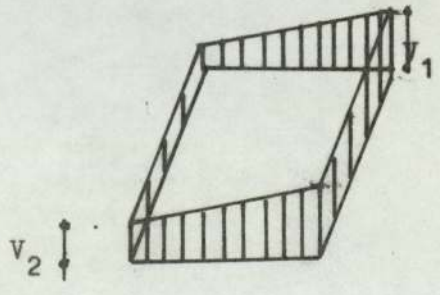

(d) Combined distribution of shear stresses.

Fig. 2.3 Distribution of shear stresses at ultimate.

Important variables in Moe's study were column size and the yield strength of the reinforcing steel. Only two specimens contained compressive as well as tensile reinforcement. He suggested that if $\frac{M}{V}$ is small, i.e. less than $\frac{r}{2}$, where r is the width of a square column, the behaviour of the slab was approximately the same as for slabs loaded by axial load through column stub only. If $\frac{M}{V}$ is greater than $\frac{r}{2}$ or if the slabs are subjected to bending moments only, the problem becomes more complicated than that of normally loaded slabs. From the test results Moe derived an empirical equation which has been shown to predict the strength of the tested slabs with sufficient accuracy for design. Moe's strength method of analysis is summarised as follows:

Fig. 2.3 (a) shows a square column stub loaded with an axial force, V, and a moment, M, in one of the planes of symmetry parallel to two faces of the column. The slab is not shown in the figure, but the forces and moments resisted by the assumed slab critical section immediately at the column-slab interface are shown in this figure.

In developing his strength criteria Moe assumed that:-

(1) The axial load V results in producing uniform nominal shear stresses in the critical section given by

$$v_v = \frac{V}{A} \qquad (a)$$

where

$A = 4rd$

r = side width of a square column.

(2) The bending moment, M, is resisted by:

(a) flexural moment of slab section AD and BC (Fig. 2.3 (a))

(b) torsional moments, M_t, on sides AB and CD, and

(c) vertical shear stresses on the four sides of the critical section. They are assumed to be constant along the critical sections perpendicular to the plane in which the applied moment acts and vary linearly along the other two planes as illustrated in Fig. 2.3 (c).

The resultant of the internal moments produced in (a), (b) and (c) must balance M. The fraction of the total bending moment resisted by the vertical shear stresses was assumed equal to KM where K is a constant which was determined from the test results. Considering the distribution of the vertical shear stresses shown in Fig. 2.3 (c) Moe determined v_m as

$$v_m = \frac{KM}{\frac{4}{3}r^2 d}$$

or

$$v_m = \frac{KMC}{J_c} \qquad (b)$$

where

v_m = maximum vertical shear stress produced by the bending moment portion KM

C = half width of a square column = $\frac{r}{2}$

$J_c = \frac{2r^3d}{3}$

Moe advanced that failure of a column-slab connection subjected to the present case of loading (Fig. 2.3 (a)) takes place when the maximum value of the shearing stress, v, (Fig. 2.3 (d)), reaches a critical value equal to the shearing strength of the same slab under concentric load determined from Equation (2.4). The maximum shear stress, v_1, is obtained as the summation of v_v and v_m as follows:

$$v_1 = v_v + v_m$$

or

$$v_1 = \frac{V}{4rd} + \frac{KMC}{J_c} \qquad (2.12)$$

Using the above assumption Moe worked backwards from his test data and concluded that the value of K in Equation (2.12), and therefore the fraction of the total moment transferred by shear stresses, was approximately one third. In calculating v_1 for the case of concentric load Equation (2.4) was used. For design Moe recommended a limiting vertical shear stress of $(9.23 - 1.12 \frac{r}{d})\sqrt{f'_c}$ for $\frac{r}{d}$ ratio less than 3 and $(2.5 + 10 \frac{r}{d})\sqrt{f'_c}$ for $\frac{r}{d}$ ratio greater than 3. These were conservative limits, intended to produce flexure rather than shear failure.

In 1962 ACI-ASCE committee 326[5] conducted a study of Moe's work which resulted in a recommendation that a limiting shear stress v_u be established using the following expression in which the critical section follows the periphery of the column:

$$v_u = 4\left(\frac{r}{d} + 1\right)\sqrt{f'_c} \qquad (2.13)$$

Therefore the shear load capacity of a concentrically loaded connection can be evaluated as

$$V = v_u b'd \qquad (2.14)$$

where b' is the perimeter of the critical section taken at the periphery of the column.

To develop design recommendations for ACI 1963 code for moment and shear transfer, ACI-ASCE committee 326[5] reviewed the foregoing investigations and in addition took into account some preliminary information on work by Hanson and Hanson.[12] The committee recommended a procedure similar to Di Stasio and Van Buren's,[11] but with two modifications. It was proposed that the critical section be taken at d/2 from the faces of the column, and that the effective depth rather than the total depth be used in calculation of A_c and J_c.

At interior columns the equation recommended for design was

$$v_u = \frac{V}{A_c} + \frac{KMC}{J_c} < 4\sqrt{f'_c} \qquad (2.15)$$

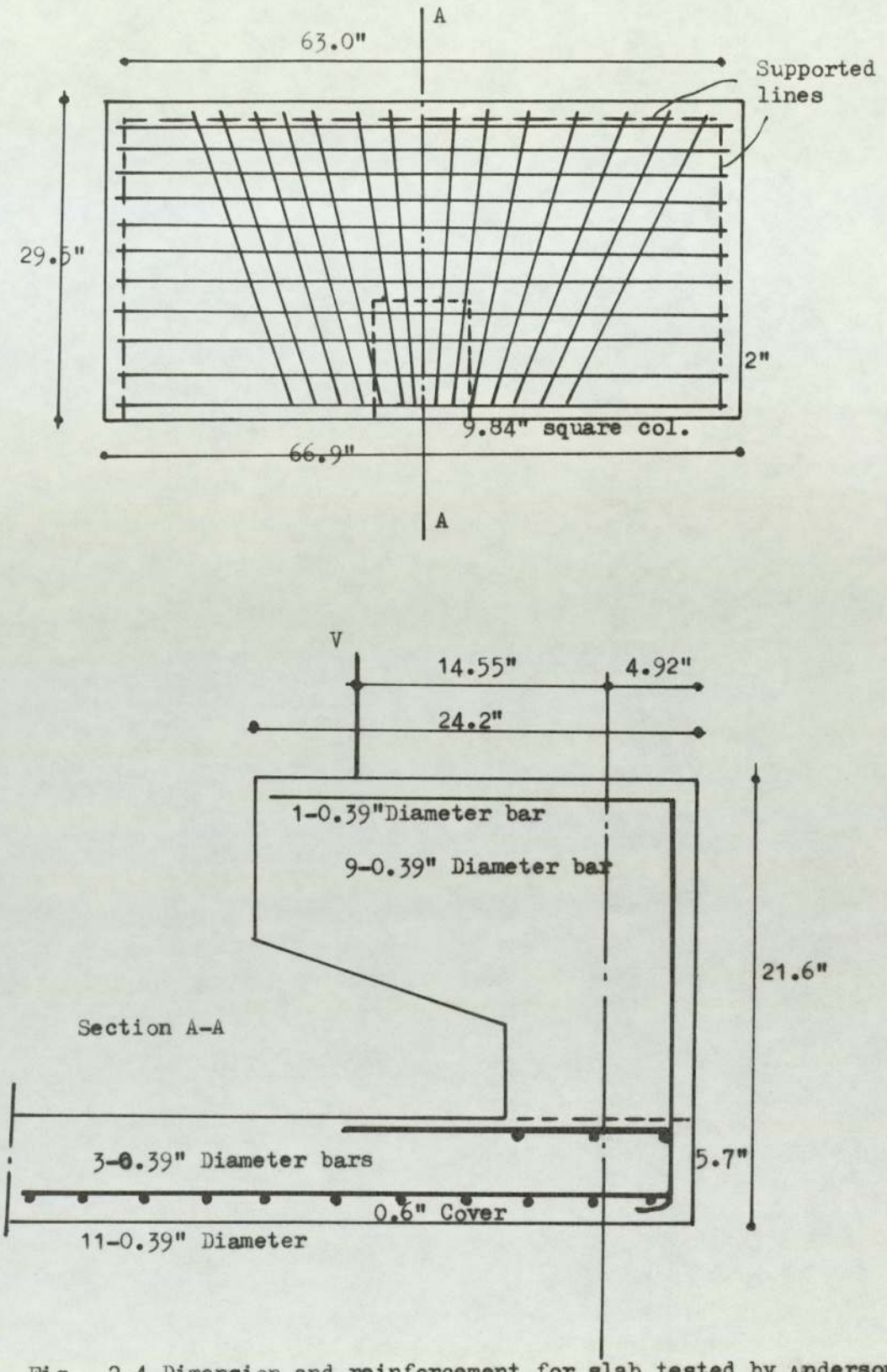

Fig . 2.4 Dimension and reinforcement for slab tested by Anderson

where v_u = ultimate shear stress.

Best agreement with available tests (10 of which were Moe's[2], 10 were Hanson's and Hanson's[12] and 5 reported by Kreps and Reese[44]) was obtained with a K value of 0.20.

The ACI commentary[42] gave a working stress design method similar to that of Di Stasio and Van Buren but dropped out the $\frac{7}{8}$. Also it did not take into account the dowelling effect of the steel. A critical section $(r_1 + d)$ and $(r_2 + 3t)$ for interior columns was allowed by this method, where r_1 is the side width of a rectangular column in the direction of the plane in which the bending moment acts and r_2 is the width of the other side of the column. The following equation is given to calculate the limiting stress

$$v = \frac{V}{A_c} + \frac{(M - M_{AD} + M_{CB})}{J_c} \left(\frac{C_1}{2}\right) \qquad (2.16)$$

The calculated shear stress by this method is limited to allowable values specified in the ACI 318-63 Building Code[6].

In 1966 Anderson[43] reported test specimens simulating edge connections in flat plate structures. The slabs, which were approximately 5 ft. by 2 ft. 6 in. with a thickness of 5 inches to 7 inches, were supported on neoprene pads closely spaced along all edges except the one containing the column. The dimensions and reinforcement for a representative specimen are shown in Fig. 2.4. The specimens were loaded by means of a hydraulic jack through

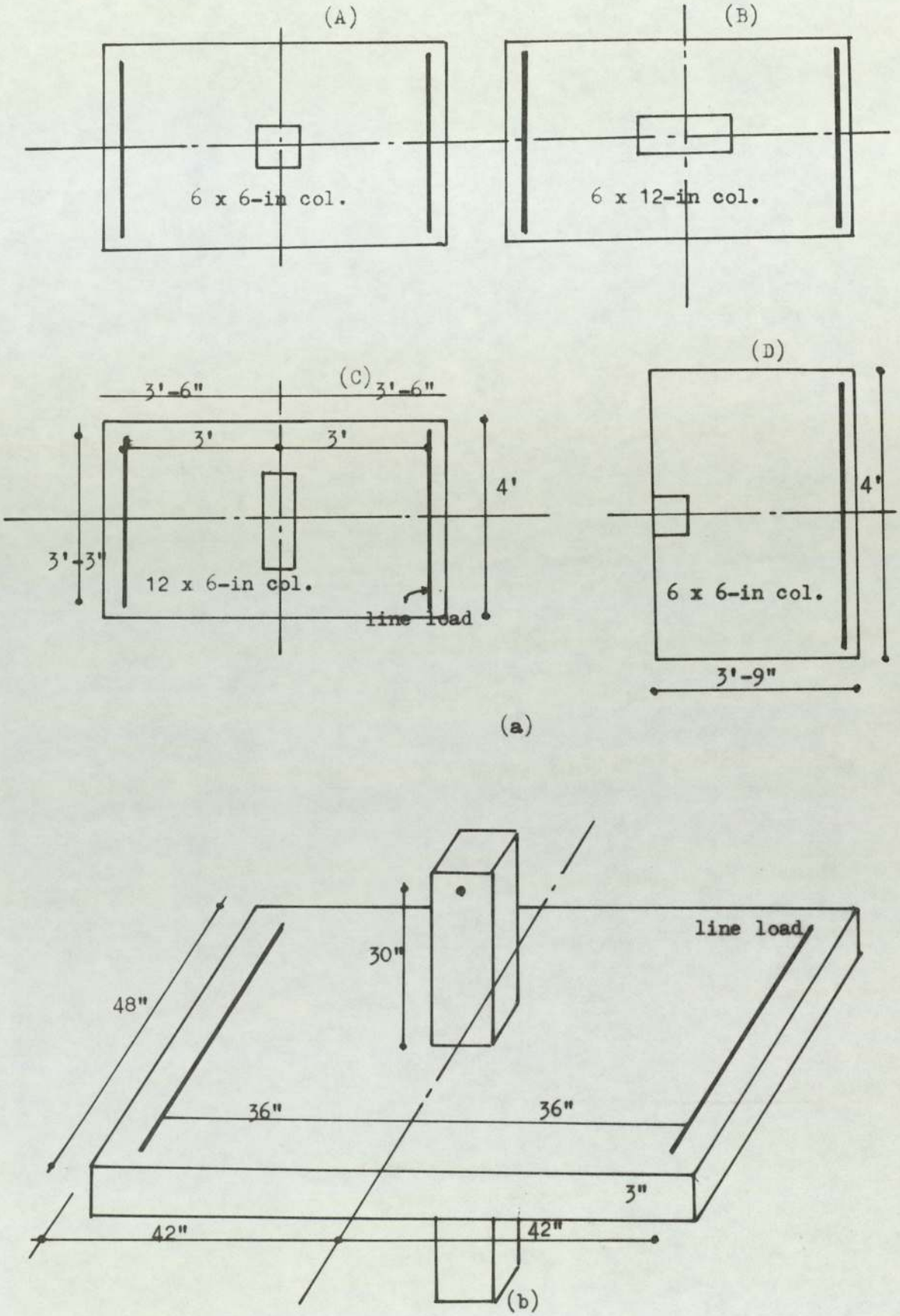

Fig. 2.5 Hanson and Hanson's test specimens and loading arrangement.

a column stub extended on one side of the slab only. The variables were the eccentricity of the load on the column slab, column size and slab reinforcement.

He concluded that the eccentricity of the column load produced a great effect on the ultimate load. When the eccentricity was small the failure was a pure flexural failure, in spite of the fact that nominal shear stress was high. When the eccentricity was great the failure was by punching, and the value of the nominal shear stress was lower. Anderson also suggested an expression for calculating the nominal shear stress at a critical section located at the column faces.[4]

In 1968, Hanson and Hanson[12] reported 17 tests involving combined shear and bending moment. Ten of these slabs had been reported in 1962 by ACI-ASCE committee 326.[5] Sixteen of the specimens contained 6 in. square or 6 in. x 12 in. rectangular concentric columns. Only one specimen was tested which had an edge column 6 in. square simulating conditions at an edge connection (Fig.2.5). The slabs were reinforced with two mats of No. 3 deformed bars spaced 3 in. centre-to-centre in each direction. The mats were placed so that the bars parallel to the long side of the slab were covered by $\frac{3}{8}$ in. of concrete. Pairs of 1 in. x 6 in. holes were blocked out of the slab in eight of the specimens with square columns. These holes were located adjacent to the column and either parallel to the long sides (free edges)

or the short sides (loaded sides) of the slab. The slab reinforcement was continuous through the holes.

The columns had hinged reaction points 30 in. above and below the surface of the 3 in. thick slabs. The principal variables were the location of the holes blocked out of the slab and the loading arrangement. Loads were applied to the slab along lines 36 in. from the centre line of the column (Fig. 2.5(a)). The three loading arrangements considered caused eccentricities varying from zero to almost infinity. For type 1 loading, the line loads in Fig. 2.5(b) were equal in magnitude and opposite in direction. For type 2 the line loads were equal and acting in the same direction and for type 3 only were acting downward. Three of the interior column-slab connections were subjected to reversal of loading. In these tests, the direction of the applied loads was reversed after reaching 25, 50 and 75 percent of the expected ultimate load (determined from companion specimens tested under monotonically increased loads up to collapse).

As a result of the examination of their tests and previous tests reported by Moe[2], the following were some of their important conclusions:

(1) The working stress method in section 2102 of the commentary on the 1963 ACI Building Code[6] was found to have a factor of safety less than 2 for some of the slab-column connections under combined

shear and moment.

(2) The working stress method recommended by Di Stasio and Van Buren[11] modified to agree with 1963 ACI code, was found to have a variable factor of safety always greater than 2. However, the method did not agree with the trend of the test data.

(3) The ultimate strength design method recommended by Moe[2] was found to be simple in application and to give good results except for the case of the edge connection.

(4) The ultimate strength design method recommended by ACI-ASCE committee 326[5] was found to give a good prediction of the strength of the column-slab connection only when the moment reduction factor, K, was changed from 0.20 to 0.40.

During the preparation of a proposed revision to the 1963 ACI Building Code[6] committee 318[7] adopted the method of the joint committee[5] for calculating the ultimate capacity of a column slab connection when moment and shear are to be transferred with the modification proposed by Hanson and Hanson.[12] In addition it was noted that most of the test data considered by Hanson and Hanson[12] to reach their findings mentioned above, involved square columns. In practice, however, for architectural reasons rectangular columns are frequently used, particularly at edges of buildings. It is logical to assume that the fraction of the bending moment

transferred by flexure, across the periphery of the critical section defined earlier[5] by the joint committee, increases as the width of the face of the critical section resisting the moment increases. Accordingly, it was suggested that the fraction, K, of the bending moment transferred by eccentricity of the shear about the centroid of the critical section be taken as

$$K = 1 - \frac{1}{1 + \frac{2}{3}\sqrt{\frac{r_1 + d}{r_2 + d}}} \qquad (2.17)$$

where $(r_2 + d)$ is the width of the face of the critical section resisting the moment, and $(r_1 + d)$ is the width of the face at right angles to $(r_2 + d)$. Equation (2.17) gives K = 0.40 for square columns.

In 1968, and later in 1970, Zaghlool, de Paiva and Glockner[9,10] reported the results on four flat plate structures. Each structure was a full size, square, single panel flat plate structure cast monolithically with a square column at each corner. The structures measured 10 ft. centre to centre of columns, with column height constant at 5 ft. The column bases rested on steel balls so that rotation but not translation of the lower end of the column was permitted. The variables studied were the column width to slab depth ratio and the concrete strength. Two column sizes were used 5½ in. and 6½ in. square. The slab thickness was constant at 5½ in. The reinforcement in the slab consisted of ½ in. diameter deformed bars having an average

yield stress of 55 ksi. The positive reinforcement was placed parallel to the edges of the slab and spaced uniformly over the entire width. In the negative moment region of the slabs adjacent to the columns only continuity bars were provided by three of the column bars bent into the slab, the outside corner bar was bent along the diagonal, the other two outside bars were bent parallel to the edges, and two other continuity bars were placed parallel to the slab edges and bent down adjacent to the outside corner bar. The structures were loaded by uniform loads simulated by 16 point loads through 15 in. square by $\frac{3}{4}$ in. thick steel plates resting on rubber pads on the surface of the slab. The loads were provided by four hydraulic jacks through distributing members.

In connection with the shear strength of the slab at its connection with the column, they found that the existing methods for predicting the column-slab connection strength for interior columns, when extrapolated to corner columns, produced extremely conservative results. Considering a simplified approach to the analysis of their tests, using the principal tensile strength of the failure cone, they obtained the following expression for the shear stress at ultimate:

$$v_u = \frac{V}{b'd} = (5.6 + 2.0(\frac{d}{r}))\sqrt{f'_c} \qquad (2.18)$$

where

$$b' = 2r$$

v = vertical shear force.

This expression showed good correlation with the tests.

In 1969 Stamenkovic[44] tested 52 half scale models of column-slab connections designed to simulate interior, edge and corner connections in a flat plate structure. They were tested under the action of axial load, bending moment or a combination of both. Of interest are the exterior column-slab connections which are described below:

All specimens had 3 ft. square by 3 in. thick reinforced concrete slabs with column stubs above and below the slab. In all the tests the slabs were supported by 1½ in. diameter tie-rods, 6½ in. centre to centre along the edges.

The edge connections were supported along three edges with the column stub being located at the centre of the free edge and the corner connections had two free edges adjacent to the column.

The loads were applied to each specimen through 1 in. thick steel plates attached to the ends of the column stubs at 13 in. from the top and bottom faces of the slab.

The slabs were reinforced with two similar mats at the top and bottom faces. Each mat consisted of $\frac{5}{16}$ in. diameter bars of hot rolled high tensile steel with a guaranteed

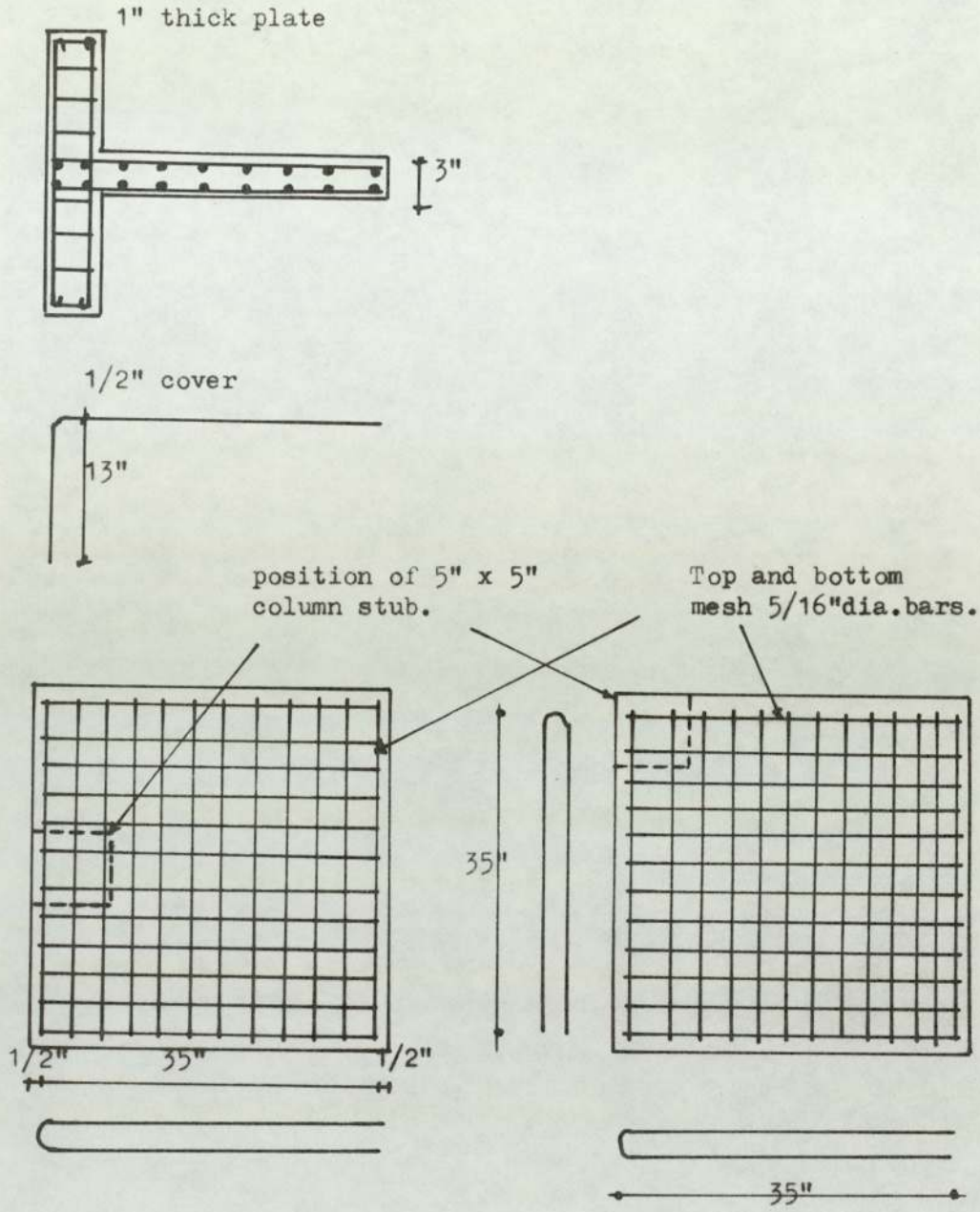

Fig. 2.6 Dimensions and reinforcement for edge and corner connections tested at Imperial College by Stamankovic.

yield stress of 60,000 psi. Typical slab reinforcement for edge and corner connections is shown in Fig. 2.6. The principal variables were the type of loading and the location of slots in the slabs at the column faces with respect to the plane in which the bending moment acts.

Nine of the edge column-slab connections were loaded as follows:

One specimen was loaded by axial load only. Four were loaded by bending moment in a plane perpendicular to the free edge; the first one had openings in the slab adjacent to the column sides, the second one had an opening in the slab at the inside face of the column, and the third and fourth did not have holes. The other four specimens were tested under varying ratios of bending moment to axial load.

The analysis of the test specimens given by Stamenkovic are summarised as follows:

(1) For the slab specimens which were provided with holes through the slabs parallel to the plane in which the bending moment acts, the bending capacity of the connection was assumed to be expressed by the ultimate strength formula given by the ACI 1963 Building Code[6] for corner and edge connection as follows:

$$M_b = 0.9bd^2 f'_c \, q(1 - 0.59\, q) \qquad (2.19)$$

where

b = width of the column face perpendicular to the plane of applied bending moment

d = effective depth of the slab

q = reinforcement index = $P \frac{f_y}{f'_c}$

p = ratio of the tension steel crossing the inside column face of width "b".

(2) For the case of specimens in which the bending resistance of the slab section perpendicular to the plane of bending was omitted by introducing a hole through the slab, the bending moment applied through the column stub was assumed to be resisted by the capacity of the slab section (or sections) at the column side (or sides) parallel to the plane of applied moment in torsion.

For obtaining the torsional capacity of the slab section it was recognised that the torsional resistance depends on the area of the slab-column interface, concrete strength, the amount of transverse reinforcement and the degree of containment. The contribution of the reinforcement was rationalised by assuming the friction develops at the irregular interface of a crack, the frictional stress depending on the contact pressure developed by the tensile force in the reinforcement. This concept has been used

for calculating the shear strength.[45] It was further assumed that at failure, this friction stress is uniform on the whole area of the column-slab interface. He suggested that the plasticity formula (2.20) would hold in such a case:

$$M_t = N\tau \frac{t^2}{2}\left(a - \frac{t}{3}\right) \qquad (2.20)$$

where

N = number of column-slab interfaces parallel to the plane of the applied moment

τ = represents the nominal shear stress associated with the tensile force in the reinforcement

$$= K_t \frac{A_{st} f_y}{at}$$

K_t = friction coefficient

A_{st} = total area of transverse steel crossing the column-slab interface

f_y = yield of steel

a = width of column-slab interface

t = total slab thickness

Using a single test for each type of connection he worked backwards from Equation (2.20) and found that

for corner connection	$K_t = 0.7$
for edge connection	$K_t = 0.7$
for interior connection	$K_t = 1.0$

For connections subjected to axial load he modified Moe's Equation (2.4) in the following form:

(a) For interior connection

$$v_u \underset{(psi)}{=} \frac{V}{4rd} = 0.90\left[\frac{15(1 - 0.075\, r/d)}{1 + 5.25\,\frac{4rd\sqrt{f'_c}}{V_{flex}}}\right]\sqrt{f'_c} \qquad (2.21)$$

(b) For edge connection

$$v_u \underset{(psi)}{=} \frac{V}{3rd} = \frac{3r + 4d}{4r + 8d}\left\{0.90\left[\frac{15(1 - 0.075\, r/d)}{1 + 5.25\,\frac{3rd\sqrt{f'_c}}{V_{flex}}}\right]\sqrt{f'_c}\right\} \qquad (2.22)$$

(c) For corner connection

$$v_u \underset{(psi)}{=} \frac{V}{2rd} = \frac{2r + 2d}{4r + 8d}\left\{0.90\left[\frac{15(1 - 0.075\, r/d)}{1 + 5.25\,\frac{2rd\sqrt{f'_c}}{V_{flex}}}\right]\sqrt{f'_c}\right\} \qquad (2.23)$$

Equations (2.22) and (2.23) for edge and corner connections respectively were obtained by modifying Equation (2.4) by a factor which expresses the relative lengths of the critical sections taken at a distance d from the column perimeter. The basis of this correction was recognised to be inconsistent with the critical section recommended by Moe.[2] It was considered, however, that the number of tests on edge and corner columns (one test for each connection) was insufficient to justify modifying Moe's formula for internal columns, and the inconsistency was accepted at that time.

For the case where there were no holes the capacity of the corner or edge connection in bending was calculated as follows:

$$M = 0.90bd^2f'_c\, q\,(1 - 0.59q) + N\tau\,\frac{t^2}{2}\left(a - \frac{t}{3}\right) \qquad (2.24)$$

where n = 1 for corner connections of the type tested and n = 2 for edge connections.

For the combined bending and axial load cases he proposed an interaction equation in the following form:

$$\left(\frac{V}{V_0}\right)^2 + \left(\frac{M}{M_0}\right)^2 = 1 \qquad (2.25)$$

where M_0 and V_0 are to be calculated from Equations (2.22) or (2.23) respectively and M was defined as follows:

for an edge connection

$$M = Mtest - V\,\frac{a}{2}$$

and for a square corner connection with side width equal to r

$$M = \left(Mtest - V\,\frac{r}{2}\right)\left(0.6 + \frac{0.40}{M_t/M_{tu}}\right)$$

where

$$M_t = 0.40\left(Mtest - V\,\frac{r}{2}\right)$$

$$M_{tu} = \tau\,\frac{t^2}{2}\left(r - \frac{t}{3}\right)$$

It is of interest to mention that Stamenkovic also found, as did others,[9,10] that extrapolation of the existing

methods of analysis for interior columns[2,12] to predict the ultimate capacity of exterior connections gave extremely conservative results.

In 1970 Mast[46, 47] presented an analytical method for calculating the stresses in flat plates near interior[46] and edge columns.[47] The method was based on the theory of elastic plates.[48] The background for the method was given elsewhere.[48, 49] He calculated the amount of column moment transmitted to the slab by flexure, torsion and vertical shear stresses.

According to this method the following are the proportions of the total applied moment which are balanced by flexure, torsion and shear for a square periphery of a critical section of a side width equal to 0.20L where L is one panel width.

Table 2.2 Moment balancing by flexure, torsion and shear.

	Flexure	Torsion	Shear
Interior connection (Table 3)[46]	0.340	0.156	0.504
Edge connection (Table 3)[47]	0.254	0.264	0.482

From the above table the coefficient K which allocates the portion of the column moment transmitted by torsion and vertical shear combined to conform with Di Stasio and Van

Buren[11] method is equal to 0.66 for interior columns and 0.746 for edge columns. Also K which allocates the amount to be transmitted by vertical shear stresses to conform with the formula due to Moe[2] is 0.504 and 0.482 for interior and edge columns respectively.

It is important to know that the mathematical model was assumed as an infinitely long plate in one direction and simply supported along the other two sides which are perpendicular to the plane of the applied moment with the moment applied at the centre. Mast suggested that the use of simple supports at the ends rather than the actual columns does not affect the stresses at the simulated loaded column to any significant degree since the location of the approximation is remote from the area of study. But at the same time it has to be noticed that the moment was applied at the central point, and the proper boundary conditions at the periphery of the loaded column were not reproduced.

Hawkins and Corley in 1970[50] developed an ultimate strength procedure for interior and exterior column-slab connections based on a beam analogy. The slab framing into each column face was idealised as beams running in two directions at right angles. The ultimate capacity of the connection was obtained by summing the ultimate bending moment, torsional moment and shear forces of the beams for the given loading condition.

In the revised 1971 ACI Building Code (ACI 318-71)[51] Section 11.13.2 states that

> "when unbalanced gravity load, wind, earthquake or other lateral forces cause transfer of bending moment between slab and column, a fraction of the moment given by
>
> $$1 - \frac{1}{1 + \frac{2}{3}\sqrt{\frac{C_1 + d}{C_2 + d}}} \qquad (2.26)$$
>
> shall be considered transferred by eccentricity of the shear about the centroid of the critical section defined in section 11.10.2. Shear stresses shall be taken as varying linearly about the centroid of the critical section and the shear stress v_u shall not exceed $4\sqrt{f'_c}$."

In section 11.10.2 it is stated that

> "The critical section shall be perpendicular to the plane of the slab and located so that its periphery is a minimum and approaches no closer than d/2 to the periphery of the concentrated load or reaction area."

In ACI 318-77 Building Code the shear stress v_u changed from $4\sqrt{f'_c}$ to $4\phi\sqrt{f'_c}$, where ϕ is a reduction factor equal to 0.85.

In the British Code of Practice for the structural use of concrete CP110, Part 1, 1972,[52] section 3.6.2 states

> "In the case of structures in which stability is provided by shear walls or other bracing designed to resist the lateral forces and where the ratio between adjacent spans does not exceed 1.25, the shear force should be calculated for the condition where the ultimate imposed loads are applied to all panels adjacent to the column being considered. The design for shear should then be in accordance with 3.4.5.2., except that the values for ultimate shear stress given by Table 5 should be reduced by 20%.

In other cases the total moment M being transmitted to the slab at each column-slab connection should be calculated and the design checked in accordance with 3.4.5.2 (as modified above) for a shear force increased by the factor

$$1 + \frac{12.5M}{V\ell}$$

where V is the shear force and ℓ is the shorter of the two spans in the direction in which bending is being considered. It will be necessary to consider various arrangements of ultimate imposed loads in cases where the ratio between adjacent spans exceeds 1.25 leading to various combinations of M and V.

The magnifying factor does not apply to corner columns or to edge columns being bent at right angles to the edge."

In 1974 Regan[53] presented a comparison between the ACI-Building Code (1971) and the British Code CP110, Part 1 (1972) on shear problem at the column head regions in flat slabs. The most important differences were as follows:

(1) The ACI Code includes torsion in its uneven shear effects.

(2) In the ACI Code uneven shear effects are greater if the column dimension parallel to the eccentricity is larger than that perpendicular to it, while in CP110 rectangularity has no effect.

(3) According to CP110 the effect of uneven shear decreases for greater slab spans. There appears to be no evidence either way on this

point for flat slabs, but there are cases in bridge decks where the ACI predictions are better.

(4) The biggest difference is in the treatment of moments perpendicular to slab edges, where the ACI code applies the above approach with a suitable modification of J_c and predicts a considerable influence on punching resistance, while CP110 totally ignores any such effect.

2.4 Summary

In reviewing the literature it was found that most of the experimental work concerning the ultimate shear strength of column-slab connections was concentrated on a study of specimens which were assumed to simulate a concentrically loaded interior connection. Only limited information is so far available, which involves bending moment or combined axial load and bending moment transfer. A lack of experimental data is apparent regarding the strength and behaviour of exterior column-slab connections, i.e. corner and edge connection.

The present methods of estimating the shearing capacity of slabs under both axial load and bending moments give different results, some of which may be unsafe, as shown by Hanson and Hanson[12] for interior connections. These methods when extended to edge connections were found to produce extremely conservative results.[9,10,44]

The following concepts are common in the present design methods:

(1) Limiting the maximum shear stresses at the remote points of an assumed critical section.

(2) Nominal shear stress to increase linearly from the centroidal axis of the peripheral section and to reach a maximum at one of the transverse sections.

(3) Flexural stresses are treated as an independent variable.

Each method uses a different position for the critical section (see Table 2.1), certain limiting shear stress and different K values to allocate a portion of the total moment to be transferred by shear and torsion.

For Di Stasio and Van Buren[11] and similarly the ACI-ASCE committee 326 and the commentary on the ACI Code 1953[6], K is considered to be the portion of the bending moment which is to be transmitted by torsion. Consequently J_c in Equations (2.10), (2.11), (2.15) and (2.16) would be the polar moment of inertia of the critical section. In Moe's Equation (2.12), K determines the portion of the total bending moment which is to be transmitted by vertical shear stresses only. In Equation (2.12), J_c is determined from equilibrium of the external moment portion KM with the moment produced by the assumed vertical shear stress

distribution. It would therefore be expected that different values for K and v_m would be obtained from the two different approaches. Also, according to Di Stasio and Van Buren, no moment will be transmitted by vertical shear and torsion if the applied moment to the connection is equal to or less than the flexural capacity of the critical section faces which are perpendicular to the plane of the applied moment.

CHAPTER III

TEST PROGRAMME

3.1 General

The discussion in section 2.4 clearly shows that the problem of moment or combined axial shear and moment transfer between columns and slabs at the connection with edge and corner columns is not yet solved and accumulation of experimental information is required.

Test programmes were undertaken in this investigation to study the effect of the basic parameters, r_1/r_2 ratio, r_1/L ratio, and r_1/d ratio on the ultimate strength of slabs at their connection with edge columns.

An outline of this test programme giving a detailed description of the test specimens and details of method of fabrication, material properties, testing equipment, instrumentation and testing procedure is presented.

3.2 Object and Scope

The object of the study was to determine the variation of strength and stiffness of the joint as the ratio of the column sides was changed and the ratio of moment and shear was changed. The main test piece dimensions and the variable dimensions are shown in Fig. 3.1.

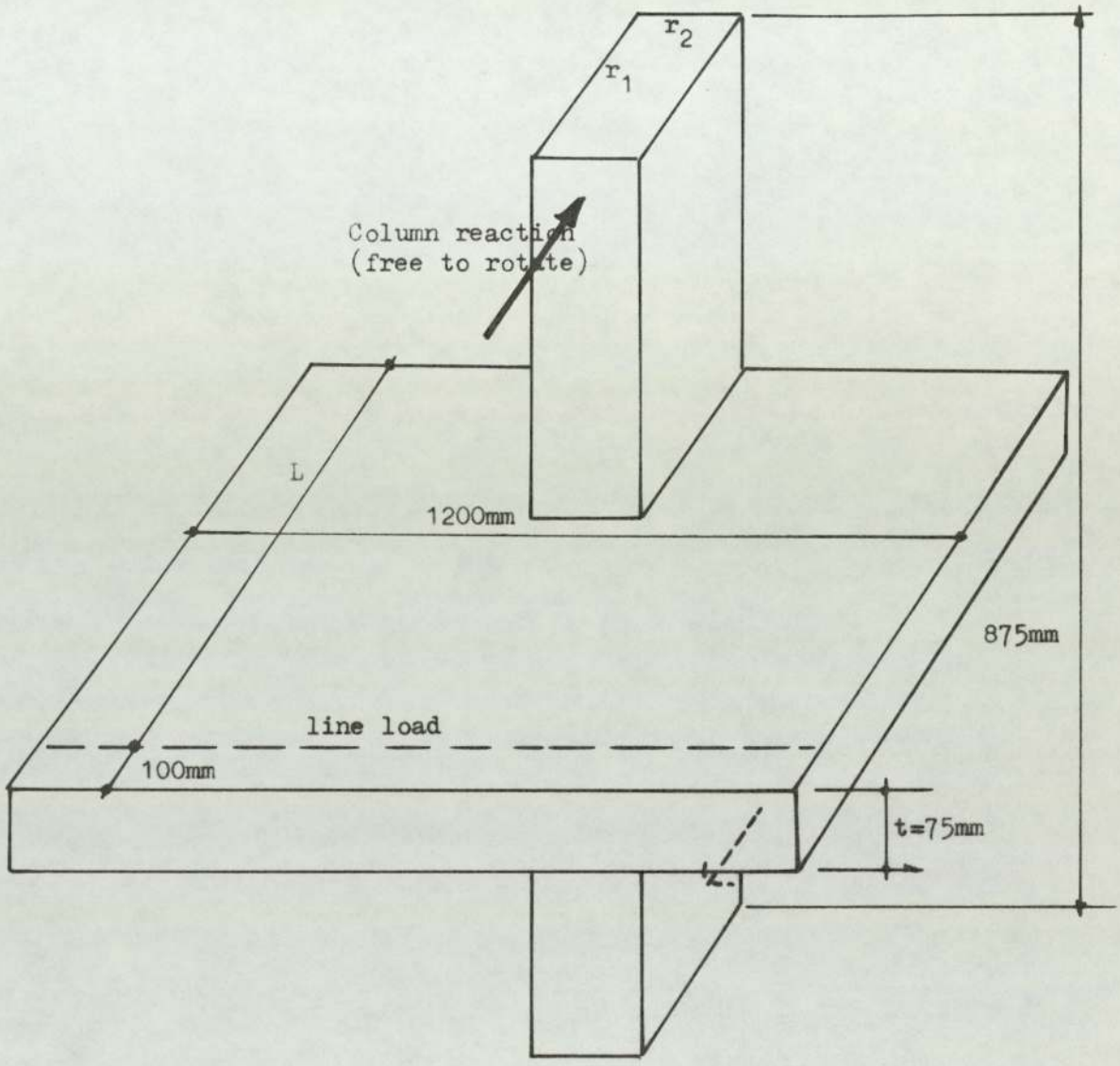

Fig. 3.1 Test specimen

The test programme was divided into four series of tests, involving a total of fifteen specimens. The principal variables considered were the column dimensions and the eccentricity of loading.

3.3 Description of test specimens

In order to obtain a realistic estimate of the behaviour of a real flat slab structure at failure, it was necessary to use test specimens that would represent the appropriate part of such a structure. Each of the fifteen specimens was intended to represent, in reduced scale, an isolated portion of slab surrounding a column as shown in Fig. (3.1).

It has been shown in tests on flat slab structures carried out in Illinois[54] that no undesirable scale effects occur for half full scale of actual structures.

All slabs tested in this investigation were 75 mm thick with the slabs cast monolithically with their column stubs. The column sizes changed from one series to another. The column stubs were kept constant at 400 mm above and below the surface of the slab. The columns had hinged reactions at their ends.

The column perimeter (three sides only) for all specimens was kept constant at 540 mm.

The position of the line load was chosen to represent the point of contraflexure of the slab which is assumed to be 15% of the span between columns. The distance from the line load to the exterior face of the column (L) was varied from 500 mm up to 1100 mm in 200 mm steps for each series, as shown in Table 3.1 below.

Table 3.1 Dimensions of test specimens and loading

Specimen No.	Column size (mm)		L (mm)	Specimen No.	Column size (mm)		L (mm)
	r_1	r_2			r_1	r_2	
1	140	280	500	9	180	180	500
2	"	"	700	10	"	"	700
3	"	"	900	11	"	"	900
4	"	"	1100	12	"	"	1100
5	160	220	500	13	200	140	500
6	"	"	700	14	"	"	700
7	"	"	900	15	"	"	900
8	"	"	1100				

The length of the other side of the slab was kept constant at 1200 mm.

3.4 Material

3.4.1. Concrete

The concrete mix was designed for a cube crushing strength of 25N/mm^2 at seven days. One cubic metre of the

mix contained:

395 kg of cement

229 kg of water

682 kg of fine aggregate

1034 kg of coarse aggregate.

Ordinary Portland cement and a 10 mm maximum aggregate size were used.

The concrete for the specimens was mixed in one or two batches according to the size of the slab, as shown in Table 3.2 below, and the concrete strengths are listed in Table 3.3

Table 3.2 Volumes and Number of Batches of the Mix

Specimen No.	Volume of mix (m^3)	Number of batches
1, 5, 9,13	0.15	1
2, 6,10,14	0.17	1
3, 7,11,15	0.19	2
4, 8,12	0.21	2

Compressive strength was determined from tests on standard 150 mm control cubes. The average of 3 specimens was considered to represent the strength, f'c , of the concrete in the test structure.

Table 3.3 Strength properties of concrete used in test specimens.

Specimen No.	Compressive strength (f'_c) N/mm^2	Modulus of rupture (f_r) N/mm^2	Tensile strength splitting test (f_t) N/mm^2
1	27.76	2.626	2.092
2	25.93	2.626	2.425
3	29.00	2.940	2.622
4	26.20	2.900	2.120
5	26.80	3.567	2.079
6	27.30	3.175	2.221
7	29.80	3.097	2.544
8	29.20	2.979	1.995
9	22.50	2.744	2.073
10	29.00	3.018	2.156
11	22.90	2.979	1.431
12	26.30	3.254	2.037
13	30.30	3.214	2.249
14	26.20	2.979	2.577
15	28.90	3.254	1.948

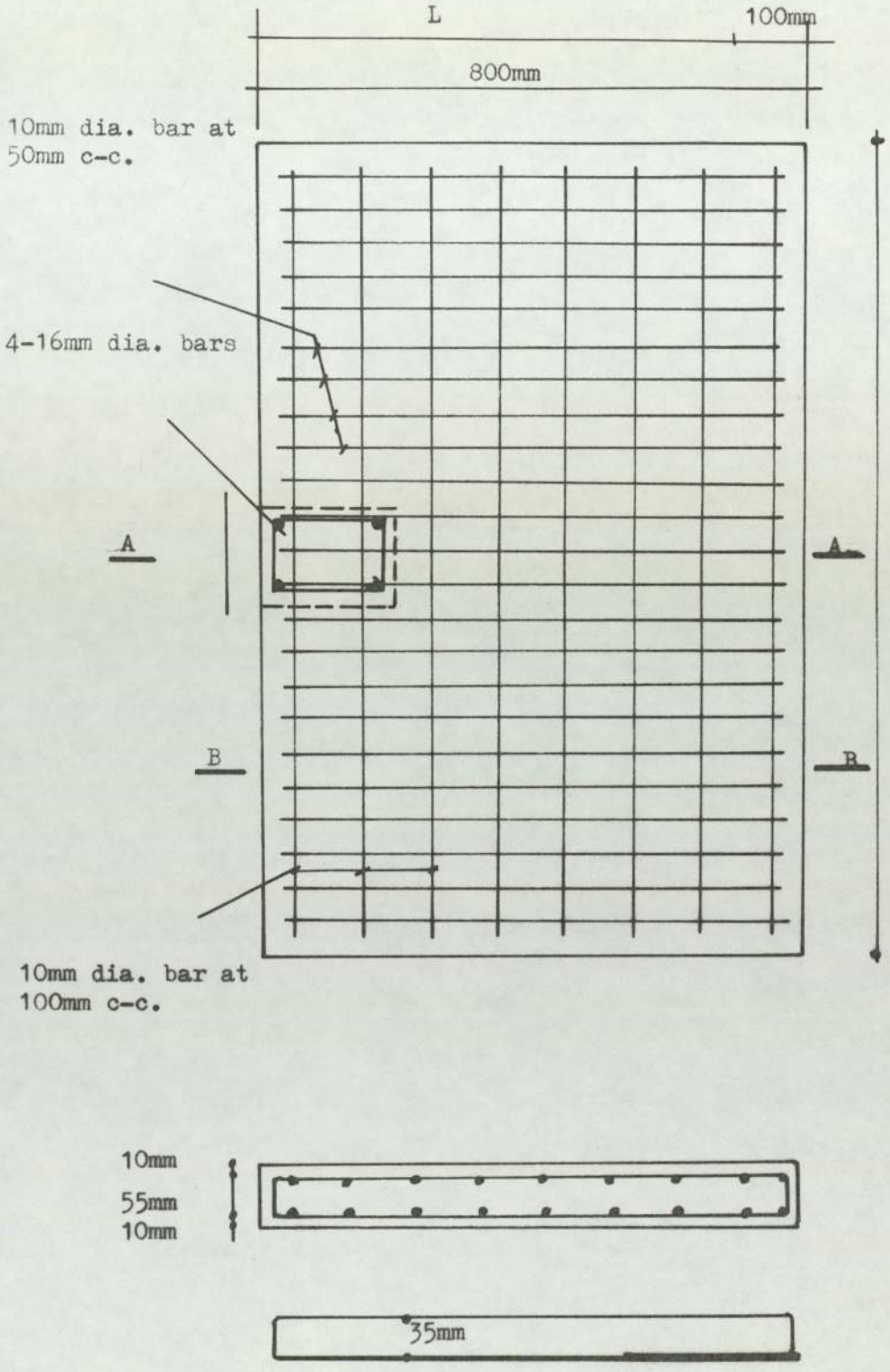

Section B-B

Fig. 3.2 Typical slab and column reinforcement.

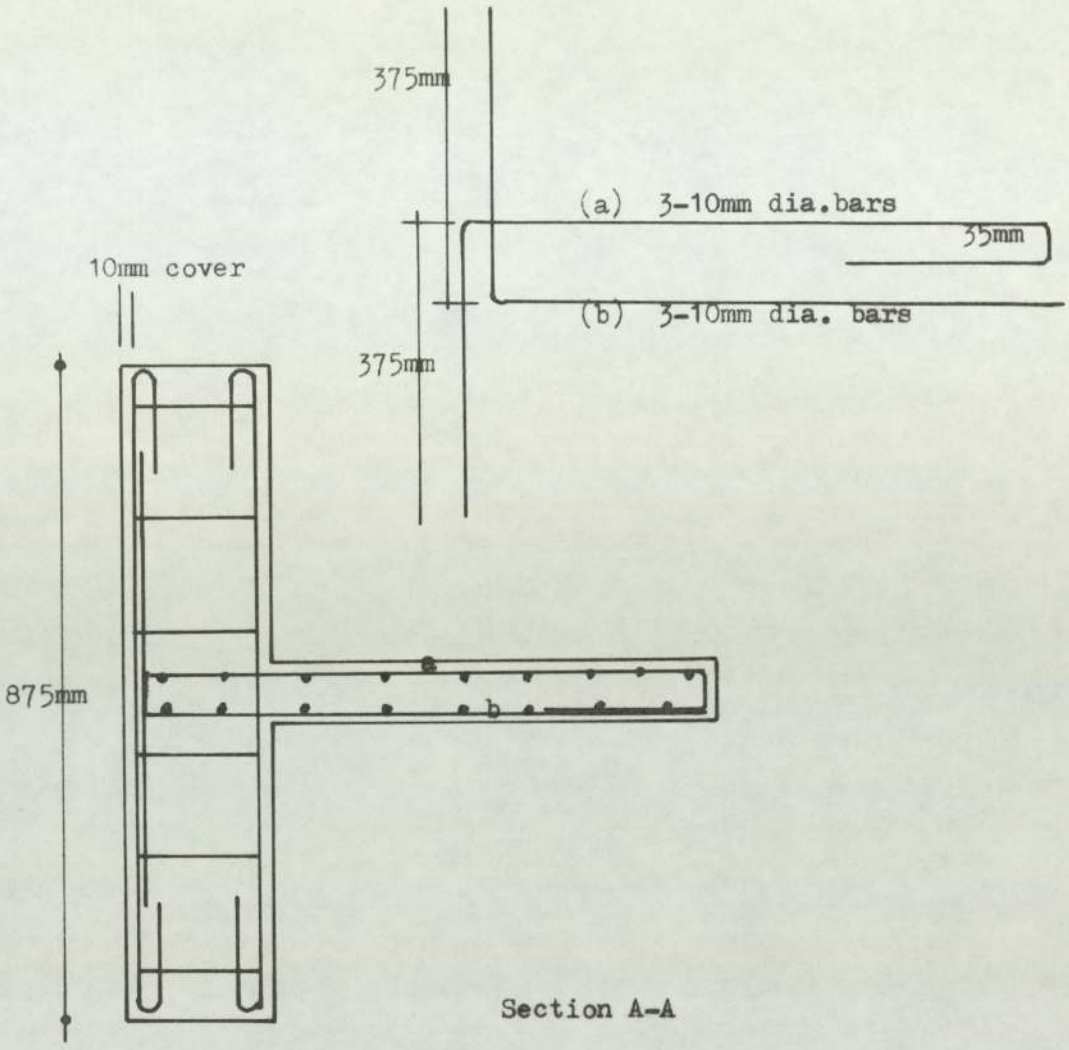

Fig. 3.2 (Continued)

Modulus of rupture strength was obtained from the average of 3 tests on 100 mm by 100 mm by 400 mm beams using third point loading.

Tensile strength in splitting was determined from the average of 3 tests on 150 mm x 300 mm control cylinders using 10 mm wide timber strips. After casting, the slab and cubes were kept for forty eight hours under wet sacking and then stored in the laboratory until tested.

3.4,2. Reinforcement

(i) Column stub reinforcement

The longitudinal reinforcement used in the column stubs consisted of 4-16 mm diameter plain bars of intermediate grade steel. (See Fig. 3.2) Stirrups were 8 mm diameter plain intermediate grade steel.

(ii) Slab reinforcement

The slabs were reinforced with two mats of 10 mm diameter plain bars spaced 50 mm centre to centre in the direction perpendicular to the exterior free edge of the slab. In the other direction of the slab, two mats were used of 10 mm diameter plain bars spaced 100 mm centre to centre. The mats were placed so that the bars perpendicular to the free edge were covered by 10 mm of concrete, all as shown in Fig. 3.2.

The steel properties for the specimens were obtained

from 3 samples cut from the bars used in each slab, see Table 3.4.

Table 3.4 Physical Properties of Reinforcement Steel

Specimen	f_y in N/mm^2	Specimen	f_y in N/mm^2
1	414.2	9	352.20
2	299.60	10	327.98
3	335.46	11	379.84
4	375.60	12	354.38
5	329.22	13	375.60
6	341.63	14	381.96
7	326.36	15	333.16
8	358.60		

In order to prevent flexural failure occurring before the punching shear failure, the amount of reinforcement was approximately 30% greater than that obtained by yield line method. Typical stress-strain relationships for 10 mm. and 16 mm. diameter bars are shown in Fig. 3.3.

3.5 Fabrication of test specimen

3.5.1. Formwork

The form was made such that the column was cast in the horizontal position while the slab was vertical, and both the column stubs and the slab were cast at the same time. Special attention was given to the rigidity necessary to control the dimensions of the slabs and column stubs.

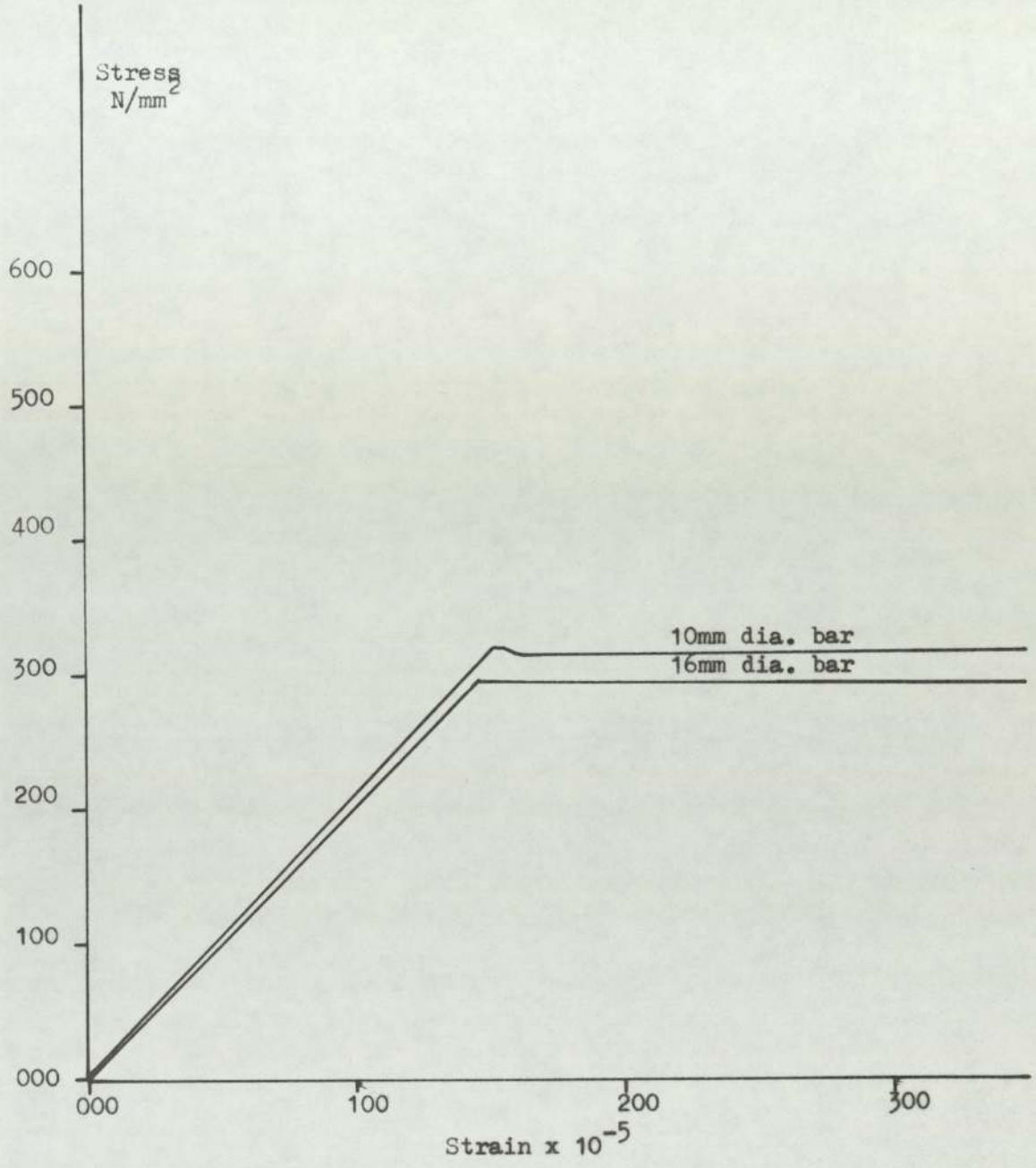

Fig. 3.3 Typical stress-strain relationships for reinforcement steel

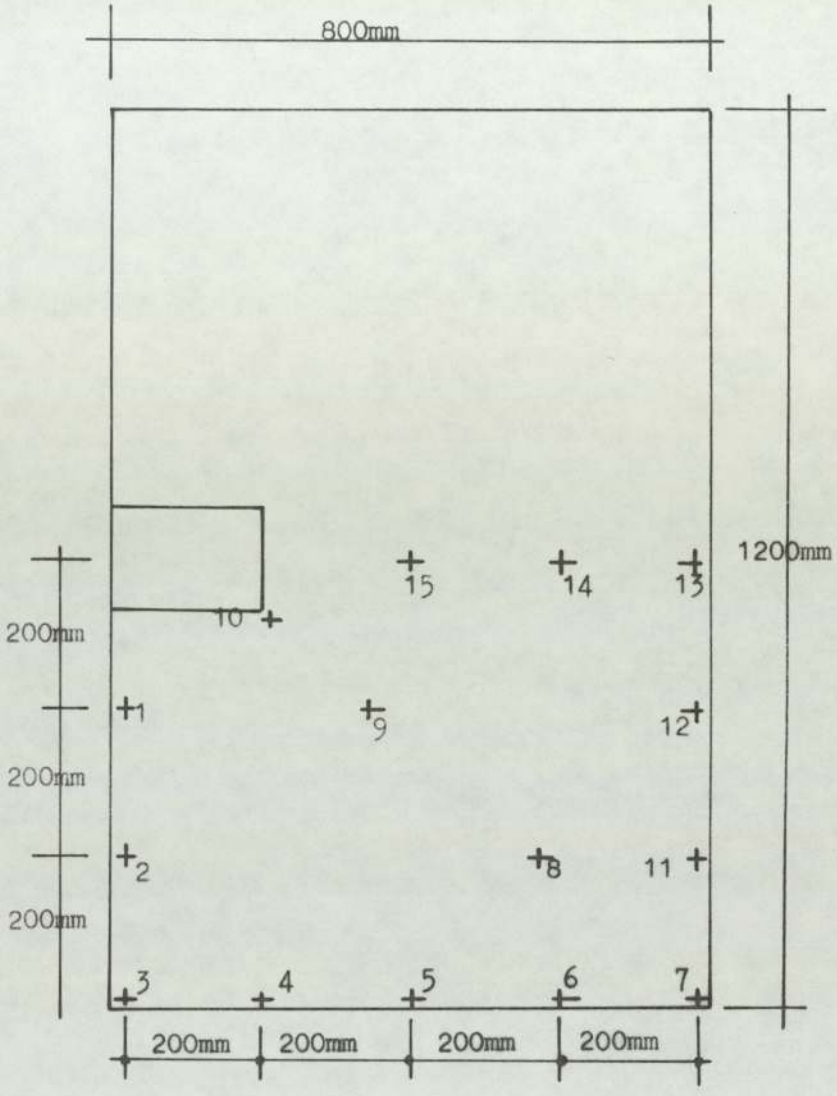

Fig. 3.4 Dial gauges (deflectometers) layout for a typical specimen.

3.5.2. Fabrication of reinforcement

The bars were assembled in the form with the configuration shown in Fig. 3.2. Bar spacings were carefully checked before casting.

3.6 Casting and Curing

Concrete was placed manually with compaction of the concrete by table vibrator. The control specimens were cast at the same time. Curing consisted of keeping the slabs and the control specimens damp by means of wet sacking and polythene sheets.

3.7 Deflectometers

The deflections of the slab of each test specimen were measured at the positions indicated in Fig. 3.4. The dial guage used for measuring these deflections had graduations of 0.01 mm.

3.8 Supporting Condition and Loading System and Apparatus.

The downward line load on the slab was applied through a 100 mm x 100 mm steel tube crosshead, 700 mm long, as shown in Fig. 3.5. Each end of this tube applied a concentrated load to the centre of another steel tube of the same cross-section and 420 mm long. The load on each tube was distributed on the slab by two 200 x 100 x 20 mm steel pads. The load was applied by a 10-ton hydraulic ram at the centre of the top beam. The applied load was measured by means of a proving ring placed between the ram and the top beam.

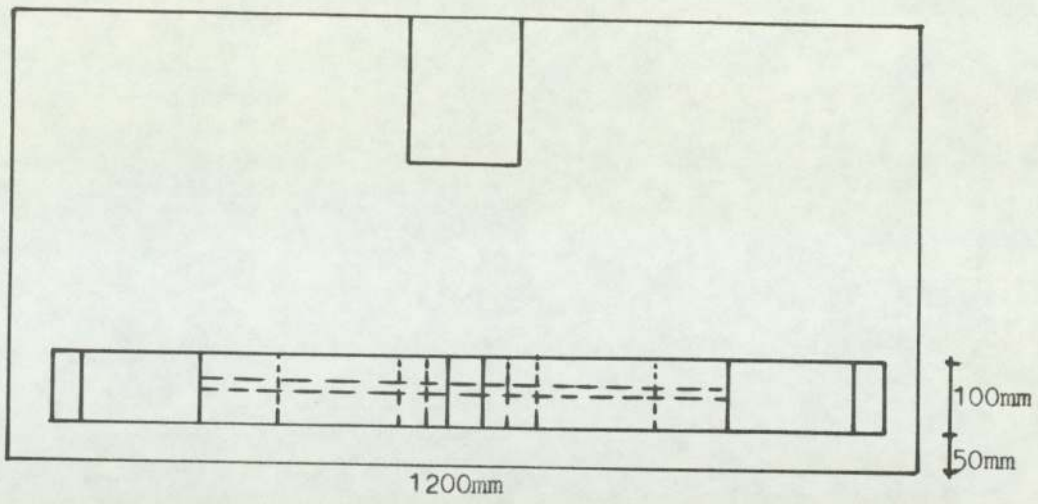

Top view

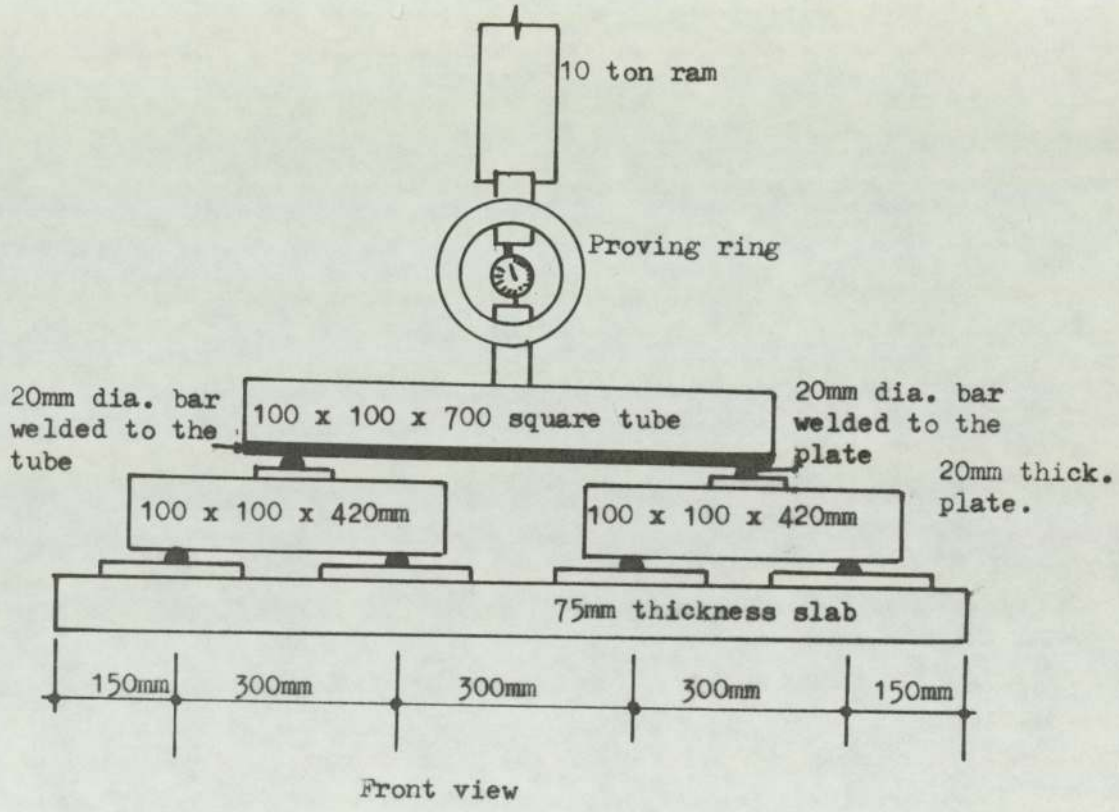

Front view

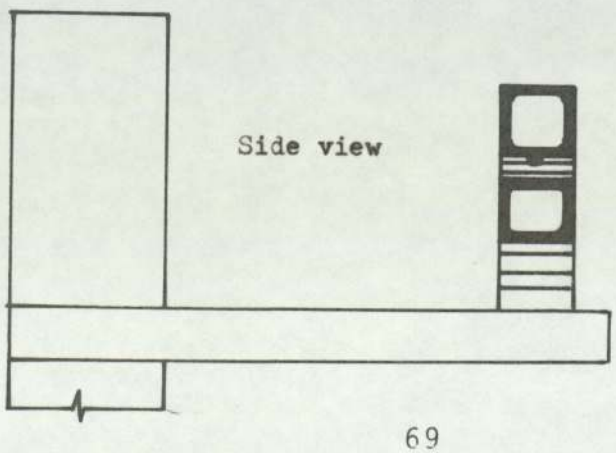

Fig. 3.5 Layout for the loading system

3.9 Testing Procedure and Measurements

One day before testing, the specimen was placed, centred and levelled in the testing rig and the necessary testing equipment assembled.

The testing of each specimen involved the recording of three separate items of information during the course of loading.

1. The applied load (proving ring reading)
2. The deflectometer reading (dial guage)
3. The general behaviour of the specimen, including cracking, was observed and recorded.

Immediately prior to testing, zero readings on all the measuring devices were taken and recorded. The load was increased in increments to failure. The magnitude of the increments was reduced at higher load levels near failure.

After the application of each load increment the readings on the measuring devices were recorded. The locations of the cracks were marked on the surface and free edges of the slab. The time required until failure varied between one and two hours.

CHAPTER IV

TEST RESULTS

4.1 General

The variables considered in the experimental investigation were the column side ratio r_1/r_2, the column side to the eccentricity ratio r_1/L, and the column side to the effective slab depth ratio r_1/d.

In this chapter, observations during the progress of the tests, deformations of the slabs and the failure mechanism of connections are reported and discussed.

4.2 Behaviour of the test specimens and modes of failure

In this section the behaviour of the test specimens throughout the course of loading is discussed.

The fifteen tests were carried out to study the effects of the variables on the behaviour and ultimate capacity of an edge column connection under the application of an axial load and a bending moment acting in a plane perpendicular to the free edge of the slab. They were classified as follows:

(1) The first series consisted of four specimens in which the principal variable was the eccentricity of the load (L) which was varied from 500 mm to 1100 mm. The column size was kept constant at

(r_1 = 140, r_2 = 260). The slab reinforcement in the direction of bending moment was 2.3%, and 1.5% in the other direction.

(2) The second series consisted of four specimens with the same variable as in Section 1 above, but with a different constant column size (r_1 = 160, r_2 = 220). The same slab reinforcement as before was used.

(3) The third series consisted of four specimens with the same variables but the column size was (r_1 = 180, r_2 = 180).

(4) The fourth series consisted of three specimens with (L) varying from 500 mm up to 900 mm; the column size was (r_1 = 200, r_2 = 140). The same amount of slab reinforcement was used in this series.

Note that in all specimens the column perimeter was kept constant at 540 mm.

In the present section a comparison is drawn between the different specimens to show the effect of the variables considered on the behaviour and on the variation of deflection of the slab.

I. Appearance of the test specimen at various loading stages.

In all tests the cracks formed on the surface of the slab in approximately the following sequence. The first cracks were probably due to torsion on the sides of the column and

(a) Top view

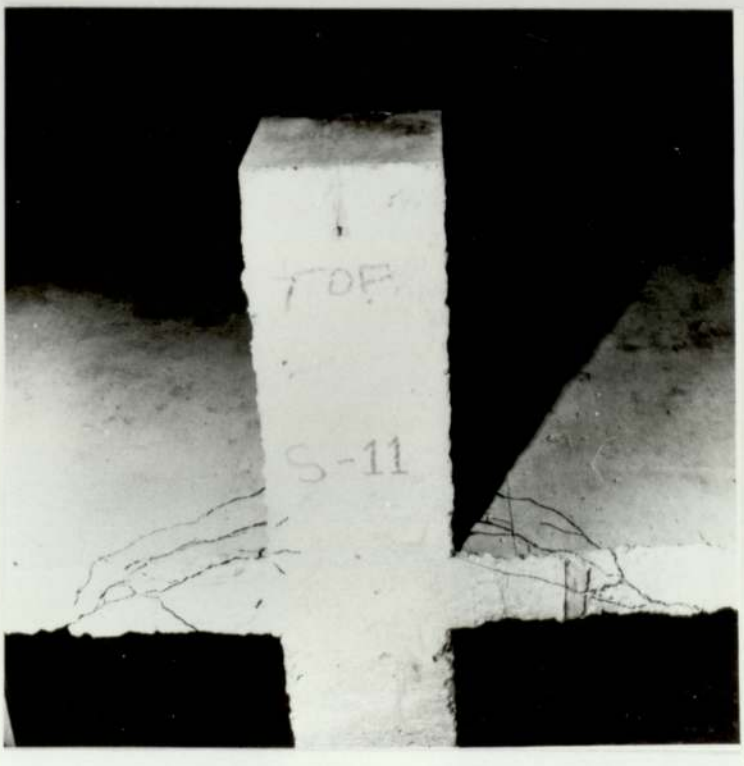

(b) Back view

Fig. 4.1 Typical specimen

they appeared at a load level equal to 0.50 - 0.68 times the failure load.

The cracks started at the inner face of the column in the slab and ran from the inner corner of the column towards the free edge. They followed first the column sides perpendicular to the free edge of the slab for a short distance and then deviated in the slab away from the column. Two or three of these cracks formed and one of them near the column developed into a large crack directly associated with the eventual failure of the specimen, see Fig. 4.1. With increasing load this crack extended from the column side to the free edge, having an inclination of about 35° to the side face of column, and then continued across the free edge. The crack, in progressing towards the compression side of the slab across the free edge, was inclined to the plane of the slab. The average inclination was about 45° in the direction away from the column stub to the compression side of the slab.

In addition to these cracks, others formed at the central part and progressively extended over the entire slab with increasing load, but they stopped some distance before the edge of the slab.

Some other tangential cracks appeared at different distances from the column faces. Finally the failure occurred in a form of a wide inclined crack from the inner

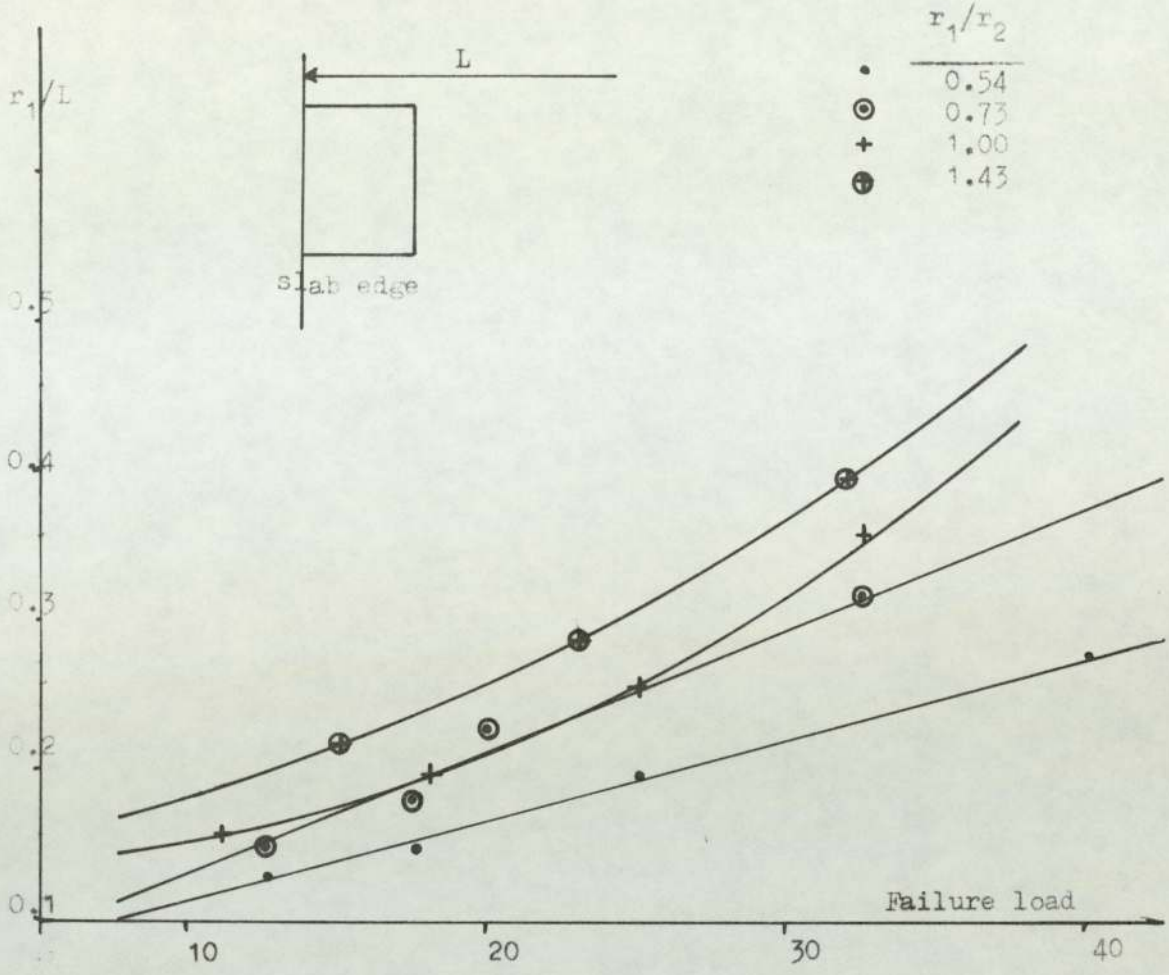

Fig. 4.2 Load-eccentricity relationship

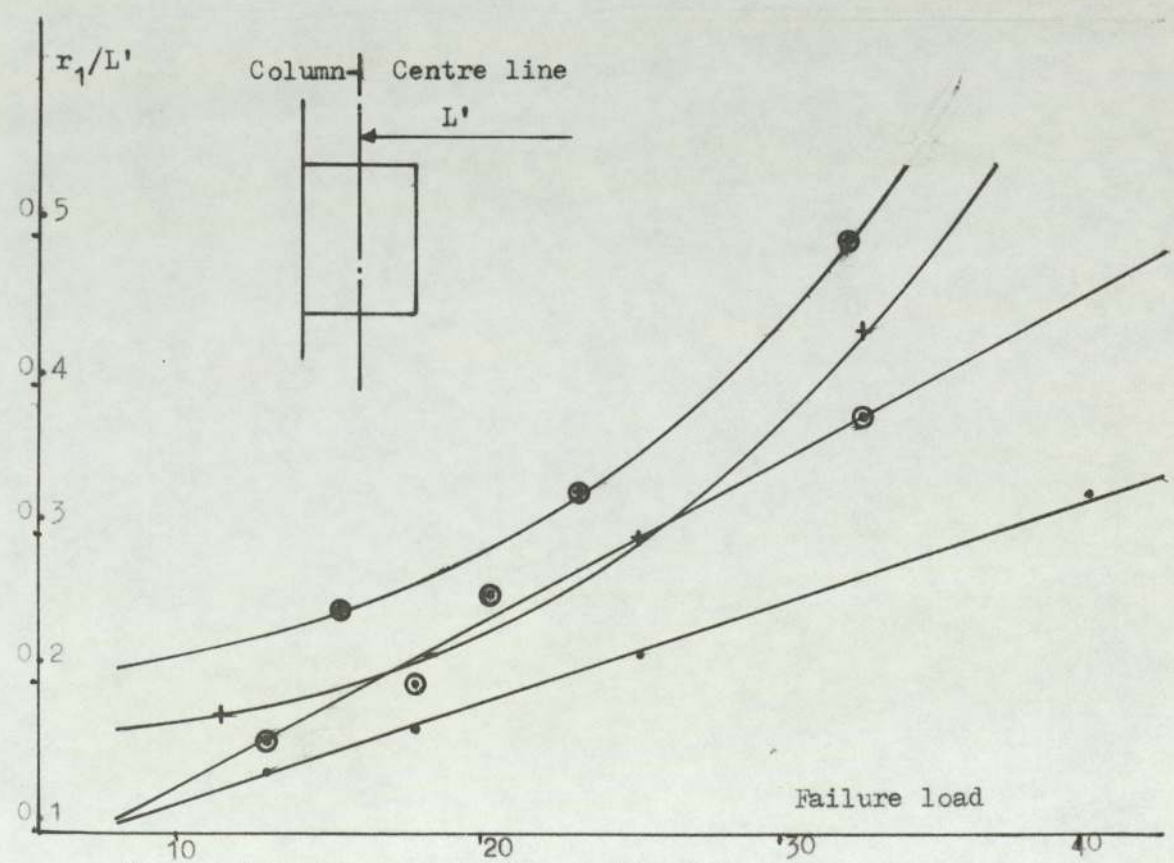

Fig. 4.3 Load-eccentricity relationship

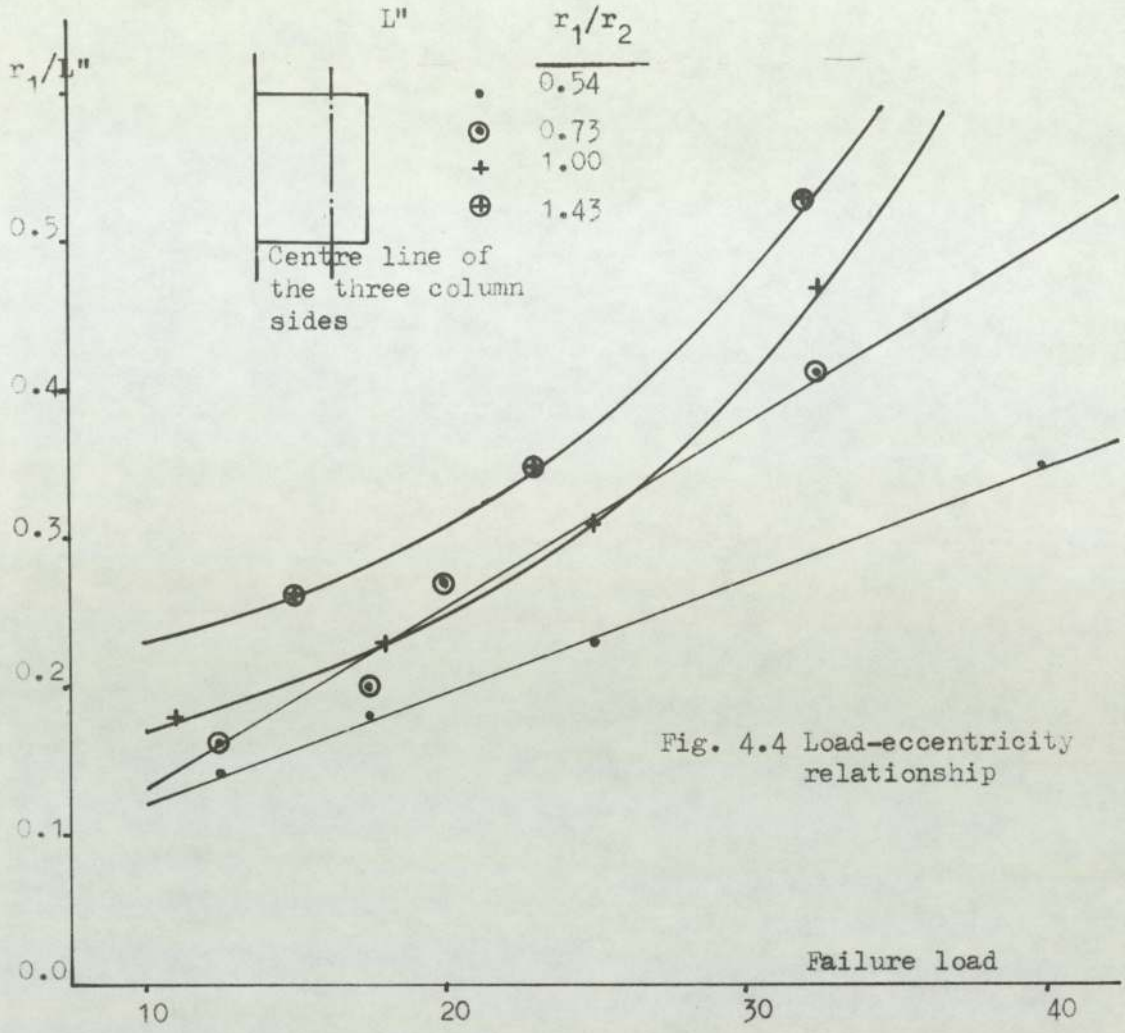

Fig. 4.4 Load-eccentricity relationship

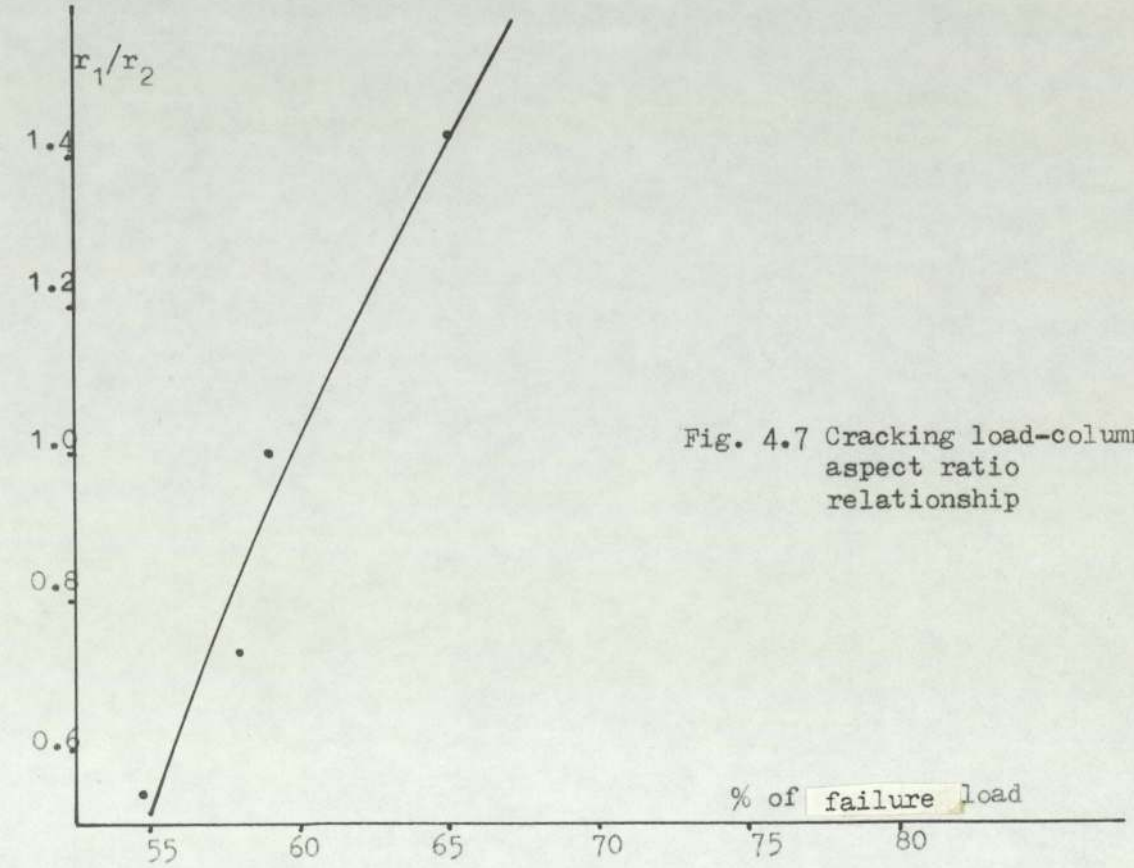

Fig. 4.7 Cracking load-column aspect ratio relationship

corner of the column to the free edge of the slab.

It is believed that the idealised mode of failure was the prime mode of failure and was mainly due to the formation of the torsional cracks on the column sides and flexural shear cracks at the inner side of the column. (see Fig. 4.1)

There was not much difference in the crack pattern and mechanism of failure in all specimens, The major difference was that the cracks were wider and more noticeable for specimens with the greater eccentricities.

II Ultimate Capacity

The load carrying capacities of the specimens in the four test series are listed in Table 4.1. Comparing the capacities of the series, as in Fig. 4.2., shows that the axial load carrying capacity of the connection increases approximately linearly with the increase of r_1/L ratio, where r_1 is the column side perpendicular to the free edge of the slab and L is the distance from the line load to the free edge of the slab. Fig. 4.3. and 4.4. have been drawn like Fig. 4.2. by using L' and L" instead of L, where L' is the distance from the line load to the centre of column, and L" is the distance from the line load to the centre of three sides of column. As may be seen in these figures, the effect of using different starting points for measuring eccentricity is small.

Specimen No.	r_1/r_2	r_1/L	V_{test} (KN)	$V_{cracking}$ (KN)	$\frac{V_{cra}}{V_{test}}$		r_1/d
1	0.54	0.28	40.0	20.0	0.50		2.333
2	"	0.20	25.0	15.0	0.60	0.56	"
3	"	0.15	17.5	10.0	0.57		"
4	"	0.13	12.5	7.5	0.60		"
5	0.73	0.32	32.5	17.5	0.54		2.666
6	"	0.23	20.0	12.5	0.63	0.58	"
7	"	0.18	17.5	10.0	0.57		"
8	"	0.15	12.5	7.5	0.60		"
9	1.00	0.36	32.5	17.5	0.54		3.000
10	"	0.26	25.0	15.0	0.60	0.59	"
11	"	0.20	18.0	10.0	0.55		"
12	"	0.16	11.0	7.5	0.68		"
13	1.43	0.40	32.0	20.0	0.63		3.333
14	"	0.28	23.0	15.0	0.65	0.65	"
15	"	0.22	15.0	10.0	0.66		"

Table 4.1 Test results

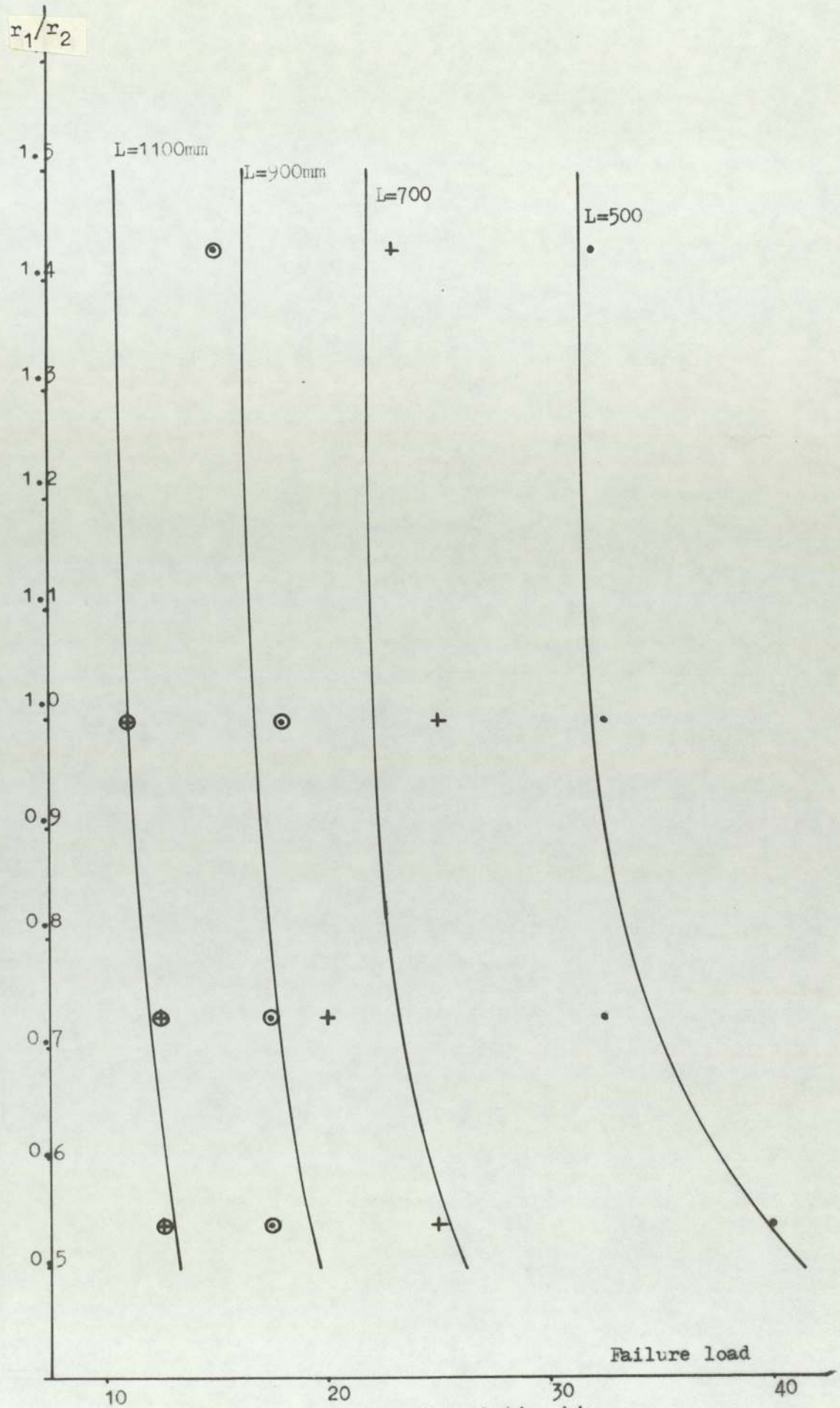

Fig. 4.5 Load-column aspect ratio relationship

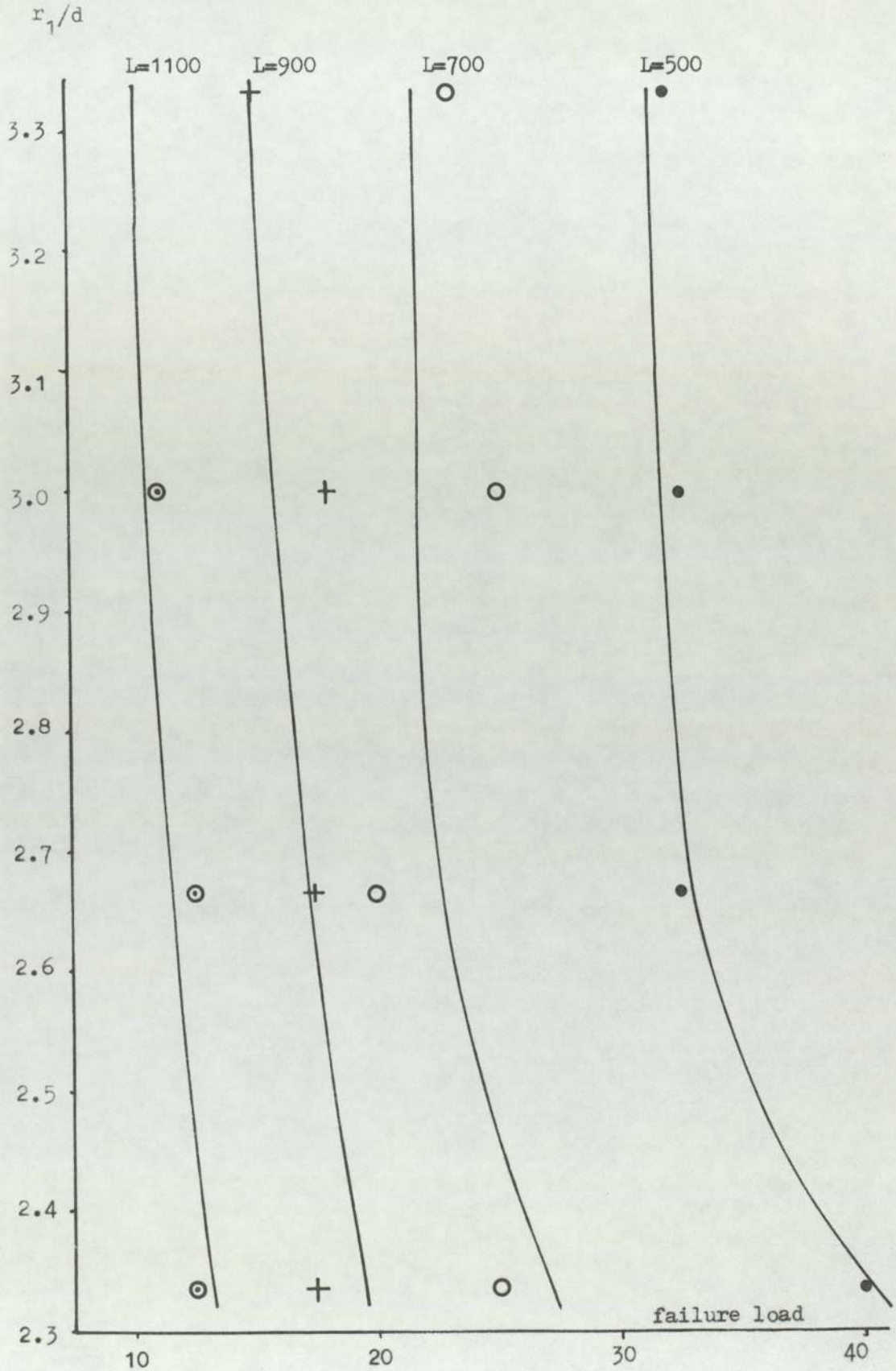

Fig. 4.6 Load-r_1/d ratio relationship

Also it was noticed that the load carrying capacity of the connection reduced slightly as r_1/r_2 and r_1/d increased, (see Figs. 4.5 and 4.6) Thiseffectwas noticed by Hawkins[3] in his tests on interior slab-column connection.

Hawkins found that both the cracking and failure loads decreased as the column sides ratio r_1/r_2 increased. This is contrary to that observed in the present investigation for edge connection. (See Fig. 4.7).

This probably related to the difference between the type of specimens used by Hawkins and specimens used in this investigation. Hawkins' specimens were rectangular columns with square slabs concentrically loaded; the columns had aspect ratio ranging between 1 and 4.3, while the specimens of this research were rectangular columns with rectangular slabs subjected to axial load and bending moment; the column aspect ratio varied from 0.54 to 1.43. In the case of edge connection, high bending moment is applied to the column, while in the case of interior connection loaded concentrically there is no bending moment carried by the column. Additionally, slab continuity or lack of slab continuity must have a considerable effect; other difference in variables may also have some effect on the cracking pattern.

III Deflections

The deflection of the slab was measured at different

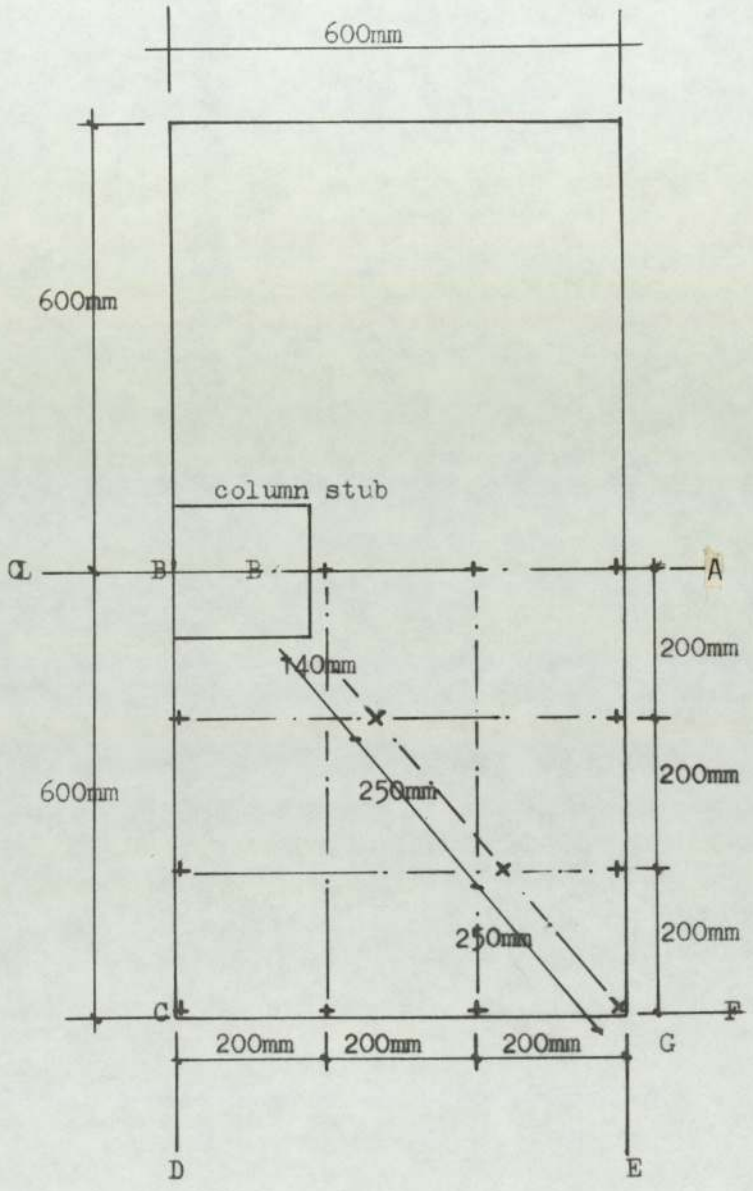

Fig. 4.8 Dial gauges outline (slab size 600mm x 1200mm)

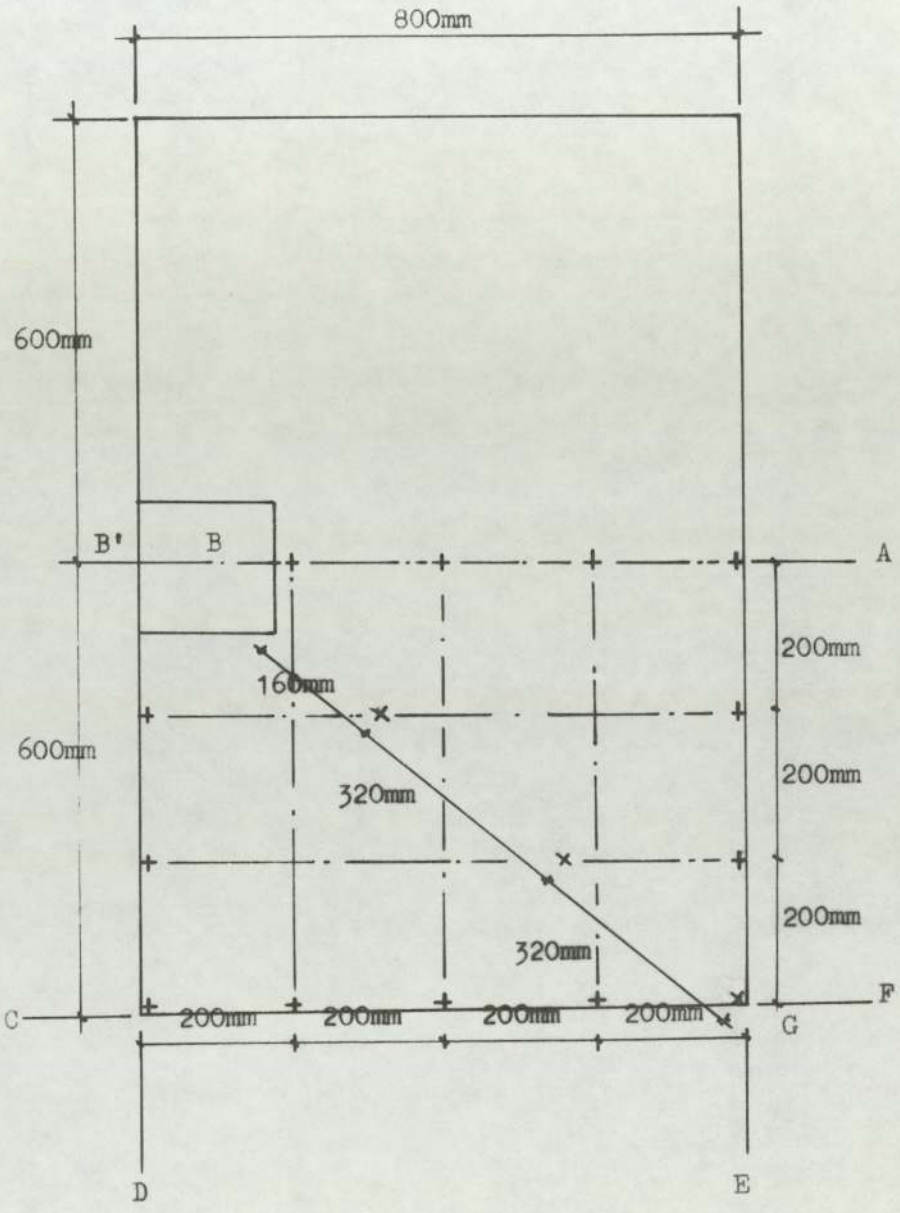

Fig. 4.9 Dial gauges outline (slab size 800mm x 1200mm)

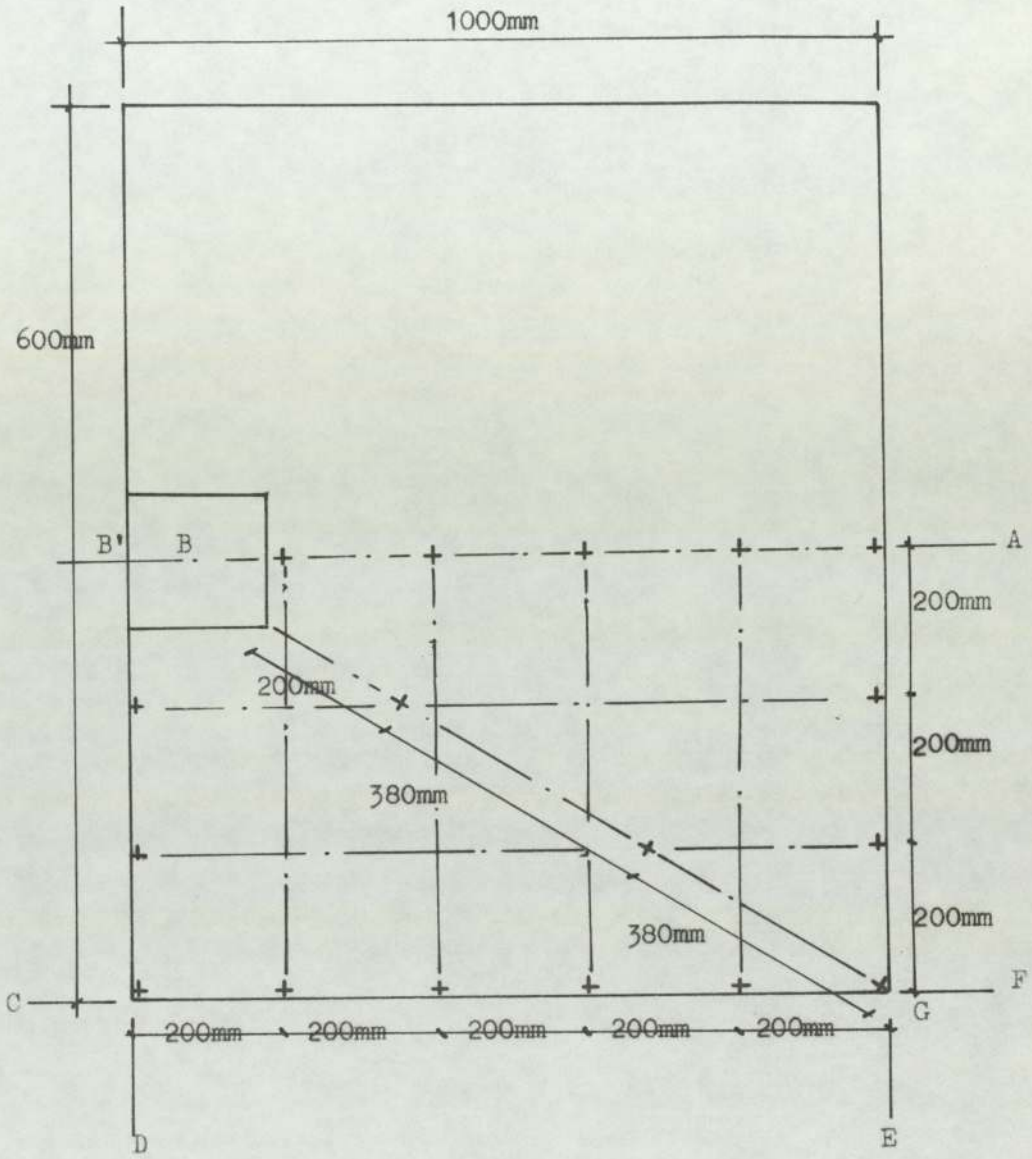

Fig. 4.10 Dial gauges outline (slab size 1000mm x 1200mm)

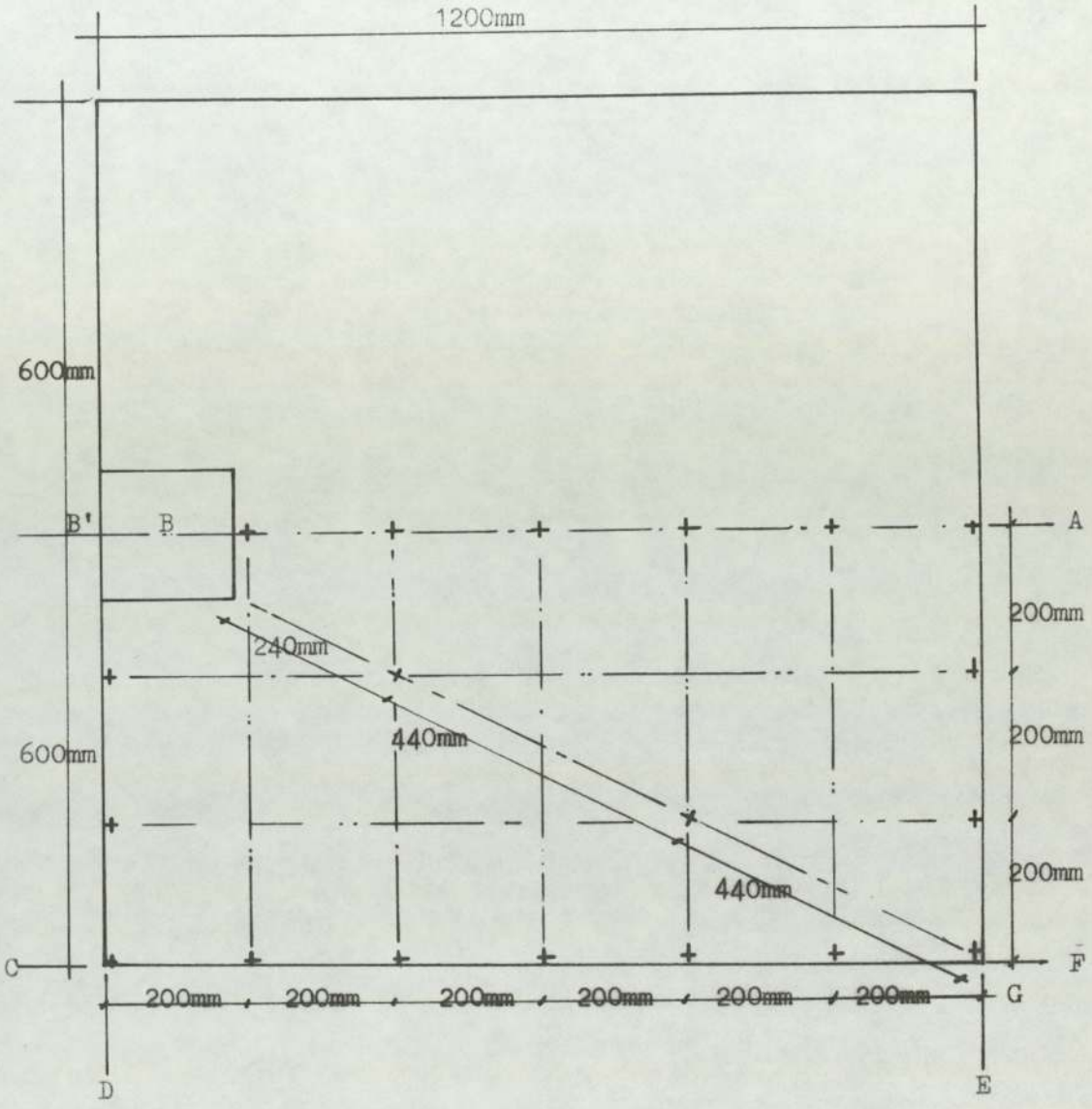

Fig. 4.11 Dial gauges outline (slab size 1200mm x 1200mm)

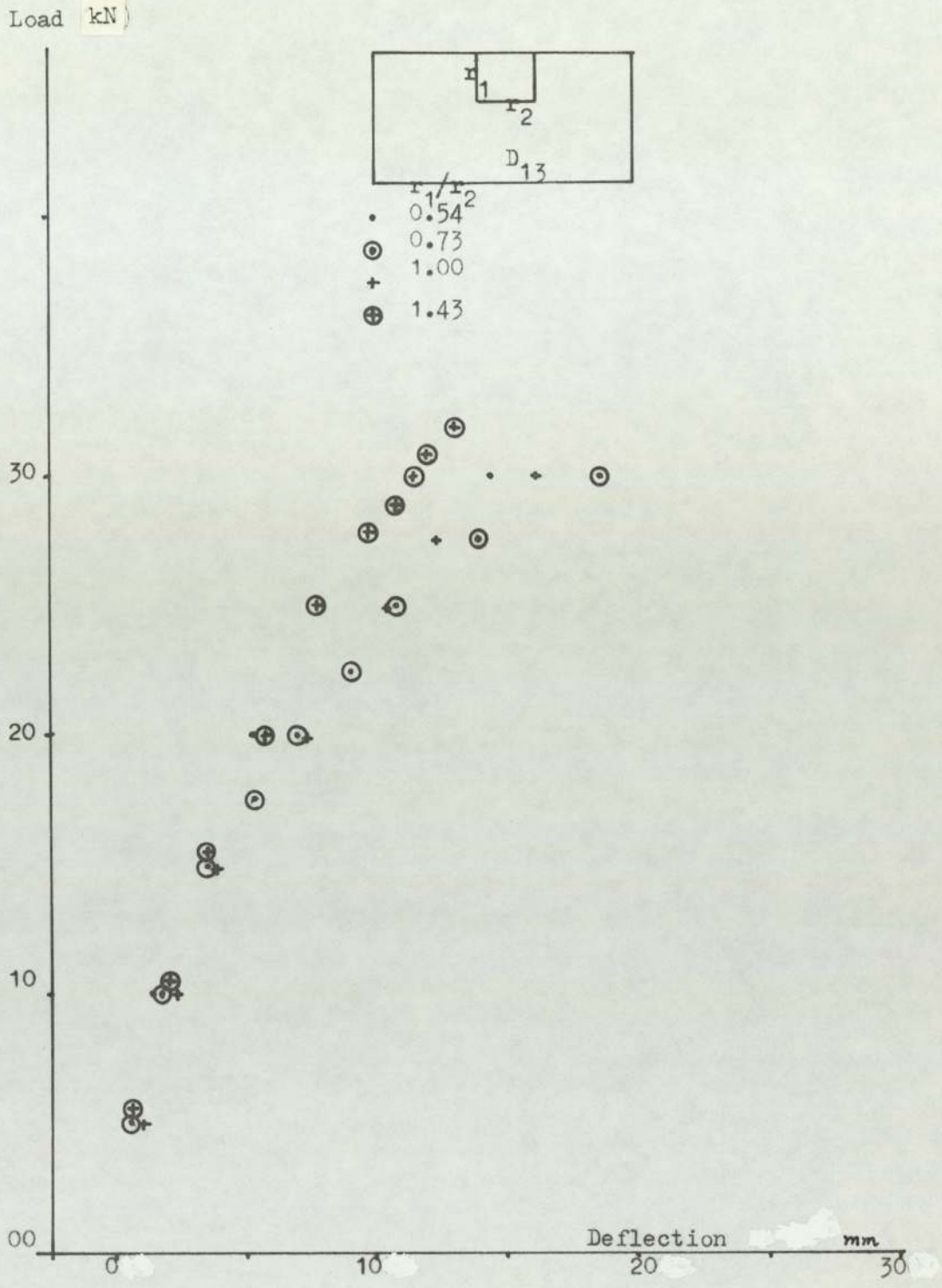

Fig. 4.12(a) Load-deflection curve at D_{13} (slab size 600mm x 1200 mm)

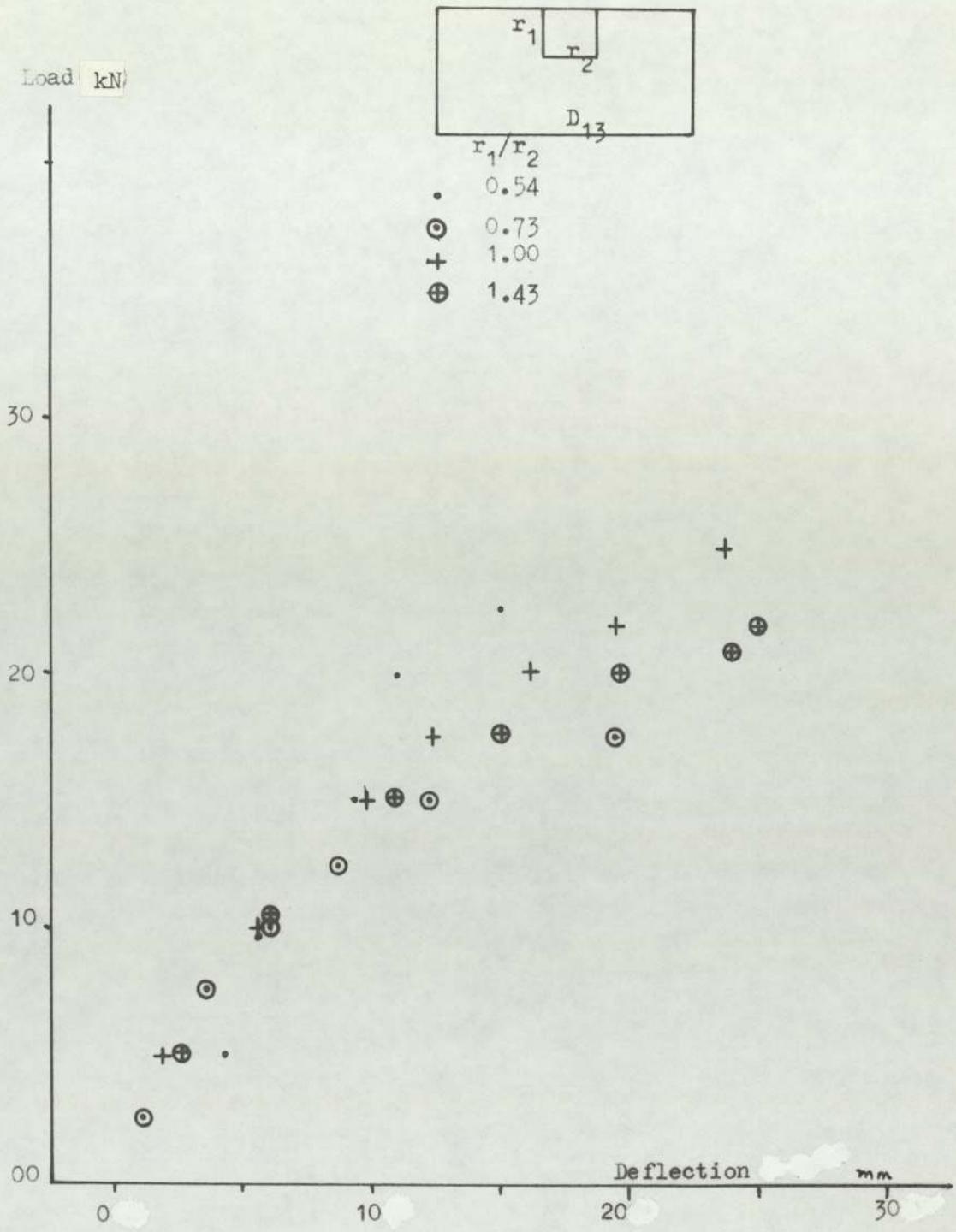

Fig. 4.12(b) Load-deflection curve (slab size 800mm x 1200mm) at D_{13}

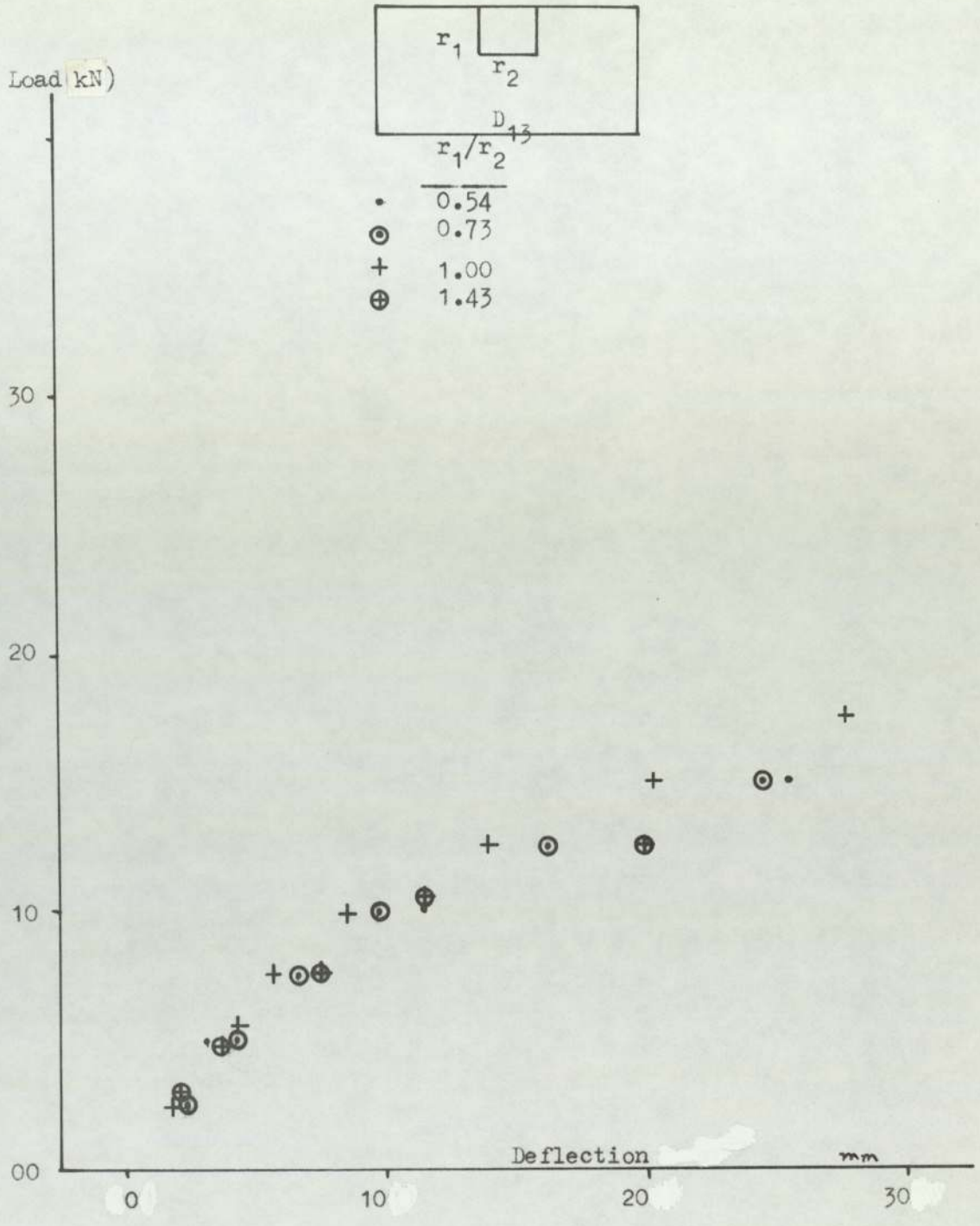

Fig. 4.12(c) Load-deflection curve (slab size 1000mm x 1200mm) at D_{13}

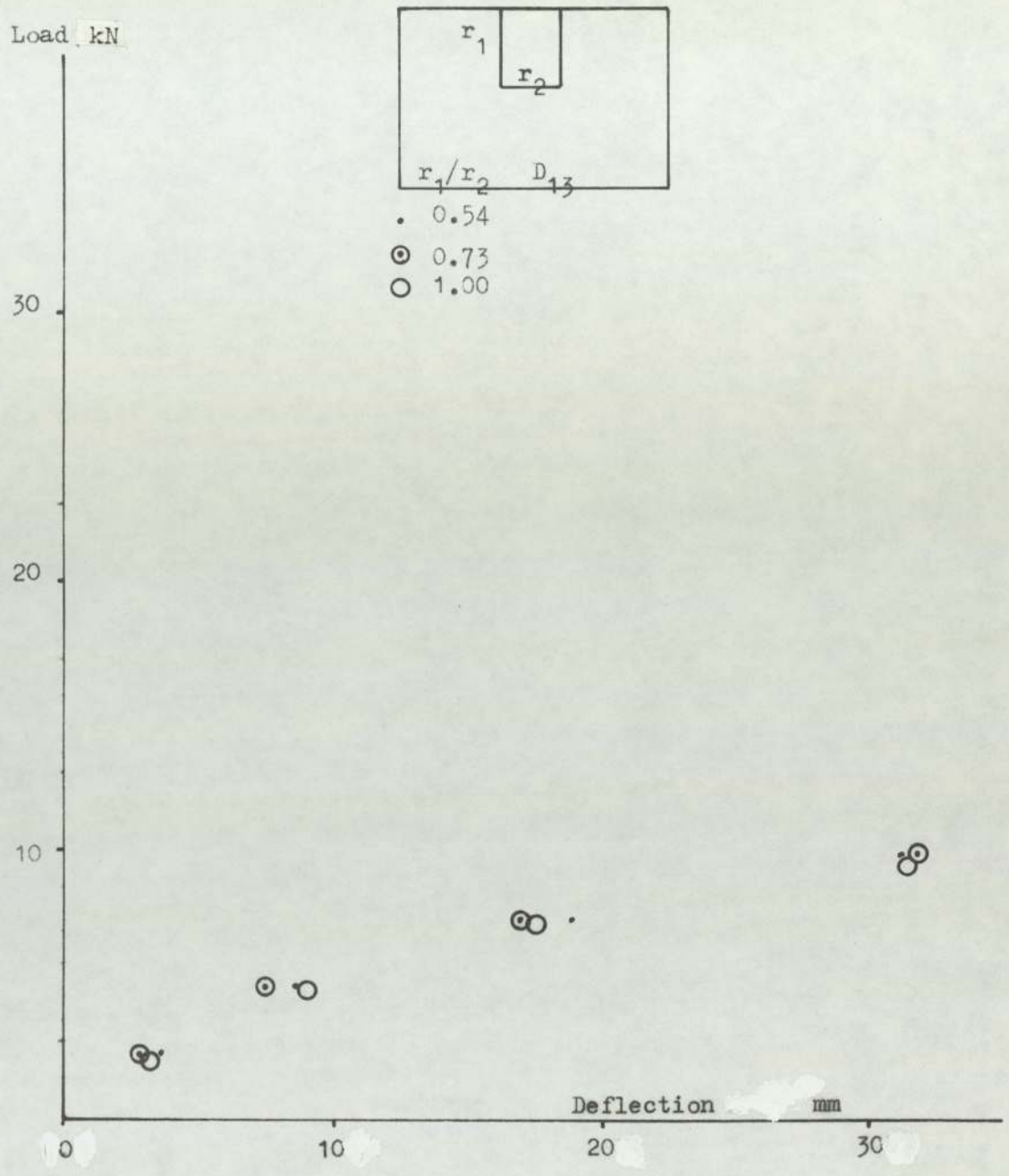

Fig. 4.12(d) Load-deflection curve at D_{13} (Slab size 1200mm x 1200 mm)

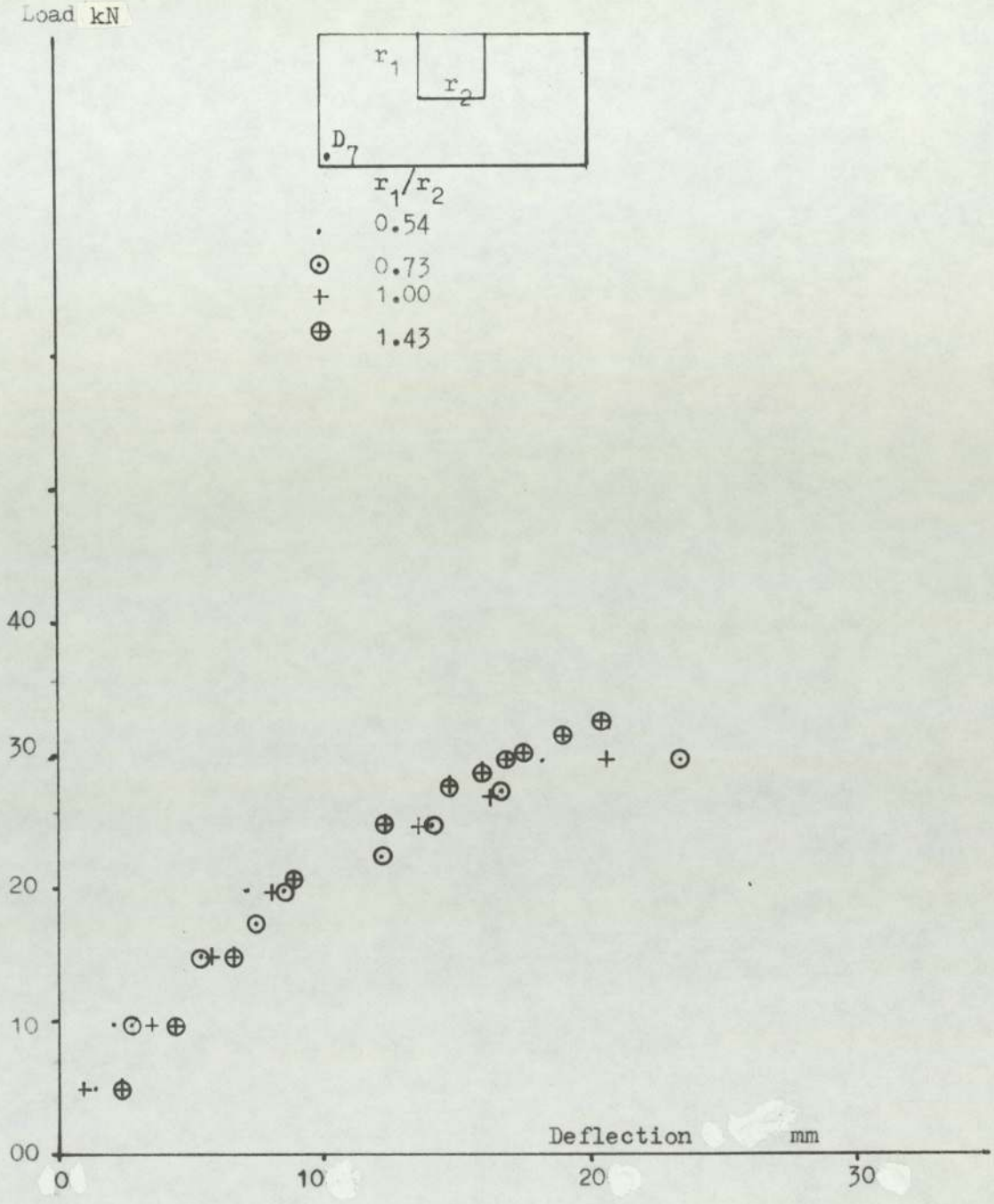

Fig.4.13(a) Load-deflection curve at D_7 (slab size 600mm x 1200mm)

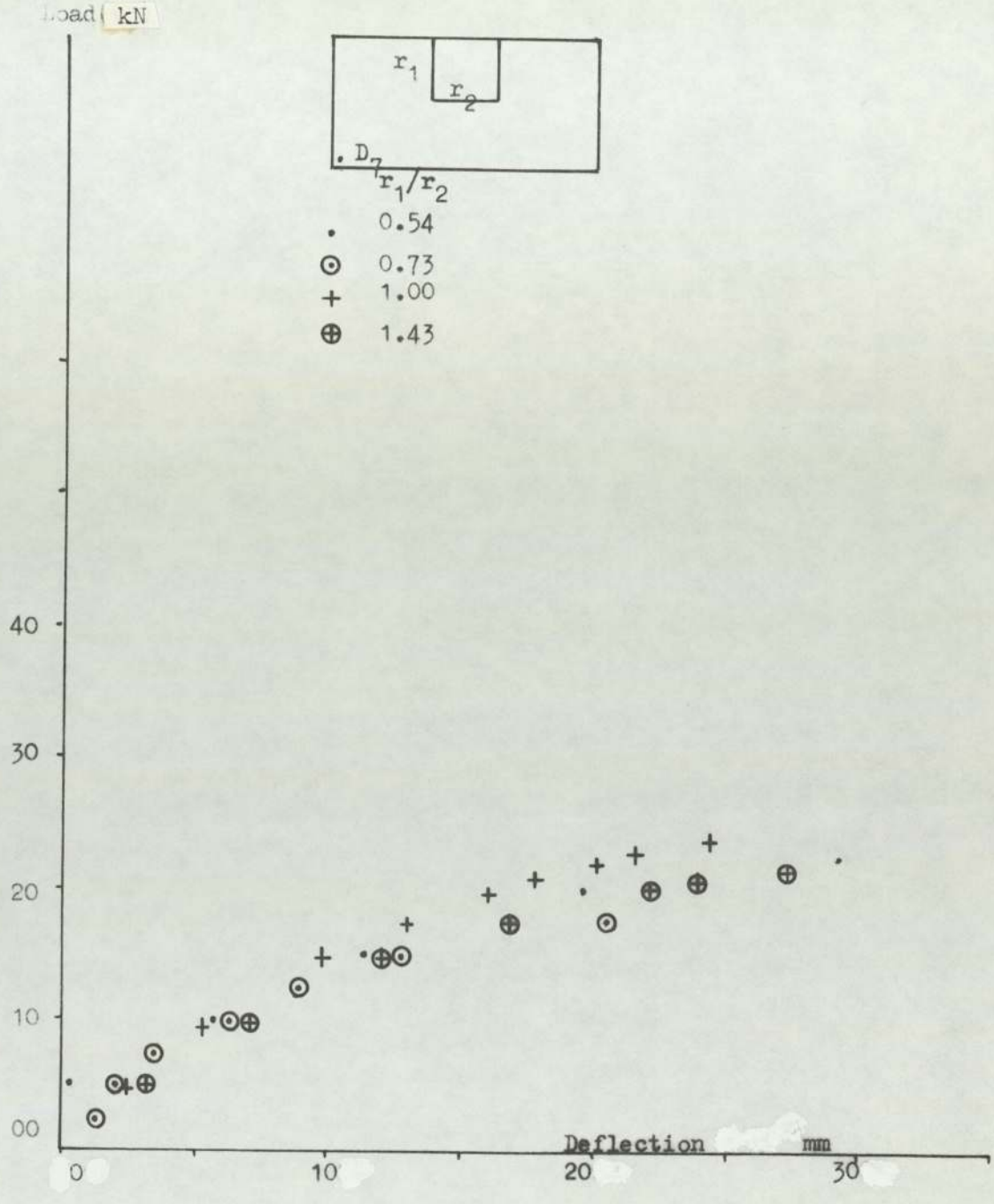

Fig. 4.13(b) **Load-deflection curve at D_7** (slab size 800mm x 1200mm)

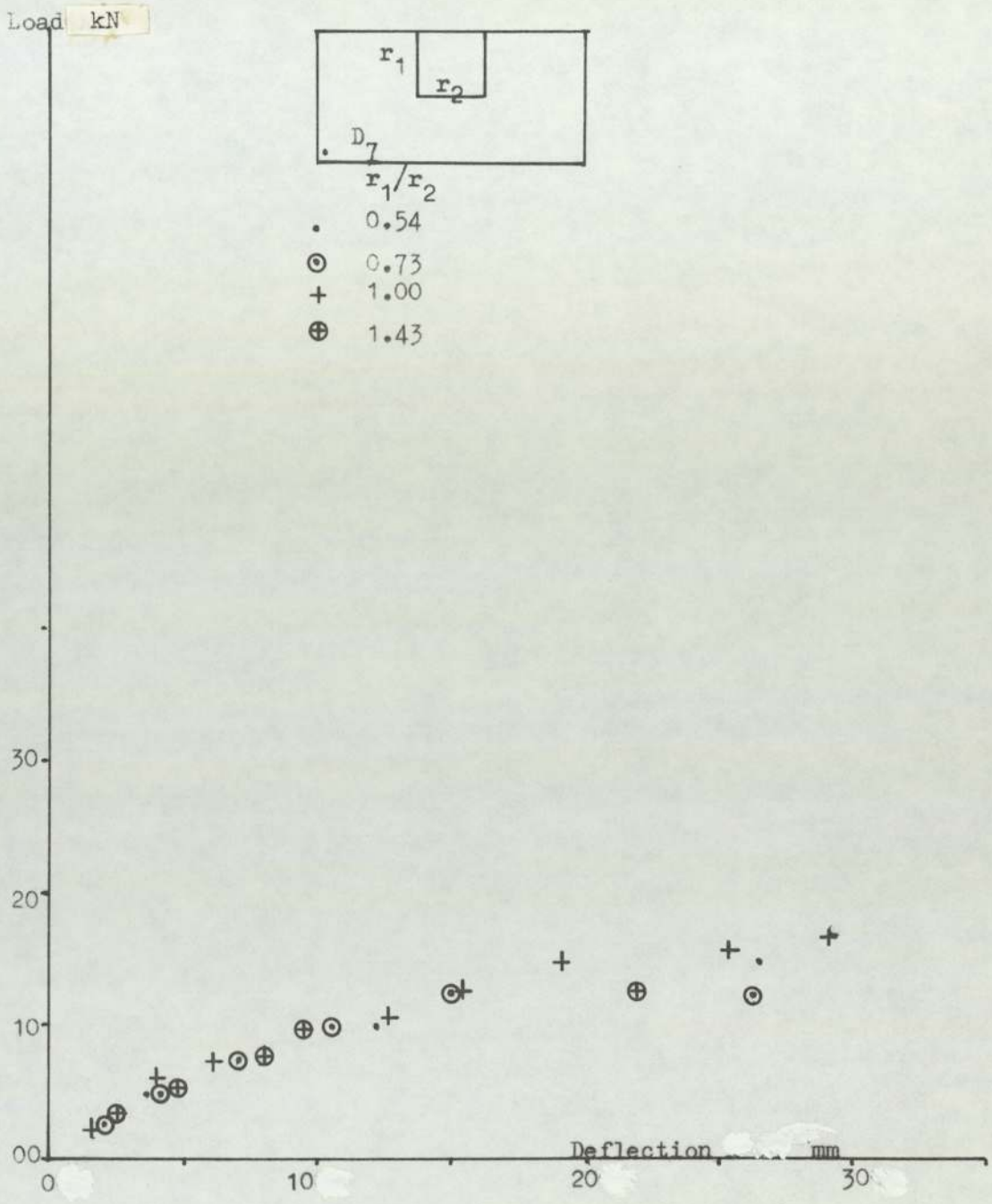

Fig. 4.13(c) Load-deflection curve at D_7 (slab size 1000 x 1200mm)

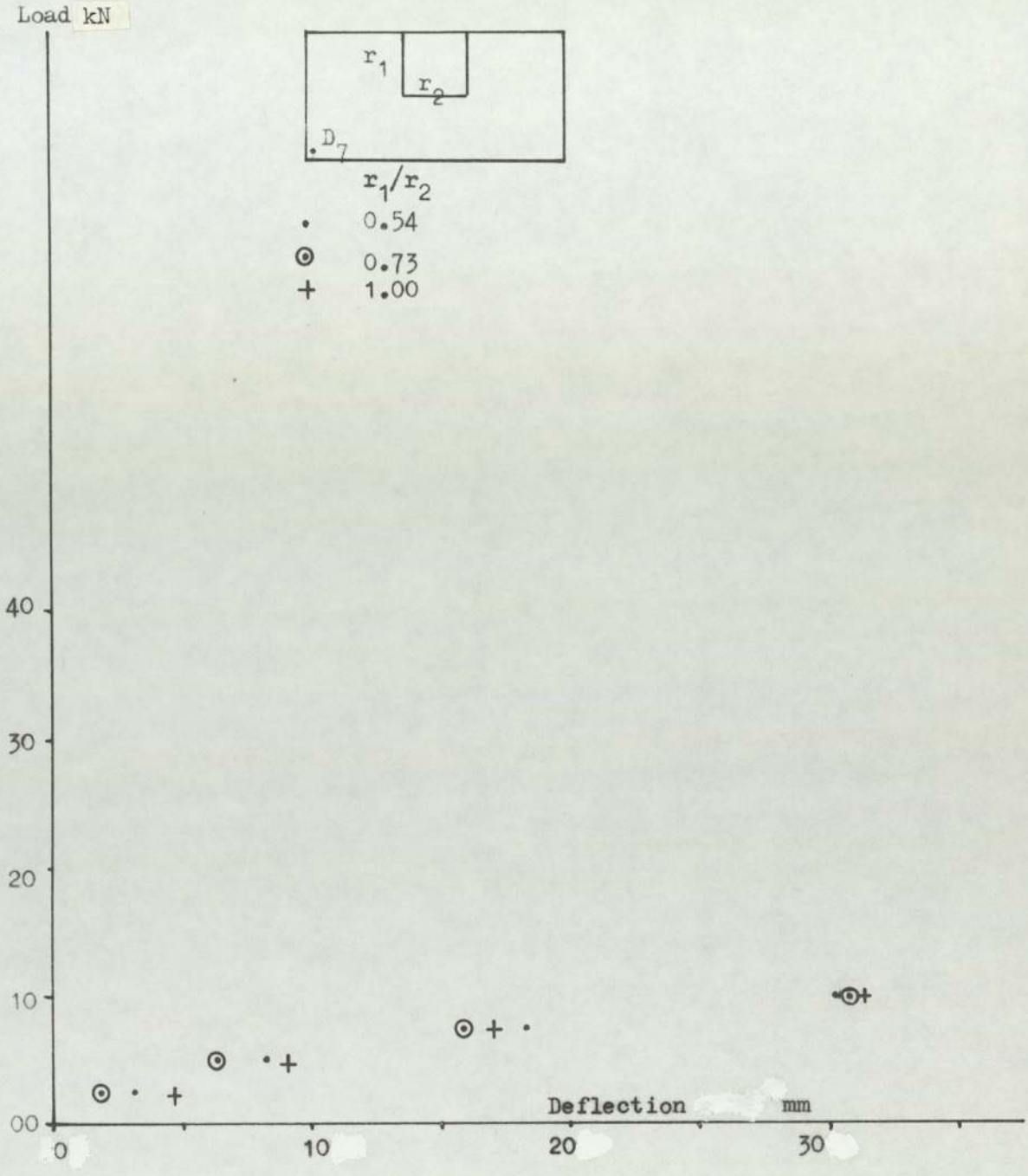

Fig. 4.13(d) Load-deflection curve at D_7 (slab size 1200mm x 1200mm)

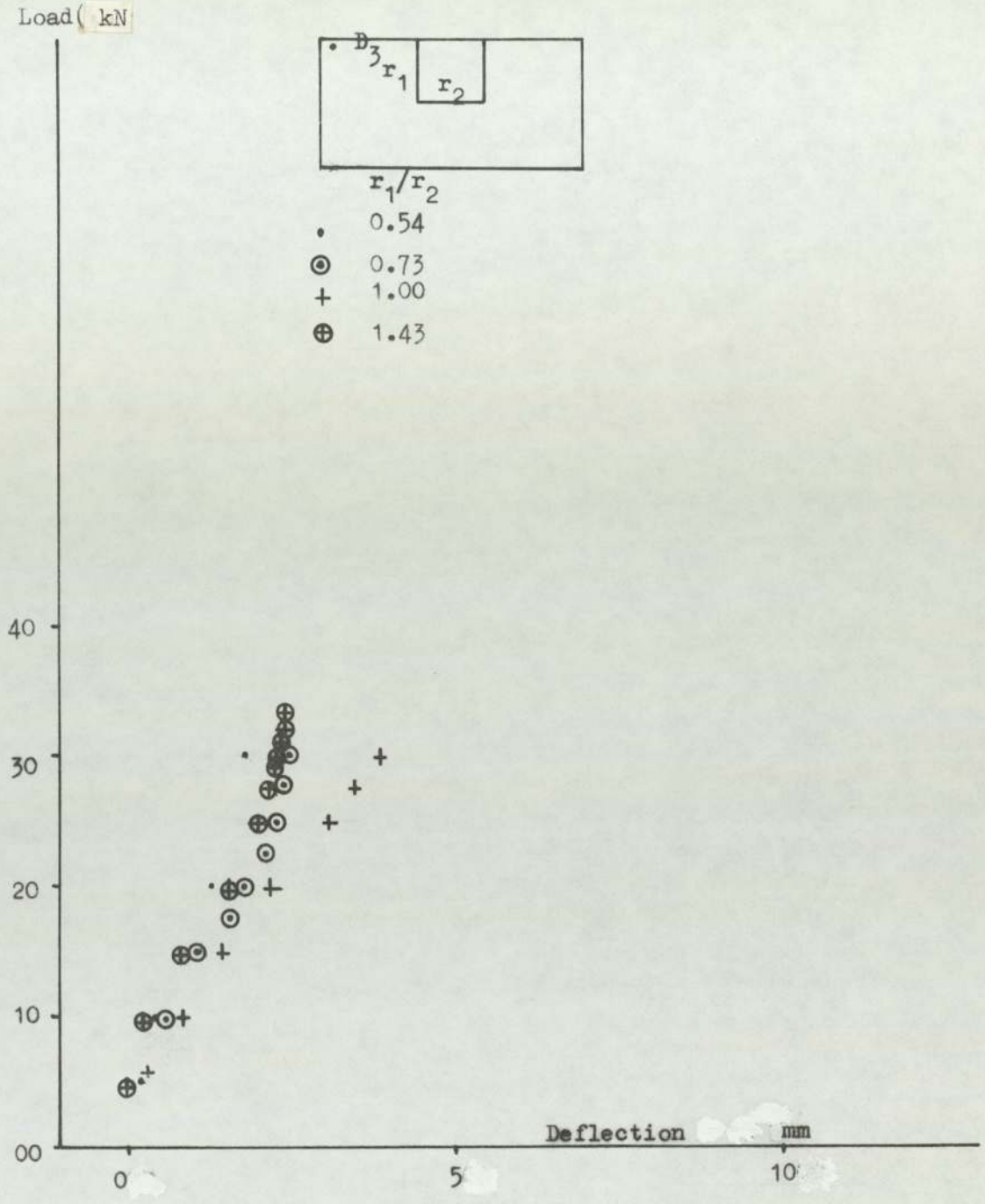

Fig. 4.14(a) Load-deflection curve at D_3 (slab size 600mm x 1200mm)

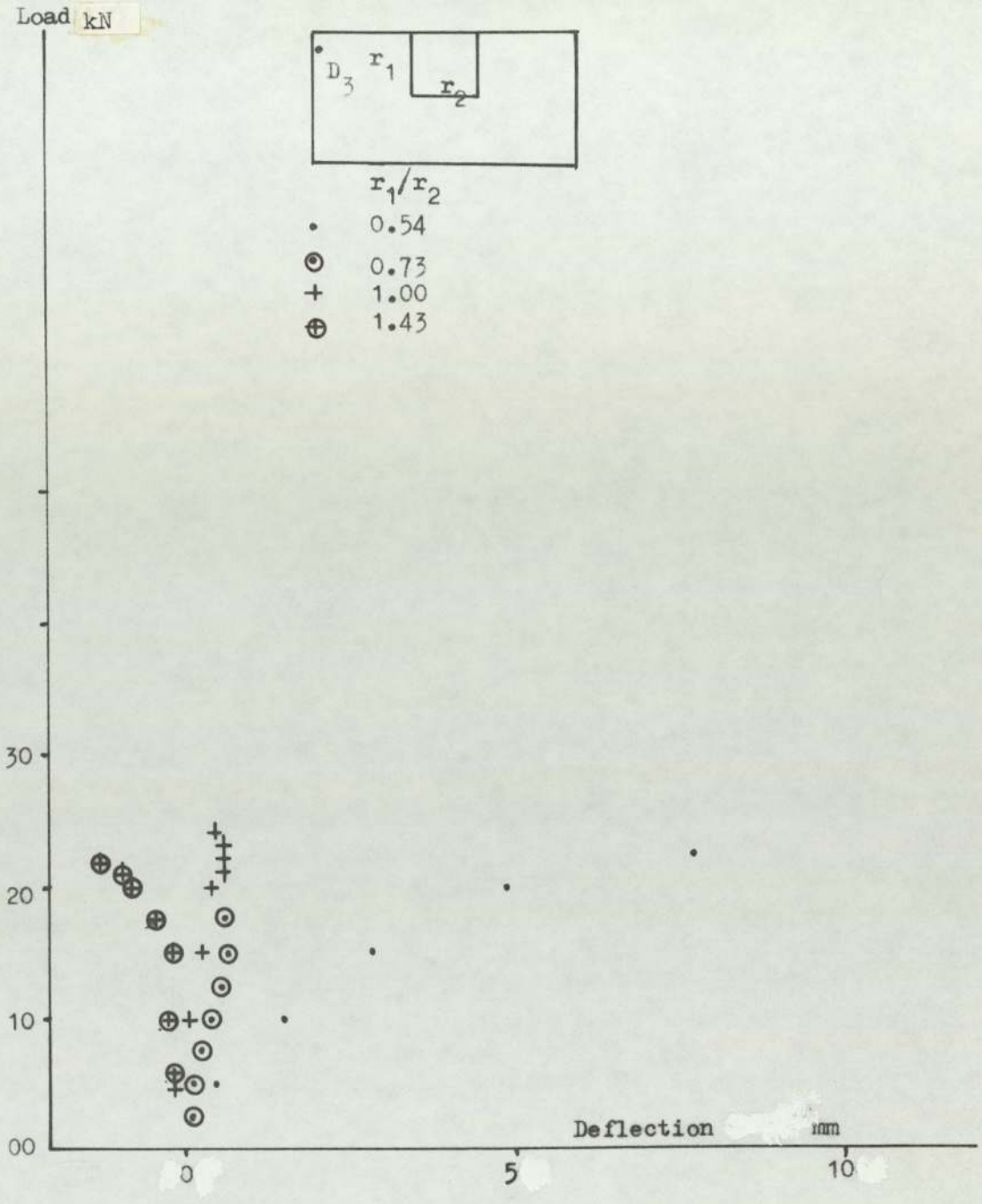

Fig. 4.14(b) Load-deflection curve at D_3 (slab size 800mm x 1200mm)

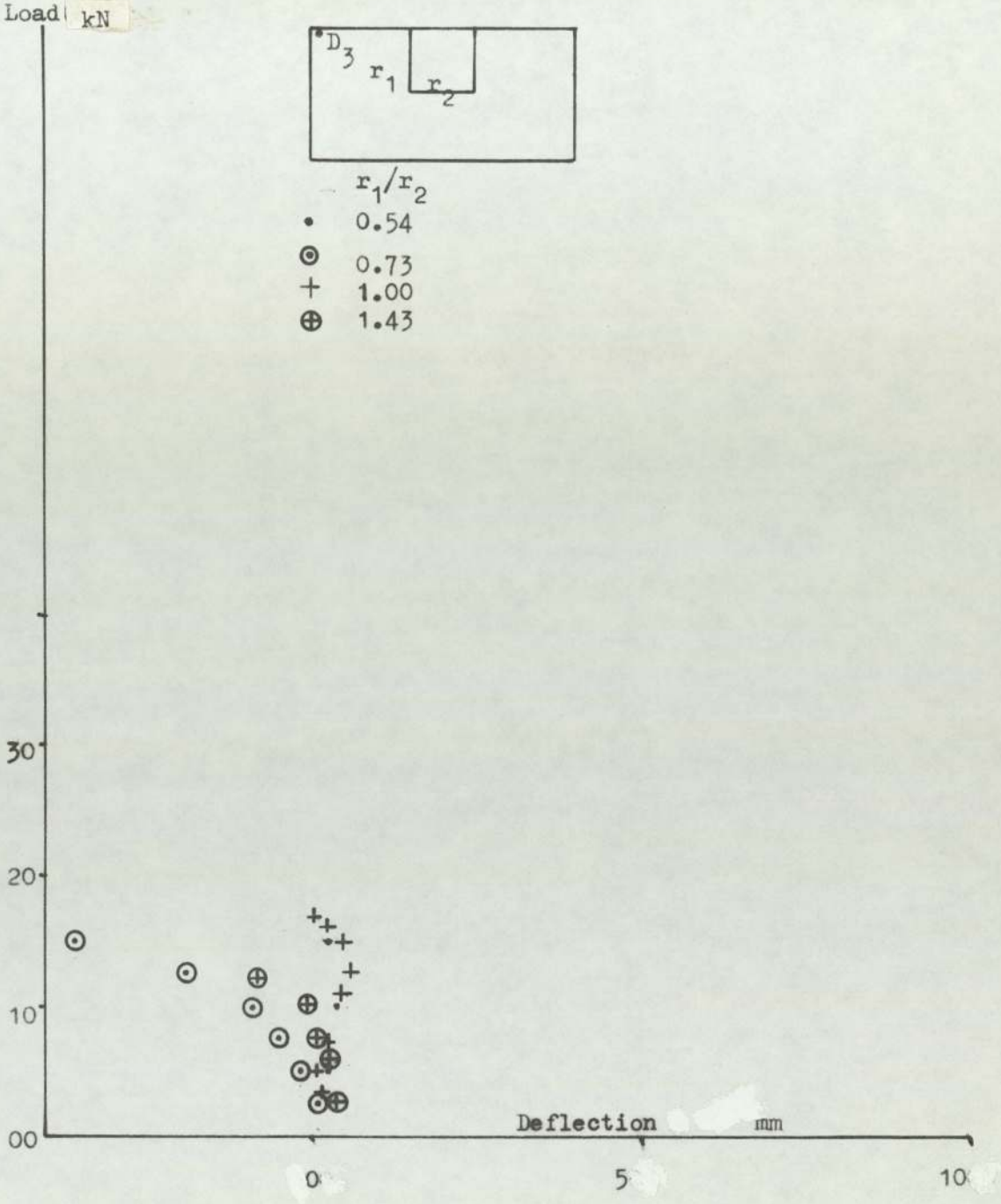

Fig. 4.14(c) Load-deflection curve at D_3 (slab size 1000mm x 1200mm)

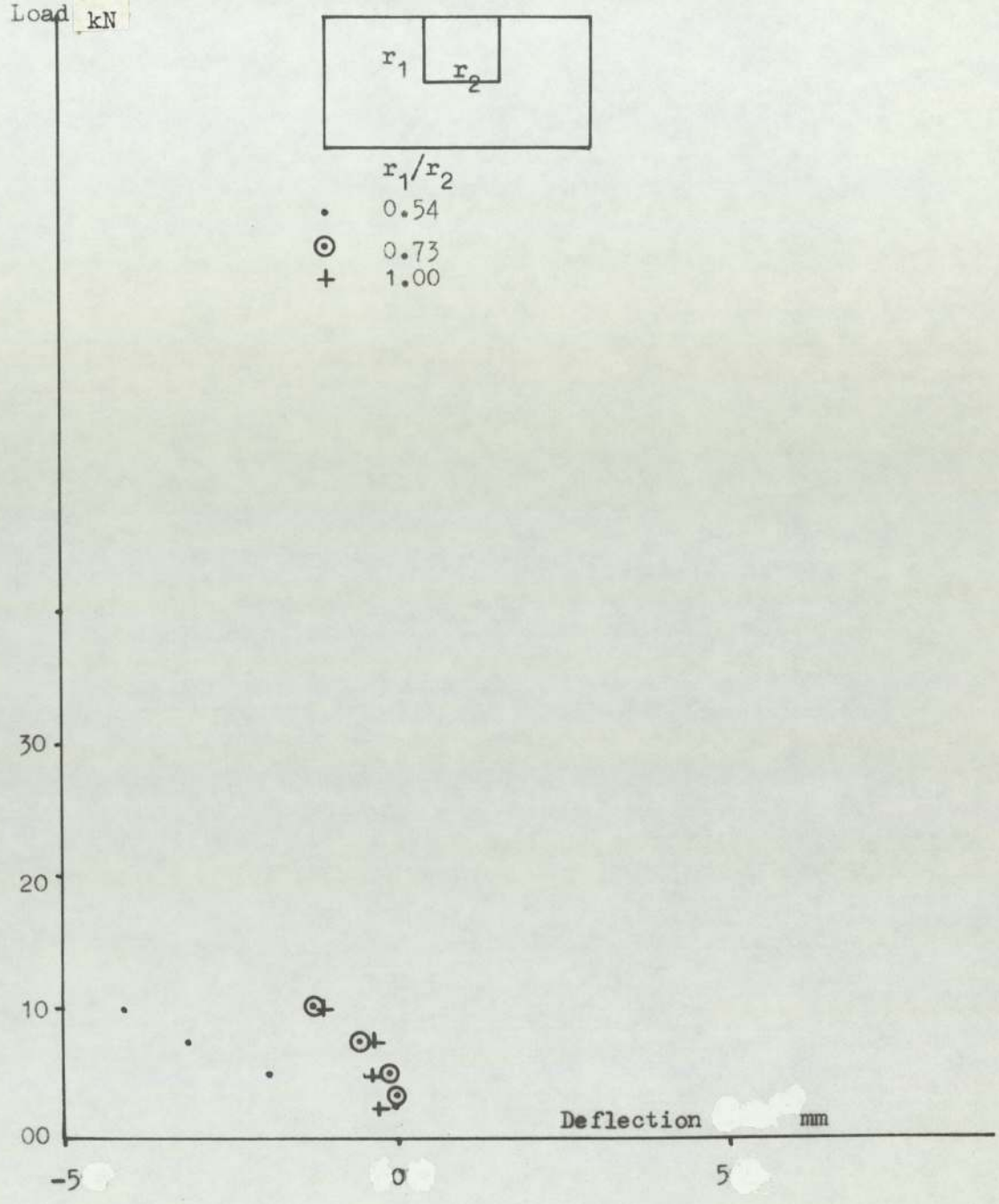

Fig. 4.14(D) Load-deflection curve at D_3 (slab size 1200mm x 1200mm)

locations throughout the slab for all specimens, (see Figs. 4.8 to 4.11). Representative load-deflection curves for the connections tested in the present investigation are given in Figs. 4.12 (a-d), 4.13 (a-d) and 4.14 (a-d). These figures are for displacements in different locations as shown in the key sketch in each figure.

In Fig. 4.15 the r_1/L ratio is plotted against deflections for three positions of dial gauges, D_3, D_7 and D_{13} measured at a load level of 10 KN.

Deflected shape curves at a load level of about 90 percent of ultimate capacity and at cracking load for different lines on the edges and centre line of the slab are given in Figs. 4.18 to 4.29. The arrangements of the dial gauges for all specimens tested are shown in Figs. 4.8 to 4.11. The indicated deflections are for the last readings of the dials taken before failure.

As shown in Fig. 4.12 (a-d) - which are the load-deflection curves of D_{13} - the influence of r_1/r_2 ratio seems to be small for all slabs and is hardly noticeable for long spans.

In Fig. 4.13 (a-d) for D_7, there is no very significant effect of the variables on the deflection of the slab at that point.

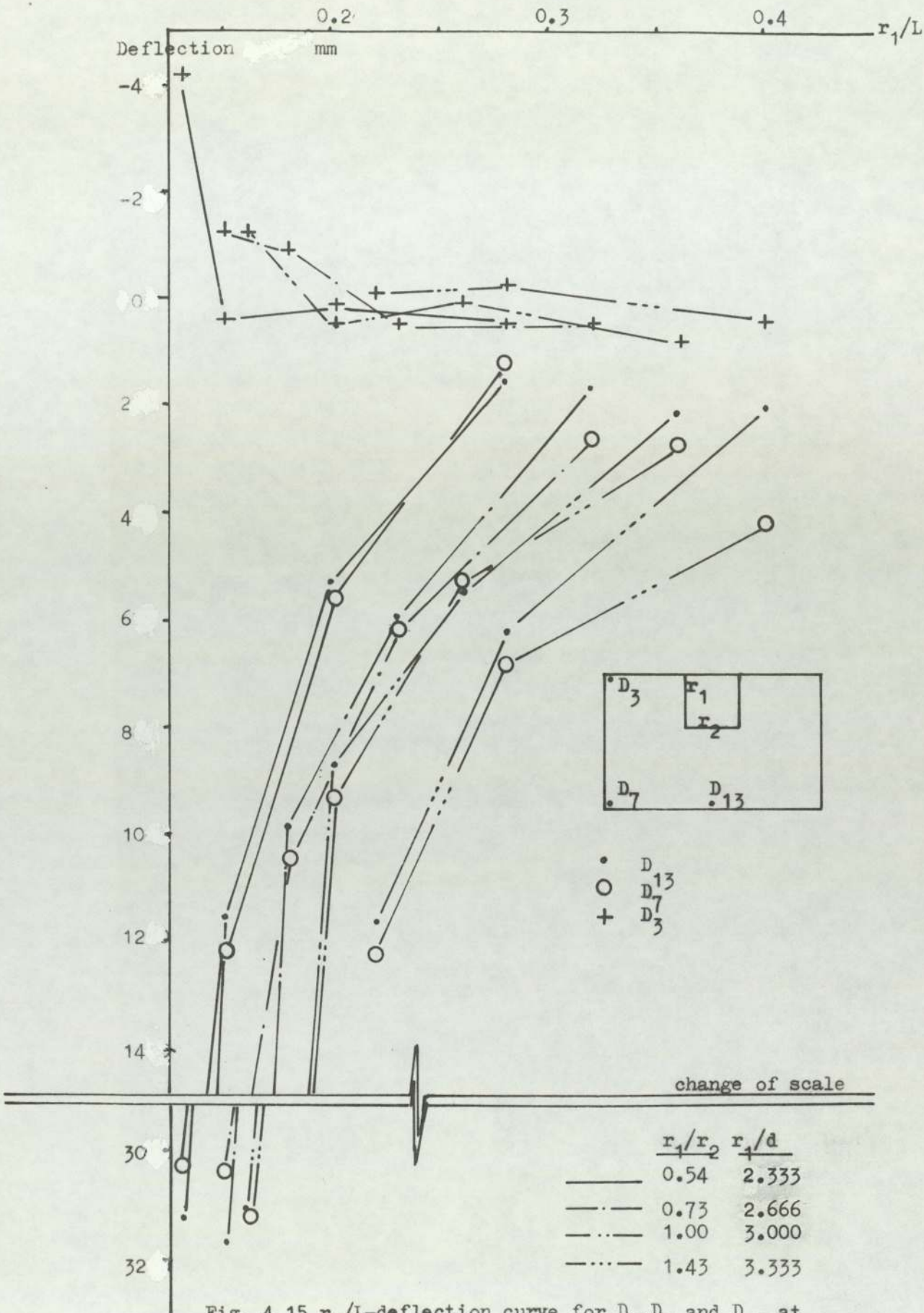

Fig. 4.15 r_1/L-deflection curve for D_3, D_7 and D_{13} at load of 10KN

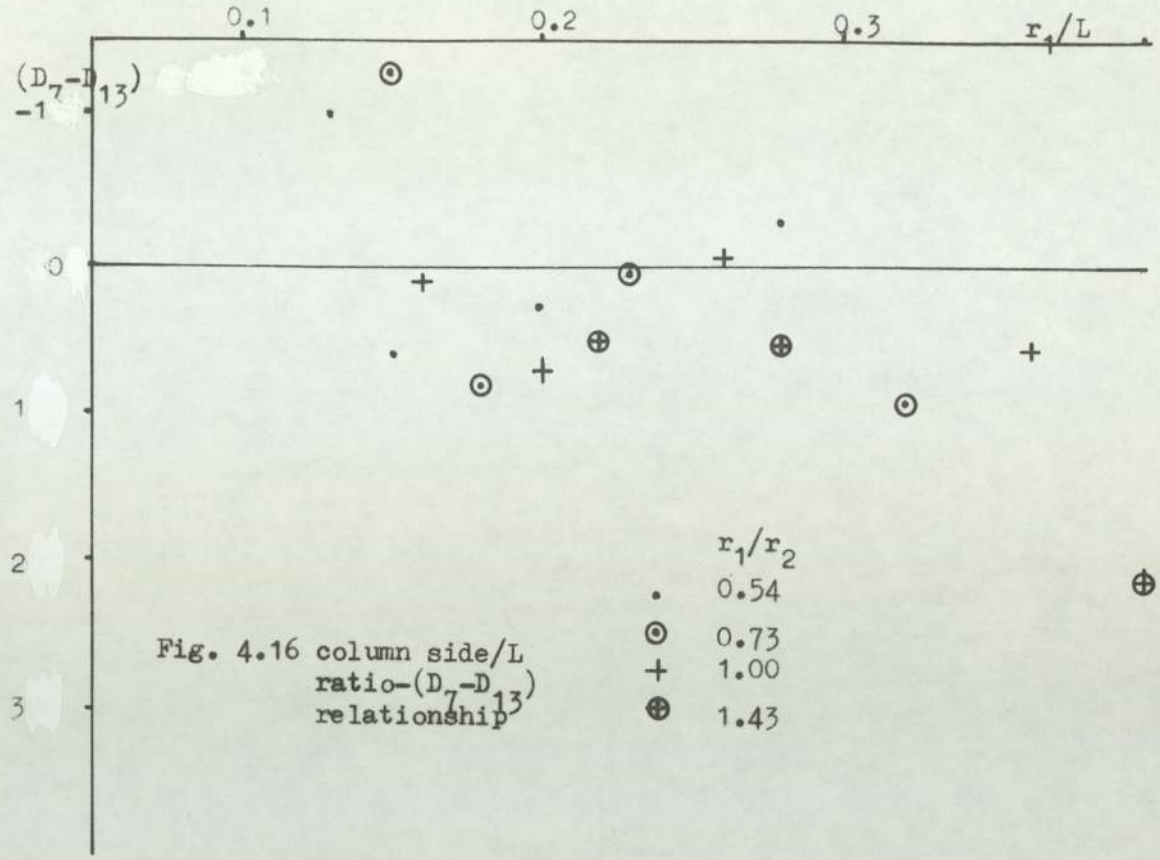

Fig. 4.16 column side/L ratio-(D_7-D_{13}) relationship

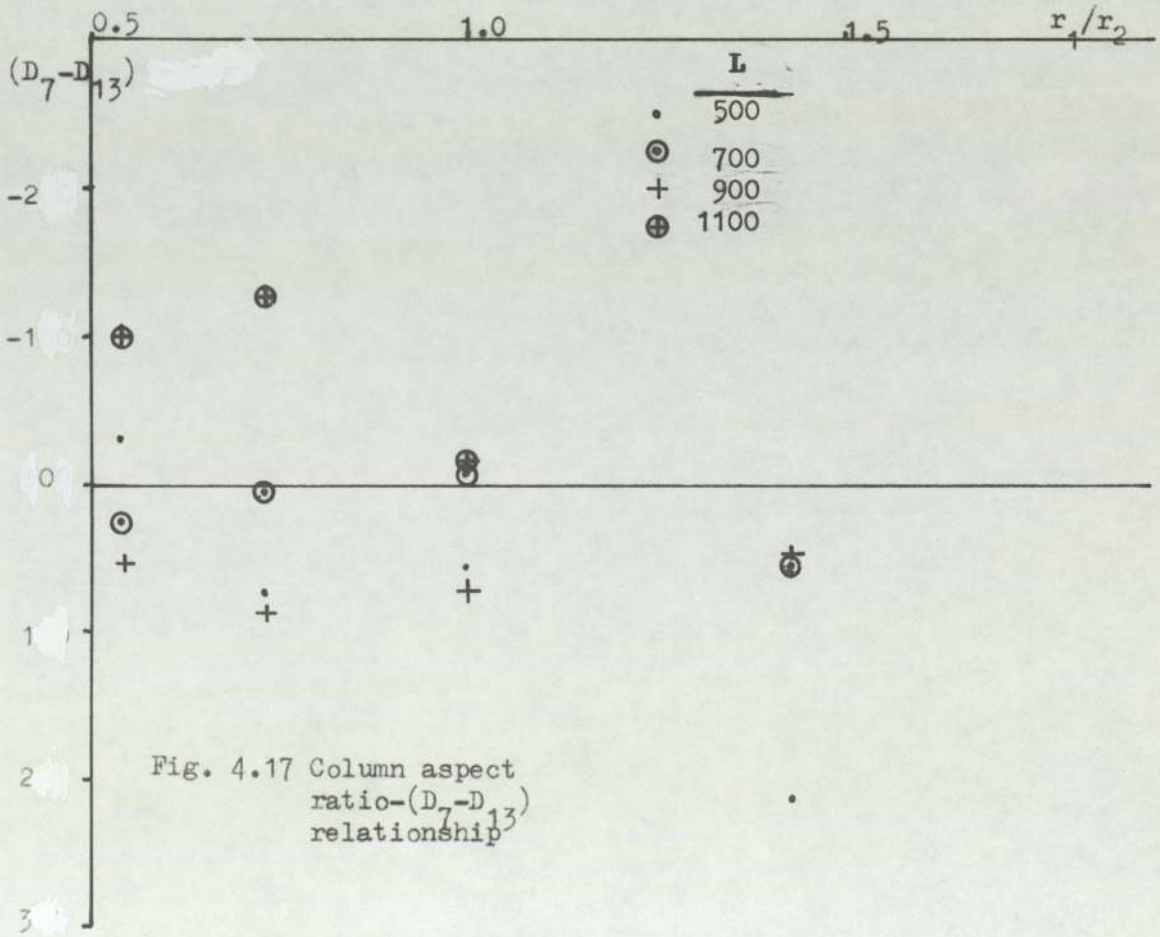

Fig. 4.17 Column aspect ratio-(D_7-D_{13}) relationship

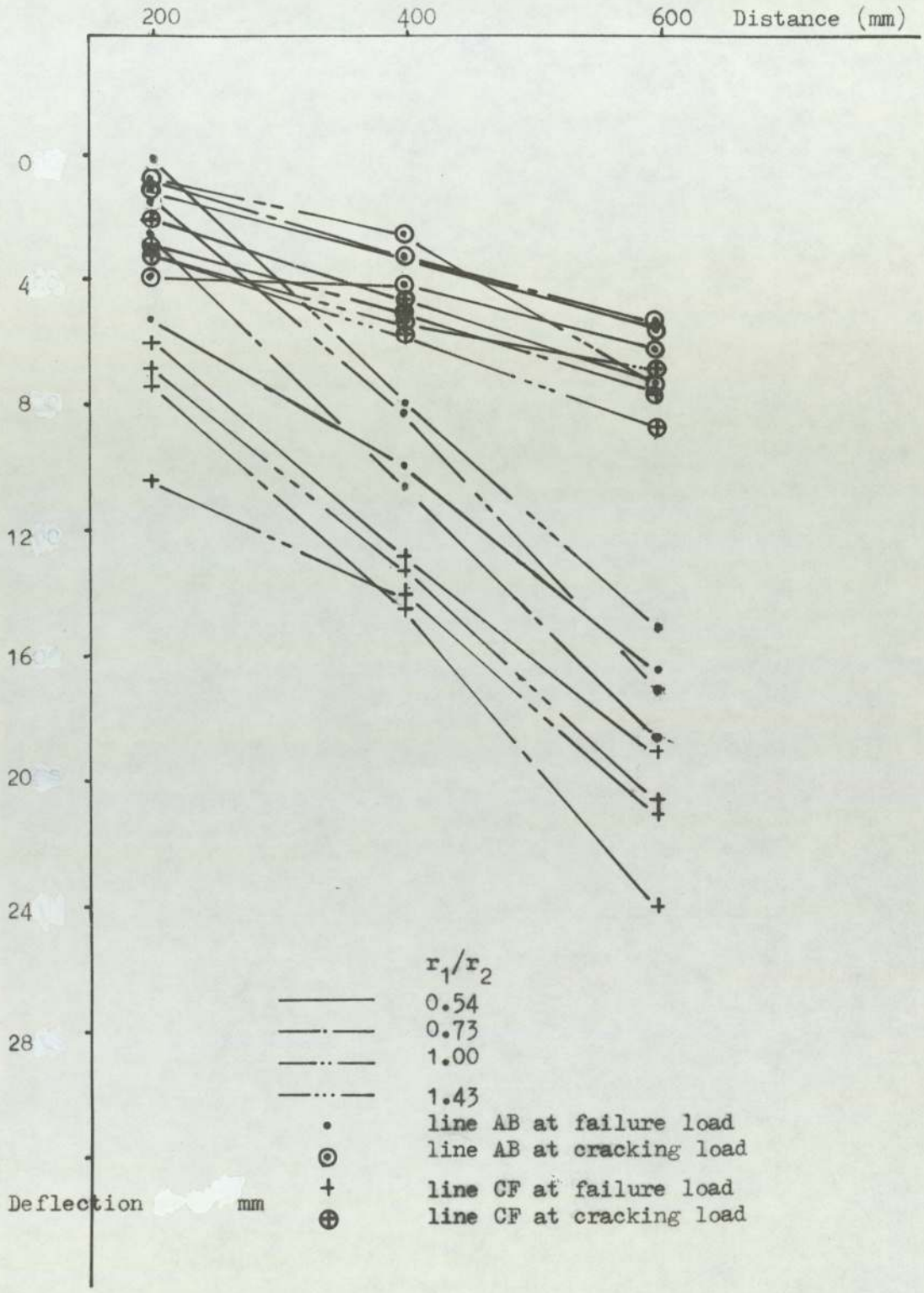

Fig. 4.18 Distance-deflection curve (slab size 600mm x 1200mm) for lines AB and CF

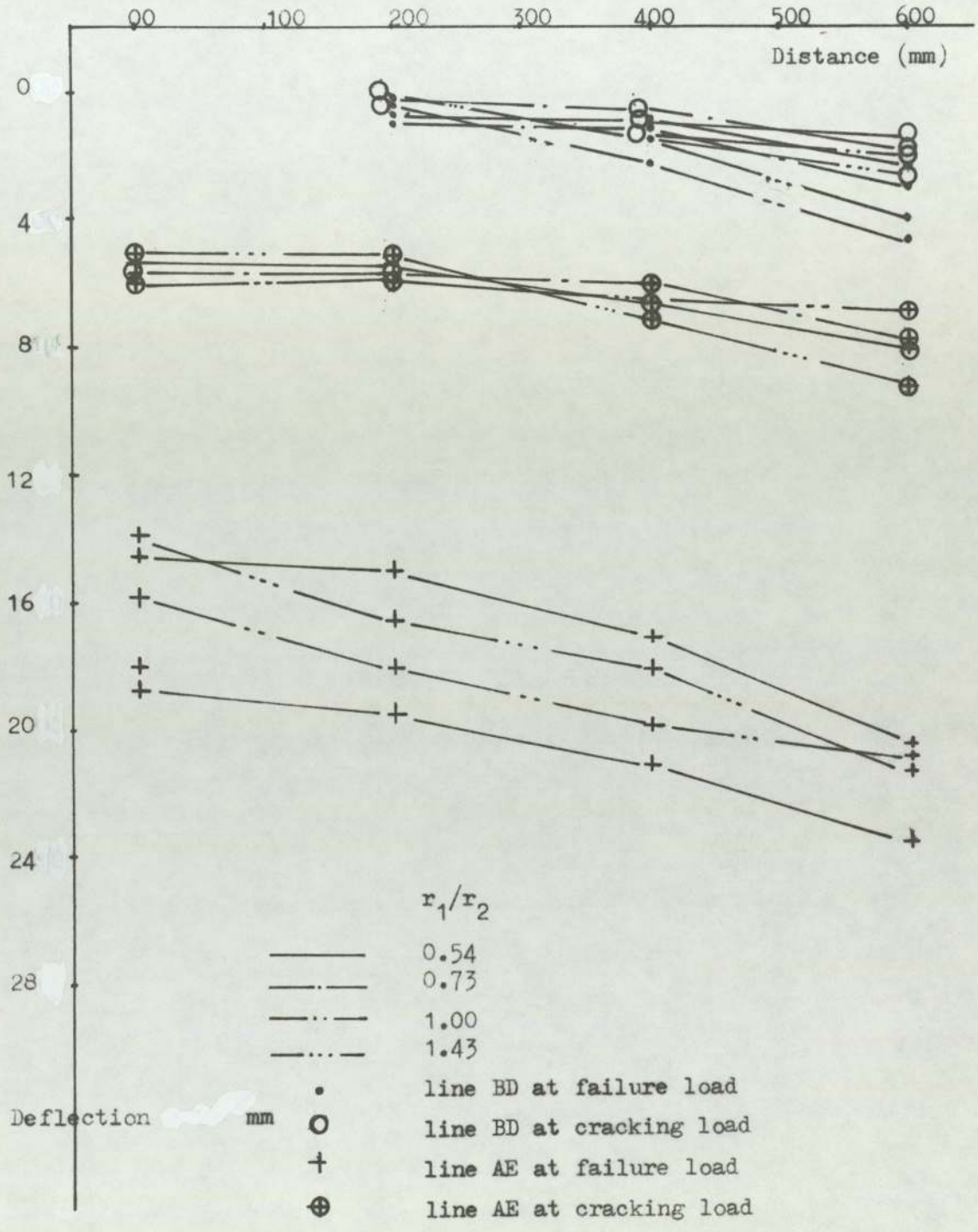

Fig. 4.19 Distance-deflection curve (slab size 600mm x 1200mm) for lines BD and AE

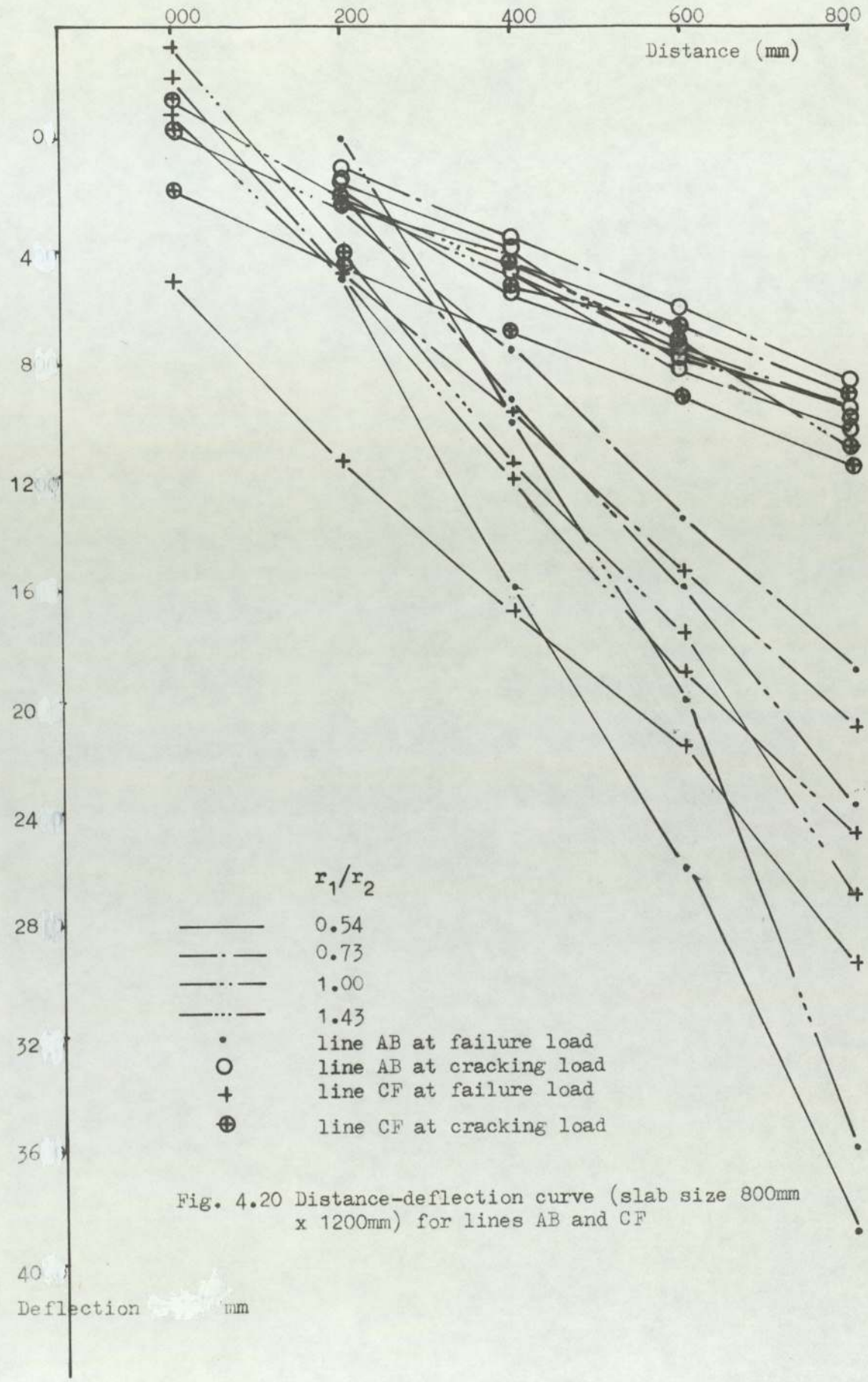

Fig. 4.20 Distance-deflection curve (slab size 800mm x 1200mm) for lines AB and CF

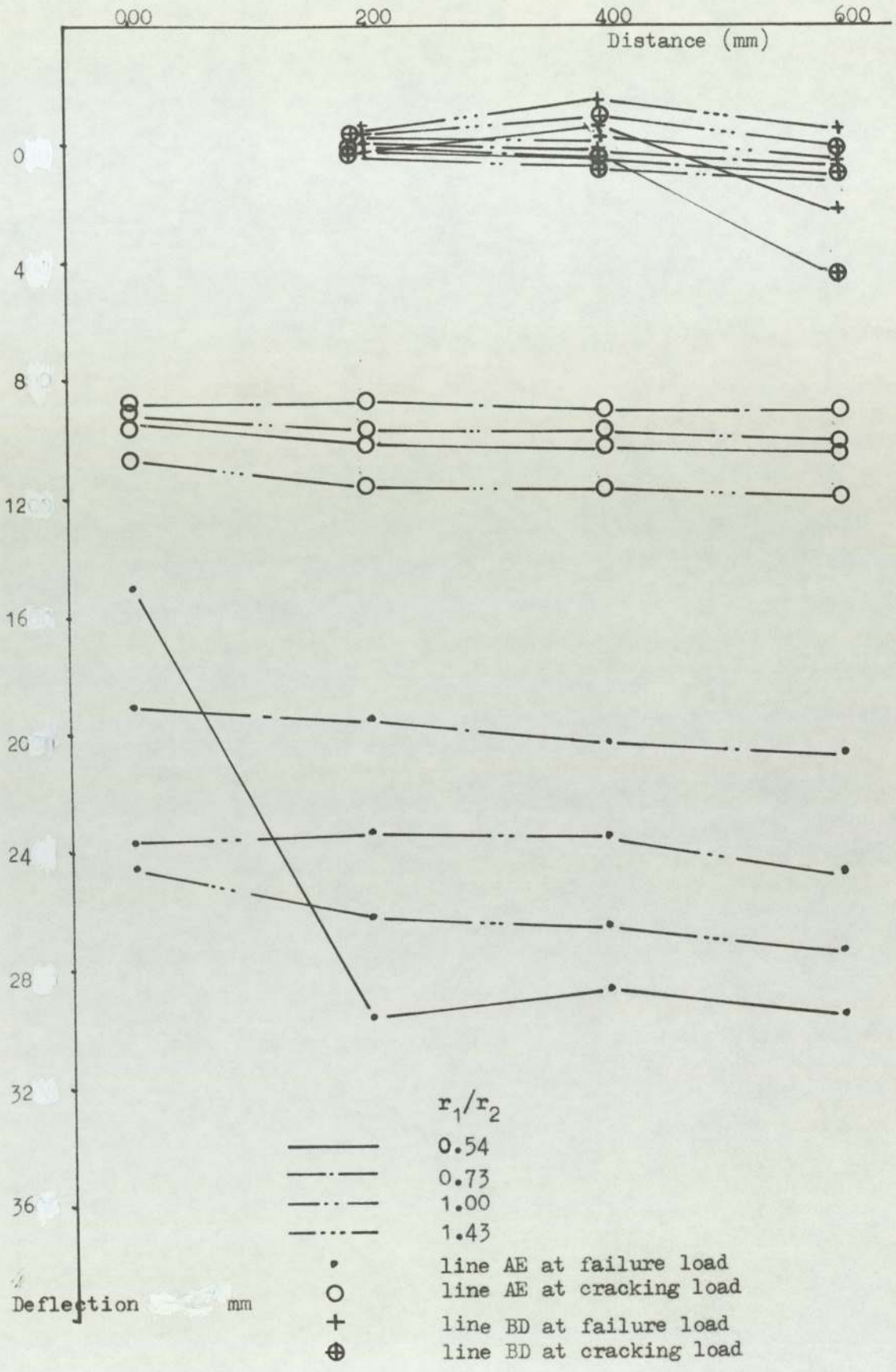

Fig. 4.21 Distance-deflection curve (slab size 800mm x 1200mm) for lines AE and BD

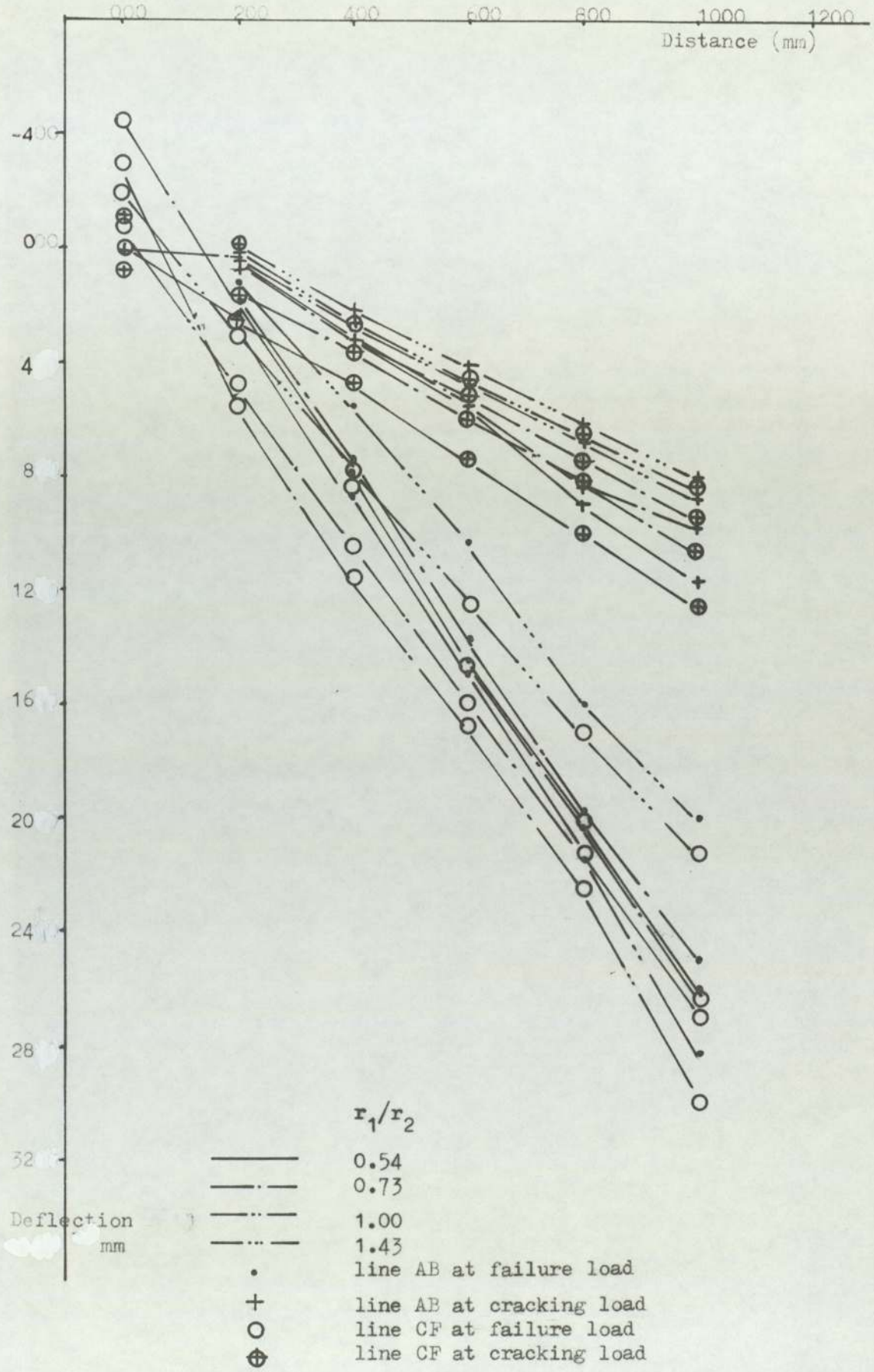

Fig. 4.22 Distance-deflection curve (slab size 1000mm x 1200mm) for lines AB and CF

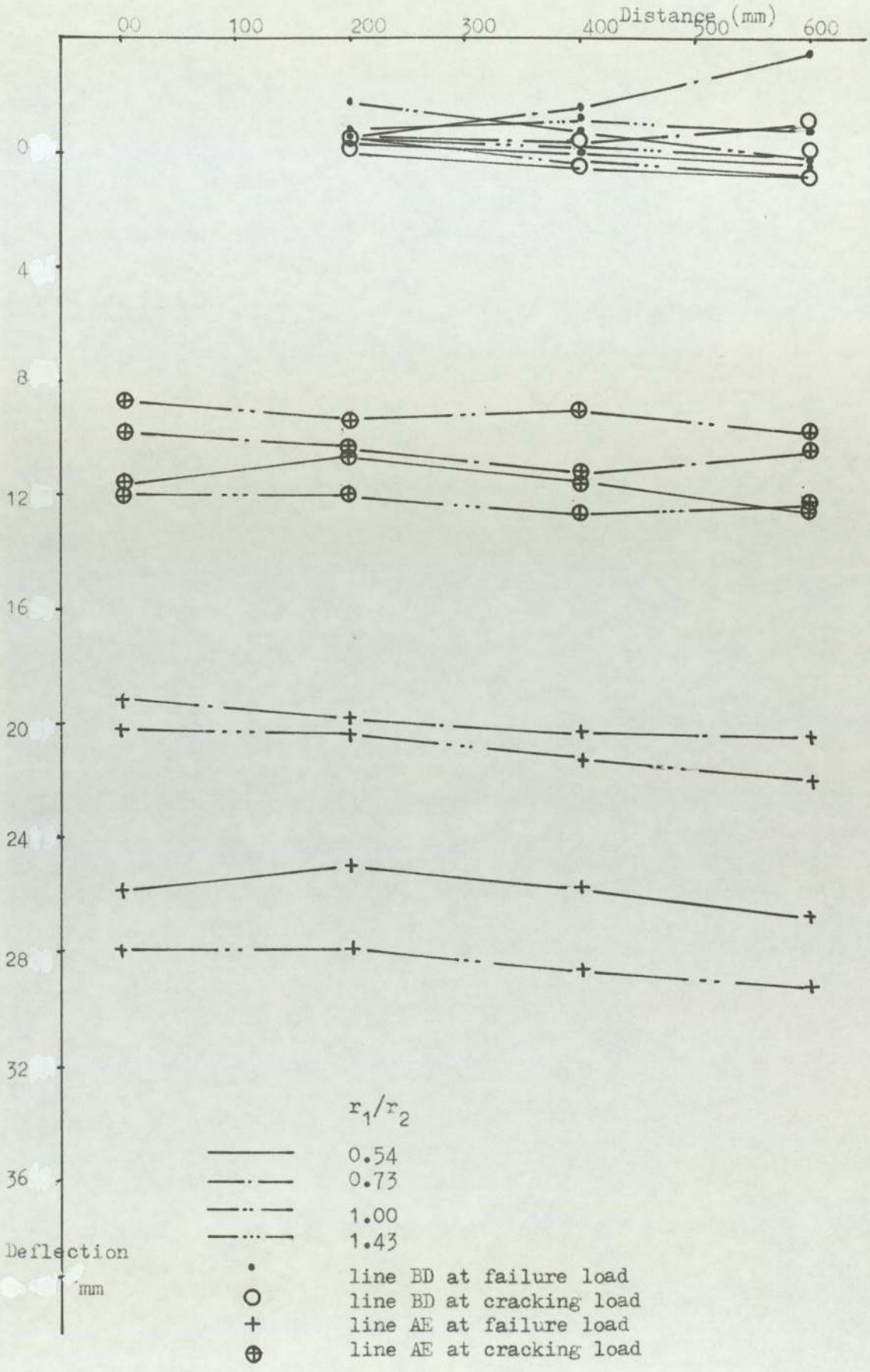

Fig. 4.23 Distance deflection curve (slab size 1000mm x 1200mm) for lines BD and AE

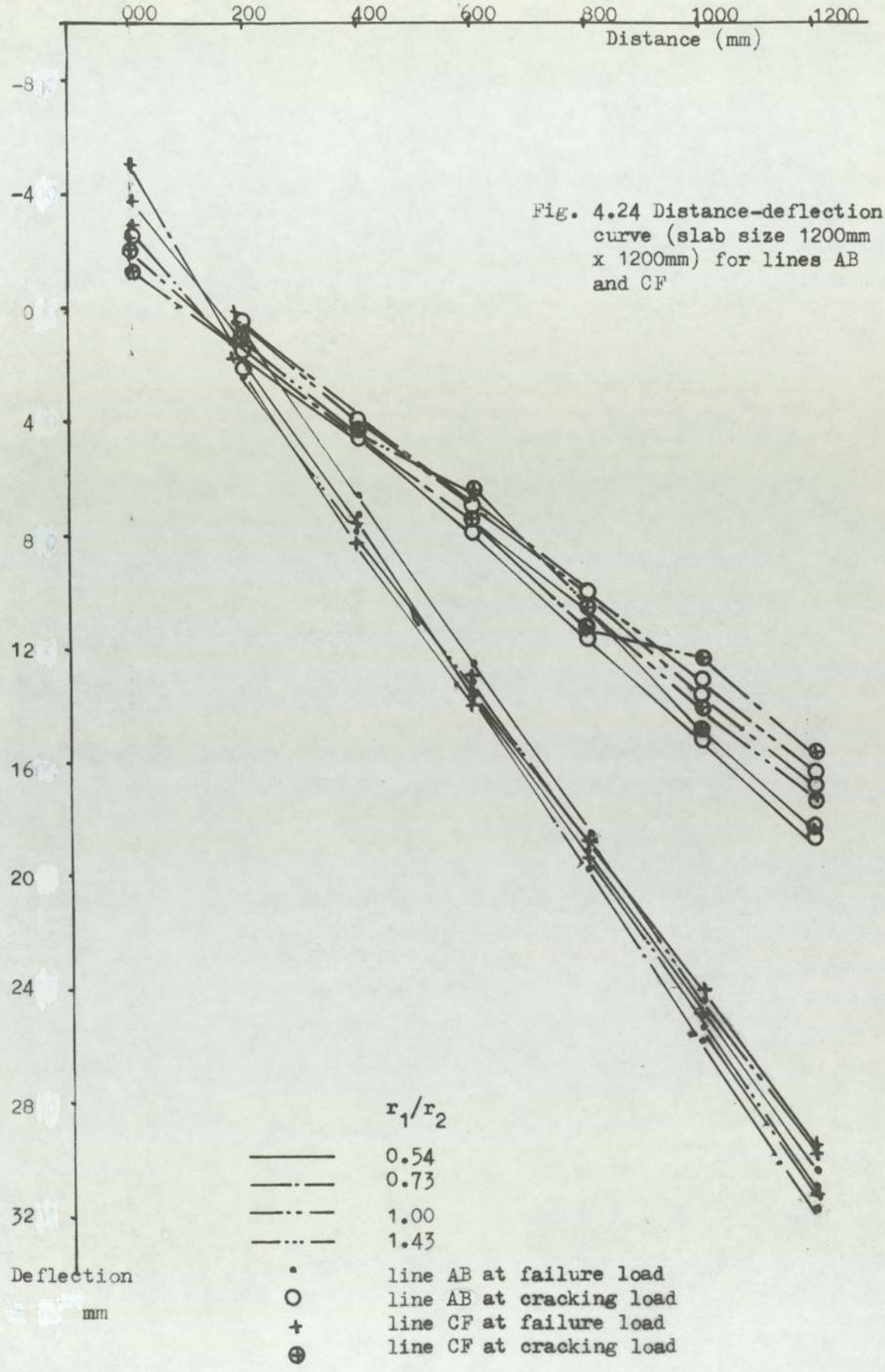

Fig. 4.24 Distance-deflection curve (slab size 1200mm x 1200mm) for lines AB and CF

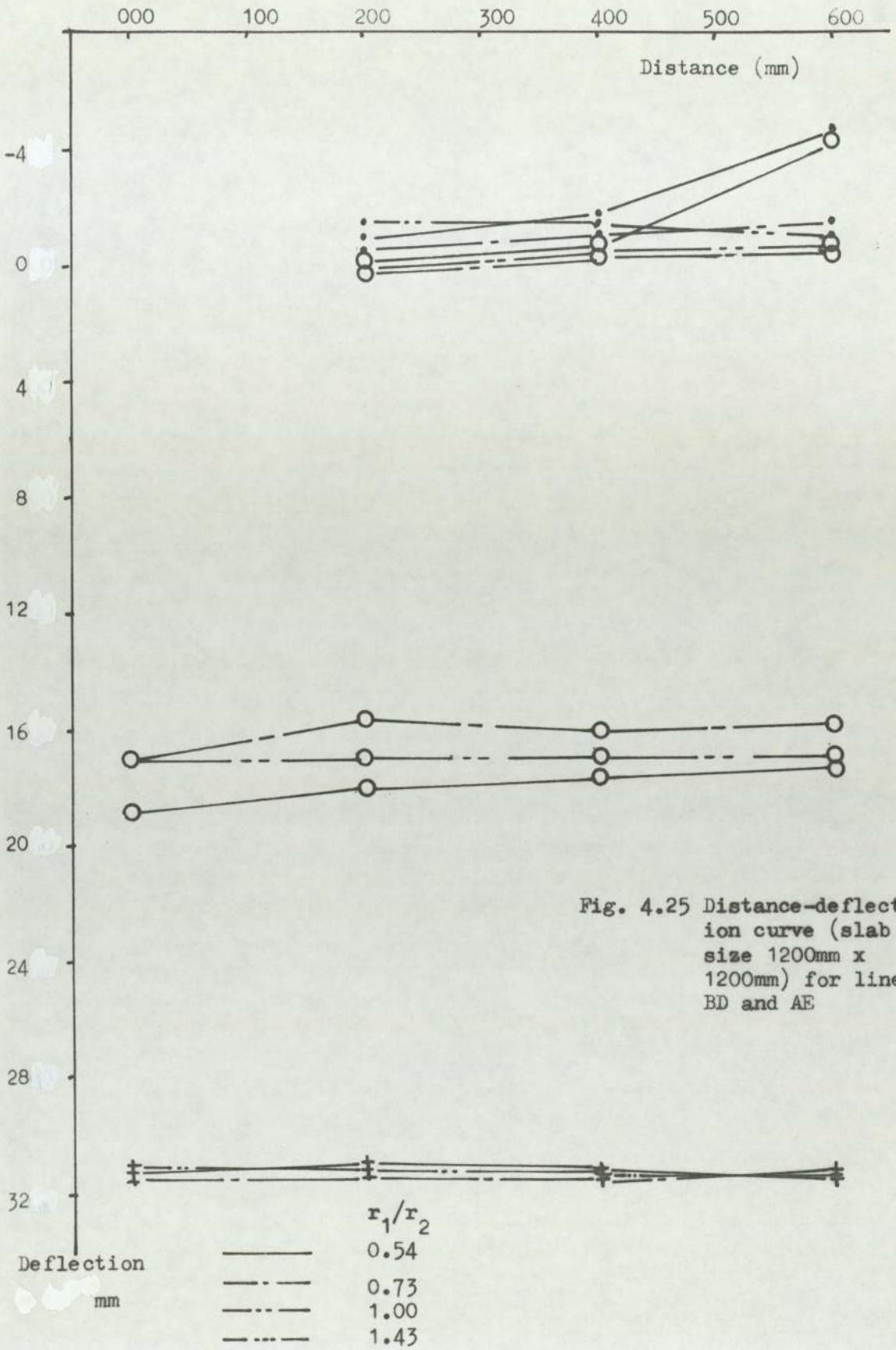

Fig. 4.25 Distance-deflection curve (slab size 1200mm x 1200mm) for lines BD and AE

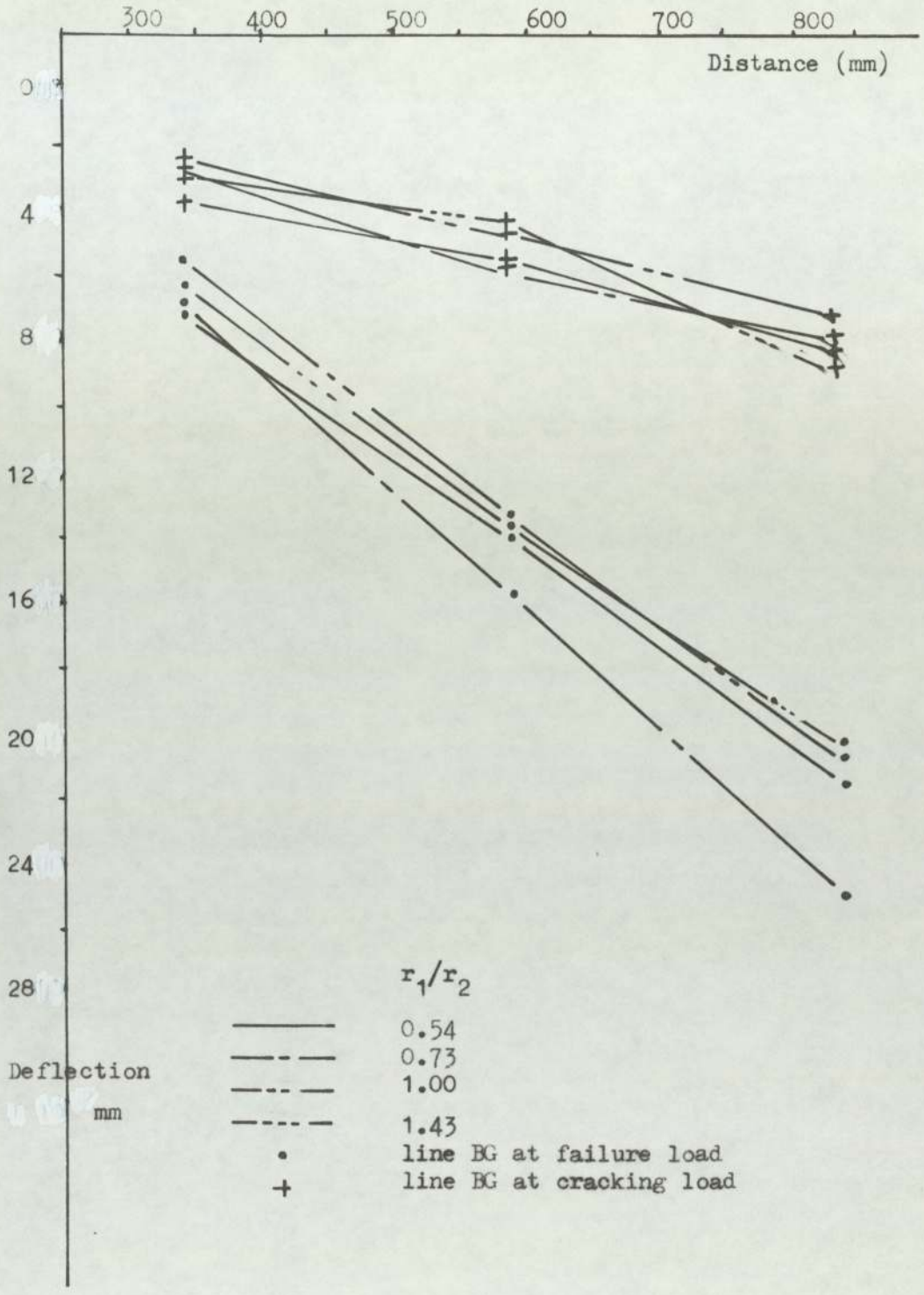

Fig. 4.26 Distance-deflection curve (slab size 600mm x 1200mm) for line BG

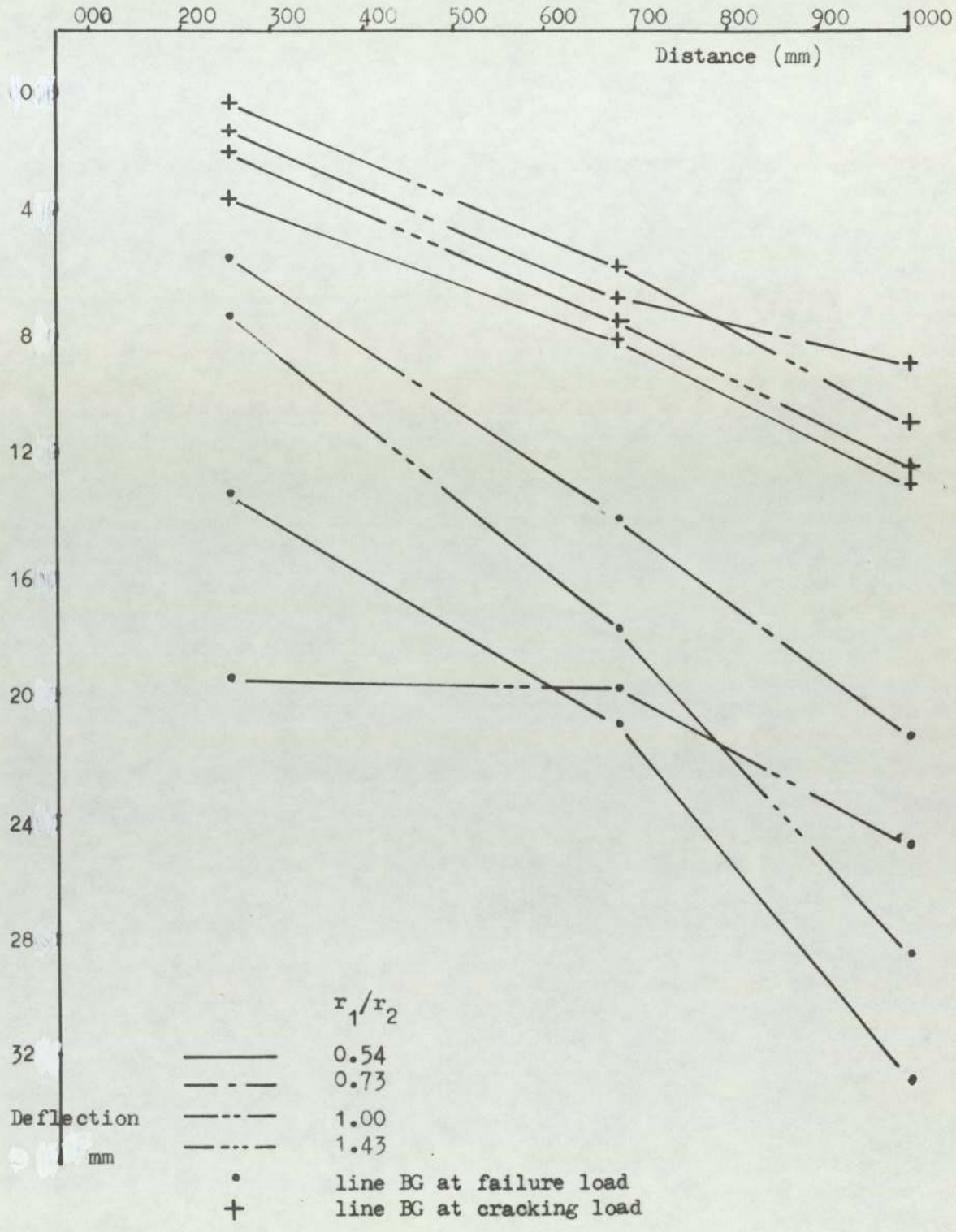

Fig. 4.27 Distance-deflection curve (slab size 800mm x 1200mm) for line BG

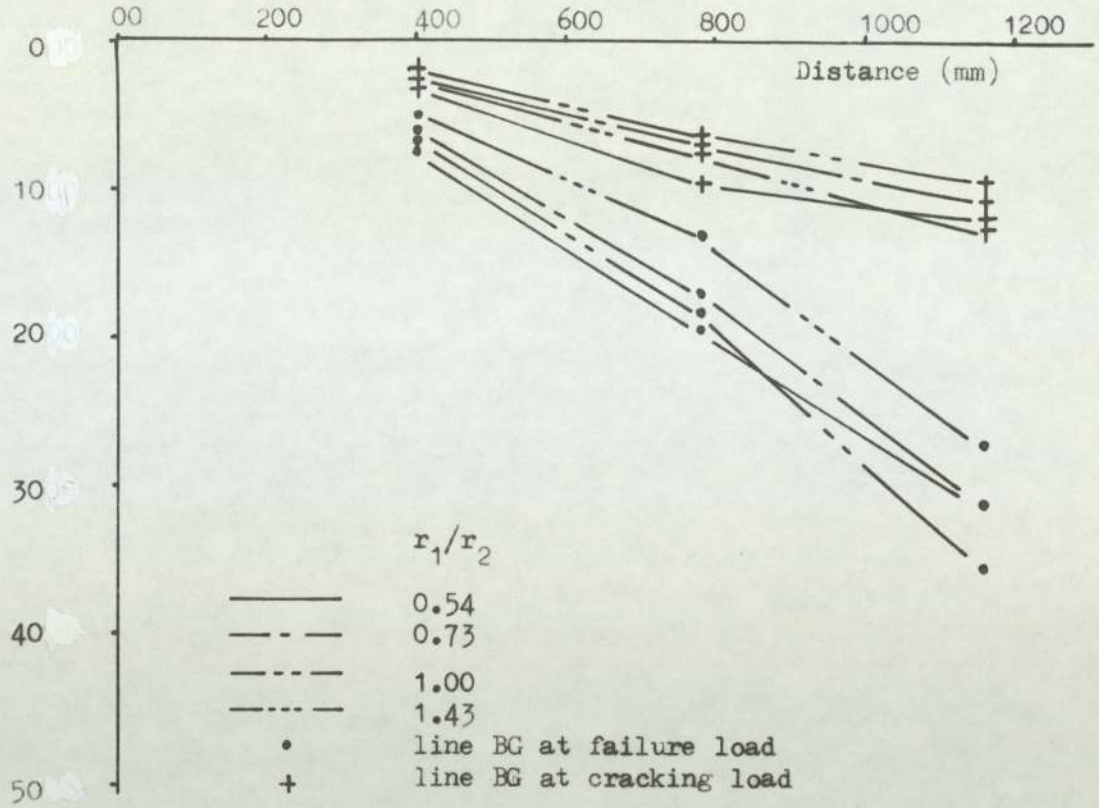

Fig. 4.28 Distance-deflection curve (slab size 1000mm x 1200mm) for line BG

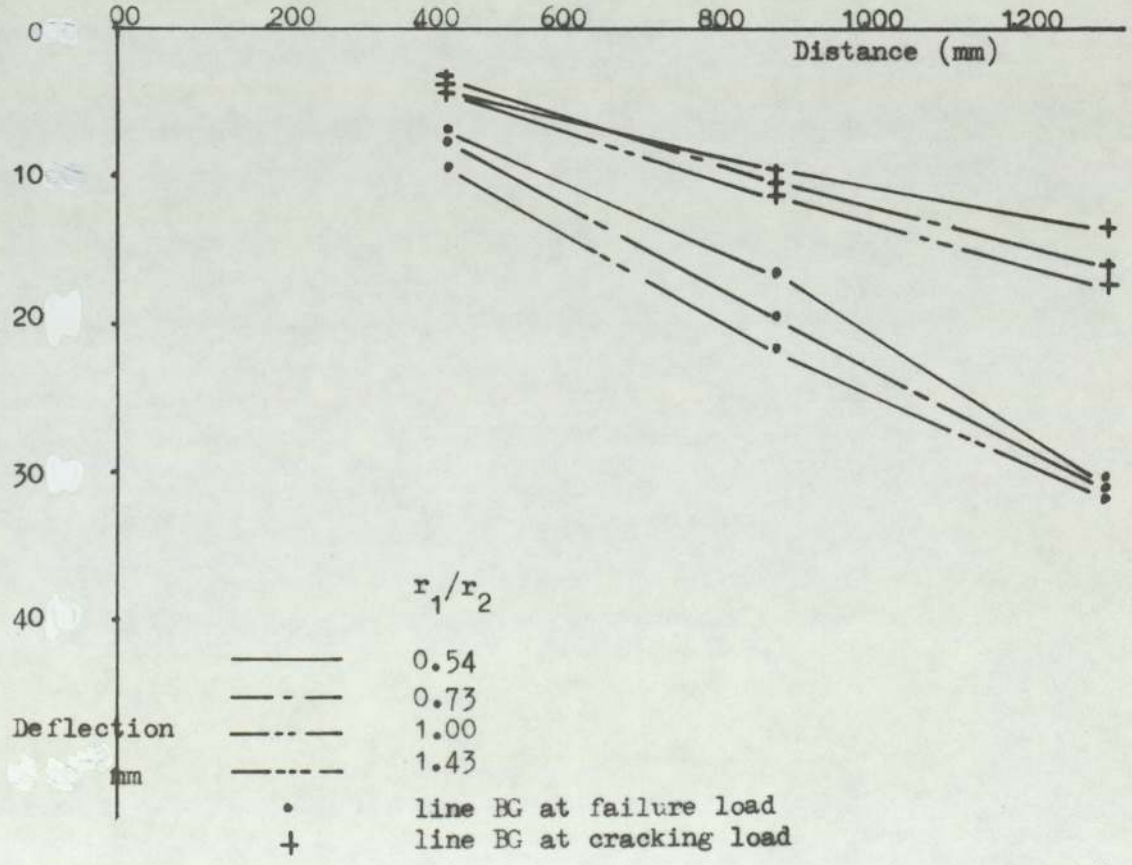

Fig. 4.29 Distance-deflection curve (slab size 1200mm x 1200mm) for line BG

In Fig. 4.14 (a-d) the deflection of D_3 becomes upward at this point for slabs with longer spans rather than for short spans.

The effect of varying r_1/L is also shown in Fig. 4.15 for the deflections D_{13}, D_7 and D_3. As shown in this figure, as r_1/L ratio increased the deflection at D_{13} and D_7 decreased. This deflection (at D_{13} and D_7) becomes very high for small values of r_1/L ratio, while there is no significant effect of r_1/L on the deflection at D_{13} except in the case where r_1/L ratio is less than 0.2, where the deflection becomes upwards and noticeable.

The effects of r_1/L, r_1/d and r_1/r_2 are also shown in Figs. 4.16 and 4.17. In these figures r_1/L and r_1/r_2 has been drawn against the difference between D_7 and D_{13}. As shown in these figures, $(D_7 - D_{13})$ seems to be increased slightly with the increase of r_1/L, r_1/d and r_1/r_2. This means that the difference between the positive moments in the column strip and middle strip of the flat plate increases with the increase of these variables and decreases with their decrease.

Deflected shape curves are shown in Figs. 4.18 to 4.29; Figs. 4.18, 4.20, 4.22 and 4.24 are for the deflection of the slab along lines AB and CF for two load levels. In these figures, as the length of the span increases the deflection of point C along line CF decreases and then

becomes upwards for longer spans. In this case high bending moments and then high torsion will take place on the connection. The differences between the deflections of the slab (at 90% of failure load) is clear for short spans. This difference is very small at cracking load.

In Figs. 4.19, 4.21, 4.23 and 4.25 the deflection of the slab along line BD at 90% of failure load and at cracking load are similar for all spans. These differences are hardly noticed for the deflection along line A E .

The effect of the variables is negligible on the deflection along line BG for all slabs.

4.3 The effect of the variables on the flexural capacity of the connection.

To assess the effect of the variables r_1/r_2, r_1/d and r_1/L on the flexural capacity of the connection, M_{test} is plotted against r_1/r_2, r_1/d, r_1/L, r_1/L' and r_1/L'' in Figs. 4.30 to 4.38, where L' is the distance from the centre line of the column to the line load, and L" is the distance from the centroid of the effective perimeter to the line load.

As shown in Figs. 4.30 to 4.35, the flexural capacity of the connection tends to decrease very slightly with the increase of r_1/r_2 and r_1/d, while in Figs. 4.36 to 4.38 the flexural capacity tends to increase with the increase of r_1/L ratio.

Fig. 4.30 Moment-column aspect ratio relationship

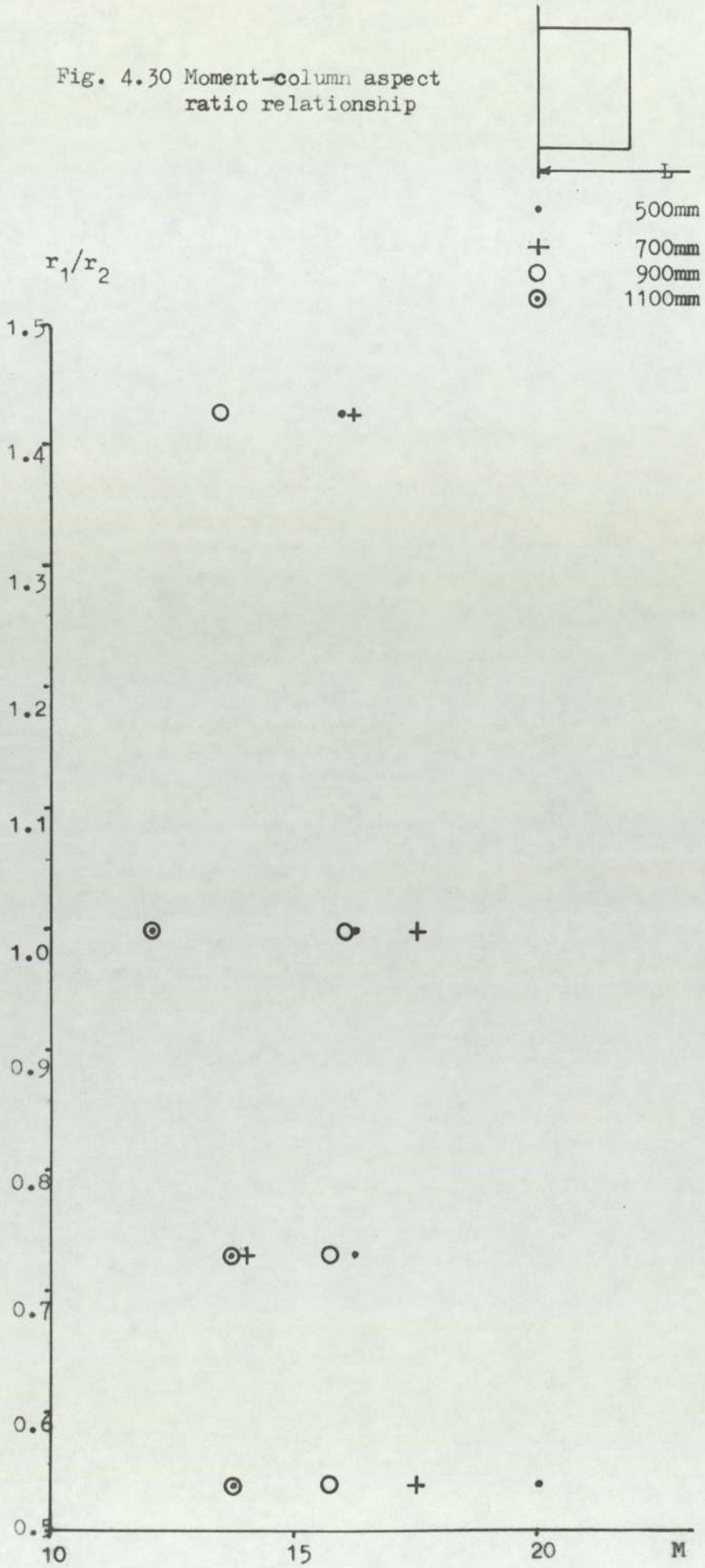

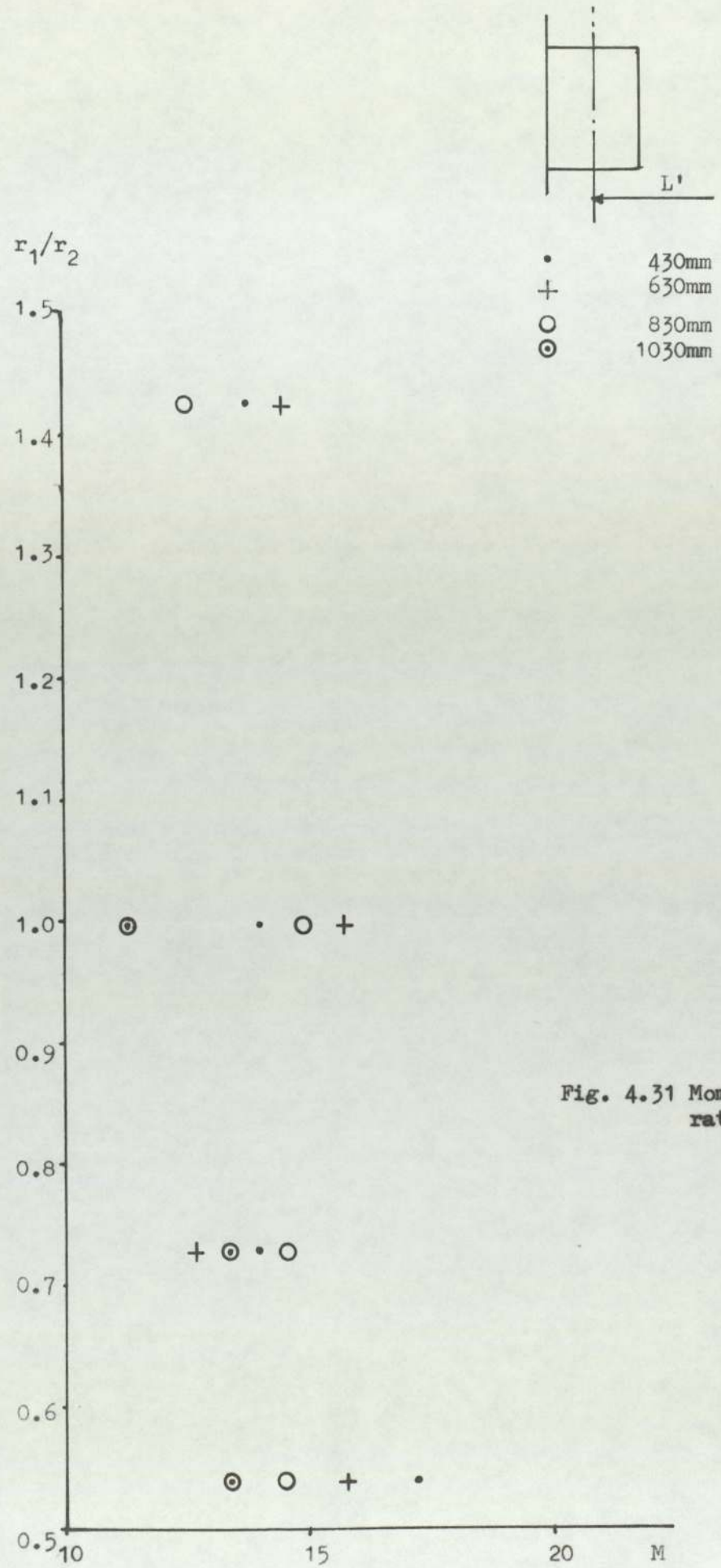

Fig. 4.31 Moment-column aspect ratio relationship

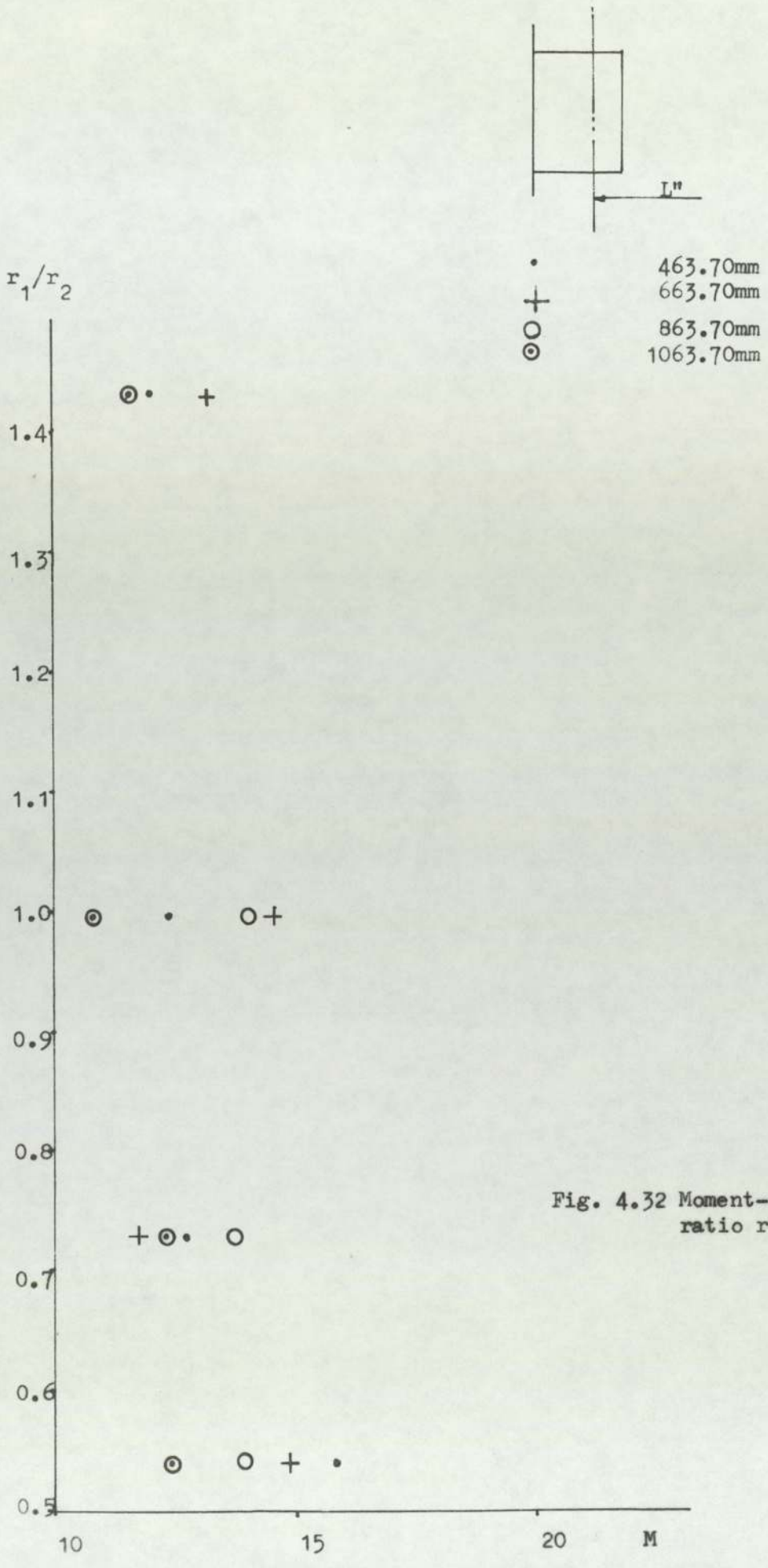

Fig. 4.32 Moment-column aspect ratio relationship

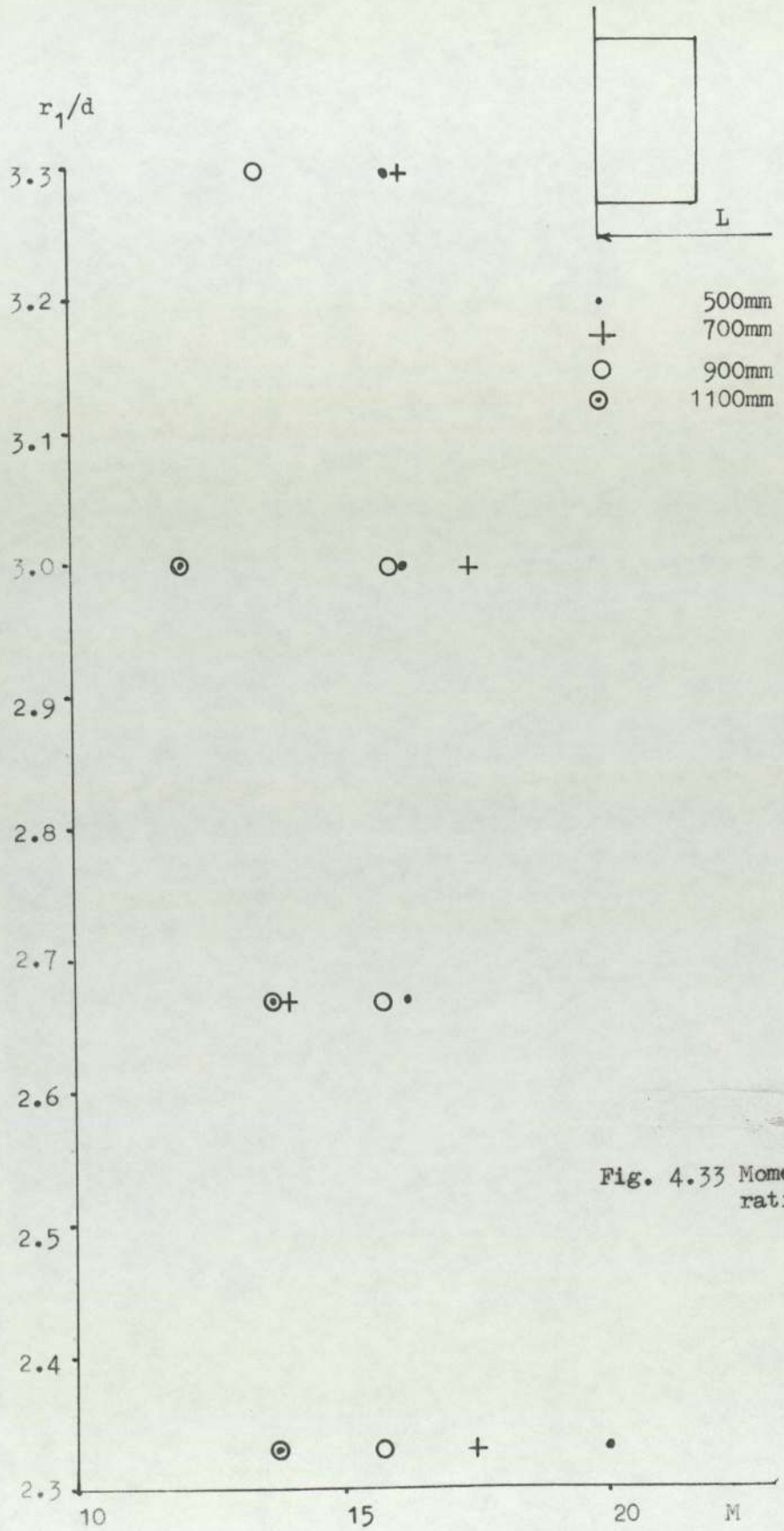

Fig. 4.33 Moment-column side/d ratio relationship

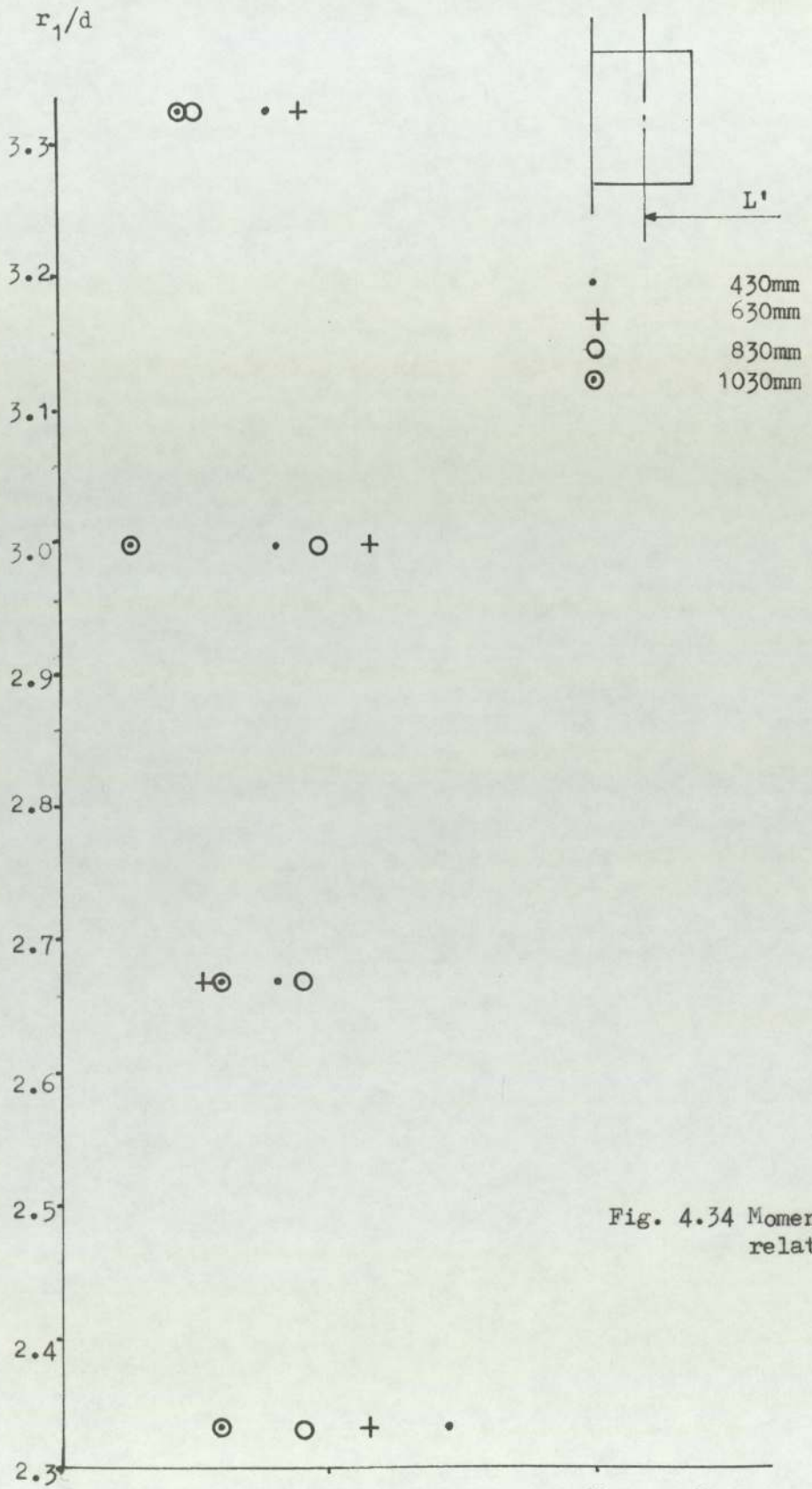

Fig. 4.34 Moment-column side/d relationship

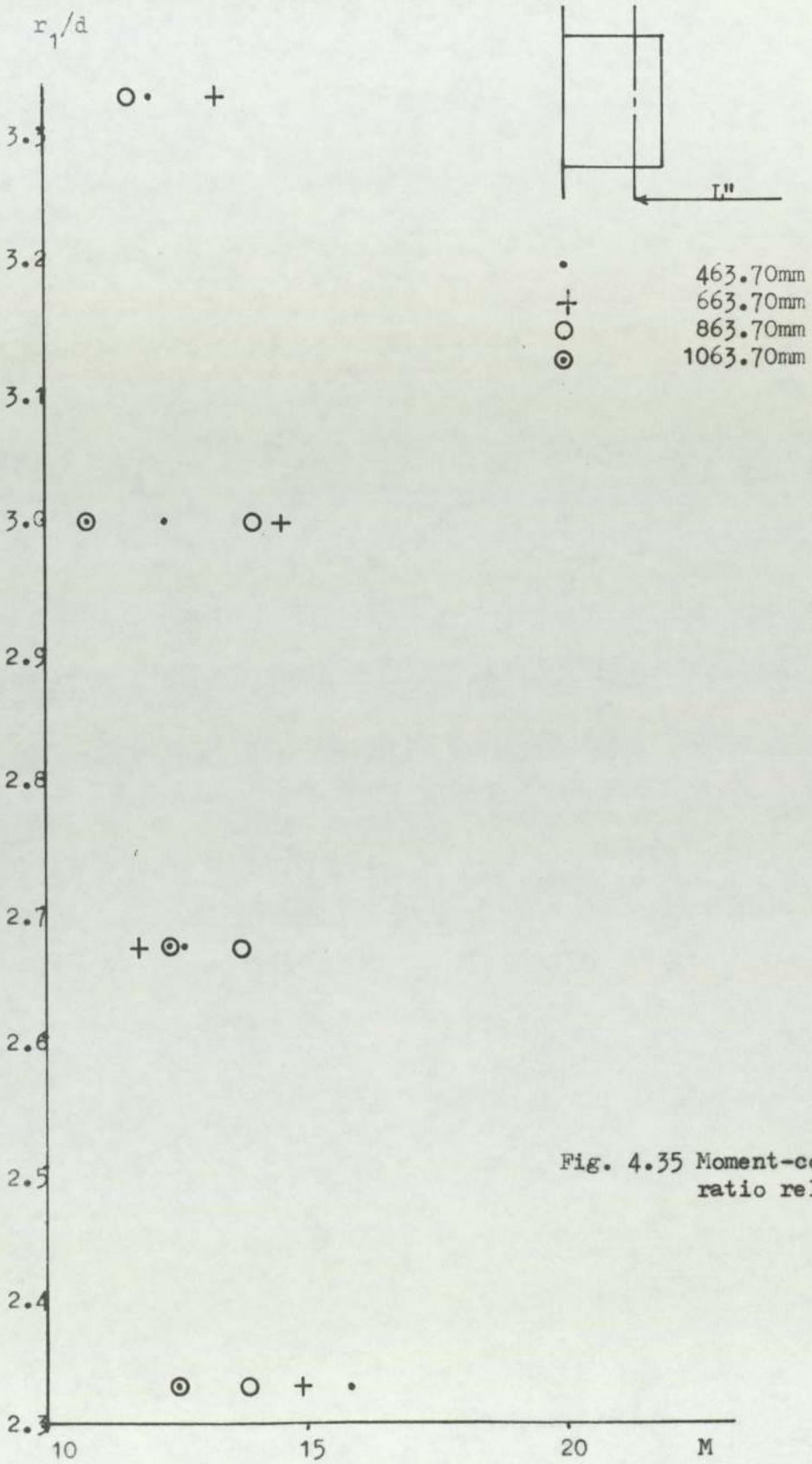

Fig. 4.35 Moment-column side/d ratio relationship

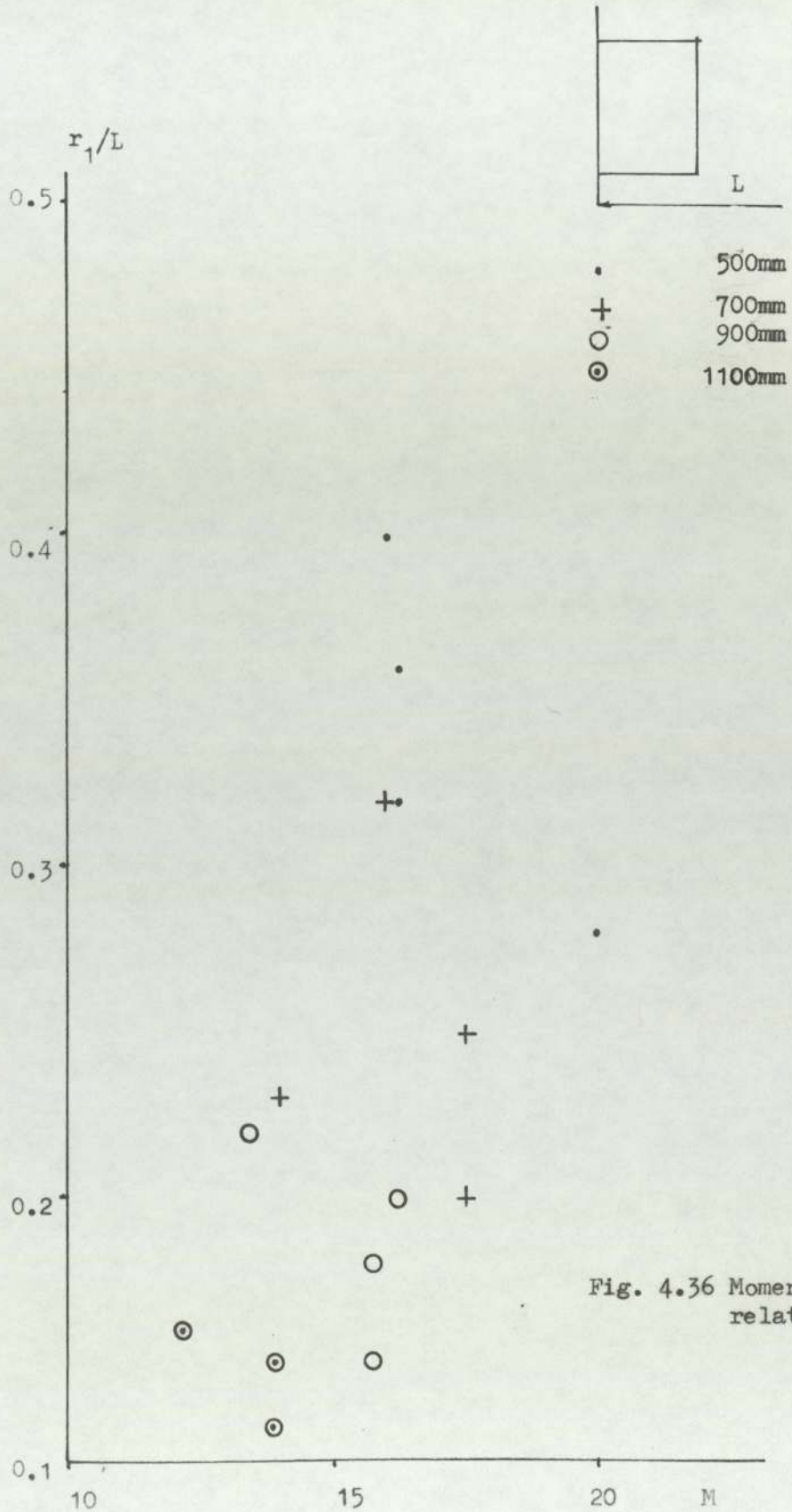

Fig. 4.36 Moment-r_1/L ratio relationship

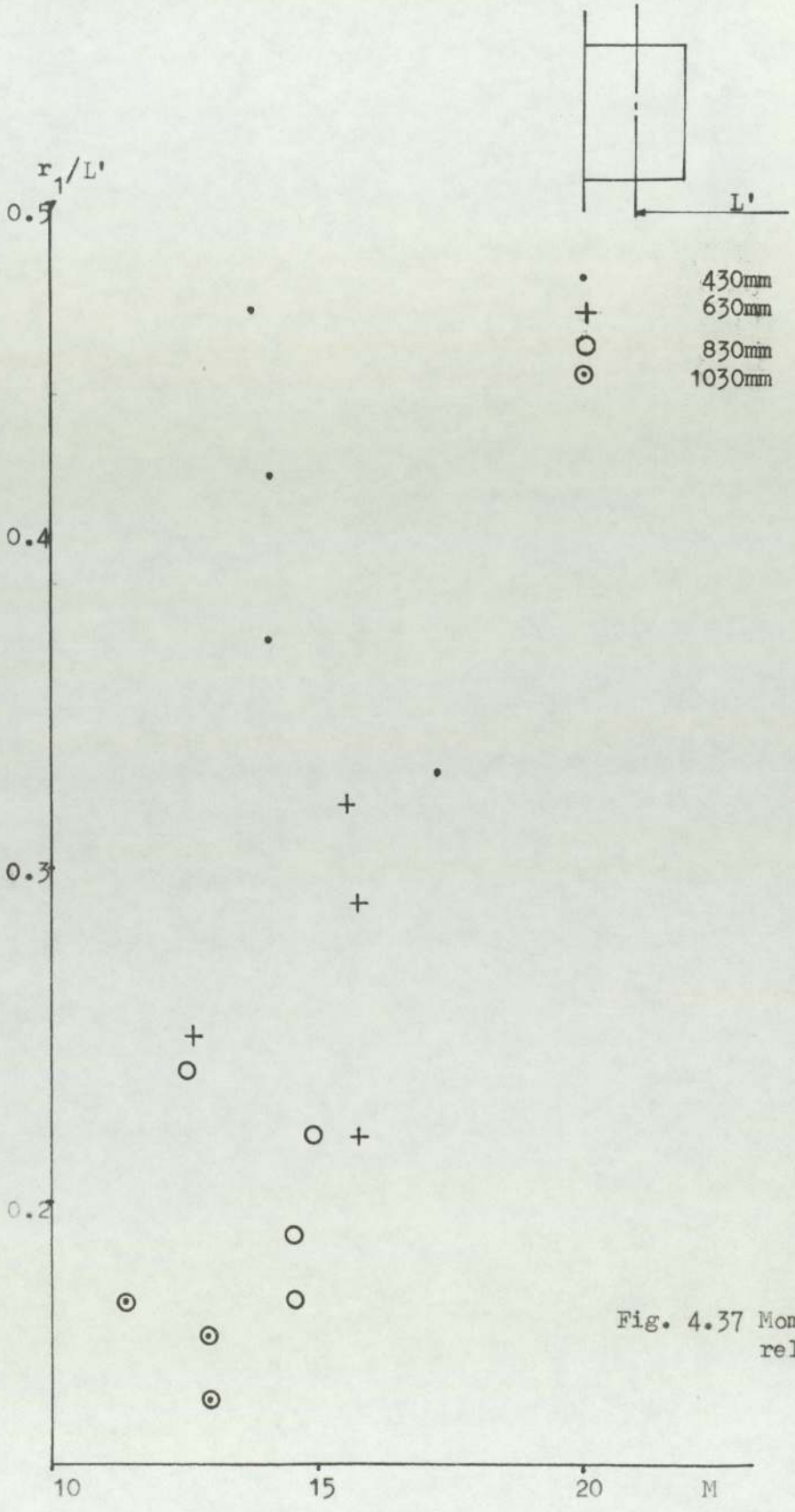

Fig. 4.37 Moment-r_1/L' ratio relationship

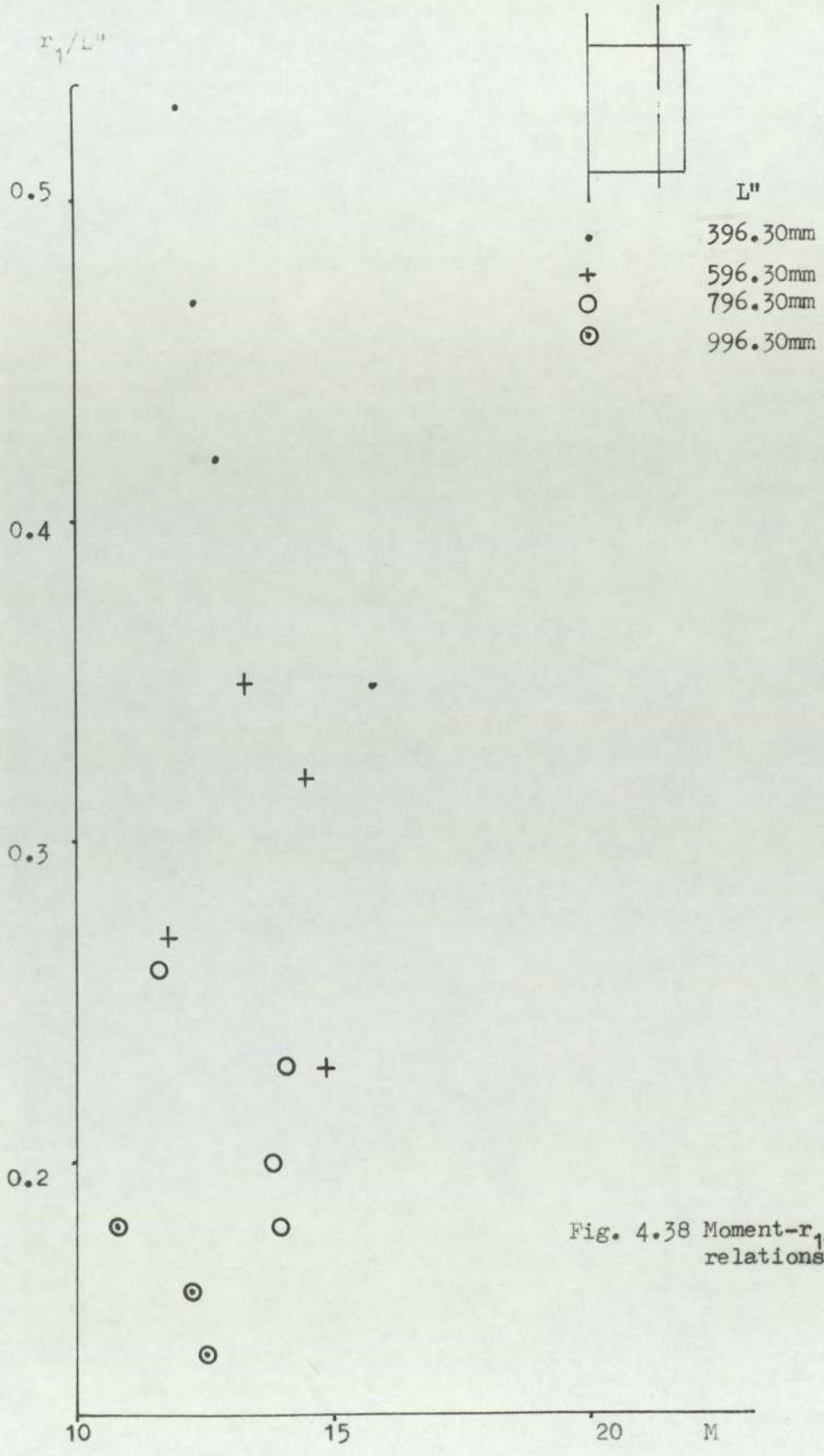

Fig. 4.38 Moment-r_1/L'' ratio relationship

The variation is greater if the bending moment is calculated using M = VL than if it is calculated using M = VL' or M = VL"; for the latter two cases the test flexural capacity appears almost constant although there is some scatter. It appears that rotation should be considered to take place about either the centroid of the column area or the centroid of the effective perimeter, but possibly with a slight margin in favour of the latter.

As shown in Figs. 4.39 to 4.42 the crack pattern does vary to some extent depending on the proportions of the column. In Fig. 4.39 it can be seen that the cracks develop at the face of the column which resists bending, and extend into the slab roughly parallel to the column face; and as would be expected by the shape of the column, a relatively small moment appears to be transferred to the column in torsion on the sides. At the other end of the scale where the longer sides are available to resist torsion, the bending cracks parallel to the column face are quite small and transverse bending cracks begin to develop as shown in Fig. 4.42.

4.4 Summary

In this chapter the test results for edge slab-column connections were presented and discussed. The following conclusions can accordingly be drawn.

(a) Top view

(b) Back view

Fig. 4.39 Specimen S-2

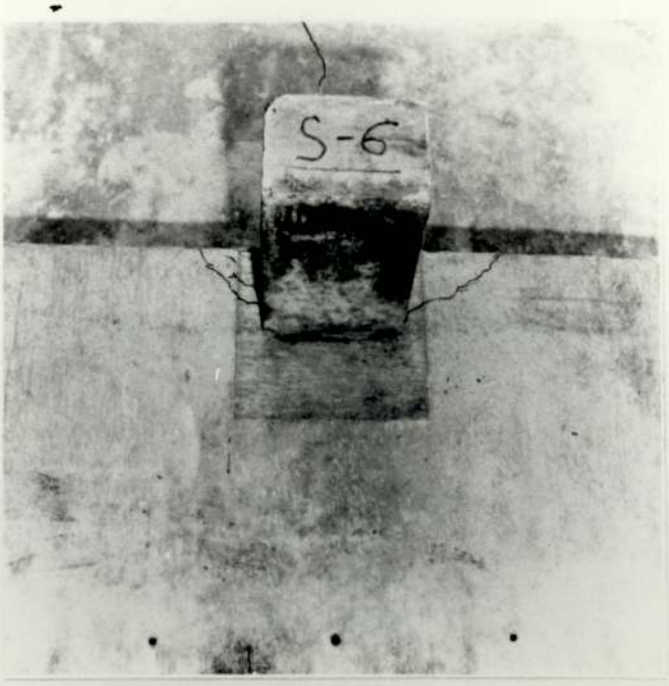

(a) Top view

(b) Back view

Fig. 4.40 Specimen S-6

(a) Top view

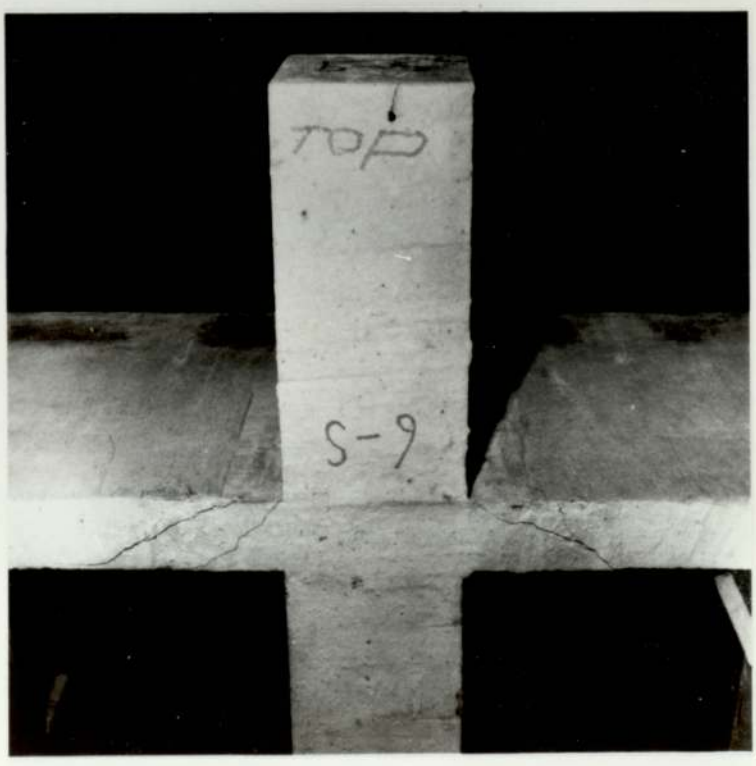

(b) Back view

Fig. 4.41 Specimen S-9

(a) Top view

(b) Back view

Fig. 4.42 Specimen S-13

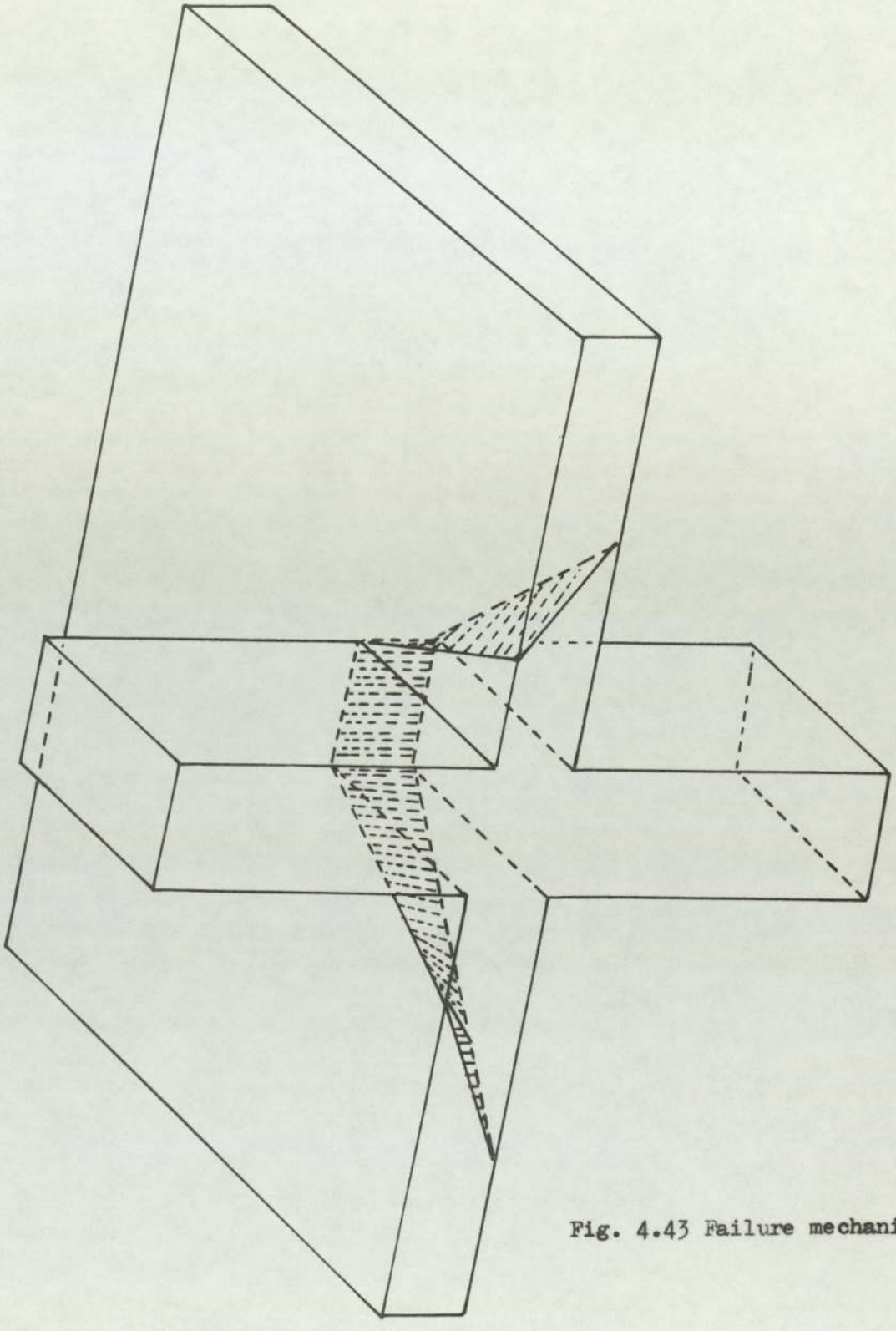

Fig. 4.43 Failure mechanism

(1) The primary failure mechanism for an edge column-slab connection subjected to moment and shear can be idealised as illustrated in Fig. 4.43. (The term mechanism refers to the last stage of the structure before failure which is capable of undergoing deformation without change in the resistance to external loads).

(2) For these structures, cracks can be expected at loads as low as 50 to 68 percent of the ultimate load.

(3) The failure of the specimen at ultimate load followed the formation of the torsional cracks on the column sides and flexural shear cracks at the inner side of the column.

(4) The flexural capacity of the joint is sensibly constant for the range of column aspect ratios tested. Such variation as can be seen indicates that as r_1 increases relative to r_2 there is a small reduction in flexural capacity of the joint.

CHAPTER V

STRENGTH ANALYSIS

5.1 Shear Strength

5.1.1. General

The effect of the variables on the shear strength of the connection is discussed and their effect on the capacity of the connection in the light of the experimental evidence is pointed out.

5.1.2. Method of analysis

It may be of interest to analyse the results obtained experimentally in the present investigation using the conventional method of analysis

$$v_u = \frac{V}{A_c} + \frac{kMC}{J_c} \qquad (5.1)$$

where

v_u = ultimate shear stress

V = shear force

A_c = Area of concrete in assumed critical section, periphery times effective slab depth d.

k = moment reduction factor

M = unbalanced moment

C = distance from centroidal axis to the most remote part of critical section

J_c = polar moment of inertia

and then compare the ultimate shear stresses obtained from

these results with the allowable ultimate shear stresses given by both ACI 318-77 Building Code and CP110 Code of Practice using both assumed critical sections.

This method (Eq. 5.1) was chosen because of its acceptance by a number of researchers[2,7,11,12] and also by ACI 317-71 and ACI 318-77 codes. This type of approach was used in comparing with the CP110 approach in obtaining the modification factor for interior slab-column connection subjected to shear and moment (see section 3.6.2 CP110 and Eq. 2.27). The differences between this approach and the approach followed by CP110 as mentioned by Regan[53] are as follows.

(1) The ACI code includes torsion in its uneven shear effects.

(2) In the ACI code uneven shear effects are greater if the column dimension parallel to the eccentricity is larger than that perpendicular to it, while in CP110 rectangularity has no effect.

(3) According to CP110 the effect of uneven shear decreases for greater slab spans. There appears to be no evidence either way on this point for flat slabs, but there are cases in bridge decks where the ACI predictions are better.

(4) The biggest difference is in the treatments of moments perpendicular to slab edges, where the ACI code applies the above approach with a suitable

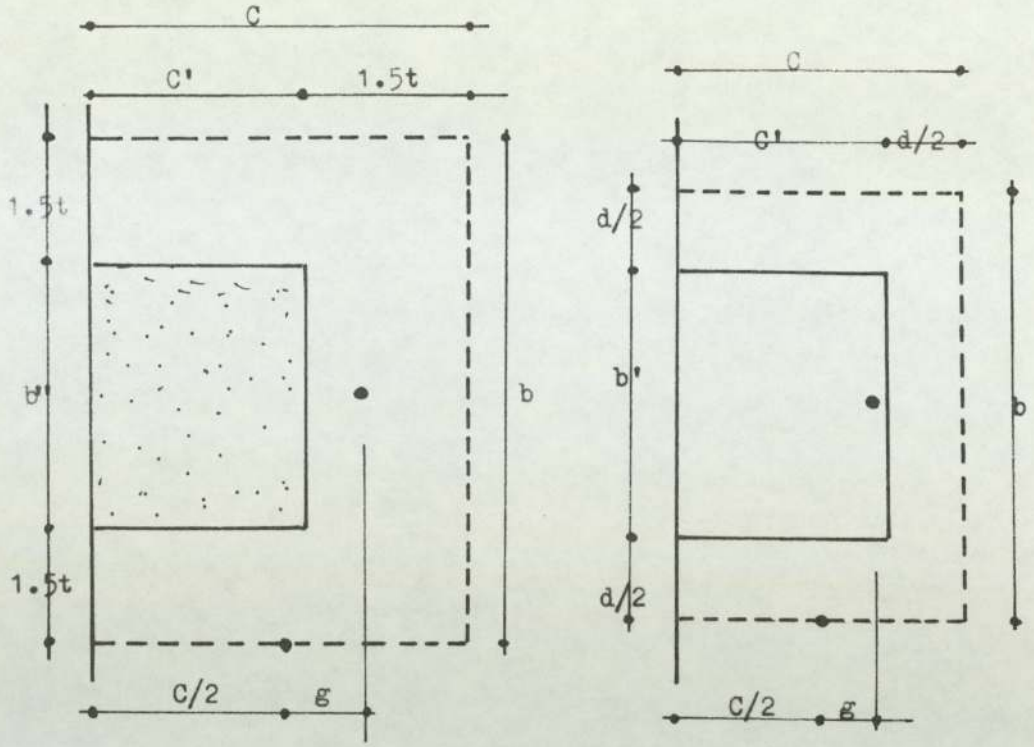

(a) CP110

(b) ACI-77

$C=C'+1.5$ or $C'+d/2$

$b=b'+3t$ or $b'+d$

$a_1=C/2+g$

$a_2=C/2-g$

$A_c=(2C+b)d$

$J_c=2dC^3/12 + 2Cd^3/12 + 2Cdg^2 + bd(C/2-g)^2$

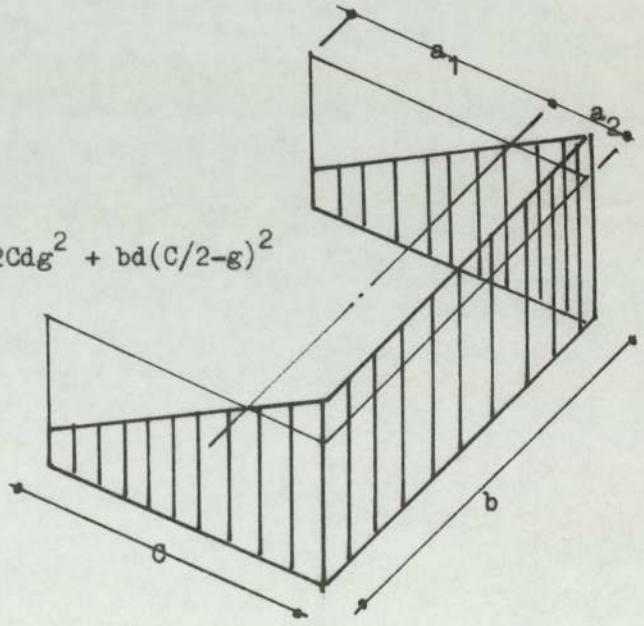

Fig. 5.A Critical sections for shear stress

modification of J_c and predicts a considerable influence on punching resistance, while CP110 totally ignores any such effect.

Eq. 5.1 was used to calculate shear stresses for comparison with CP110 using the critical section assumed by CP110. Three different values of k were used.

(1) k = 0 according to CP110

(2) k = 0.20 according to ACI-ASCE Committee 326.

(3) k = 0.40 according to Hanson and Hanson.

5.1.2.1. Typical calculation of the shear stress using Eq. 5.1

For c' = 140 mm, b' = 260 mm, d = 60 mm from Fig. 5.A we find (for CP110)

$c = 252.5$ mm, $b = 485.0$ mm

$g = 61.85$ mm, $a_2 = 64.4$ mm

$A_c = 59400$ mm^2

$J_c = 406.7 \times 10^6$ mm^4

Substitute these values in Eq. 5.1 using k = 0.2 and then get another value for v_u by using k = 0.4.

Then follow the same approach to calculate v_u according to ACI-77 assumptions (see Fig. 5.A and Table 5.1).

5.1.3. Effect of r_1/r_2 ratio

In Figs. 5.1 to 5.4 the calculated ultimate shear stress (according to CP110 assumptions) is plotted against

		CP110 (N/mm²)				AC1-77 (N/mm²)			
SP.NO	f_c' (N/mm²)	v_c (code)	v_c (k=0)	v_c (k=.2)	v_c (k=.4)	v_c (code)	v_c (k) code value	r_1/r_2	r_1/d
1	27.76	0.893	0.673	1.220	1.760	1.486	3.060	0.54	2.33
2	25.93	0.872	0.421	0.920	1.420	1.436	2.320	"	"
3	29.00	0.902	0.293	0.750	1.214	1.519	2.170	"	"
4	26.00	0.873	0.210	0.618	1.024	1.439	1.850	"	"
5	26.80	0.881	0.547	0.970	1.390	1.461	2.520	0.73	2.67
6	27.30	0.905	0.336	0.720	1.103	1.475	2.050	"	"
7	29.80	0.910	0.295	0.738	1.182	1.540	2.230	"	"
8	29.20	0.904	0.210	0.600	0.999	1.525	1.910	"	"
9	22.50	0.840	0.547	0.950	1.349	1.339	2.590	1.00	3.00
10	29.00	0.902	0.421	0.880	1.337	1.519	2.660	"	"
11	22.90	0.843	0.303	0.740	1.177	1.359	2.390	"	"
12	26.30	0.876	0.185	0.518	0.851	1.448	1.750	"	"
13	30.30	0.915	0.539	0.925	1.311	1.554	2.650	1.43	3.33
14	26.20	0.875	0.387	0.804	1.220	1.444	2.560	"	"
15	28.90	0.901	0.252	0.615	0.976	1.516	2.110	"	"

Table 5.1: Shear stresses

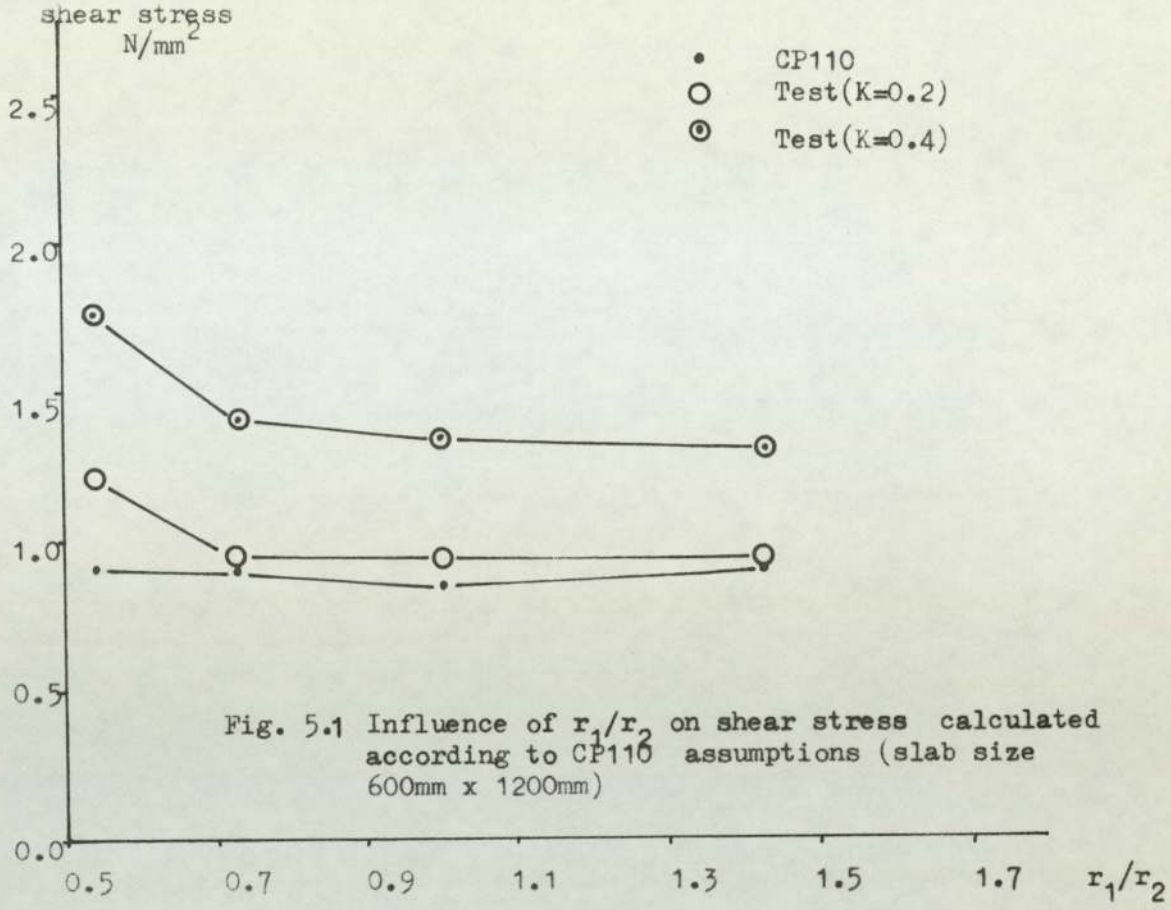

Fig. 5.1 Influence of r_1/r_2 on shear stress calculated according to CP110 assumptions (slab size 600mm x 1200mm)

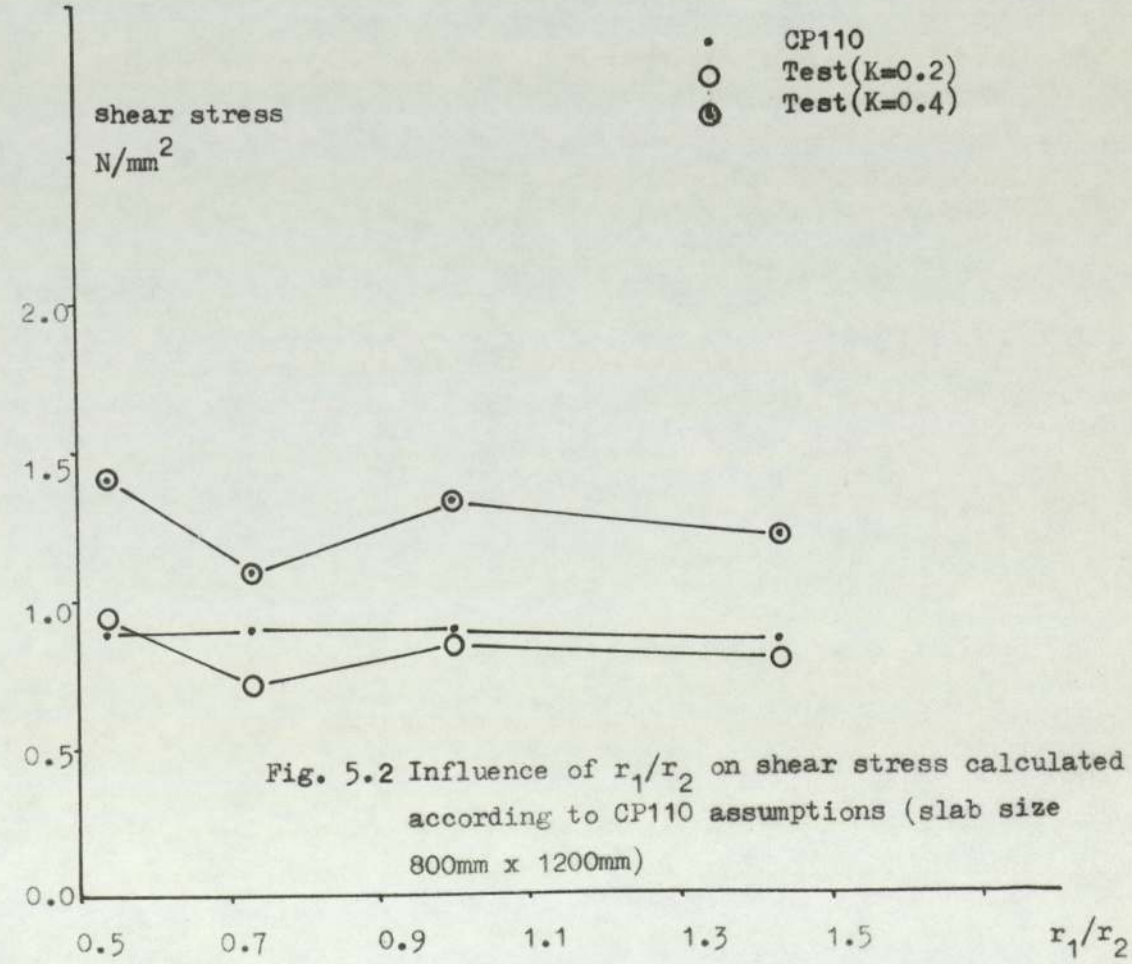

Fig. 5.2 Influence of r_1/r_2 on shear stress calculated according to CP110 assumptions (slab size 800mm x 1200mm)

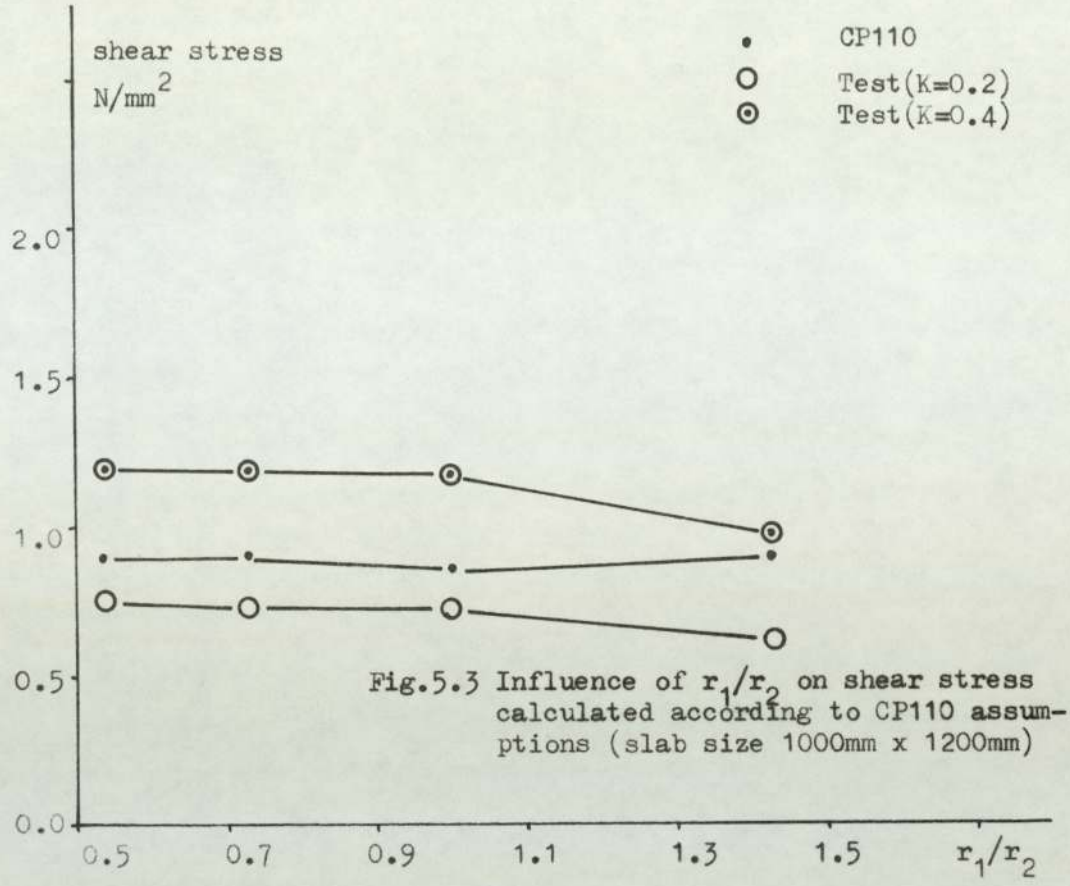

Fig.5.3 Influence of r_1/r_2 on shear stress calculated according to CP110 assumptions (slab size 1000mm x 1200mm)

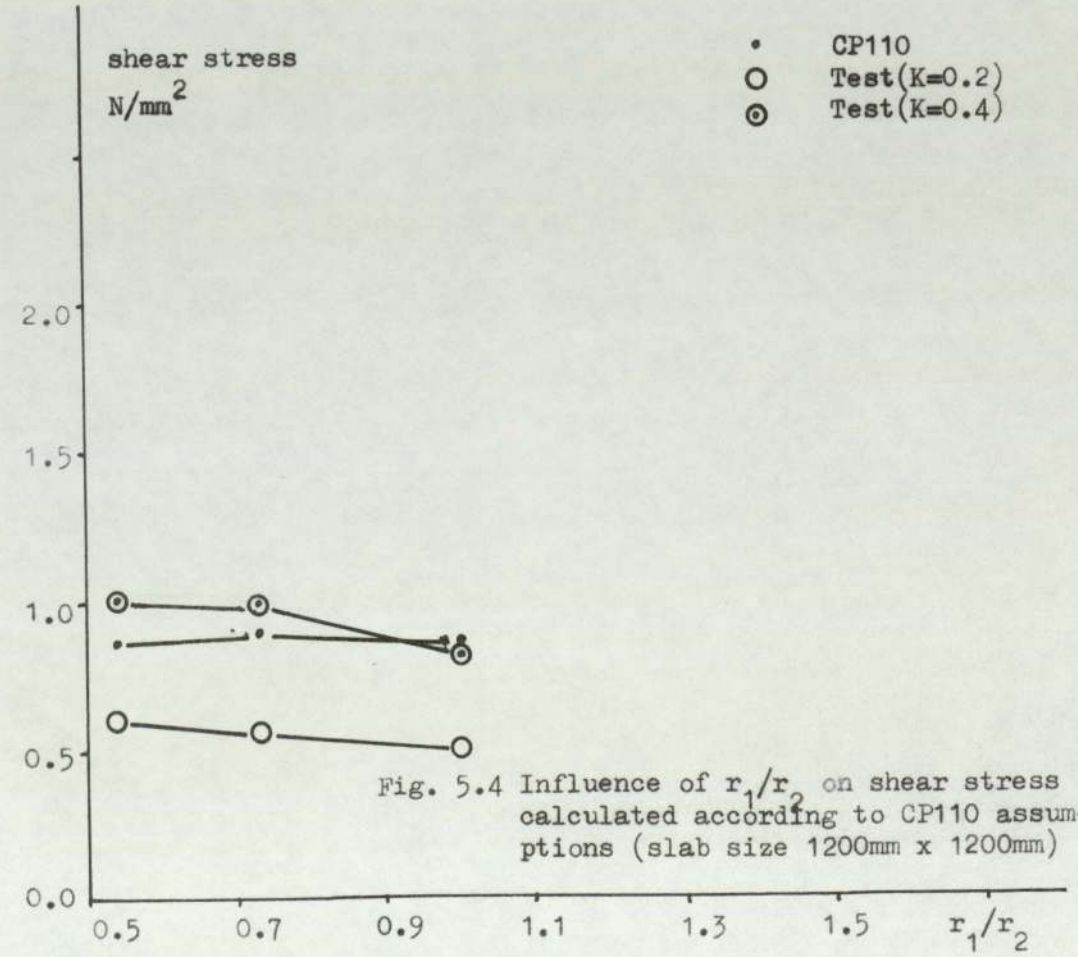

Fig. 5.4 Influence of r_1/r_2 on shear stress calculated according to CP110 assumptions (slab size 1200mm x 1200mm)

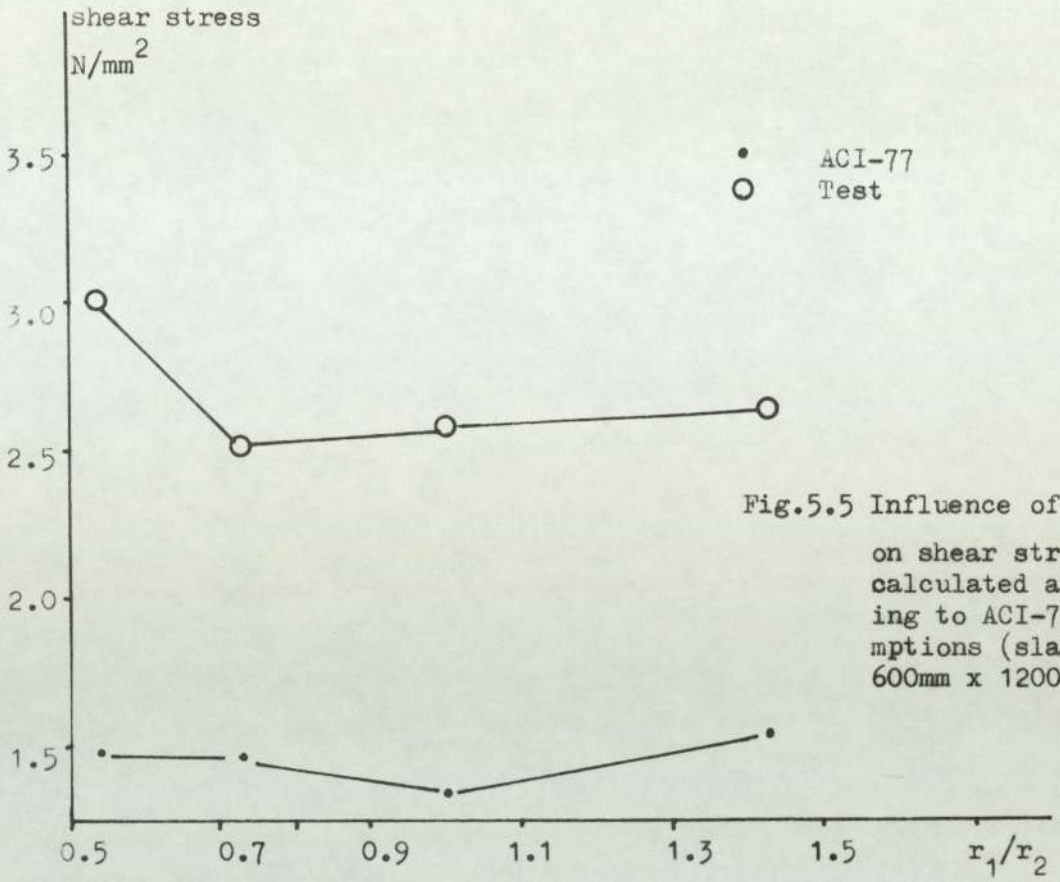

Fig.5.5 Influence of r_1/r_2 on shear stress calculated according to ACI-77 assumptions (slab size 600mm x 1200mm)

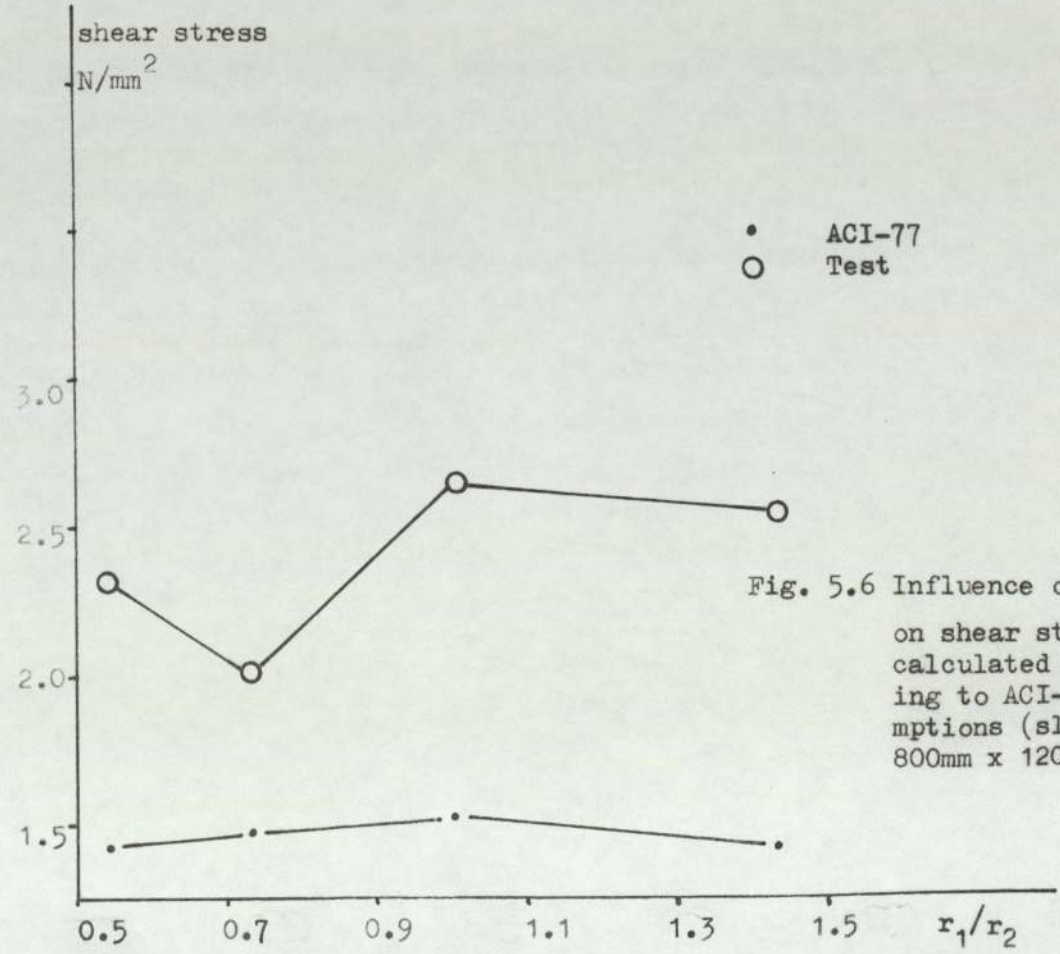

Fig. 5.6 Influence of r_1/r_2 on shear stress calculated according to ACI-77 assumptions (slab size 800mm x 1200mm)

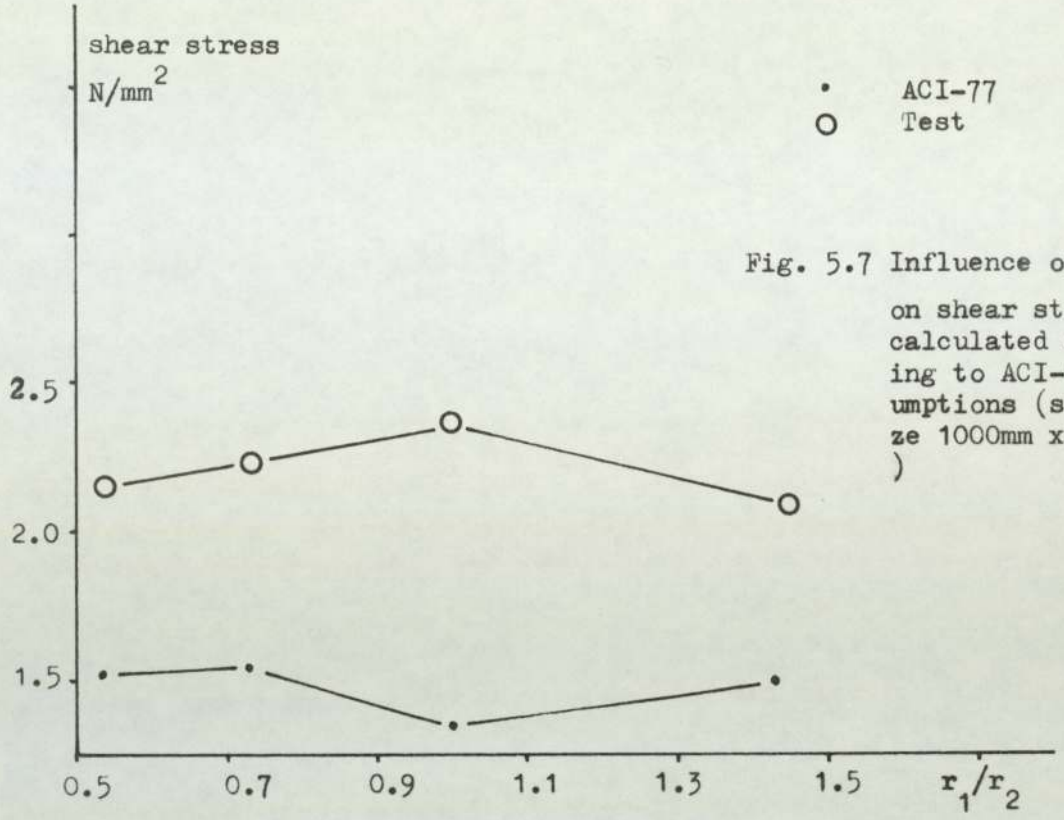

Fig. 5.7 Influence of r_1/r_2 on shear stress calculated according to ACI-77 assumptions (slab size 1000mm x 1200mm)

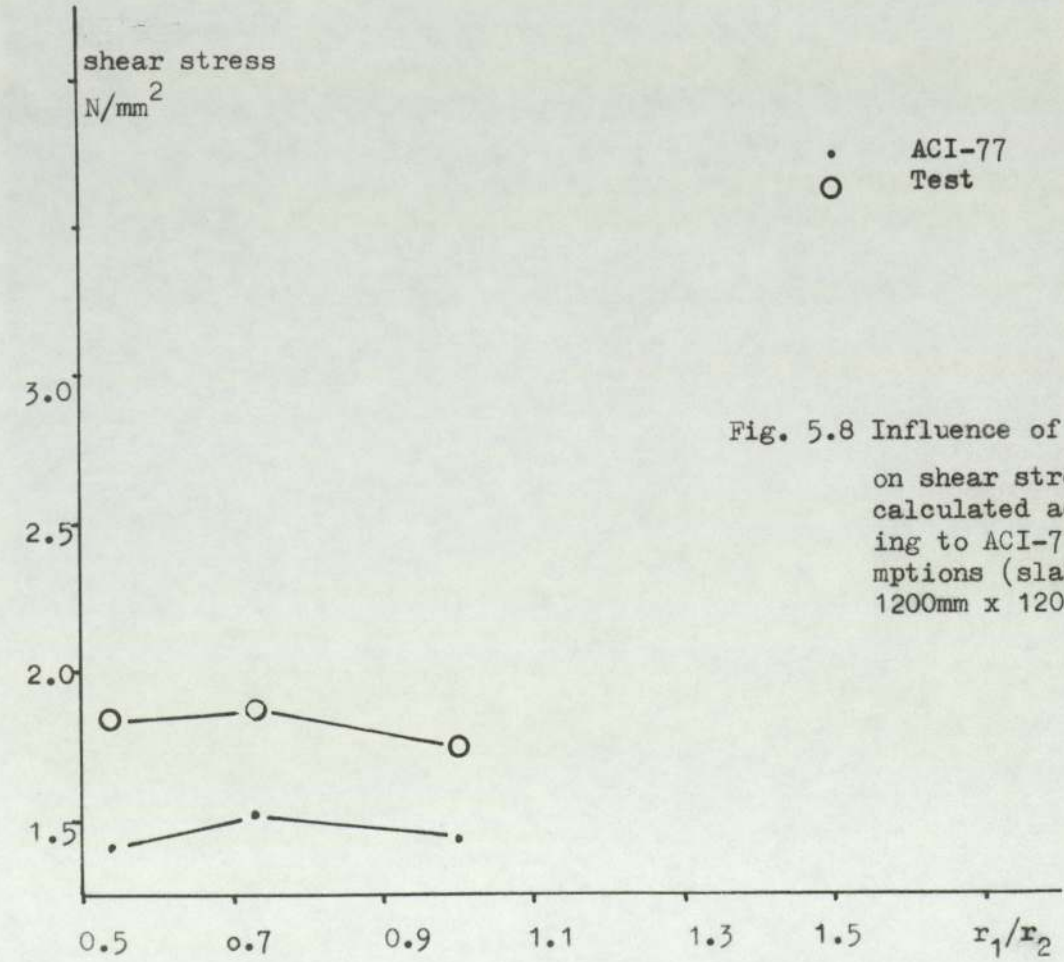

Fig. 5.8 Influence of r_1/r_2 on shear stress calculated according to ACI-77 assumptions (slab size 1200mm x 1200mm)

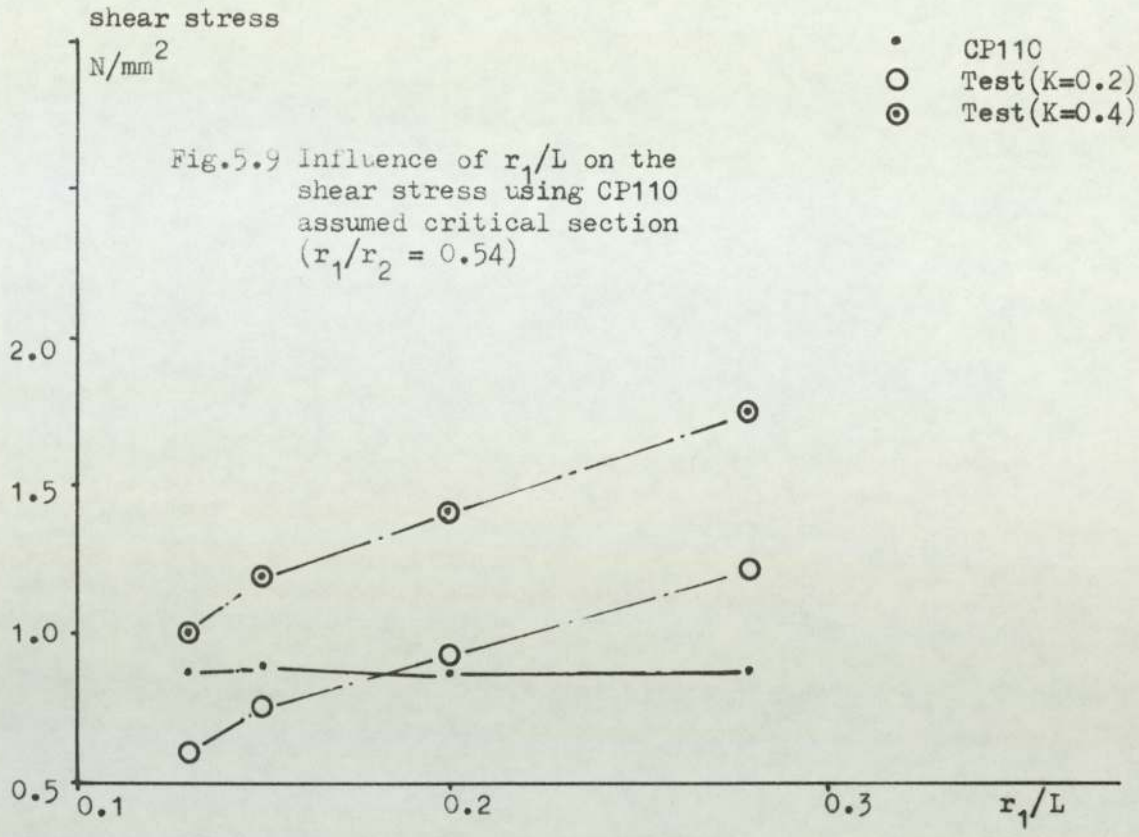

Fig.5.9 Influence of r_1/L on the shear stress using CP110 assumed critical section ($r_1/r_2 = 0.54$)

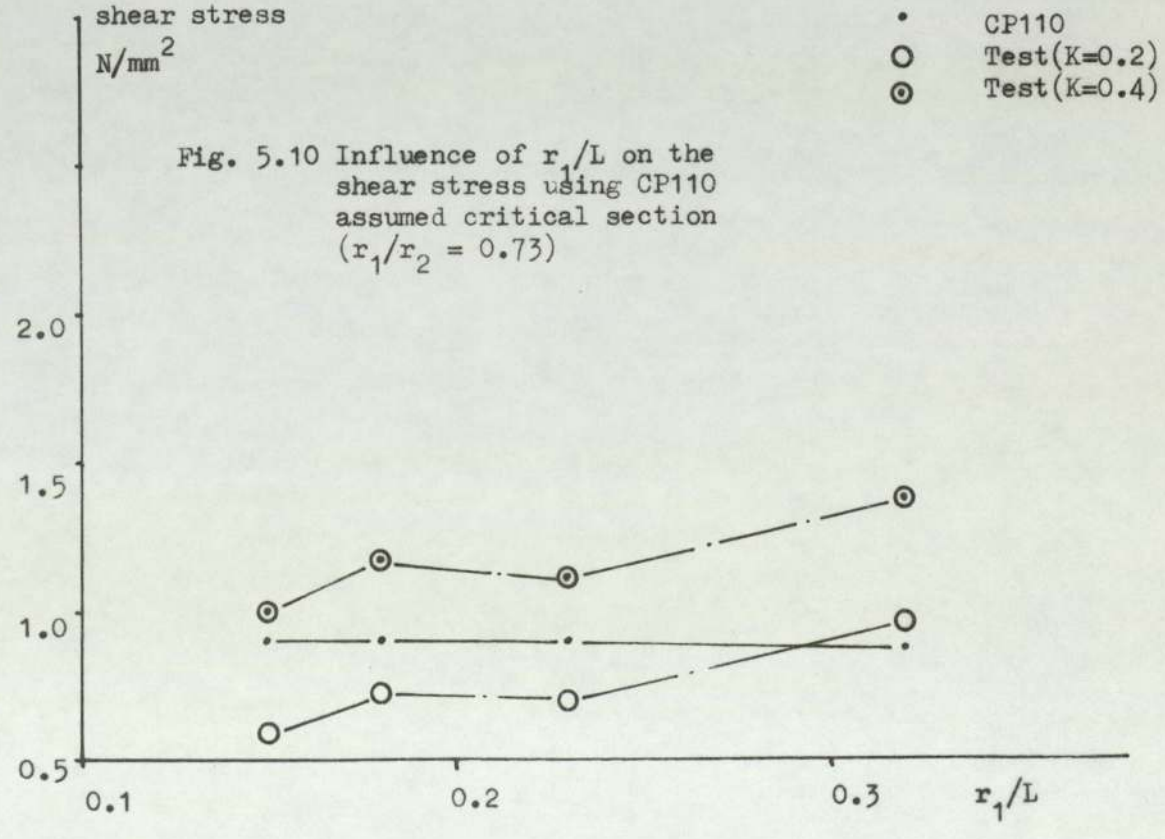

Fig. 5.10 Influence of r_1/L on the shear stress using CP110 assumed critical section ($r_1/r_2 = 0.73$)

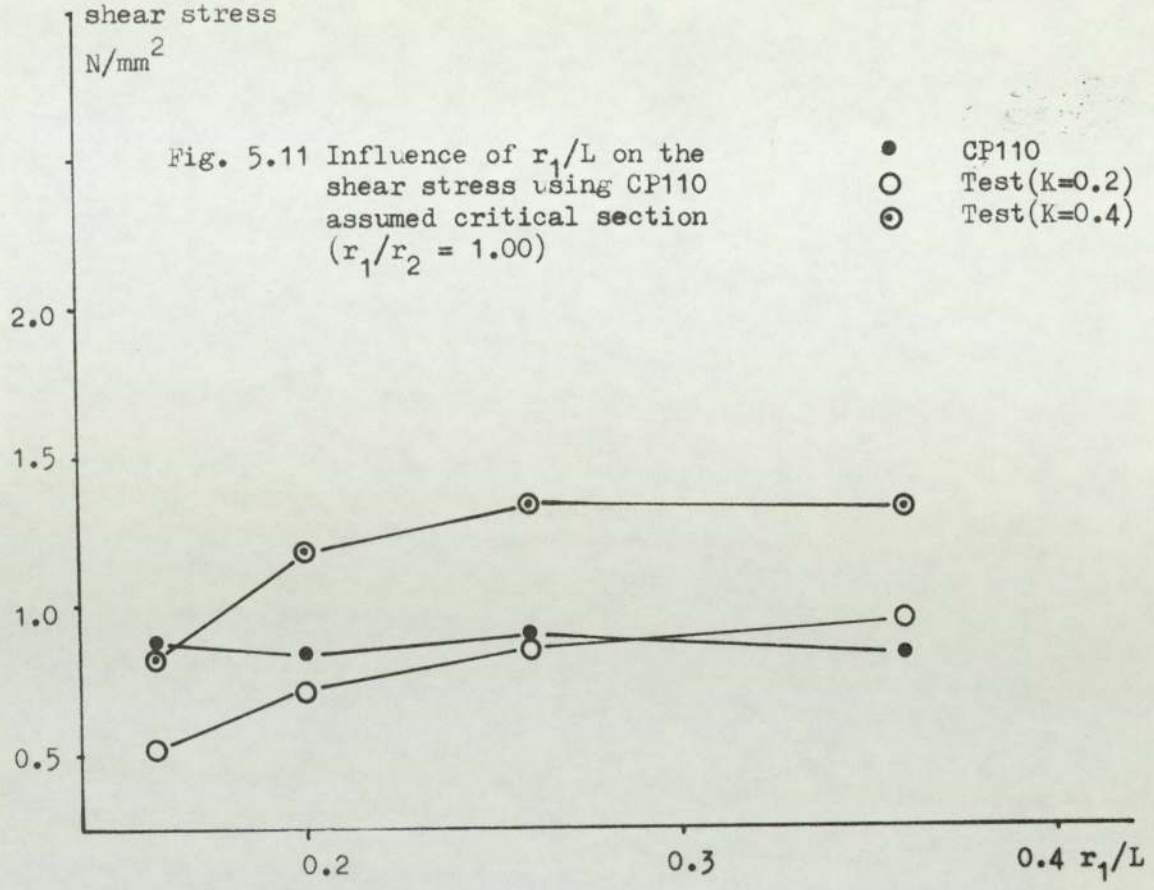

Fig. 5.11 Influence of r_1/L on the shear stress using CP110 assumed critical section (r_1/r_2 = 1.00)

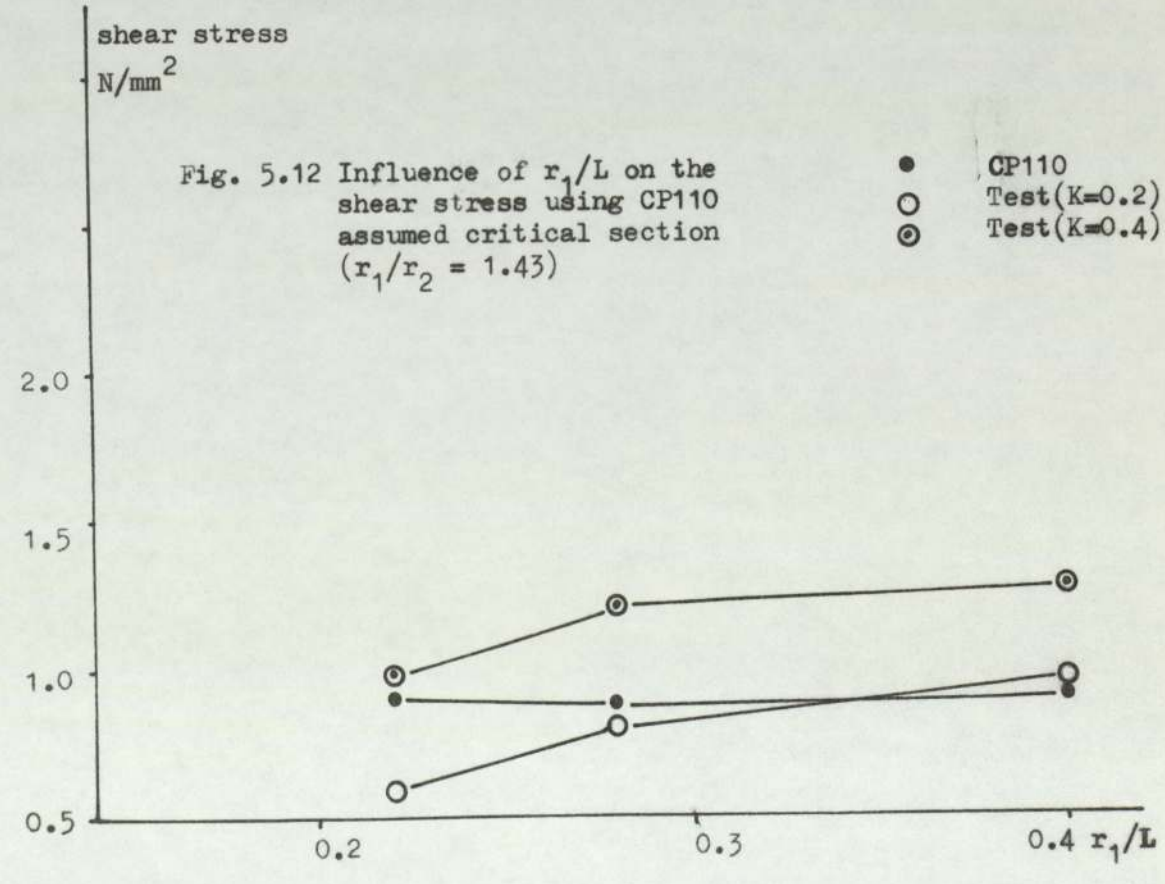

Fig. 5.12 Influence of r_1/L on the shear stress using CP110 assumed critical section (r_1/r_2 = 1.43)

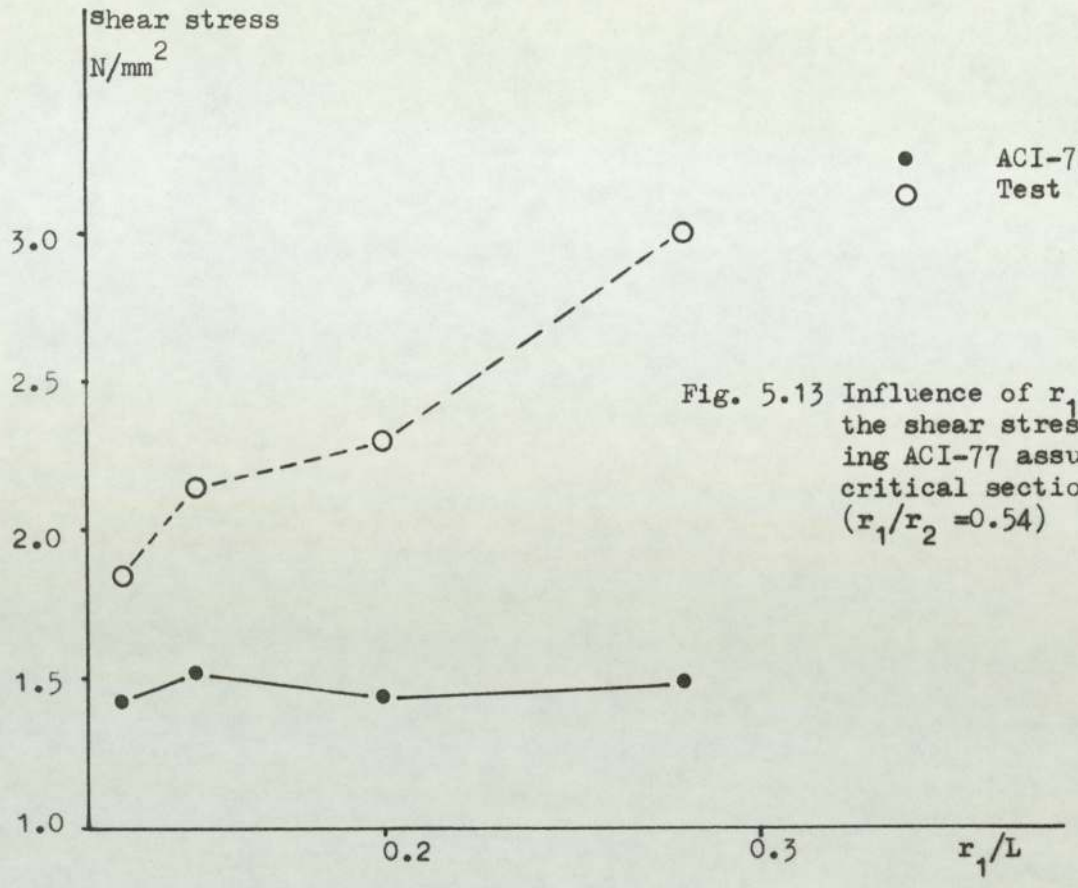

Fig. 5.13 Influence of r_1/L on the shear stress using ACI-77 assumed critical section (r_1/r_2 =0.54)

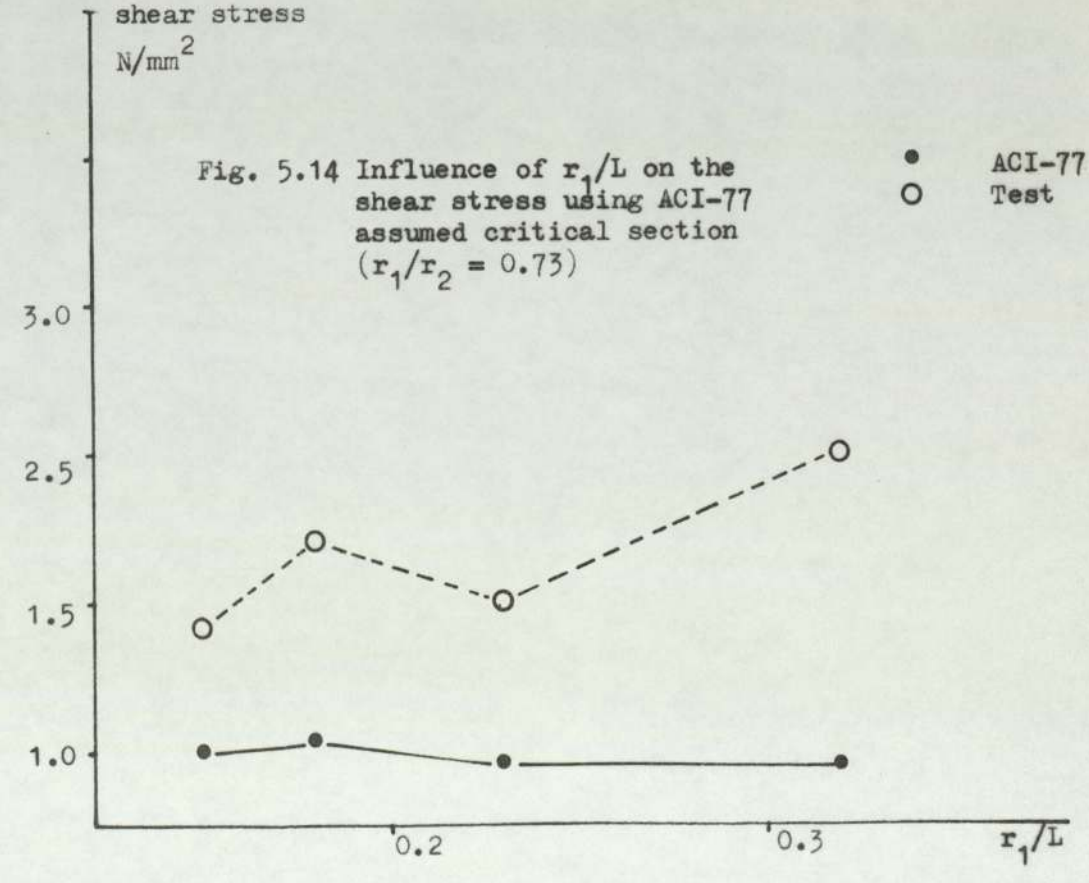

Fig. 5.14 Influence of r_1/L on the shear stress using ACI-77 assumed critical section (r_1/r_2 = 0.73)

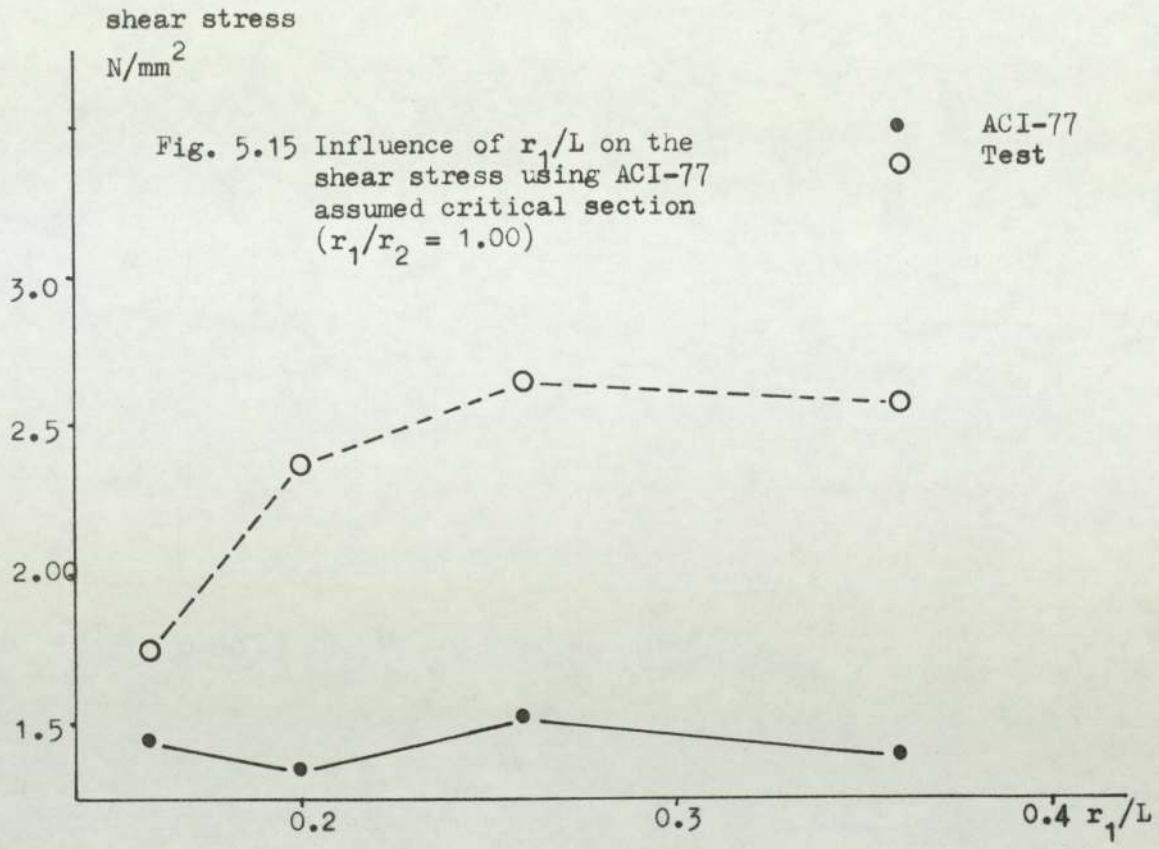

Fig. 5.15 Influence of r_1/L on the shear stress using ACI-77 assumed critical section (r_1/r_2 = 1.00)

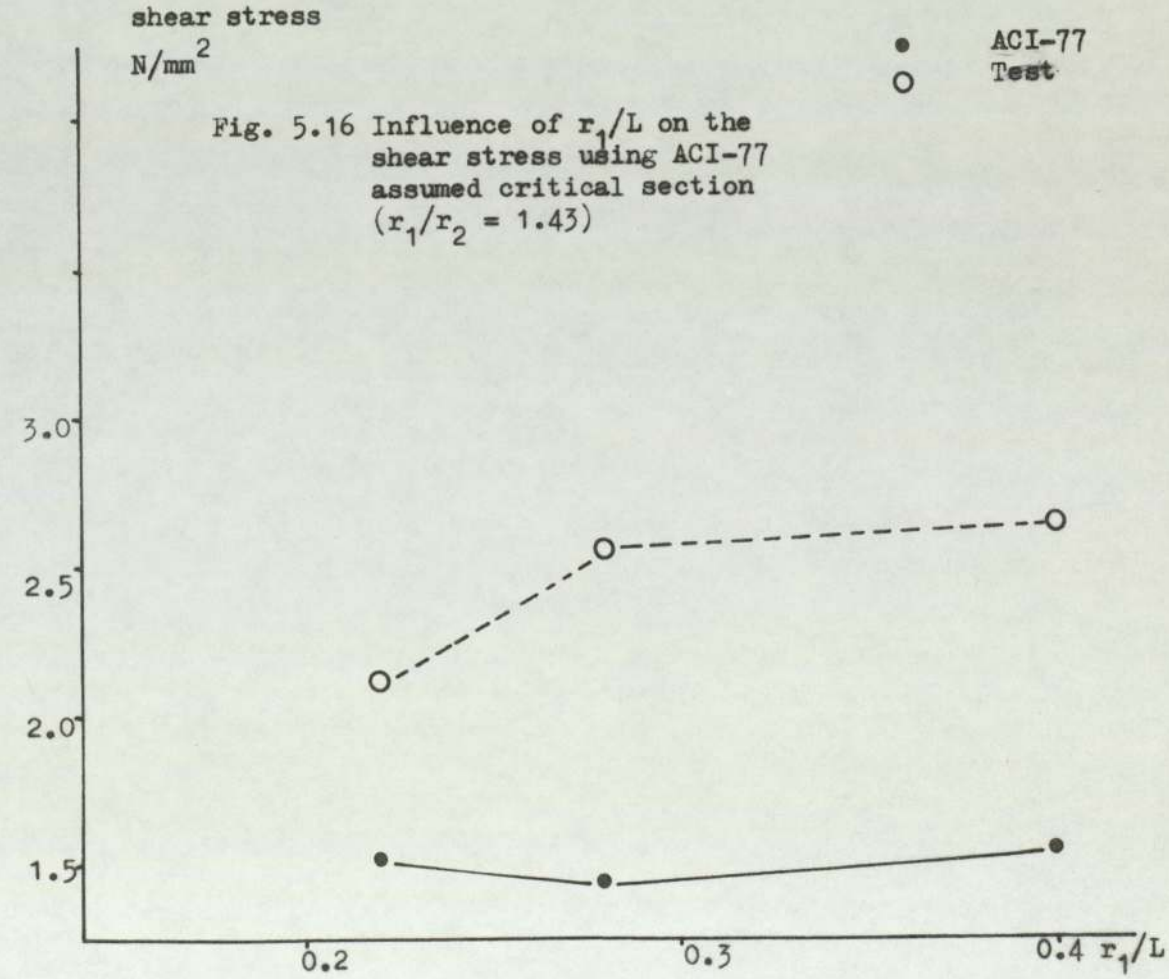

Fig. 5.16 Influence of r_1/L on the shear stress using ACI-77 assumed critical section (r_1/r_2 = 1.43)

r_1/r_2 ratio. Also in Figs. 5.5 to 5.8 the calculated ultimate shear stress (according to ACI-77) is plotted against r_1/r_2 ratio. As shown in these figures, the effect of r_1/r_2 ratio on the ultimate shear stress is small. As r_1/r_2 increases the ultimate shear stress decreases slightly, while the allowable shear stress given by the codes remains practically constant. Also we can notice from those figures that the code values are not on straight line because they are dependent on concrete strength.

The allowable ultimate shear strength under ACI-77 code seems to be highly conservative when the value of k is taken according to the code equation (Eq. 2.26), while the ultimate shear strength under CP110 appears to be unsafe for all tests when k = 0 and unsafe for high values of r_1/r_2 when k = 0.20. If the value of k = 0.40 is used in calculating the shear stress using the CP110 assumptions for critical section, and the results are compared with CP110, it can be seen that all specimens produce safe results except those with high values of r_1/r_2.

5.1.4 Effect of r_1/L ratio

In Figs. 5.9 to 5.12 the calculated ultimate shear stress,using a critical plane at 1.5h from the column as is done in CP110,is plotted against r_1/L ratio. In Figs. 5.13 to 5.16 the calculated ultimate shear stress,using a critical section at d/2 from the column as in ACI-77 code, is plotted against r_1/L ratio.

As shown in these figures the ultimate shear stress calculated using Eq. 5.1 tends to increase with the increase in r_1/L while the allowable shear stress remains practically constant. These figures also demonstrate that the ratio v_{test}/v_{code} increases as r_1/L ratio increases, therefore for high values of r_1/L the allowable ultimate shear strength under the present codes seem to be more conservative than for low values of r_1/L; while it seems to be unsafe for small values of r_1/L (see Fig. 5.17). Fig. 5.18 shows the effect of the ratio P/L (where P is the perimeter of the column for three sides). As shown from this figure, for high values of P/L the allowable shear strength under the present codes is conservative and it is unsafe for small values of P/L.

5.1.5. Effect of r_1/d ratio

In Figs. 5.19 to 5.22 the calculated ultimate shear stress (according to CP110 assumptions) is plotted against r_1/d ratio. In Figs. 5.23 to 5.24 the calculated ultimate shear stress (according to ACI-77) is plotted against r_1/d ratio.

As shown in these figures, the effect of r_1/d ratio seems to be similar to the effect of r_1/r_2 ratio. As r_1/d ratio increased the calculated ultimate shear stress decreased slightly while the allowable shear stress remained constant.

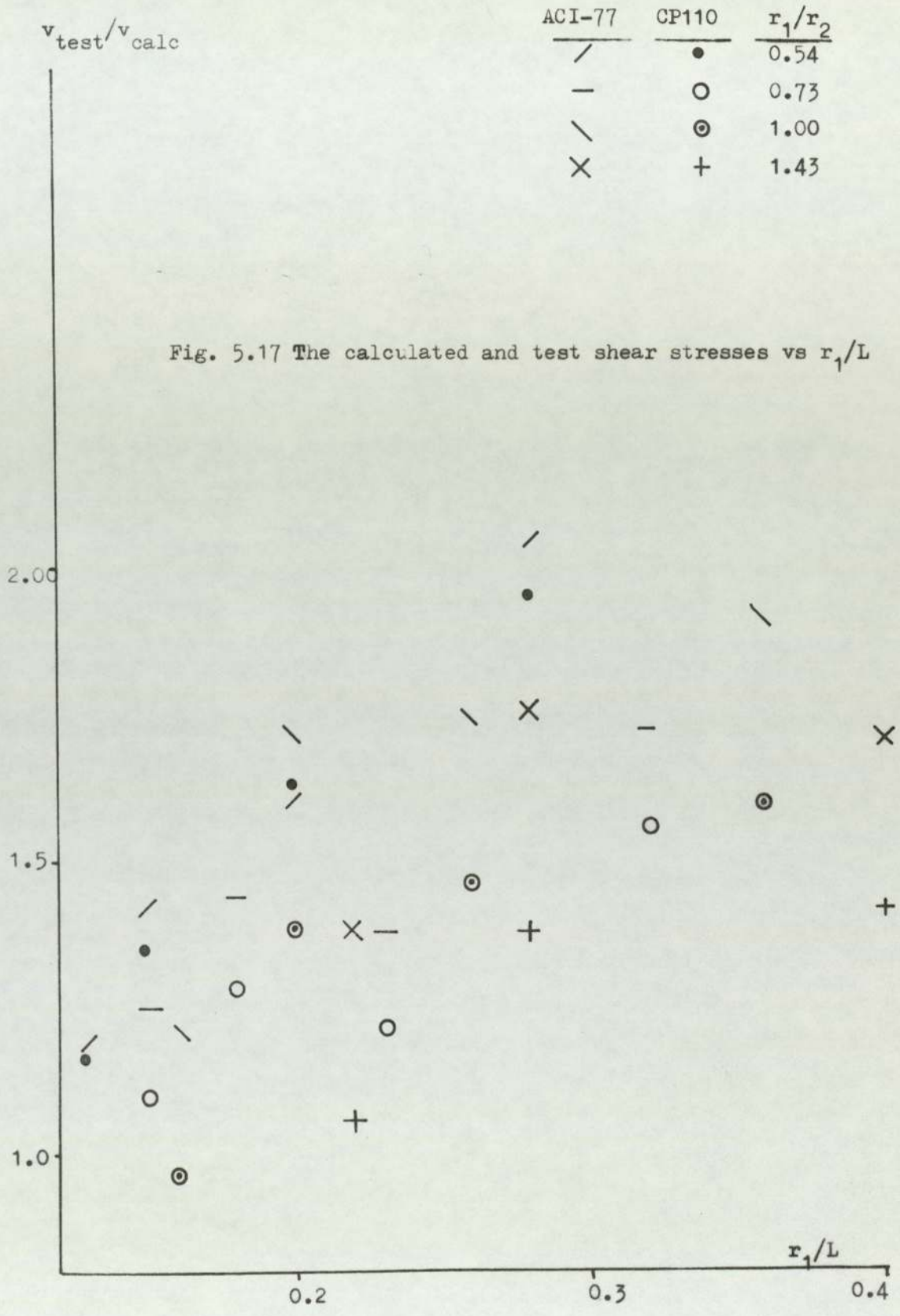

Fig. 5.17 The calculated and test shear stresses vs r_1/L

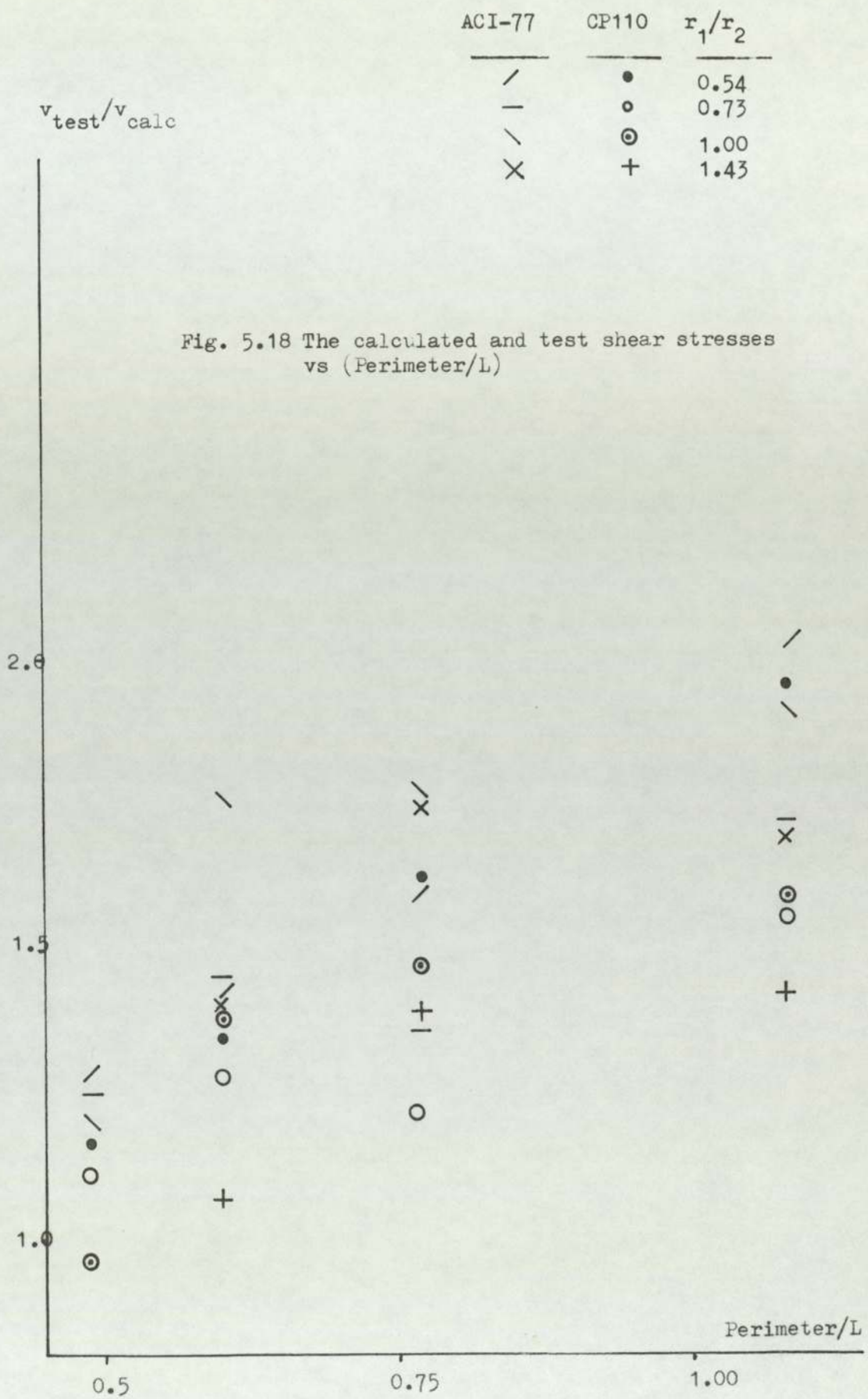

Fig. 5.18 The calculated and test shear stresses vs (Perimeter/L)

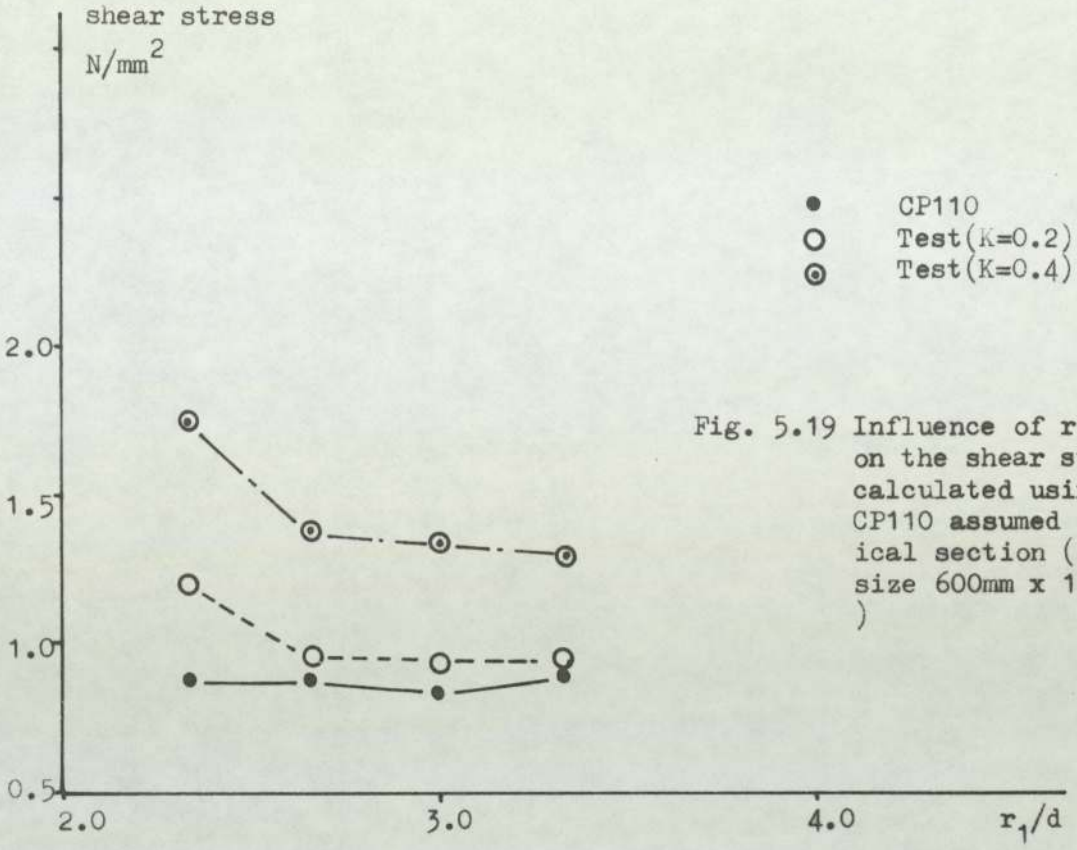

Fig. 5.19 Influence of r_1/d on the shear stress calculated using CP110 assumed critical section (slab size 600mm x 1200mm)

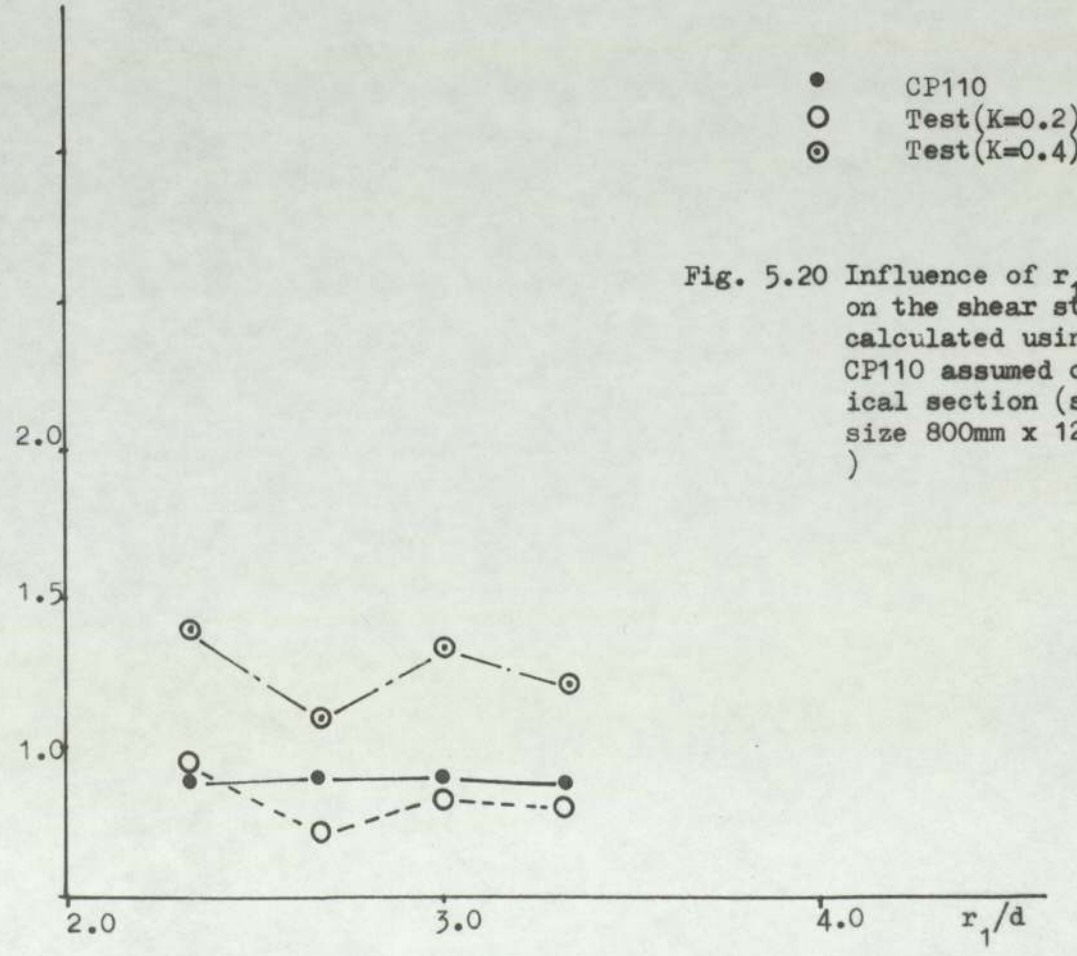

Fig. 5.20 Influence of r_1/d on the shear stress calculated using CP110 assumed critical section (slab size 800mm x 1200mm)

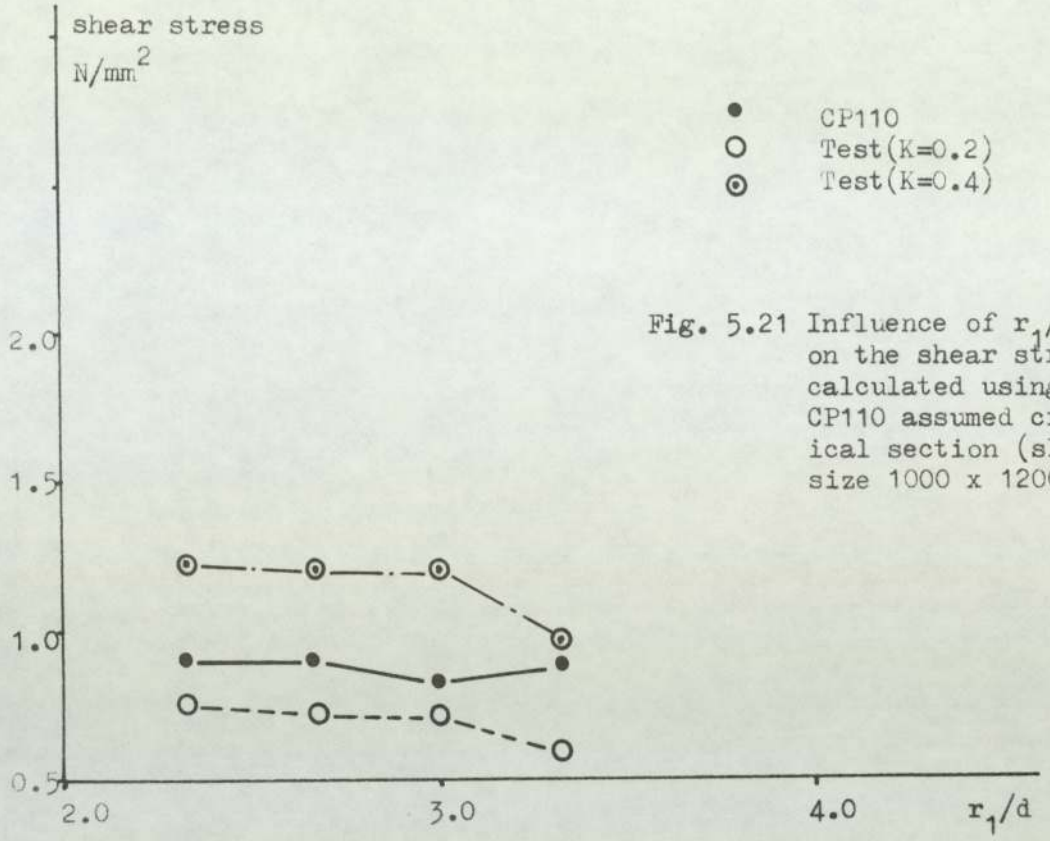

Fig. 5.21 Influence of r_1/d on the shear stress calculated using CP110 assumed critical section (slab size 1000 x 12000mm)

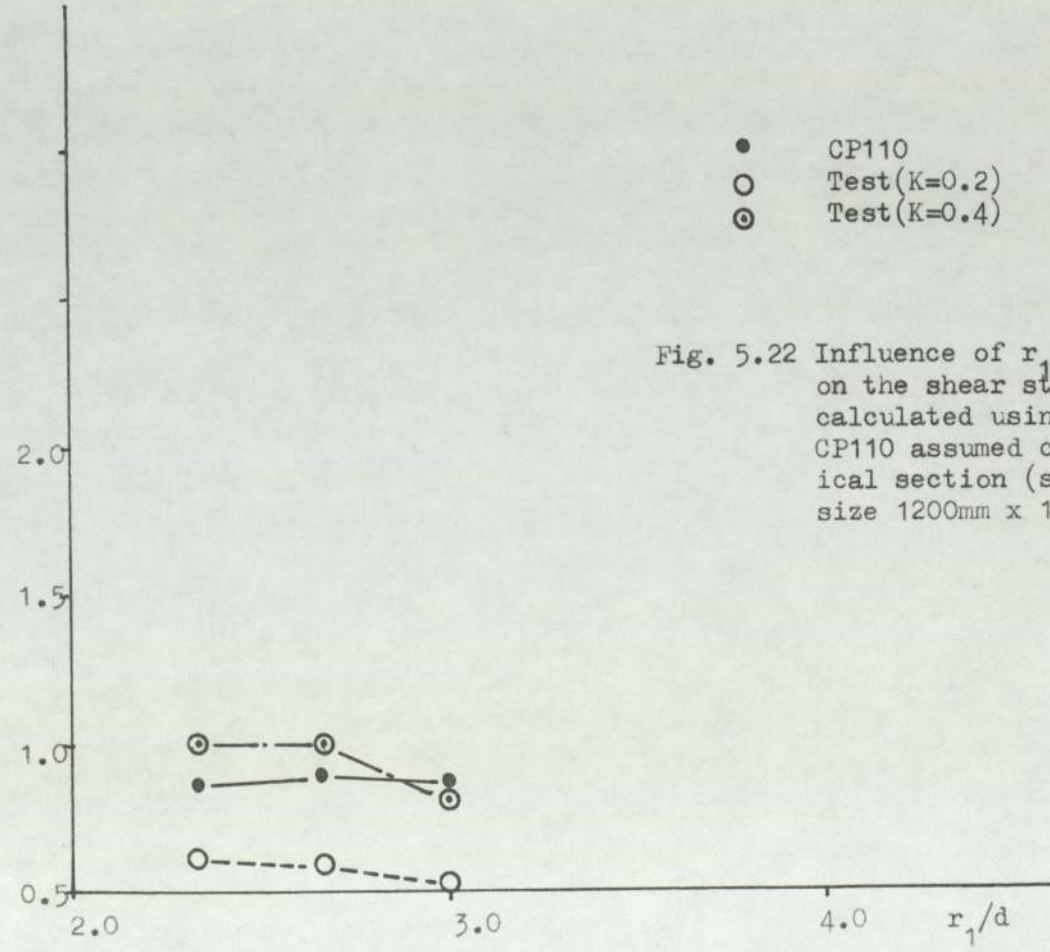

Fig. 5.22 Influence of r_1/d on the shear stress calculated using CP110 assumed critical section (slab size 1200mm x 1200mm)

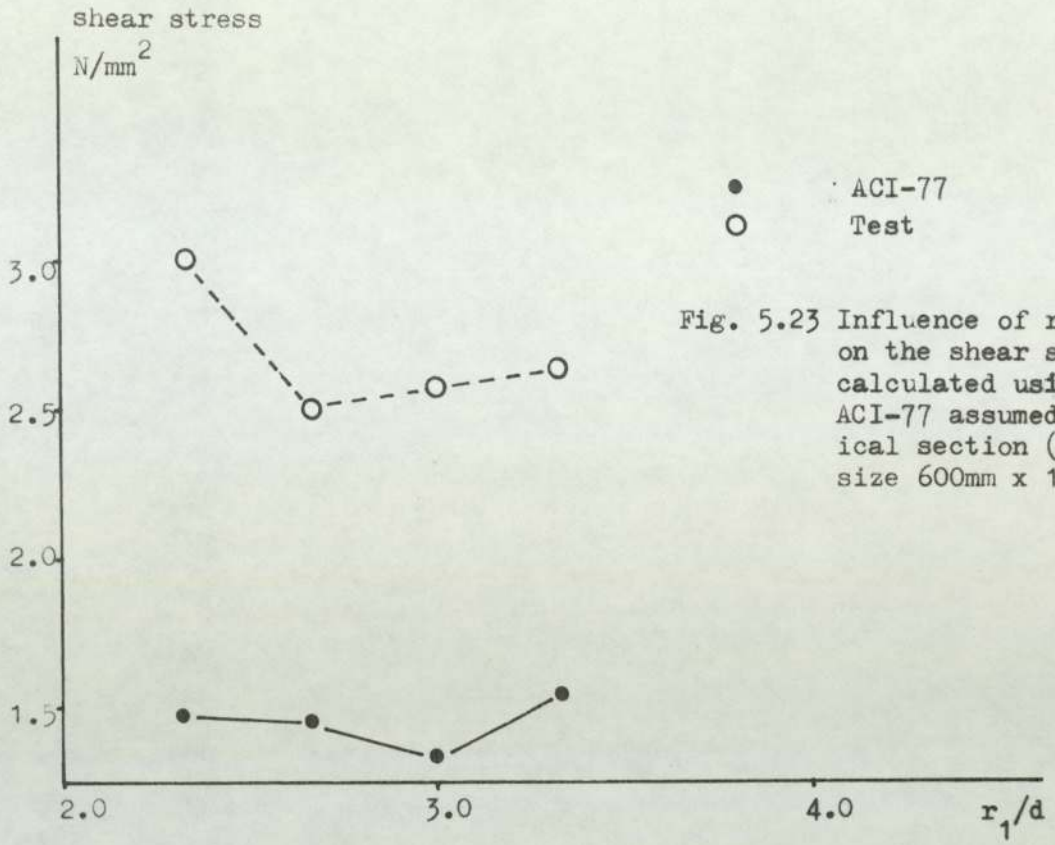

Fig. 5.23 Influence of r_1/d on the shear stress calculated using ACI-77 assumed critical section (slab size 600mm x 1200mm)

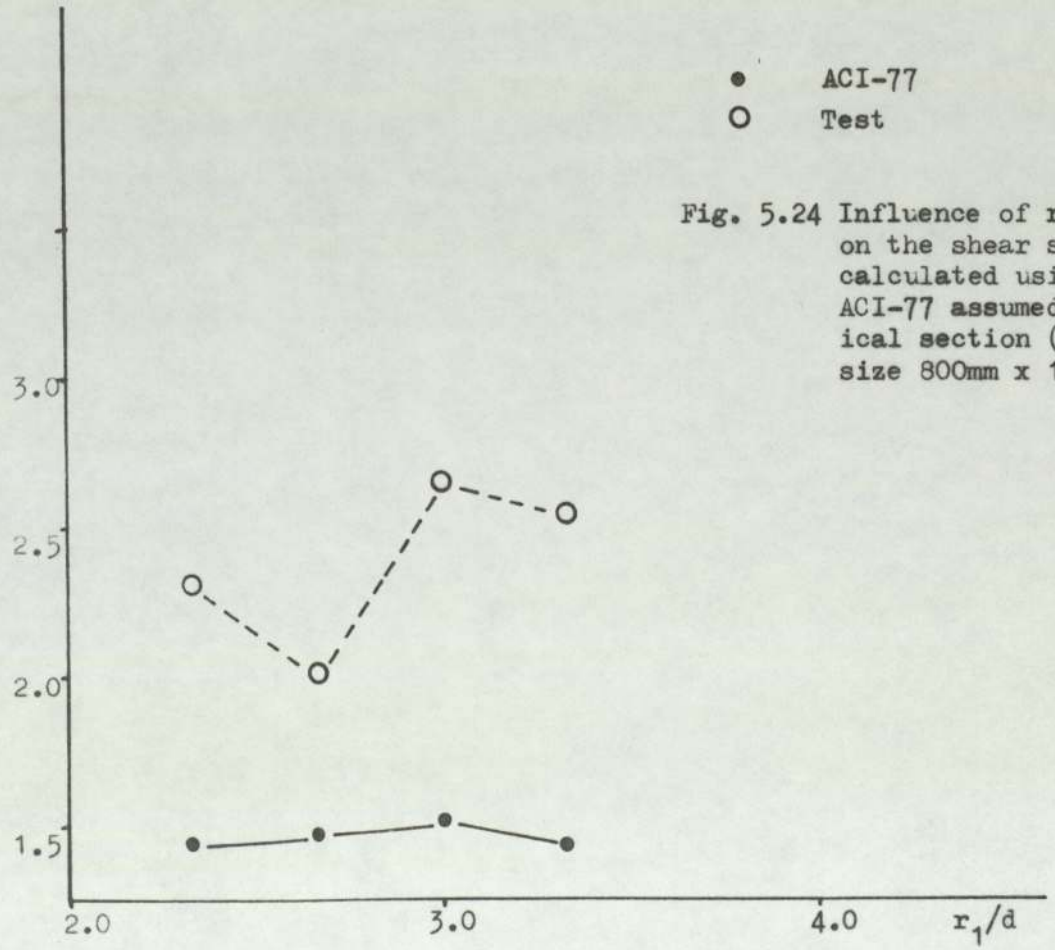

Fig. 5.24 Influence of r_1/d on the shear stress calculated using ACI-77 assumed critical section (slab size 800mm x 1200mm)

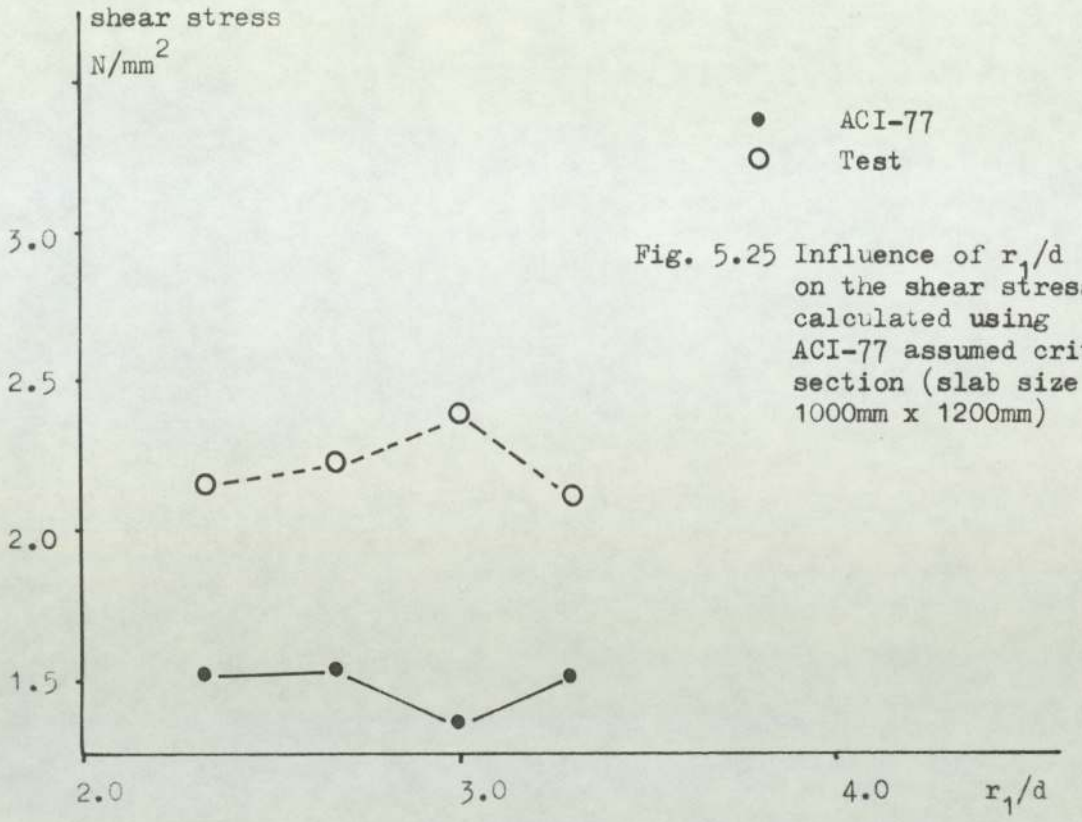

Fig. 5.25 Influence of r_1/d on the shear stress calculated using ACI-77 assumed critical section (slab size 1000mm x 1200mm)

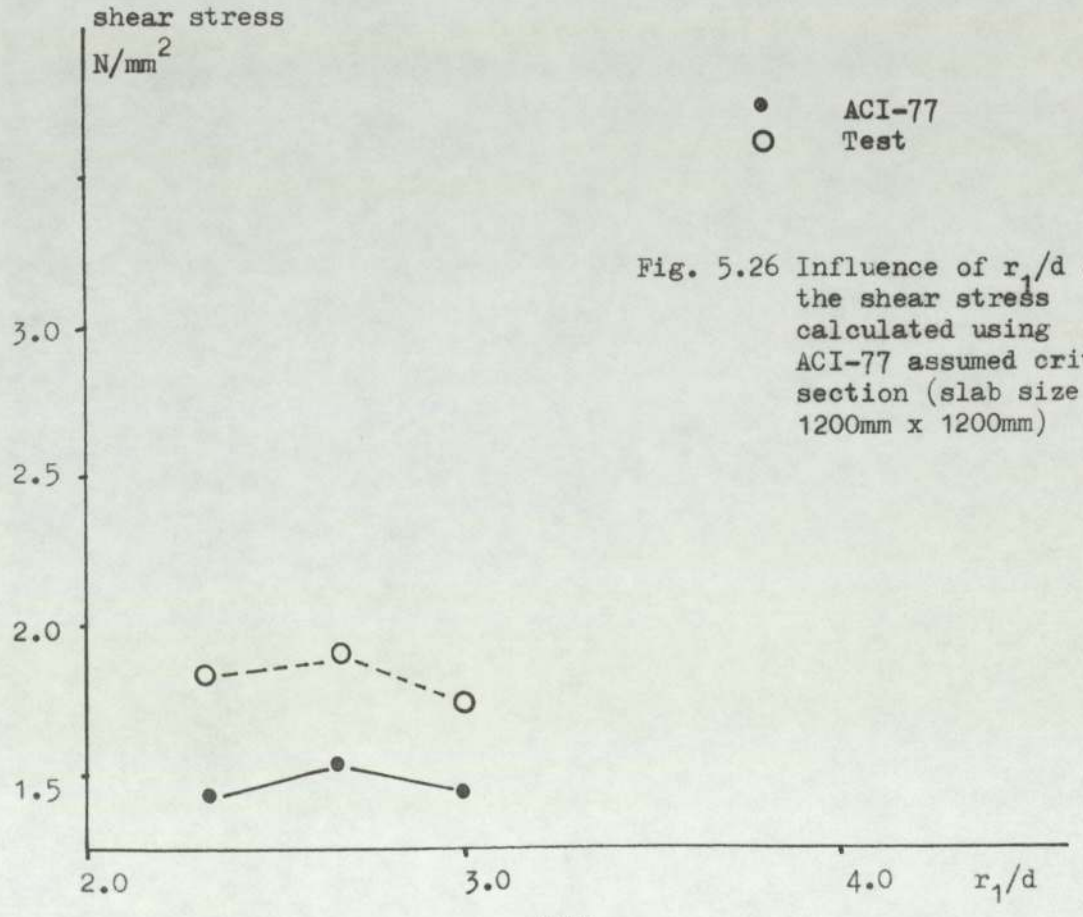

Fig. 5.26 Influence of r_1/d on the shear stress calculated using ACI-77 assumed critical section (slab size 1200mm x 1200mm)

5.1.6. Effect of $\frac{M}{V}$

From Figs. 5.27 to 5.34 the calculated ultimate shear stress decreases slightly as M/V increases. From these results it can be said that the current codes do not recognise the variation in the ultimate shear stress due to the variation in the M/V ratio.

5.1.7. Comparison with Regan's analysis for the edge connection.

To determine the punching resistance of an edge column, Regan used the following equation:

$$V_c' = 0.8\xi_s v_c b_p d \qquad (5.2)$$

where $b_p = b_o + 1.5\pi h$

He assumed that "The three-sides shapes of these perimeters are such as to offer very little bending stiffness, and it can be assumed that, so long as the combined flexural and torsional resistances are not exceeded, the shear distribution remains substantially uniform."

He supported this assumption by some test results from various sources as shown in Fig. 5.35. The moment resistances of this figure were calculated as

$$M_u = m_x b_y + 2\sqrt{m_x m_y}\, b_x$$

where M_u = ultimate bending resistance about an axis through the 'centre of gravity of the column perimeter

m_x, m_y = flexural resistance moments per unit width in x and y directions

$\sqrt{m_x m_y}$ = torsional resistance moments per unit width.

b_x, b_y = column dimensions.

By applying these equations on the present test results we find that these results give low shear strengths similar to the shear strengths obtained for the tests by Stamenkovic and shown in Fig. 5.35. This effect may be due to their small scale as suggested by Regan, h = 75 mm, and this scale is similar to Stamenkovic's scale (h = 76 mm).

5.2 Flexural Strength

5.2.1. General

The calculation of the ultimate flexural strength of the various test structures was made ignoring the possibility of a premature shear failure. The yield line theory as developed by K W Johanson[55] and discussed by others[56, 57, 58] was used for this purpose.

An evaluation of the strength of a test structure is important, not only because the computed or the observed strength of structures have general application to other structures of the same type, but also because a comparison of the computed and observed strength of the test structures is indicative of the reliability of the known methods of analysis in predicting the strength of relatively complex slabs.

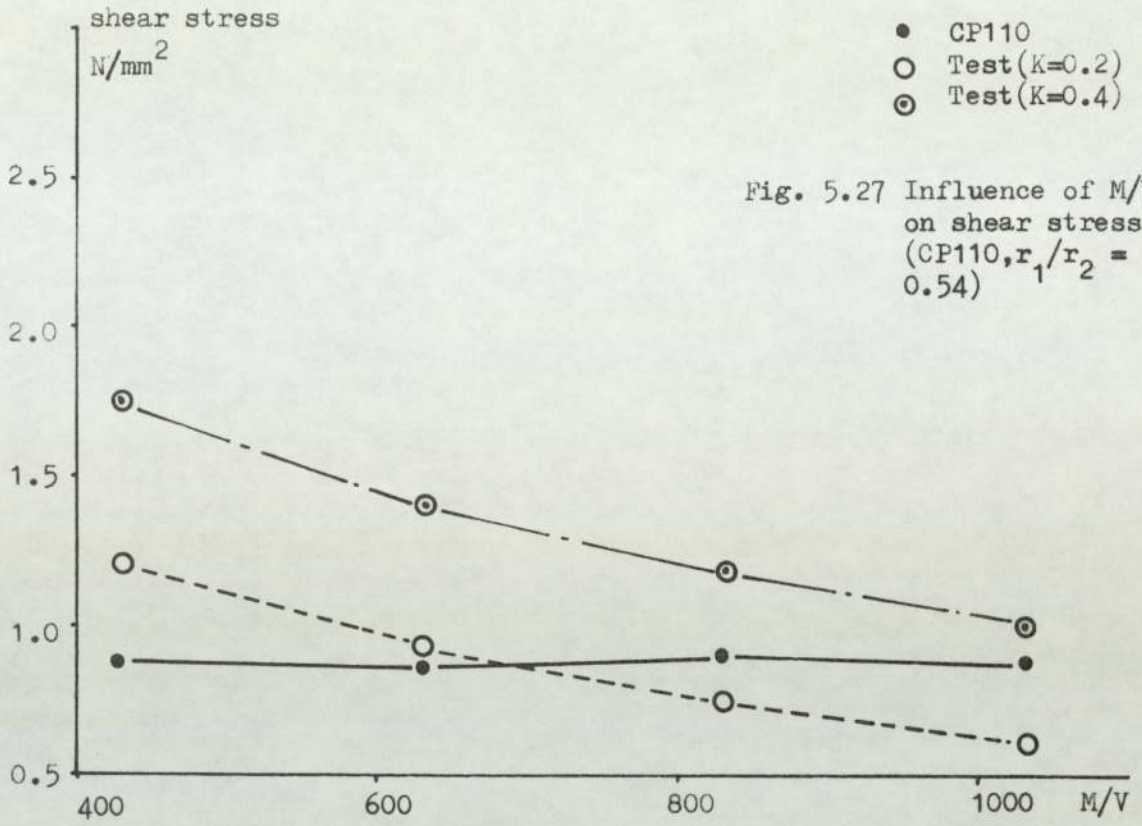

Fig. 5.27 Influence of M/V on shear stress (CP110, r_1/r_2 = 0.54)

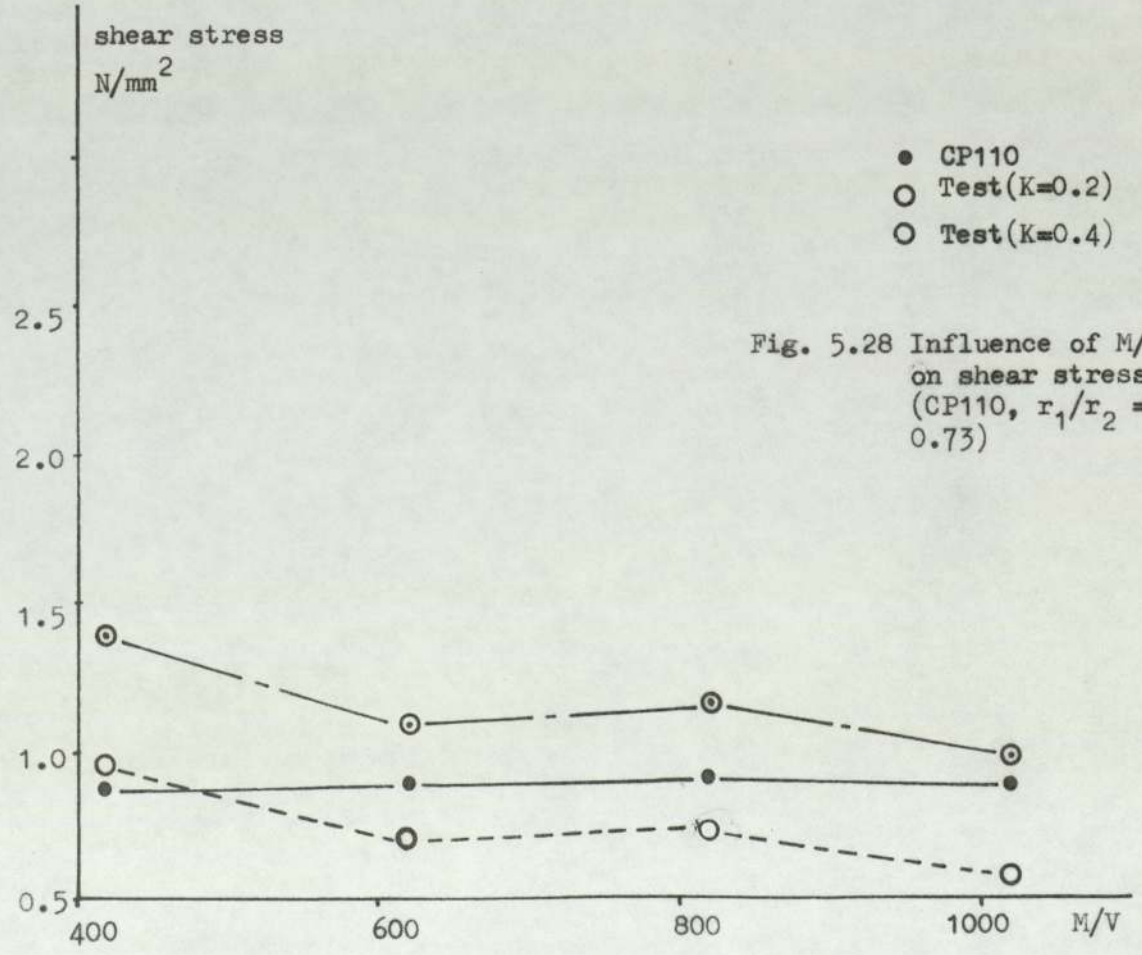

Fig. 5.28 Influence of M/V on shear stress (CP110, r_1/r_2 = 0.73)

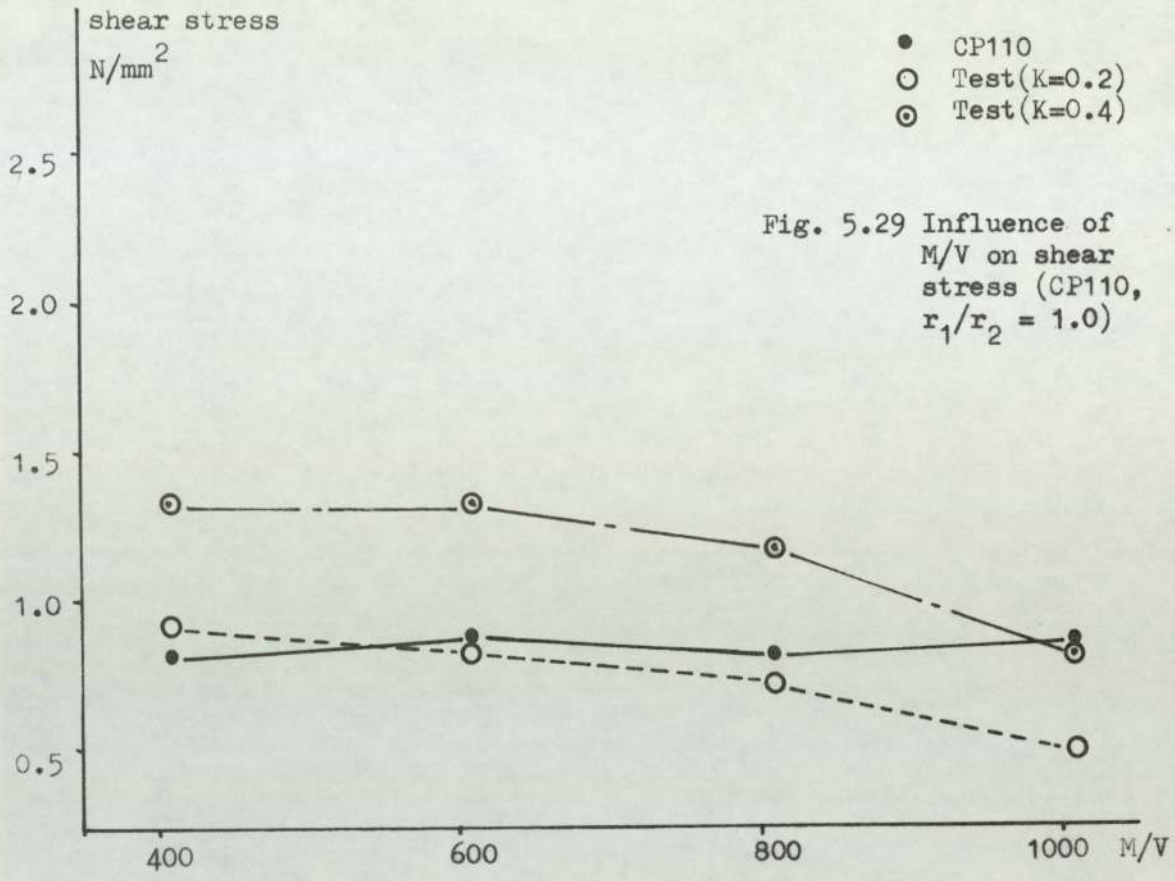

Fig. 5.29 Influence of M/V on shear stress (CP110, $r_1/r_2 = 1.0$)

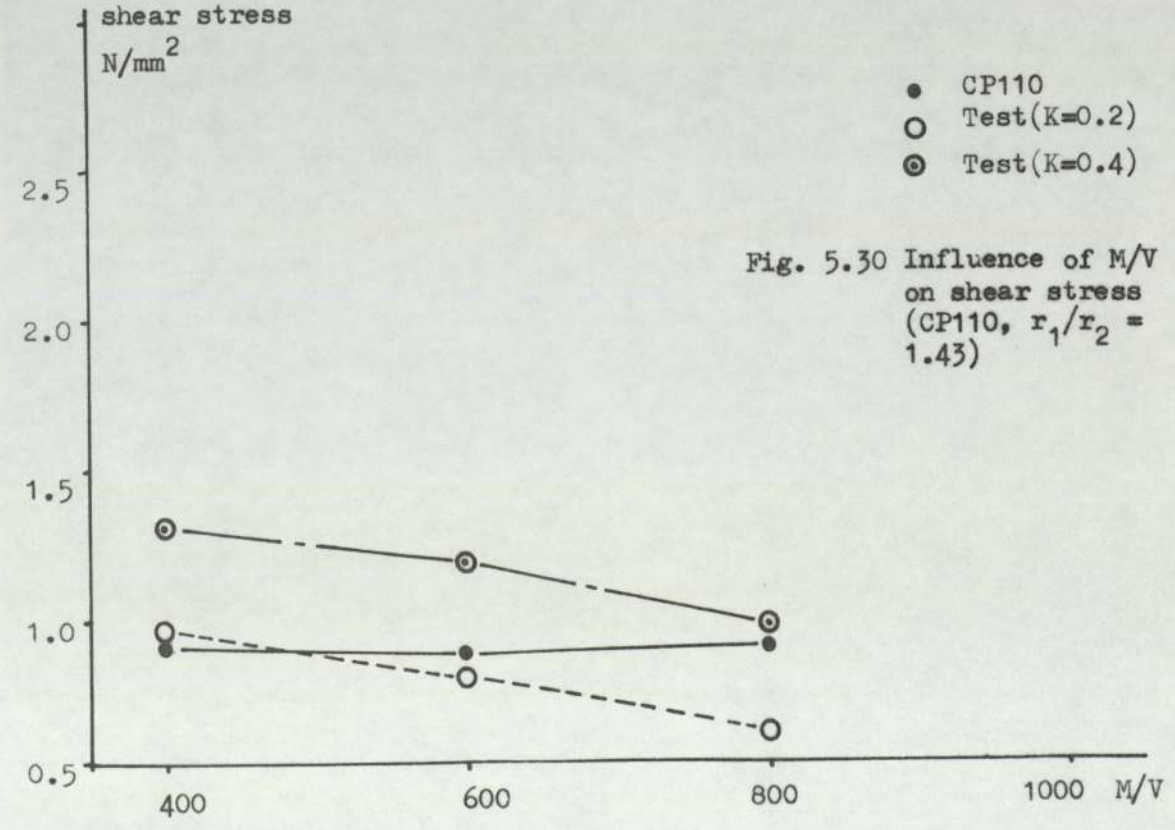

Fig. 5.30 Influence of M/V on shear stress (CP110, $r_1/r_2 = 1.43$)

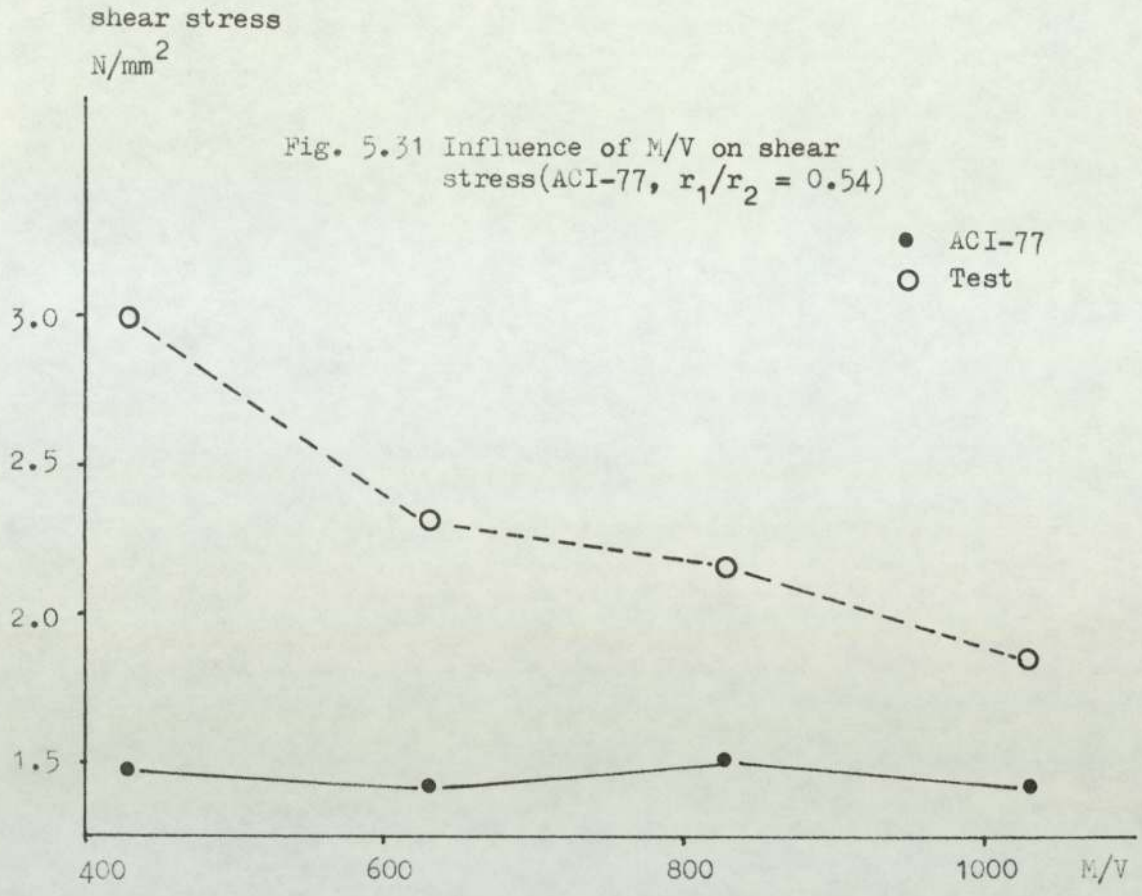

Fig. 5.31 Influence of M/V on shear stress(ACI-77, $r_1/r_2 = 0.54$)

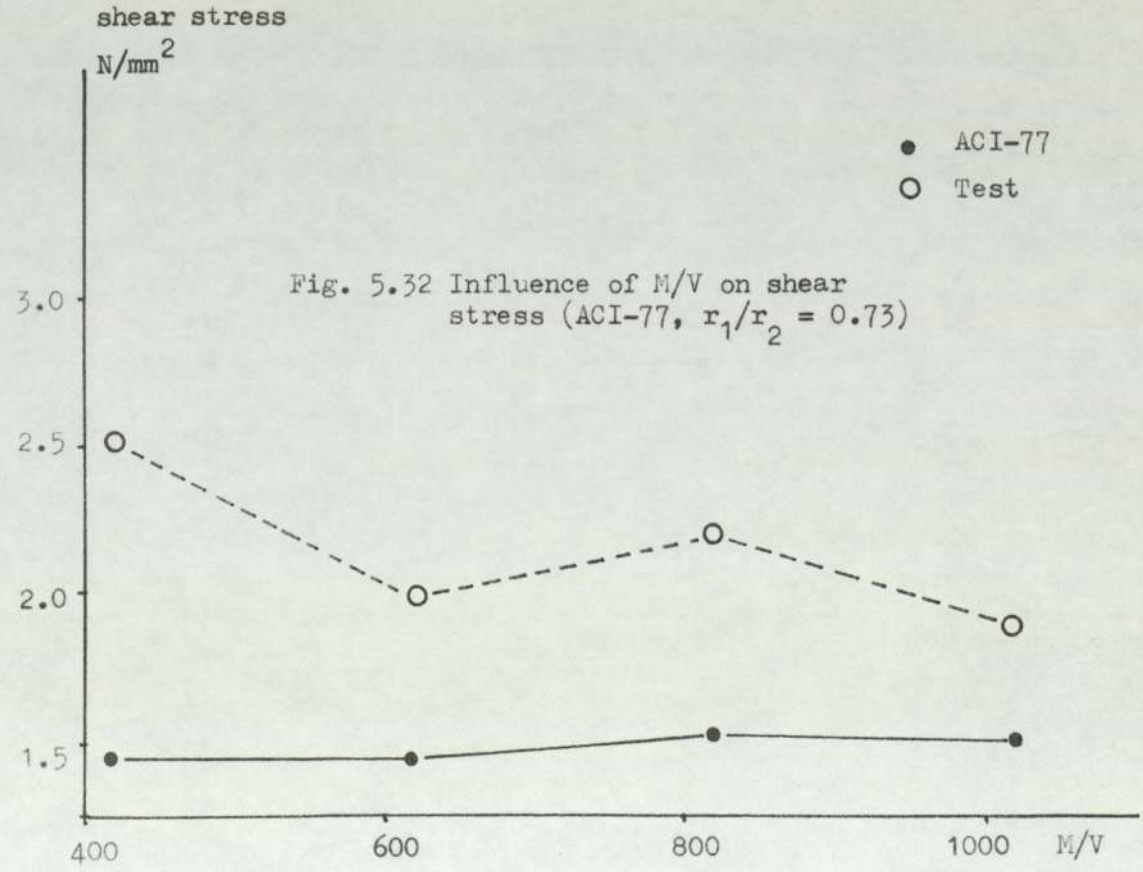

Fig. 5.32 Influence of M/V on shear stress (ACI-77, $r_1/r_2 = 0.73$)

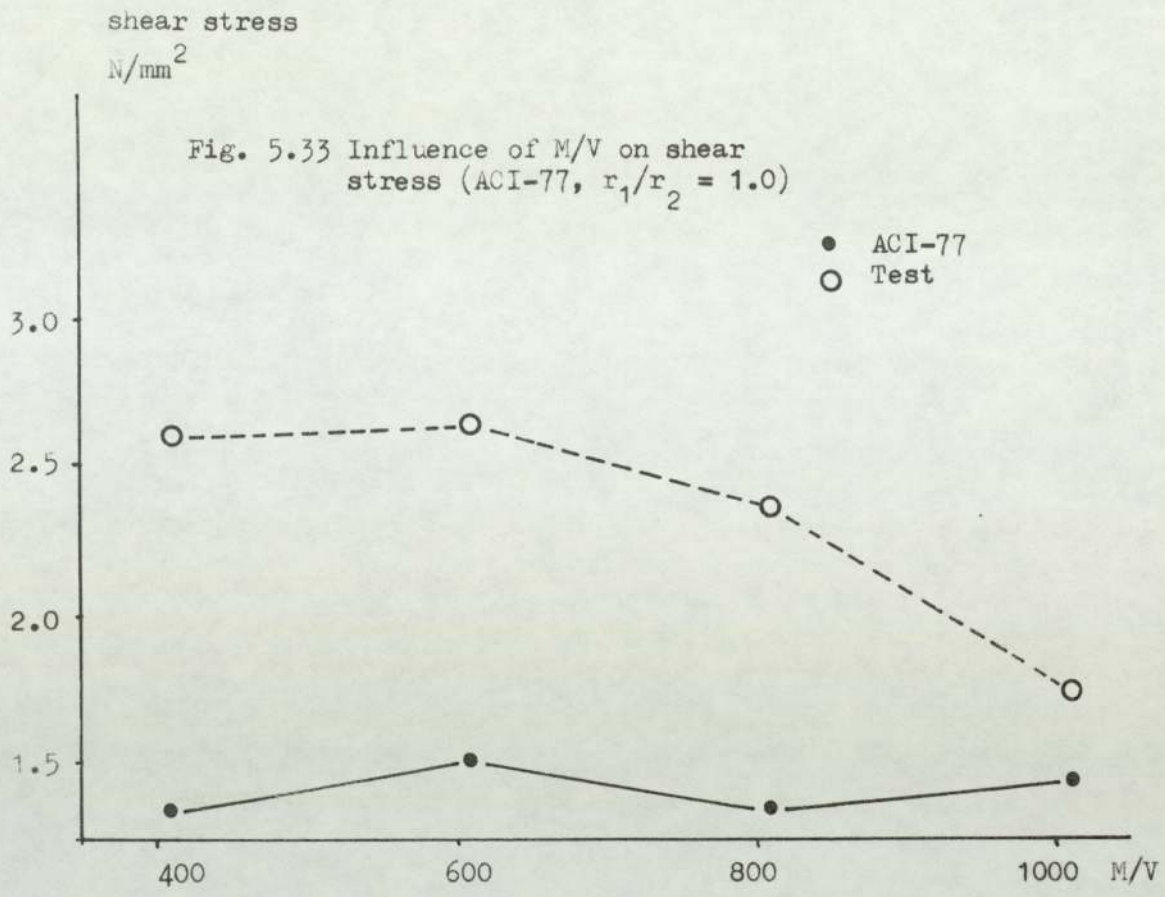

Fig. 5.33 Influence of M/V on shear stress (ACI-77, r_1/r_2 = 1.0)

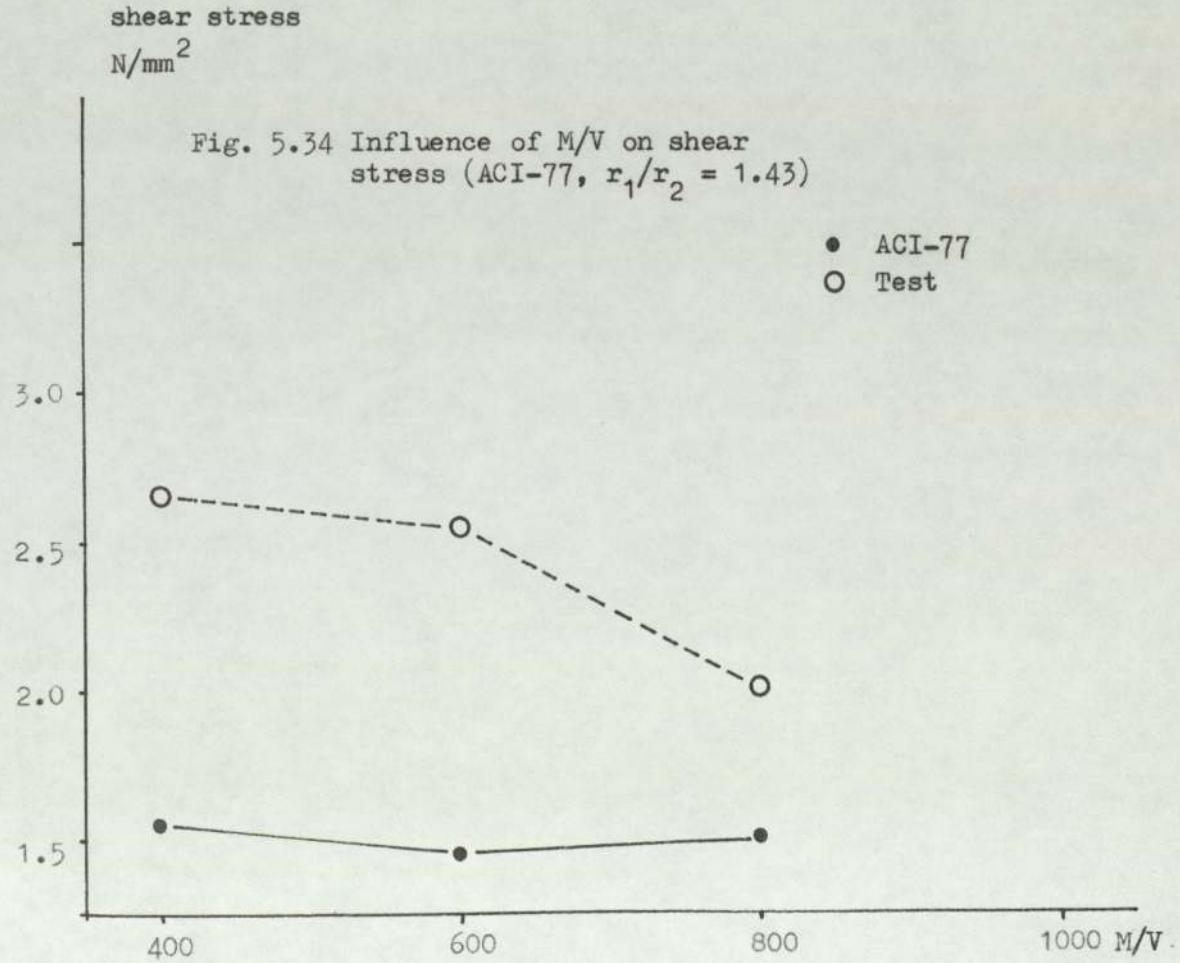

Fig. 5.34 Influence of M/V on shear stress (ACI-77, r_1/r_2 = 1.43)

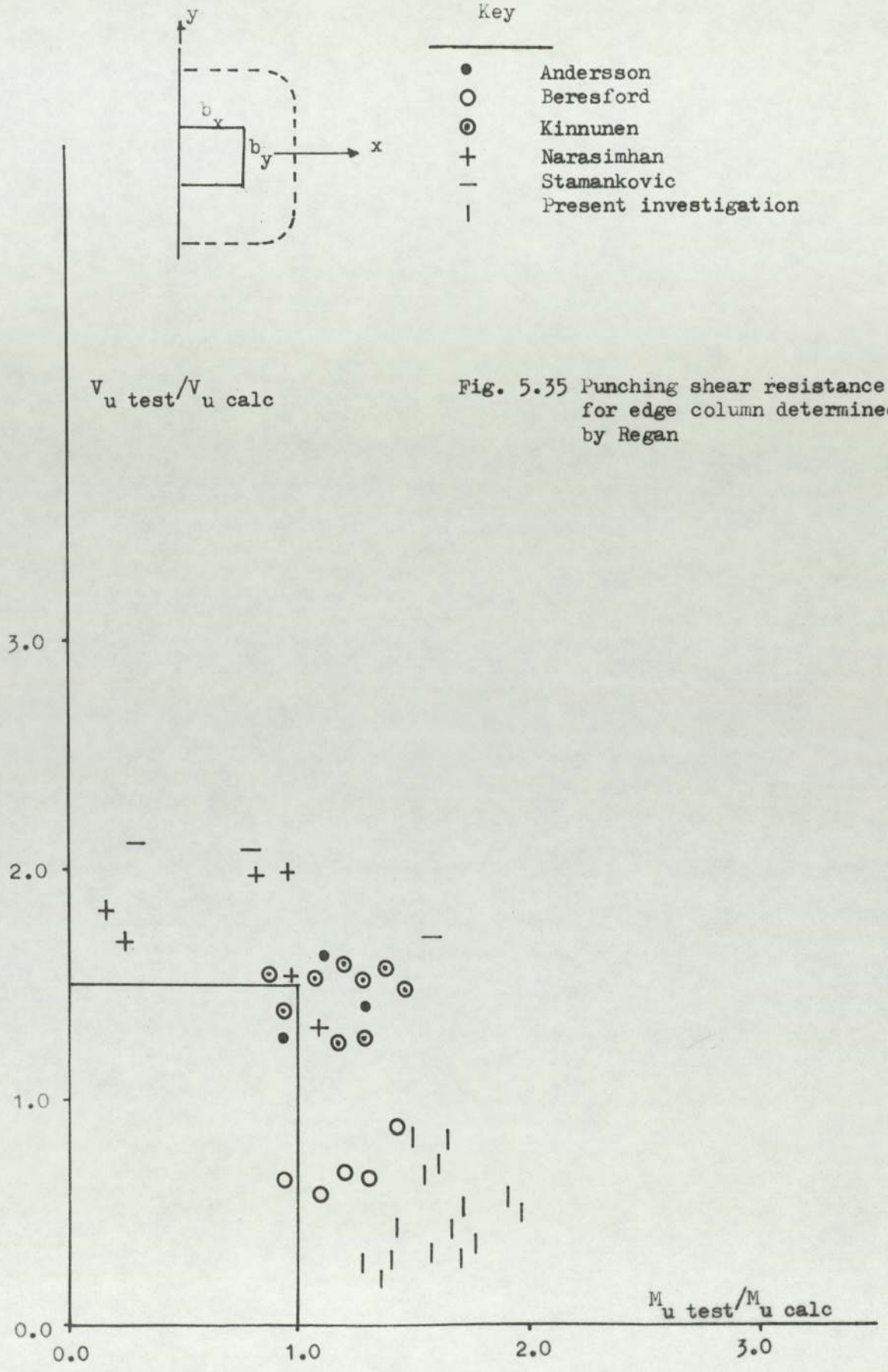

Fig. 5.35 Punching shear resistance for edge column determined by Regan

In applying the yield line theory, the yield moments of the slabs were based on the ultimate strength. Certain assumptions were applied in calculating the ultimate flexural capacities of the test structures.

5.2.2. Application of yield line analysis to the test structures.

To determine the collapse load of a given slab the sequence of the steps may be summarised as follows:

(1) A possible yield line pattern is adopted.

(2) The ultimate moment (m) per unit length is calculated for various yield lines.

(3) The collapse load (Wu) which corresponds to the assumed yield line pattern is calculated by the use of virtual work.

(4) The dimensions of the particular failure pattern are adjusted to minimise (Wu).

(5) Different trial yield line patterns are assumed and steps 2, 3 and 4 are repeated.

(6) Provided all possible collapse mechanisms (yield line patterns) have been investigated, the lowest computed value of (Wu) is theoretically the correct collapse load (because of the approximation in the theory).

The virtual work theorem states that the "external work" U_{ext}, and the "internal work", U_{int}, are equal. The term external work is the summation of the products of

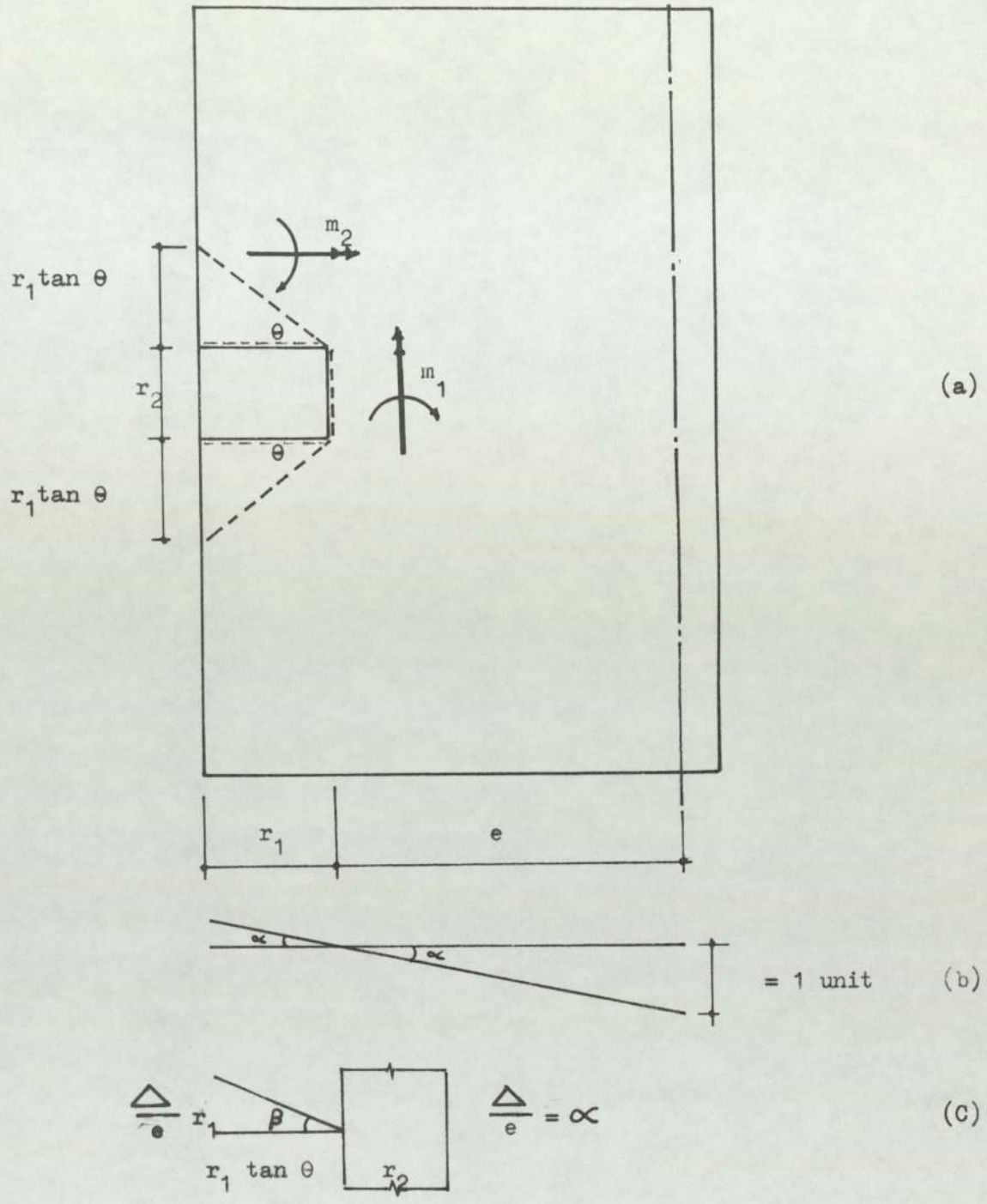

Note: The same layer of reinforcement used at the top and bottom of the slab.

Fig. 5.36 First yield line pattern

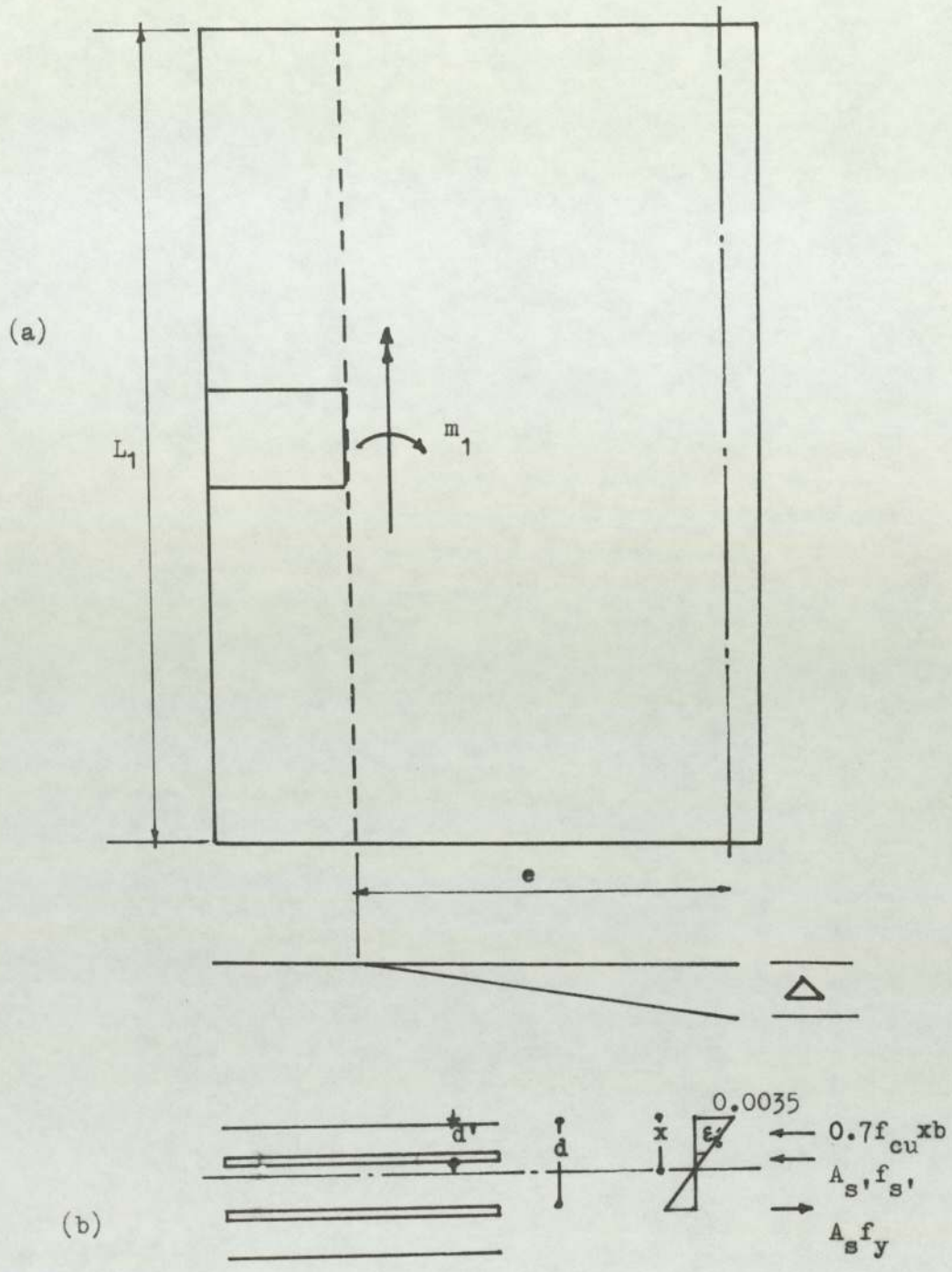

Fig. 5.37 Second yield line pattern

external forces and their conjugate displacements which arise from the virtual displacement system. The term internal work is the summation of the products of the internal stresses and displacements.

If a vertical load is applied on the free edge of a slab, then the possible failure patterns are as follows:

(1) The first yield line pattern is shown in Fig. 5.36 If the load is given a vertical deflection of unity, then the solution for the slab is obtained by following the above six steps.

To calculate the ultimate moment per unit length, the following method was used.

From Fig. 5.37(b) we have

$$\varepsilon'_s = \frac{x - d'}{x} \times 0.0035 \qquad (5.2)$$

$$A'_s f'_s + 0.7 f_{cu}.x.b = A_s f_y \qquad (5.3)$$

$$f'_s = E\varepsilon'_s \quad (\text{where } E = 213333 \text{ N/mm}^2) \qquad (5.4)$$

By solving these equations to find f'_s and x, the ultimate moment can be determined as:

$$M_u = 0.70 f_{cu}.x.b.(d-\frac{x}{2}) + A'_s f'_s (d-d') \qquad (5.5)$$

The external work of the slab is

$$U_{ext} = We\alpha \qquad (5.6)$$

The internal work is

$$U_{int} = m_1 r_2 \alpha + 2m_1 r_1 \tan\theta\alpha + 4m_2 r_2 \beta$$

where $\beta = \frac{\frac{\Delta}{e} r_i}{r_1 \tan\theta} = \frac{e\alpha}{e\tan\theta} = \frac{\alpha}{\tan\theta}$ (see Fig. 5.36(c))

By equating the external work to the internal work we obtain

$$w = \frac{m_1 r_2}{e} + \frac{2m_1 r_1 \tan\theta}{e} + \frac{4m_2 r_1 \cot\theta}{e} \qquad (5.7)$$

The minimum value of w can be found by differentiation

$$\frac{dw}{d\theta} = 0 + \frac{2r_1 m_2}{e} \sec^2\theta - \frac{4m_2 r_1}{e} \operatorname{cosec}^2\theta = 0$$

$$\therefore \quad \tan\theta = \sqrt{\frac{2m_2}{m_1}} \qquad (5.8)$$

Now substitute the values of m_1, m_2, θ, and f_y of each specimen into Eq. 5.7 to get the values of w.

(2) The second possible yield line pattern is shown in Fig. 5.37. By following the same steps as in (1) we obtain:

$$w = \frac{m_1 L_1}{e} \qquad (5.9)$$

5.2.3. Flexural strength of test structures

The two possible modes of failure shown in Figs. 5.36 and 5.37 were studied and the failure load (V_{flex}) and the ultimate capacity M_{flex} have been found. Clearly the smaller value of these two failure loads will be used.

The values of V_{flex}, M_{flex}, V_{test} and M_{test} are tabulated in Table 5.2 where M_{test} represents the maximum moment reached during testing.

SP.NO	F_y (N/mm^2)	M_1 (N-mm)	M_2 (N-mm)	e (mm)	V_{flex} (1) kN)	V_{flex} (2) (kN)	$\phi_0 = \frac{V_{test}}{V_{flex}(1)}$
1	414.42	29971.34	13541.89	360	65.96	99.90	0.61
2	299.60	22226.13	10230.79	560	31.64	47.63	0.79
3	335.46	24869.95	11457.10	760	26.10	39.27	0.67
4	375.60	27285.02	12371.81	960	22.55	34.11	0.55
5	329.22	24253.58	11124.10	340	59.42	85.60	0.55
6	341.63	25150.53	11524.85	540	38.78	55.89	0.52
7	326.36	24332.86	11235.21	740	27.46	39.46	0.64
8	358.60	26422.66	12135.10	940	23.43	33.73	0.53
9	352.20	25392.61	11395.10	320	68.41	95.22	0.48
10	327.98	24359.36	11238.25	520	40.83	56.21	0.61
11	379.84	27285.89	12135.03	720	32.56	45.48	0.55
12	354.38	25886.06	11807.14	920	24.41	33.76	0.45
13	375.60	27644.76	12691.96	300	83.54	110.58	0.38
14	381.96	27720.89	12541.60	500	49.95	66.53	0.46
15	333.16	24706.18	11387.62	700	32.05	42.35	0.47

Table 5.2 A Flexural capacities

SP. NO.	$r_1 \times r_2$	V_{test} (kN)	r_1/r_2	r_1/d	M_{flex} kN - mm	$M_{test}=Ve$ kN - mm	$\frac{M_{test}}{M_{flex}}$
1	140 x 260	40	0.54	2.33	17676.0	15852.0	0.89
2	"	25	"	"	12768.0	14907.5	1.16
3	"	17.5	"	"	14288.0	13935.25	0.97
4	"	12.5	"	"	16032.0	12453.75	0.77
5	160 x 220	32.5	0.73	2.67	14314.0	12590.5	0.88
6	"	20.0	"	"	14310.0	11748.0	0.82
7	"	17.5	"	"	14208.0	13779.5	0.97
8	"	12.5	"	"	15604.0	12342.5	0.79
9	180 x 180	32.5	1.00	3.00	15616.0	12350.0	0.79
10	"	25	"	"	14560.0	14500.0	0.99
11	"	18	"	"	16848.0	14640.0	0.83
12	"	11	"	"	15640.0	10780.0	0.69
13	200 x 140	32	1.43	3.33	16980.0	11971.2	0.71
14	"	23	"	"	17250.0	13204.3	0.76
15	"	15	"	"	15050.0	11611.5	0.77

Table 5.2 B Flexural Capacities

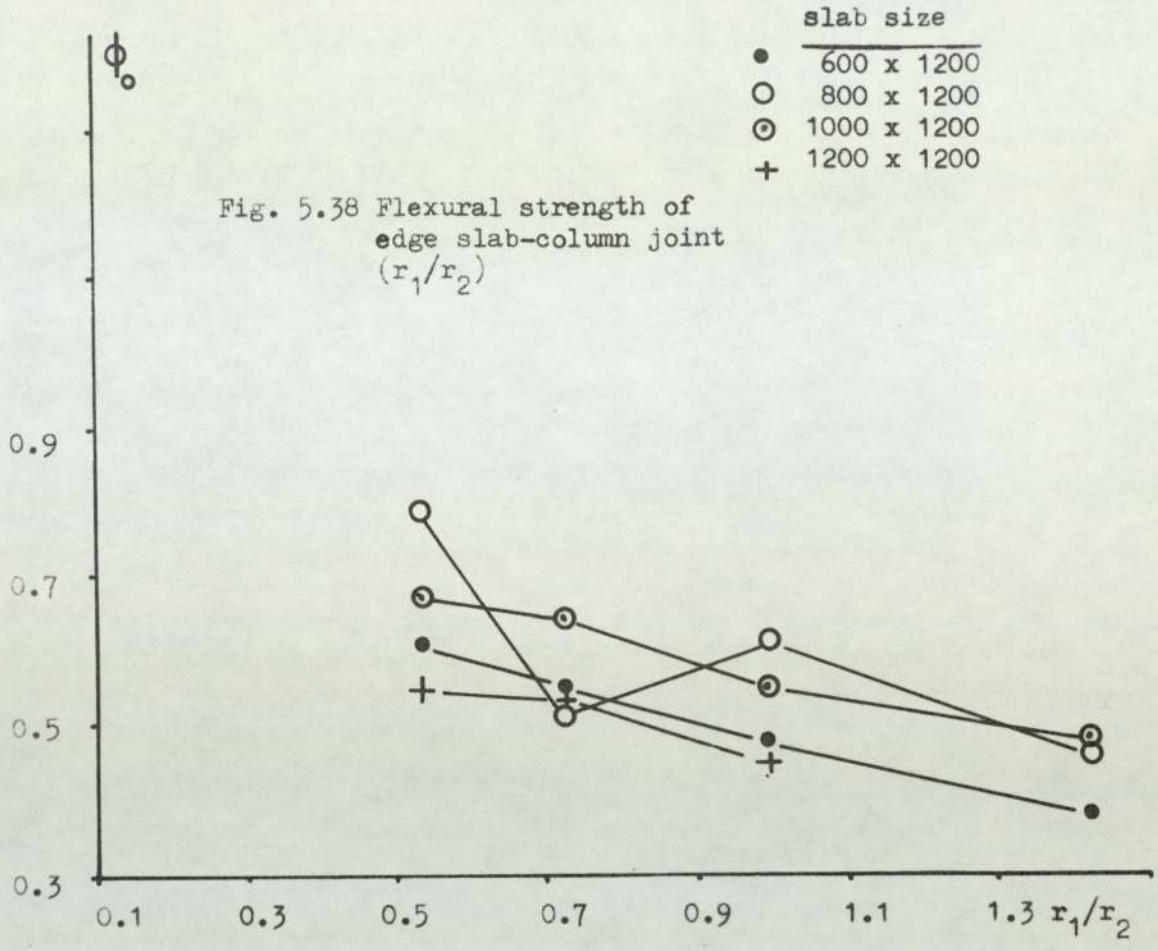

Fig. 5.38 Flexural strength of edge slab-column joint (r_1/r_2)

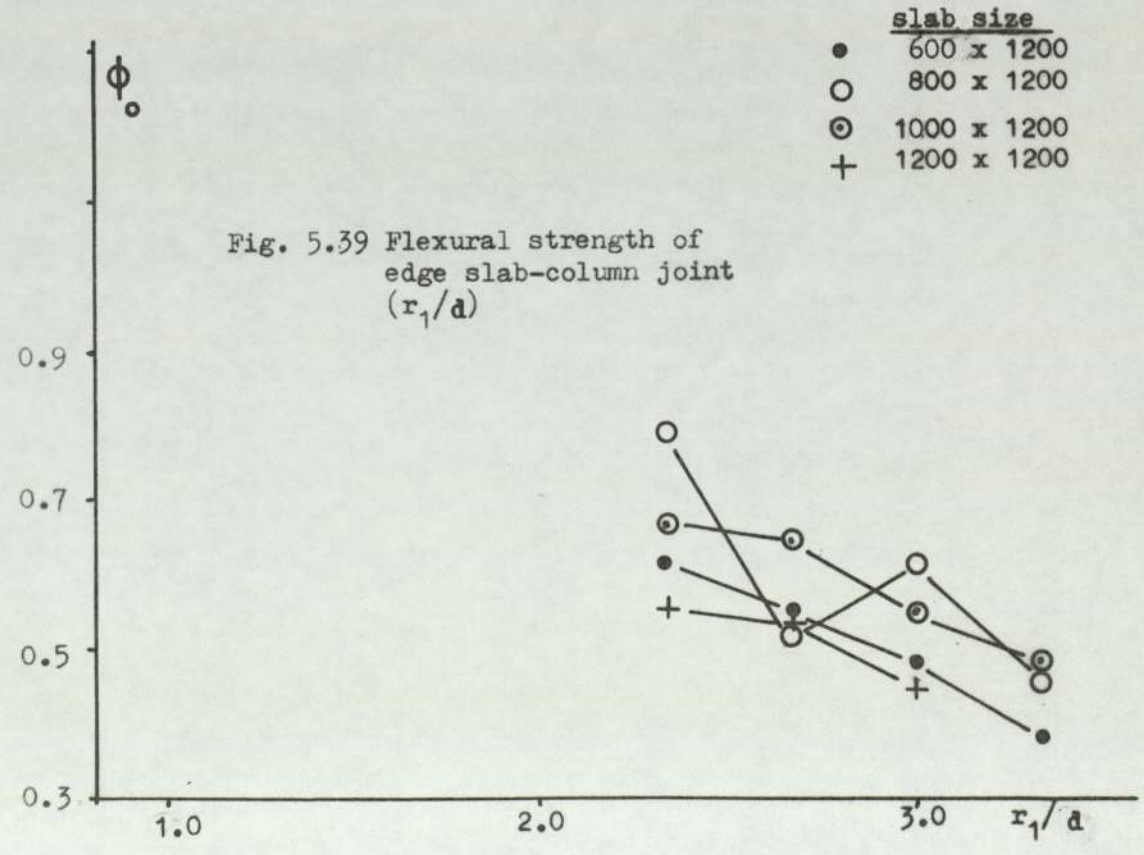

Fig. 5.39 Flexural strength of edge slab-column joint (r_1/d)

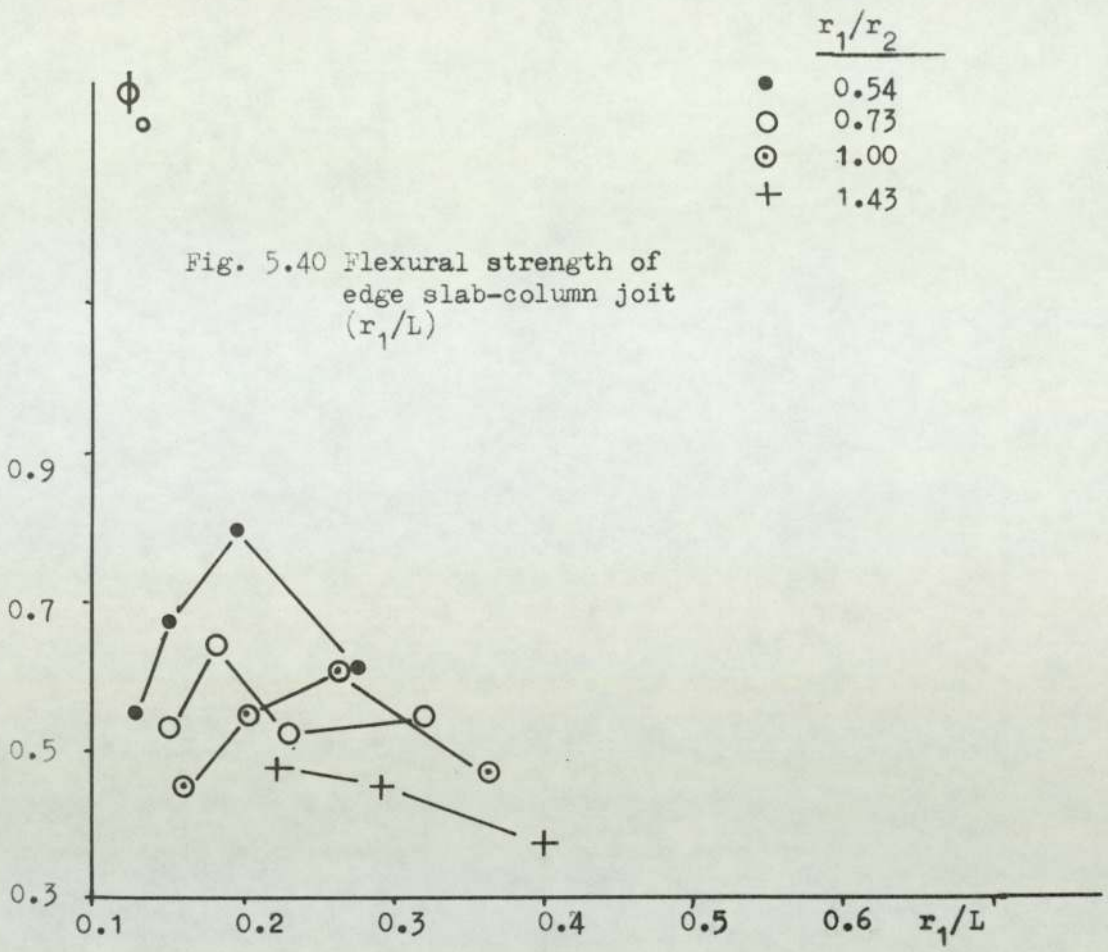

Fig. 5.40 Flexural strength of edge slab-column joit (r_1/L)

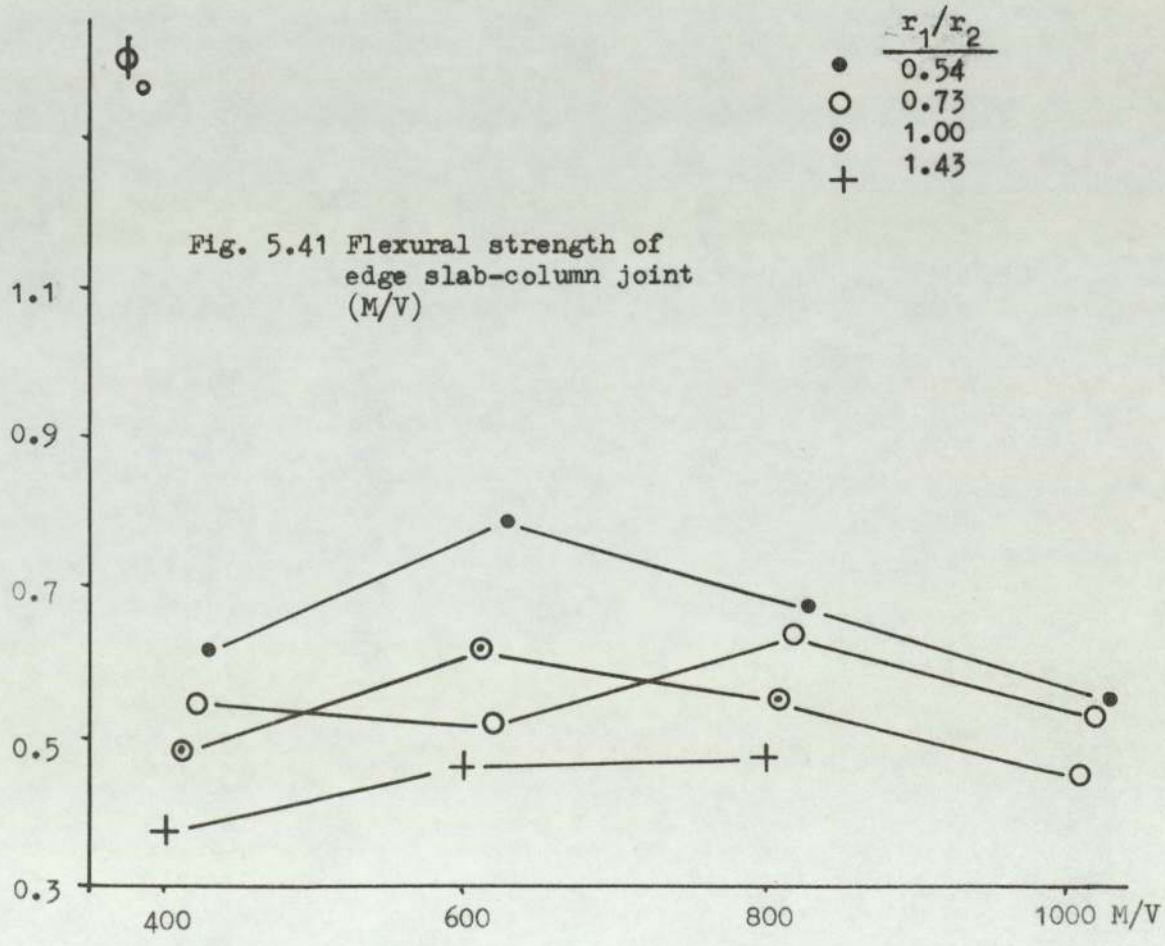

Fig. 5.41 Flexural strength of edge slab-column joint (M/V)

5.2.4. Comparison with test results

In this section the ultimate theoretical load capacity of the slab obtained from the yield line theory as described before is compared with the test ultimate capacity of the connection. ϕ_0 as shown in Table 5.2 is plotted against r_1/r_2, r_1/d, r_1/L and M/V in Figs. 5.38, 5.39, 5.40 and 5.41 respectively; where ϕ_0 is the ratio of test ultimate strength to the theoretical ultimate strength of the slab.

As shown in Fig. 5.38, for all specimens, ϕ_0 decreases as r_1/r_2 ratio increases. It appears that as r_1/r_2 ratio increases the ultimate flexural strength of the connection becomes overestimated by greater amounts. This case is the same for ϕ_0 against r_1/d (see Fig. 5.39).

In Fig. 5.40, where ϕ_0 has been drawn against r_1/L, for both low and high values of r_1/L, ϕ_0 is nearly the same, but for intermediate values of r_1/L, ϕ_0 is relatively high, which indicates that the ultimate flexural strength is overestimated specially for low and high values of r_1/L. The same conclusion can be drawn in the case of ϕ_0 drawn against M/V ratio (see Fig. 5.41).

5.3 Summary

The following conclusions from this chapter can be drawn:

(1) "k" factor was used equal to 0.4 by Hanson and

Hanson[12], in equation no. 5.1. For most specimens this value gives safe results when used with CP110 stresses and failure plane. In only one case does it give a slightly low safety factor (0.97).

(2) Equation 5.1 appears not to fully describe the failure since a constant shear stress is not obtained when using it. The calculated shear stress is higher for small eccentricities than it is for large eccentricities.

(3) The method proposed by Regan and adopted in part by CP110 appears to give safe results, although the margin of safety is very variable.

(4) The values of $\frac{M_{test}}{M_{flex}}$ and the values of ϕ_0 as shown in Table 5.2 for all specimens are less than unity. This indicates that the ultimate flexural strength is overestimated by a considerable margin for all specimens. The yield line method is therefore not suitable for the calculation of the strength of such joints, and some method which takes more account of shear would be better.

CHAPTER VI

ANALYSIS FOR ULTIMATE STRENGTH AND COMPARISON WITH TEST RESULTS

6.1 General

An ultimate strength procedure is derived for determining the shear and unbalanced moment capacity of exterior column-slab junctions. This theory is based on an extension of previous investigations. The strength of such junctions as predicted by the theory is shown to give good agreement with test results.

6.2 Introduction

In most cases the strength of flat plate column junctions without any shear reinforcement is governed by a shear-flexure failure on some critical section surrounding the column before the formation of the complete yield line pattern for the slab. On this critical section the applied shear and unbalanced moment are resisted by three actions within the slab, namely (i) flexure, (ii) shear, and (iii) torsion. The theory for the failure mode is based on the evaluation of these three quantities which are obtained from the results and previous investigations.

Fig. 6.1 shows the portion of a flat plate surrounding an exterior column. Let V be the resultant shear and M the unbalanced moment about the x-x axis acting on the

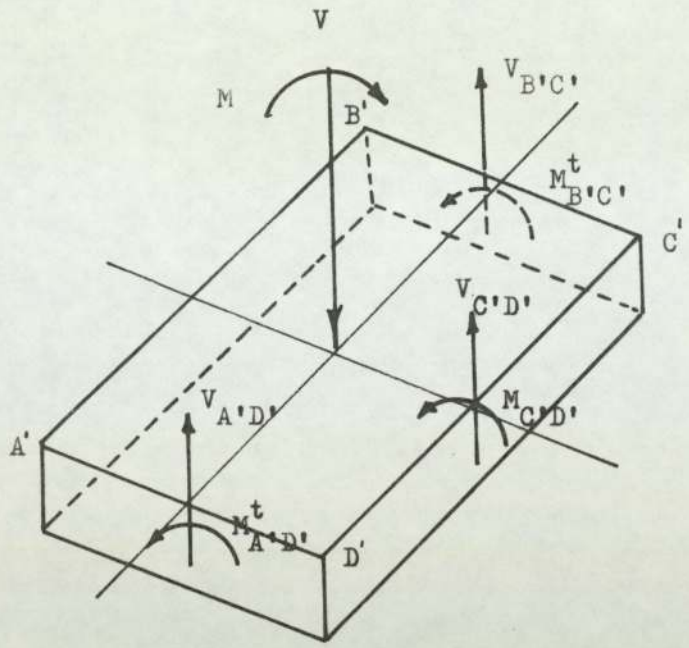

A D C B = column perimeter

A'D'C'B' = the assumed shear plane perimeter

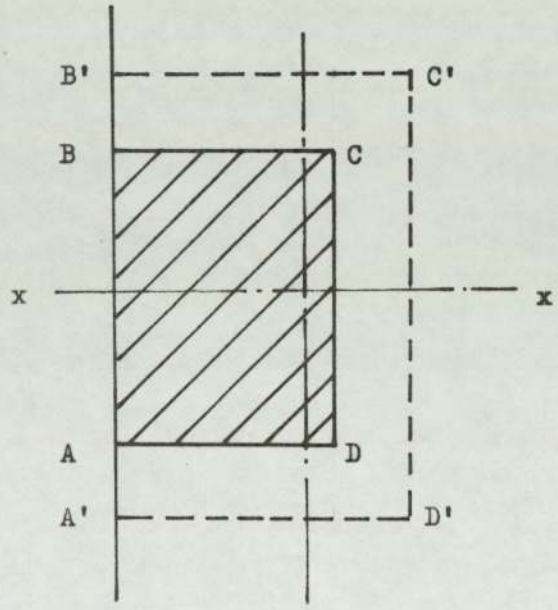

Fig. 6.1 Critical section for the shear stress of an edge slab-column junction

centroid of the slab-column junction at ultimate loading conditions. The forces and moments acting on a critical section A'B'C'D' within the slab and contributing to the transfer of the shear V and the moment M are indicated in the figure.

The unbalanced moment M is transferred by three actions, namely (i) flexure on face C'D', (ii) vertical shear on face C'D', and (iii) torsion on faces A'D' and B'C'.

The individual contributions of these actions will be determined and summed to obtain the total unbalanced moment that can be transferred with shear force at the edge column-slab junction.

The distribution of stresses in the slab around the column at the ultimate load is very complex. Mast[47] has obtained the distribution of stresses in flat plate near columns due to the moment transfer in accordance with the theory of elastic plates. This elastic stress distribution does not apply at the ultimate load because of the effect of inclined cracking in the slab around the column, which has been ignored in the theory, and is likely to alter the stress distribution; additionally the elastic theory does not account for the influence of the slab reinforcement and the concrete does not behave as an elastic homogeneous material at ultimate load. Because of this complex behaviour it is necessary to make some simplifying assumptions in order to derive design equations.

6.3 Assumptions and Prediction of Strength of Edge Column-slab Connection.

In this section a method is proposed for predicting the strength of the edge column-slab connection in flat plate slabs under combined shear and unbalanced moment loadings.

In Moe's method the ultimate strength analysis was developed by assuming that the critical section is directly adjacent to the periphery of the column and that failure takes place when the maximum shear stress reaches a limiting value equal to the shear strength of the same connection under concentric load. For an interior square column and slab connection subjected to combined bending moment M and vertical shear force V the ultimate vertical shear stress is given in Eq. 5.1 as

$$v_u = \frac{V}{A_c} + \frac{kMC}{I_c}$$

in which $A_c = bd$, and $I_c = (2/3)r^3d$, b = the perimeter of the column; r = the column width; C = one half the width of the column, and k = a moment reduction factor which accounts for that part of the shear which is resisted by bending moments and torsional moments acting at the column and slab intersection. Moe determined the constant k experimentally and found that the best correlation with his test results is obtained for $k = 1/3$.

In considering the strength of the edge column-slab

connections under the action of shear and biaxial moment, it is assumed that the critical section is located at a distance equal to half the effective depth of the slab from the periphery of the column, and, as was done by Moe, that failure takes place when the maximum shearing stress reaches a limiting value equal to the shearing strength of the same connection under concentric load. The limiting ultimate shearing stress under concentric load was calculated using the equation

$$v_{(psi)} = \frac{V}{b_o d} = \frac{15(1-0.075\frac{r}{d})\sqrt{f'_c}}{1+5.25\frac{bd\sqrt{f'_c}}{V_{flex}}} \qquad (6.1)$$

Equation 6.1 was chosen for development because of the following:

(1) This equation was found to give good results.

(2) The shear strength of a flat plate was found, as in Moe's investigations, to be affected by the ratio of column side to slab thickness.

(3) The shear strength of a flat plate is dependent upon the flexural strength.

The value of V_{flex} in equation 6.1 was calculated for the test structures by means of the yield line theory according to the modes of failure discussed in Chapter V. The application of this method, with some developments, to

the test structures will be discussed in the following sections. Note that Equation 6.1 was used after conversion to SI units, therefore it becomes:

$$v_u \text{ (N/mm}^2\text{)} = \frac{1.244\left(1-0.075\,\frac{r_1}{d}\right)\sqrt{f'_c}}{1+0.435\,\frac{b_0 d\sqrt{f'_c}}{V_{flex}}} \qquad (6.1A)$$

v_u in N/mm^2

f'_c in N/mm^2

r_1, b_0, d in mm

V_{flex} in N

6.3.1. Prediction of strength of edge column-slab connection

Referring to Fig. 6.1 which is a plan of an edge column-slab connection in a flat plate floor slab, the connection is subjected, in addition to the axial shear force, to unbalanced moment M. As mentioned before, this moment is balanced by torsional moment, vertical shear stresses and flexural moment of the slab at the critical section. The effective depth of the critical section for shear is equal to the effective depth, d, of the slab at that section.

To obtain a semi-empirical formula by which the ultimate shear strength can be predicted, the balance of the above-mentioned forces has to be achieved as follows.

Equilibrium condition in the x-direction in Fig. 6.1 gives:

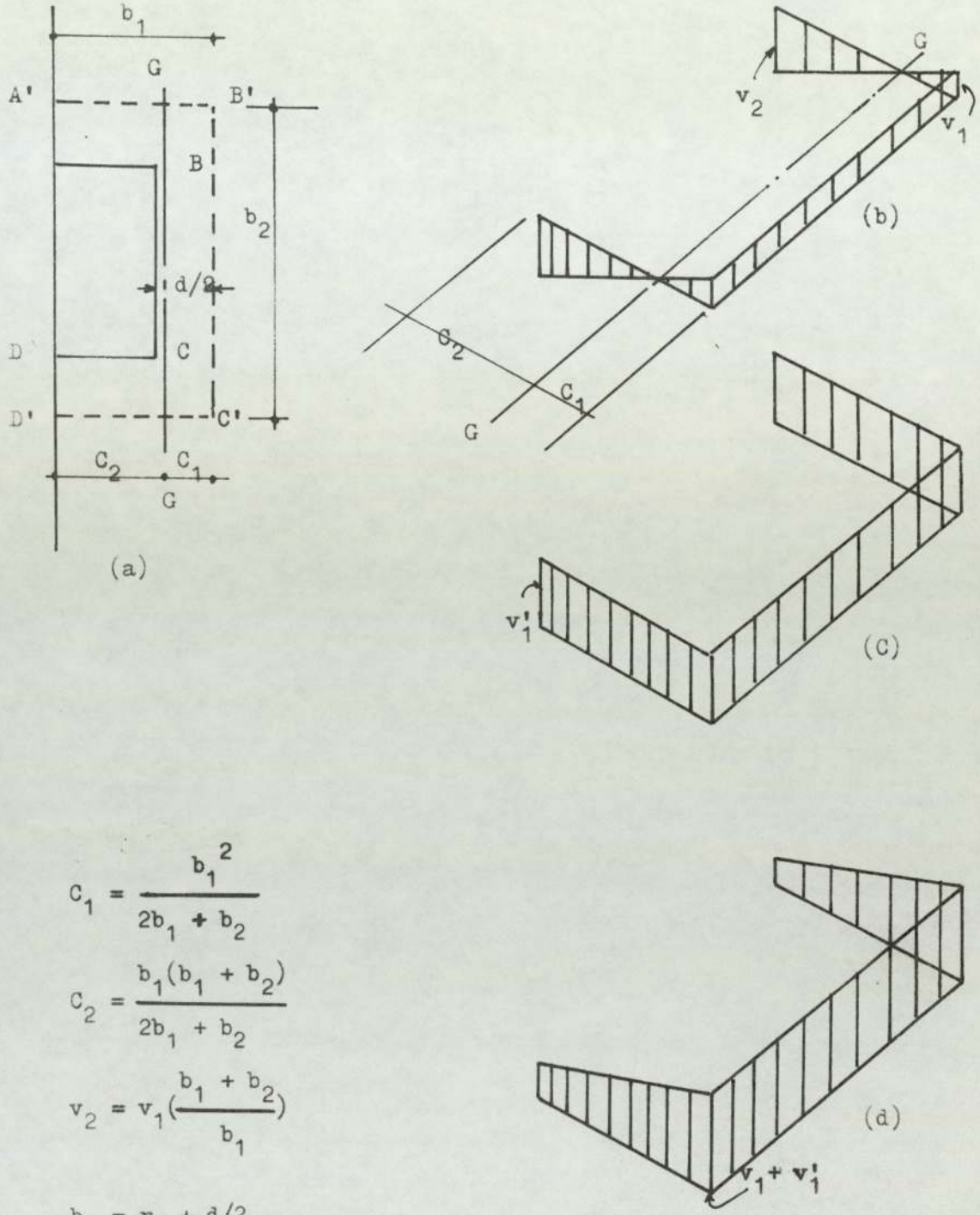

$$C_1 = \frac{b_1^2}{2b_1 + b_2}$$

$$C_2 = \frac{b_1(b_1 + b_2)}{2b_1 + b_2}$$

$$v_2 = v_1\left(\frac{b_1 + b_2}{b_1}\right)$$

$$b_1 = r_1 + d/2$$

$$b_2 = r_2 + d$$

Fig. 6.2 Assumed shear stress distribution

$$M-(M_{CD}'' + M_{BC}^{t}'' + M_{AD}^{t}'' + Vx) = 0 \qquad (6.2)$$

where x is the eccentricity of the resultant V in the x direction, M_{BC}^{t}'' and M_{AD}^{t}'' are torsional moments on section BC'' and AD'' respectively.

From Equation 6.2 we have

$$Vx = M-(M_{CD}'' + M_{BC}^{t}'' + M_{AD}^{t}'') \qquad (6.3)$$

If the part of the total external moment in the x-direction to be taken by the vertical shear stresses is assumed to be proportional to the total moment, M, Equation 6.3 becomes

$$Vx = kM \qquad (6.4)$$

where k is a coefficient which defines the amount of external moment which is carried by vertical shearing stresses between the slab and column. Furthermore, it is assumed that the shear stresses are uniformly distributed across the effective depth of the slab, and,as was assumed by Moe,that the failure takes place when the maximum shear stress reaches a value equal to the shear strength of the same connection concentrically loaded. Also it is assumed that the shear stresses are proportional to the distance from the centre line of the critical section $A''B''C''D''$ (see Fig. 6.2(a)) hence from Fig. 6.2 (b) we have:

(1) The line of zero shear stress G-G is located such that the resultant of vertical forces due to moment only is zero.

(2) The moments of shear stress areas about line G-G equal to the amount of external moment which is carried by vertical shearing stresses is kM.

By taking moments about GG we find:

$$\left[2\left(\frac{1}{2}v_2c_2\right)\left(\frac{2}{3}c_2\right) + 2\left(\frac{1}{2}v_1c_1\right)\left(\frac{2}{3}c_1\right) + v_1b_2c_1\right]d = kM \qquad (6.5)$$

By substituting c_1, c_2 and v_2 (Fig. 6.2) into equation 6.5 we have

$$v_1 = \frac{kM}{\frac{b_1 d}{3b_0^2}\left[4b_1^3+12b_1^2b_2+9b_1b_2^2+2b_2^3\right]} \qquad (6.6)$$

where $b_0 = 2b_1 + b_2$

The vertical shearing stress due to the vertical shearing force (Fig. 6.2(c)) can be expressed as

$$v_1' = \frac{V}{(2b_1+b_2)d} = \frac{V}{b_0 d} \qquad (6.7)$$

Therefore the maximum shearing stress at the inner corners of the section shown in Fig. 6.2 (d) can be expressed as:

$$v_{max} = v_s + v_m$$

$$v_{max} = \frac{V}{b_0 d} + \frac{kM}{\frac{b_1 d}{3b_0^2}\left[4b_1^3+12b_1^2b_2+9b_1b_2^2+2b_2^3\right]} \qquad (6.8)$$

but $v_{max} = \frac{V_0}{b_0 d}$

where $V_0 = v_u(2b_1+b_2)d$ = shearing capacity at zero eccentricity, and v_u is to be determined from Eq. 6.1. (Note: Eq. 6.1 must be multiplied by $\frac{2r_1+r_2}{2b_1+b_2}$ because of the new critical section assumed by the writer where $b_1 = r_1 + \frac{d}{2}$ and $b_2 = r_2 + d$

Therefore

$$V = V_0 - \frac{kM}{\frac{b_1}{3b_0^3}\left[4b_1^3+12b_1^2b_2+9b_1b_2^2+2b_2^3\right]} \qquad (6.9)$$

Substitute $M = V_e$ in Eq. 5.9 and we get

$$V = V_0 - \frac{kVe}{\frac{b_1}{3b_0^3}\left[4b_1^3+12b_1^2b_2+9b_1b_2^2+2b_2^3\right]}$$

or

$$V = \frac{V_0}{1+\frac{ke}{\frac{b_1}{3b_0^3}\left[4b_1^3+12b_1^2b_2+9b_1b_2^2+2b_2^3\right]}} \qquad (6.10)$$

The constant k can now be determined from the test results.

6.3.2. Interaction diagram

The test results may also be evaluated in terms of an interaction diagram after Hanson considering the critical section is assumed to be located at a distance d/2 from the periphery of the column, and the ultimate shear capacity of the connection is then calculated for the case of shear transfer without moment transfer as:

$$V_0 = v_u b_0 d = v_u A_c \qquad (6.11)$$

For the case of moment transfer (M_0) without shear transfer, the ultimate shear capacity of the connection is obtained from Equation (6.6) as

$$v_m = \frac{kM_0}{\frac{b_1 d}{3b_0^2}\left[4b_1^3+12b_1^2b_2+9b_1b_2^2+2b_2^3\right]}$$

therefore

$$M_0 = \frac{v_m b_1 d}{3b_0^2 k}\left[4b_1^3+12b_1^2b_2+9b_1b_2^2+2b_2^3\right] \qquad (6.12)$$

For intermediate case, the connection capacity from Equation 6.8, where the axial shear controls, becomes:

$$v_s = v_{max} - v_m$$

$$V_u = v_u A_c - A_c \frac{kM_u}{\frac{b_1 d}{3b_0^2}\left[4b_1^3+12b_1^2b_2+9b_1b_2^2+2b_2^3\right]}$$

$$V_u = A_c\left(v_u - \frac{kM_u}{\frac{b_1 d}{3b_0^2}\left[4b_1^3+12b_1^2b_2+9b_1b_2^2+2b_2^3\right]}\right) \qquad (6.13)$$

From Equations 6.11, 6.12 and 6.13 we obtain:

$$\frac{V_u}{V_0} = 1 - \frac{M_u}{M_0} \qquad (6.14)$$

6.3.3. Determination of k factor

The factor "k" in Equation 6.9 defines the portion of the column moment which is carried by vertical shear stresses as already mentioned. The results from the test structures are used in determining a value for this factor.

A trial was made to check a similar factor determined experimentally by Moe[2] from his tests for eccentric loads in one direction and Zaglool from his tests for eccentric loads in two directions. Moe found that the ultimate shear strength of all his slabs could be predicted with a standard deviation of 0.103 when k was taken as equal to $\frac{1}{3}$. The ultimate shear strength of Zaglool's slabs could be predicted when k was taken equal to 0.04. In applying these two factors to the test structures it was found that the results were a conservative lower bound when k = $\frac{1}{3}$ and unsafe when k = 0.04, as can be seen from Figs. 6.3 and 6.4 and Table 6.1. Also it is noticed from Fig. 6.3 that as r_1/r_2 increases the "k" factor increases. From this, it can be concluded that the behaviour of edge column-slab connection subjected to axial force and bending moment is nearly similar to the behaviour of the interior column-slab connection subjected to similar loads when the ratio of r_1/r_2 is more than unity, and it is nearly similar to the behaviour of the corner column-slab connection subjected to axial force and biaxial bending moment when the ratio of r_1/r_2 is less than unity.

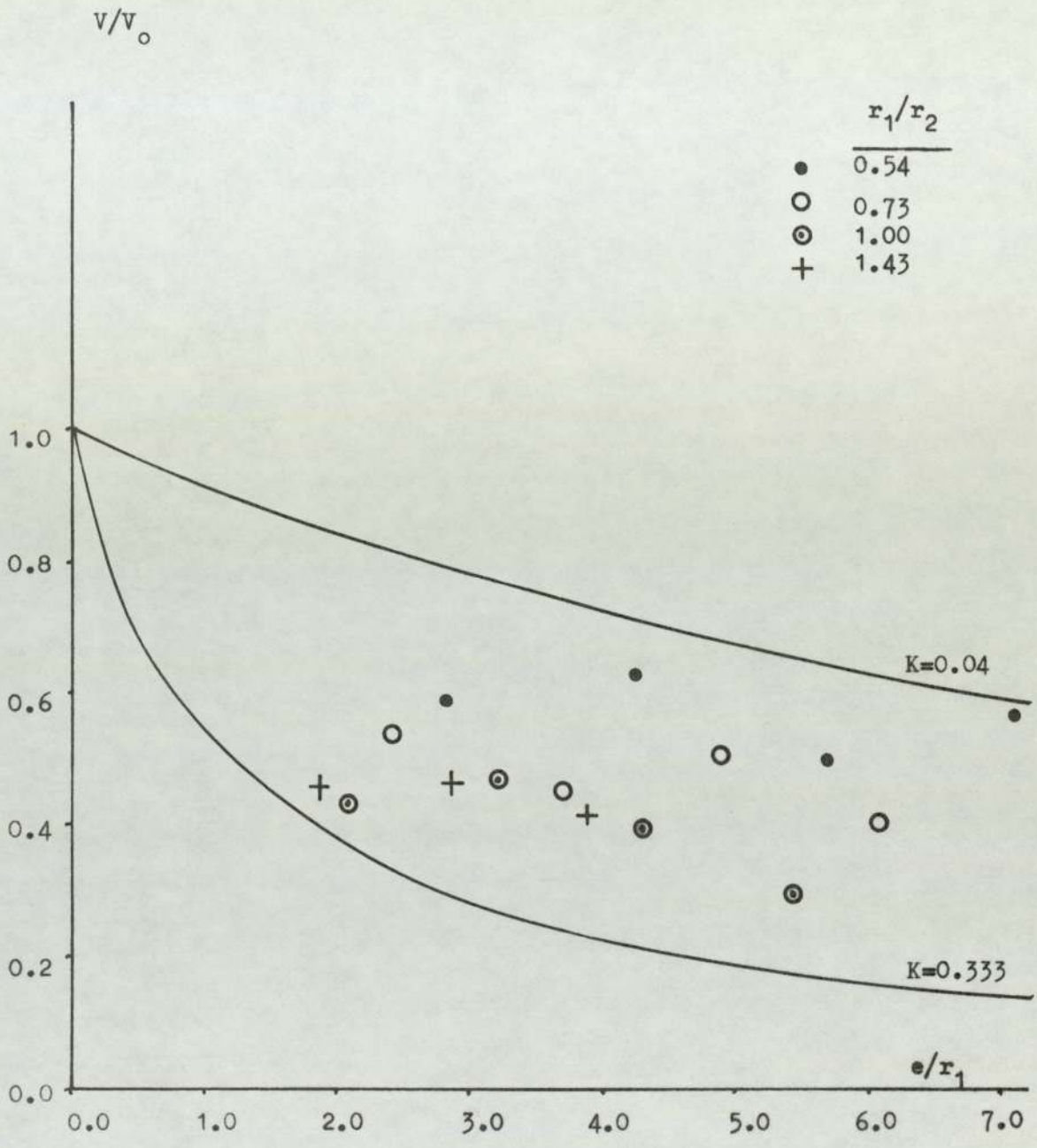

Fig. 6.3 Effect of eccentricity on ultimate shear strength of flat plates

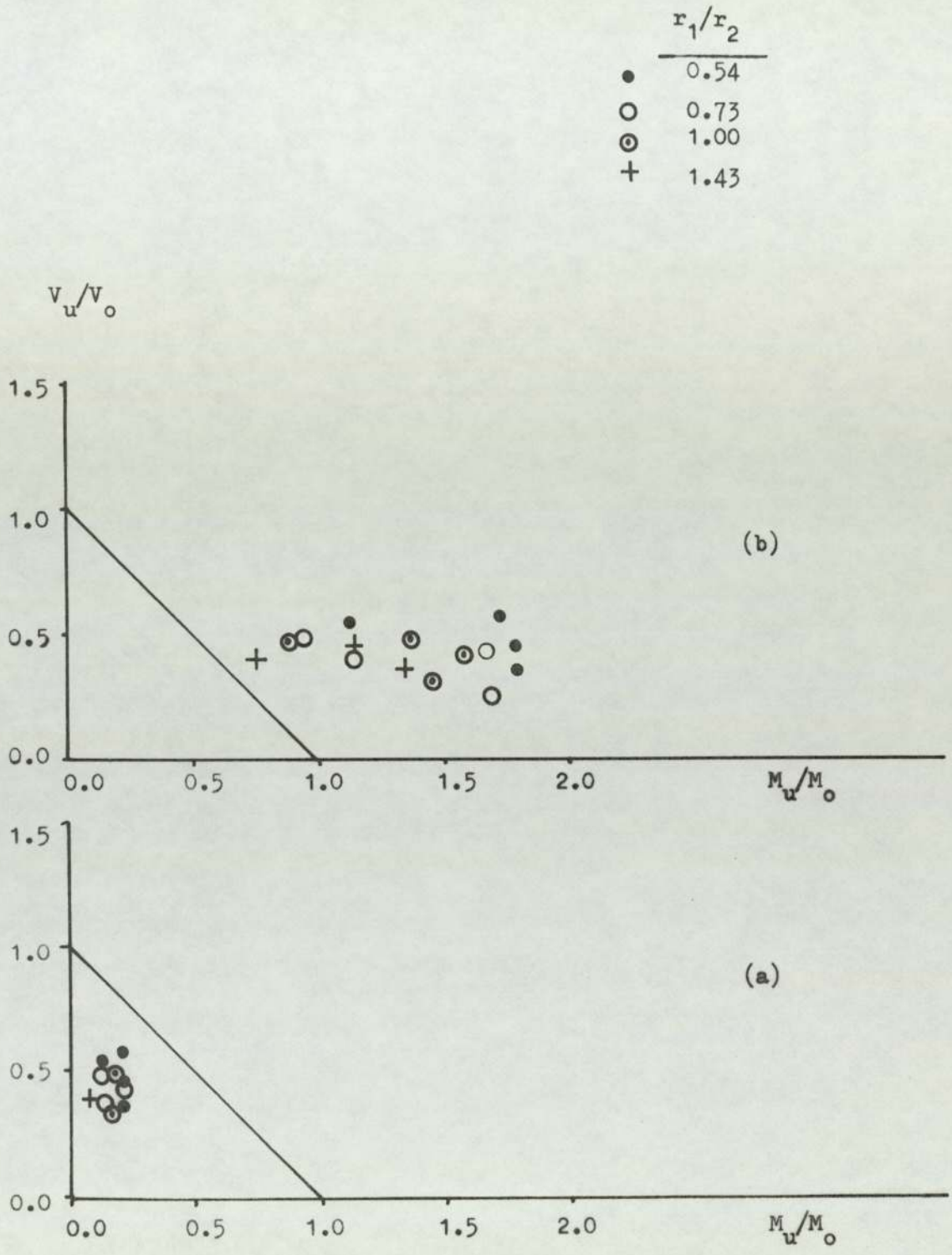

Fig. 6.4 Interaction of shearing force and bending moment of slab-column connection (a) K = 0.04 (b) K = 0.333

The deficiency of Moe's and Zaglool's factors in this case could be related to the difference between the type of specimens used by those investigators and the specimen used in this investigation. Moe's specimens were square slabs with square columns, while Zaglool's specimens were full size, square single panel flat plate structures cast monolithically with a square column at each corner. For a description of the specimens tested by the present author, refer to Section 3.3.

It was therefore felt that a determination of a more suitable moment reduction factor (taking into consideration the effect of r_1/r_2) was desired, rather than using that obtained to fit Moe's and Zaglool's results.

The determination of "k" factor proceeded as follows:

Equation 6.12 can be written in the form

$$k = \frac{v_u b_1 d}{3b_0^2 M_0}\left[4b_1^3+12b_1^2b_2+9b_1b_2^2+2b_2^3\right] \qquad (6.15)$$

Also Equation 6.14 can be written

$$M_0 = \frac{M_u}{1 - \frac{V_u}{V_0}} \qquad (6.16)$$

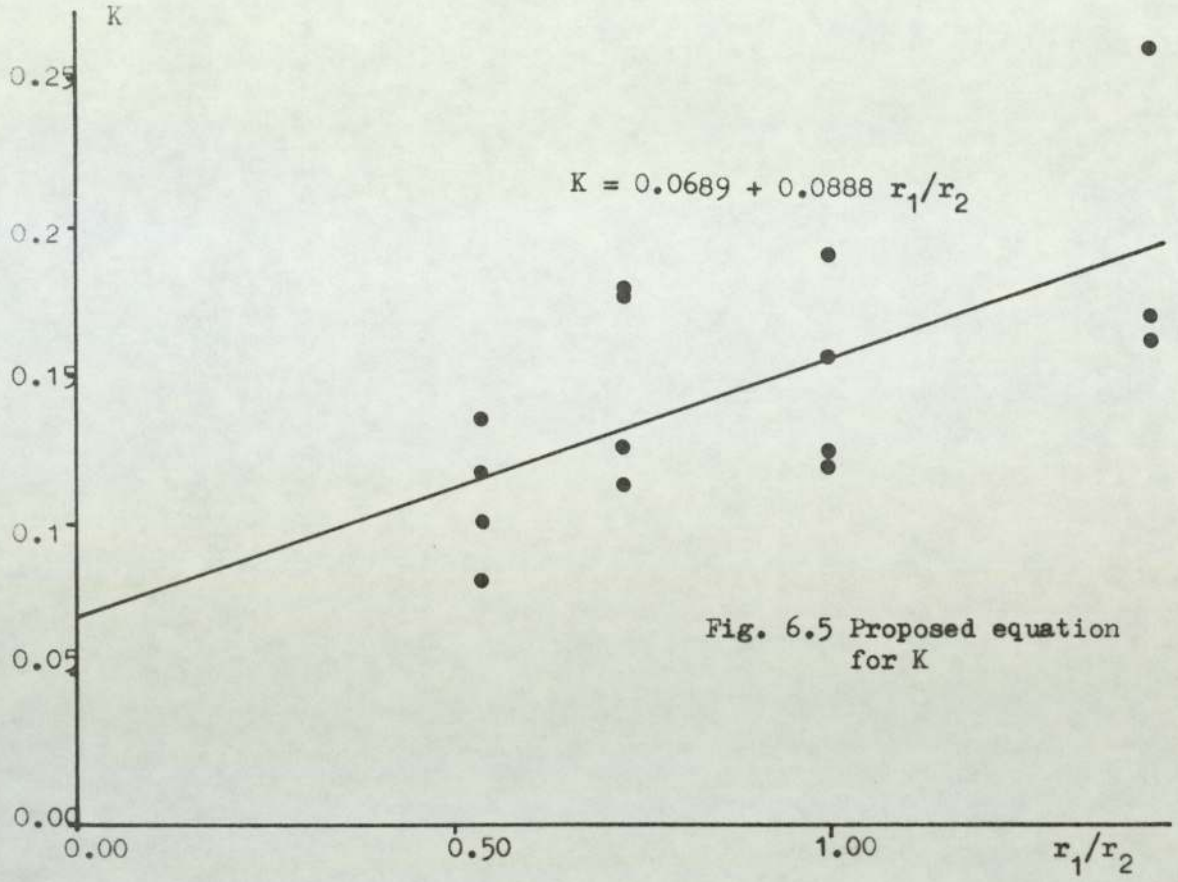

Fig. 6.5 Proposed equation for K

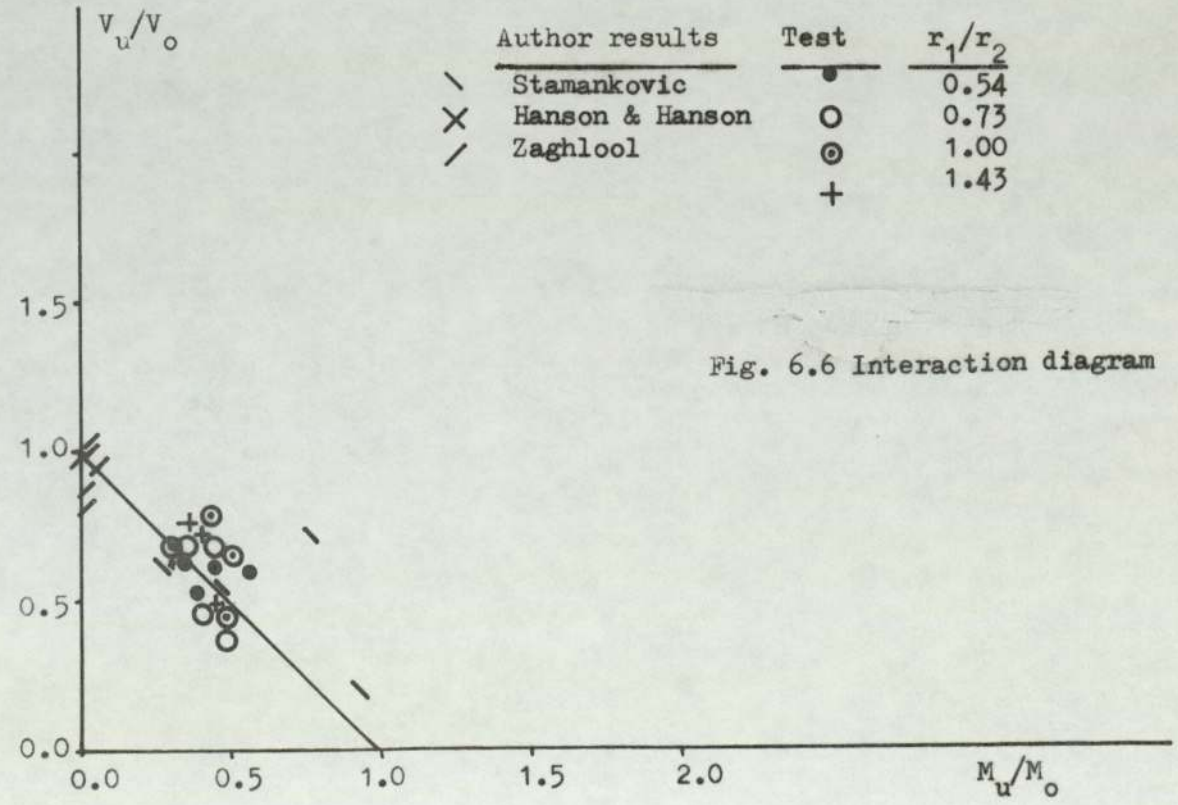

Fig. 6.6 Interaction diagram

SP. No.	v_u N/mm² (Eq. 5.1)	V_u kN (Test)	M_u kN-mm (Test)	V_0 kN (Eq. 6.11)	M_0 kN-mm k=0.333	M_0 kN-mm k=0.04	$\frac{V_u}{V_0}$	$\frac{M_u}{M_0}$ k=0.333	$\frac{M_u}{M_0}$ k=0.04
1	1.86	40.00	17200	73.70	15389.85	128120.50	0.543	1.118	0.134
2	1.10	25.00	15750	43.56	9101.53	75770.24	0.574	1.730	0.208
3	0.98	17.50	14525	38.81	8108.63	67504.34	0.451	1.791	0.215
4	0.87	12.50	12875	34.45	7198.48	59927.35	0.363	1.789	0.215
5	1.67	32.50	13650	66.13	14305.92	119096.78	0.491	0.954	0.115
6	1.28	20.00	12400	50.69	10965.01	91283.71	0.395	1.131	0.136
7	1.01	17.50	14350	39.99	8652.08	72028.57	0.438	1.659	0.199
8	0.88	12.50	12750	34.85	7538.45	62757.60	0.359	1.691	0.203
9	1.70	32.50	13325	67.32	14766.83	122933.80	0.483	0.902	0.108
10	1.29	25.00	15250	51.08	11205.42	93285.12	0.489	1.361	0.163
11	1.06	18.00	14580	41.97	9207.55	76652.85	0.429	1.583	0.190
12	0.88	11.00	11110	34.85	7644.01	63636.38	0.316	1.453	0.174
13	1.96	32.00	12800	77.62	17030.69	141780.50	0.413	0.752	0.090
14	1.40	23.00	13800	55.44	12164.78	101271.79	0.415	1.134	0.136
15	1.05	15.00	12000	41.58	9123.56	75953.64	0.361	1.315	0.158

Table 6.1

Bending moments and shear strengths for test specimens

SP. NO.	M_0 kN-mm (Eq. 6.16)	k (Eq. 6.15)	r_1/r_2	k (Eq. 6.17)	M_0 kN-mm (Eq. 6.12)	$\frac{M_u}{M_0}$	$V_{calc.}$ kN (Eq. 6.9)	$\frac{V_{test}}{V_{calc.}}$
1	37636.76	0.136	0.54	0.116	44125.85	0.390	45.02	0.888
2	36971.83	0.082	"	"	26135.25	0.603	17.30	1.445
3	26457.19	0.102	"	"	23264.08	0.624	14.59	1.200
4	20211.93	0.118	"	"	20560.41	0.626	12.98	0.960
5	26817.29	0.178	0.73	0.134	35542.92	0.384	40.74	0.798
6	20495.87	0.178	"	"	27225.86	0.455	27.62	0.724
7	25533.81	0.113	"	"	21494.13	0.668	13.30	1.316
8	19890.79	0.126	"	"	18732.97	0.681	11.13	1.123
9	25773.69	0.191	1.00	0.158	31124.18	0.428	38.50	0.844
10	29843.44	0.125	"	"	23610.32	0.646	18.09	1.382
11	25534.15	0.120	"	"	19393.02	0.752	10.43	1.726
12	16242.69	0.157	"	"	16109.05	0.690	10.82	1.017
13	21805.79	0.260	1.43	0.196	28926.05	0.443	43.28	0.739
14	23589.74	0.172	"	"	20665.09	0.668	18.42	1.249
15	18779.34	0.162	"	"	15502.54	0.774	9.39	1.597

Table 6.2 Calculated and Test Results

Average $\frac{V_{test}}{V_{calc.}} = 1.13$

Standard deviation $\sigma = 0.32$

SP. NO.	f'_c N/mm^2	f_y N/mm^2	P %	Col. size mm	V_{test} kN	M_{test} kN-mm	v_u N/mm^2	V_o kN	M_o kN-mm	$V_{cal.}$ kN	$\frac{V_{test}}{V_o}$	$\frac{M_{test}}{M_o}$	$\frac{V_{test}}{V_{cal.}}$
STAMANKOVIC'S TESTS: SLABS DEPTH 3 in., SLABS ARE 3'-0" SQUARE													
C /E/1	38.47	448.18	1.17	127x127	73.17	5593.50	2.82	77.65	26821.10	61.51	0.942	0.208	1.19
C /E/2	32.41	495.75	"	"	54.71	9175.60	2.60	71.59	24728.60	45.06	0.764	0.731	1.21
C /E/3	33.99	495.75	"	"	24.91	10057.00	1.99	54.80	18926.90	27.72	0.454	0.531	0.97
C /E/4	34.34	495.75	"	"	10.94	8842.25	1.48	40.75	14076.30	15.18	0.268	0.628	0.72
HANSON AND HANSON'S TESTS: SLABS DEPTH 3 in., SLABS ARE 3'-0" SQUARE													
D15	31.10	365.43	1.65	152.4 x 152.4	12.05	9932.70	1.18	38.57	15467.80	13.80	0.312	0.642	0.87
ZAGHLOOL'S TESTS: SLABS DEPTH 6 in., SLABS ARE 3'-2" x 6'-0"													
Z-IV(1)	27.33	475.76	1.23	177.8 x 177.8	122.32	3971.95	1.38	128.99	79848.10	118.96	0.948	0.057	1.03
Z-V(1)	34.34	473.69	"	266.7 x 266.7	277.55	7051.20	1.93	242.49	192500.0	233.61	1.145	0.037	1.19
Z-V(2)	40.40	473.69	1.65	"	306.91	7797.0	2.34	295.21	233334.0	285.39	1.040	0.033	1.08
Z-V(3)	38.75	475.07	1.23	"	339.83	8633.20	3.28	412.57	327067.0	401.79	0.823	0.026	0.85
Z-V(6)	31.30	476.44	"	"	289.12	7345.0	2.60	326.70	259260.0	317.45	0.885	0.028	0.91
Z-VI(1)	25.99	475.76	"	355.6 x 355.6	350.7	8911.18	2.23	352.22	323073.0	348.98	0.996	0.028	1.01

Table 6.3 Comparison with other results

Substitute the values of M_0 from Equation 6.16 into Equation 6.15 and then evaluate the values of "k" for each specimen (see table 6.2).

Now plot "k" against r_1/r_2 ratio and find the relation between "k" and r_1/r_2 (see Fig. 6.5). Therefore the equation of the line passing through the points in Fig. 6.5 is

$$k = 0.0689 + 0.0888 \frac{r_1}{r_2} \qquad (6.17)$$

Also it can be said that when r_1/r_2 is equal to zero, 6.8% of the total moment are assumed to contribute to the shearing stresses,which is negligible; this increases as r_1/r_2 increases, until the ratio reaches unity, where 15.8% of the total moment are assumed to contribute to the shearing stresses with the distribution assumed to be linear, as shown in Fig. 6.2.

6.4 Comparison with test results

The validity of the method for predicting the edge column-slab connection strength presented in Section 6.3 was checked using:

(1) The test results of the writer

(2) Hanson and Hanson's tests[12]

(3) Stamankovic's tests

(4) Zaglool's tests.

The theoretical predictions are tabulated against the test results in Tables 6.2 and 6.3.

In all cases the theoretical predictions were in reasonable agreement with the experimental results. Some of the measured results, however, were somewhat lower than computed. This discrepancy between the measured and computed results may be ascribed to one or more of the following causes:

(1) Variation in the yield strength of the reinforcement.

(2) Variation due to placement of steel at levels other than the assigned ones.

(3) Difficulty in obtaining uniform thickness of the slab.

(4) Local variation in concrete strength throughout the slab which was cast from two batches.

The test results are now evaluated in terms of proposed k values and Equation 6.16, and are plotted in Fig. 6.6.

SP. NO.	V_u kN (Test)	V_o kN Eq. 6.11	M_{flex} kN-mm	LV_o N-mm	V_{calc} kN Eq. 6.14a	$\frac{V_{test}}{V_{calc}}$
1	40.00	73.70	17676.0	26532.0	29.46	1.36
2	25.00	43.56	12768.0	24393.6	14.96	1.67
3	17.50	38.81	14288.0	29495.6	12.66	1.38
4	12.50	34.45	16032.0	33072.0	11.25	1.11
5	32.50	66.13	14314.0	42323.2	19.98	1.63
6	20.00	50.69	14310.0	27372.6	17.40	1.15
7	17.50	39.99	14208.0	29592.6	12.97	1.35
8	12.50	34.85	15604.0	32759.0	11.24	1.11
9	32.50	67.32	15616.0	21542.4	28.29	1.15
10	25.00	51.08	14560.0	26561.6	18.09	1.38
11	18.00	41.97	16848.0	30218.4	15.02	1.20
12	11.00	34.85	15640.0	32062.0	11.43	0.96
13	32.00	77.62	16980.0	23286.0	32.73	0.98
14	23.00	55.44	17250.0	27720.0	21.27	1.08
15	15.00	41.58	15050.0	29106.0	14.17	1.06

Average $\frac{V_{test}}{V_{calc}} = 1.24$

Standard deviation $\sigma = 0.21$

Table 6.4 Calculated and test results

6.5 Modified Interaction Formula

Hanson interaction formula (Eq. 6.14) may be re-written as follows

$$V_{calc} = \frac{V_o M_{flex}}{M_{flex} + LV_o} \qquad (6.14a)$$

where M_{flex} is the flexural capacity of the joint calculated using yield line theory. The results are presented in Table 6.4. As can be seen, the modified form of the interaction formula tends to predict failure loads generally on the safe side except for two values, and the standard deviation is 0.21, which is reasonable.

CHAPTER VII

SUMMARY AND CONCLUSION

7.1 Summary

The purpose of this investigation was to study experimentally the strength and behaviour of the edge column-slab connection of a reinforced concrete flat plate under different loading conditions. The view was to obtain data useful for establishing a method for analysis of this connection.

The experimental study involved tests on 15 reduced scale connections. The test specimens were as shown in Fig. 3.1. The column stubs were cast monolithically with the slabs. The variable parameters were:

(1) The ratio of column sides r_1/r_2.

(2) Ratio of column side to the effective depth r_1/d.

(3) Ratio of column side to the slab length L.

(4) Ratio of bending moment to axial load M/V.

The test results along with the effect of the parameters were discussed in Chapter IV.

A theoretical method for the analysis of an edge connection subjected to the effect of combined axial force and bending moment was developed in Chapter VI. The method was checked against the test results of the writer and the others. Good correlation was found between the test results and the theoretical predictions.

7.2 Conclusions

From the tests conducted and different variables parameters involved in this investigation, it was possible to obtain the following conclusions.

(1) The primary failure mechanism for an edge column-slab connection subjected to moment and shear can be idealised as illustrated in Fig. 4.7.

(2) For these structures, visible cracks can be expected at loads as low as 50% of the ultimate load.

(3) The flexural capacity of the joint is sensibly constant for the range of column aspect ratio tested. Such variation as can be seen indicates that as r_1 increases relative to r_2 there is a small reduction in flexural capacity of the joint.

(4) The critical section governing the ultimate shearing strength of the slab is located at a distance equal to d/2 from the perimeter of the column.

(5) The ultimate shearing strength of plates computed at a section at d/2 distance around the column was found to be predicted with good accuracy by the following equation

$$V = V_0 - \frac{kM_u}{\frac{b_1}{3b_0^3}\left[4b_1^3+12b_1^2b_2+9b_1b_2^2+2b_2^3\right]} \qquad (6.9)$$

(6) The portion of bending moment to be transferred through vertical shear stresses distributed along the critical section as shown in Fig. 6.2, k, was found to be as follows:

$$k = 0.0689 + 0.0888\ ^{r_1}/_{r_2} \qquad (6.17)$$

(7) The interaction between the bending moments and shearing force at the column-slab connection can be expressed by a linear function as follows:

$$\frac{V_u}{V_0} = 1 - \frac{M_u}{M_0} \qquad (6.14)$$

7.3 Suggestions for future research

On the basis of the present investigation the following suggestions for further research concerning shear and moment transfer can be recommended:

(1) A study on plates with different steel ratios in

the vicinity of the columns.

(2) A study of the effect of different slab thicknesses on the ultimate shear strength.

(3) A study of the effect of different types of shear reinforcement on the ultimate shear strength in the case of thick slabs.

(4) A study of the effect of static reversal loading on the ultimate shear strength of column-slab connection is also of great interest.

REFERENCES

1. Talbot, A. N.
"Reinforced concrete wall footings and column footings."
University of Illinois Engineering and Experiment Station, Bulletin No. 67, March 1913, 114 pages.

2. Moe, J.
"Shearing strength of Reinforced concrete slabs and footings under concentrated loads."
Research and Development Department, Bulletin D47, Portland Cement Association, Skokie, Illinois, April 1961.

3. "European Committee of Concrete", (Comite Europeen du Beton), Bulletin D'information No. 50, Paris, 1965 (In French and German).

4. "European Committee of Concrete", (Comite Europeen du Beton) Bulletin D'information No. 58, London, 1966 (In English).

5. Report of ACI-ASCE Committee 326, (Now 426)
"Shear and Diagonal Tension." ACI Journal, Proceedings Vol. 59, January to March 1962, pp1-30, and pp 352-396.

6. ACI Committee 318 Report, ACI Standard, "Building Code Requirements for Reinforced Concrete (ACI.318-63)", American Concrete Institute, June 1963, 144 pages.

7. ACI Committee 318, "Proposed Revision of ACI 318-63: Building Code Requirements for Reinforced Concrete." ACI Journal, Proceedings Vol. 67, No. 2, Febuary 1970, pp 77-186.

8. Corley, W. G. and Hawkins, N. M. "Shearhead Reinforcement for Slabs", ACI Journal, Proceedings Vol. 65, October 1968, pp 811-824.

9. Zaghlool, E. R. F. "Strength and Behaviour of Reinforced Concrete Flat Plate Floor Slabs." MSc Thesis, University of Calgary, Calgary, Alberta, Canada, 1968.

10. Saghlool, E. R. F., de Paiva, H. A. R., and Glockner, P. G. "Test of Reinforced Concrete Flat Plate Floors," Journal of the Structural Division, Proceedings of the American Society of Civil Engineers, Vol. 96, No. ST3, March 1970, pp 487-507.

11. Distasio, J. and Van Buren, M. P. "Transfer of bending moment between flat plate floor and column.", ACI Journal, Proceedings Vol 57, September 1960, pp 299-314.

12. Hanson, N. W. and Hanson, J. M. "Shear and moment transfer between concrete slabs and columns," PCA Journal, Research and Development Laboratories, V.10, No. 1, January 1968.

13. Bach, C. and Graf, O.
"Test of square and rectangular reinforced concrete slabs supportedon all sides." (In German), Deutscher Ausschuss fur Eisenbeton (Berlin) Heft 30, 1915, 309 pages. Quoted by Reference 2.

14. Graf, O.
"Test of reinforced concrete slabs under concentrated load applied near one support." (In German) Deutscher Ausschuss fur Eisenbeton (Berlin) Heft 73, 1933, 2 pages. Quoted by Reference 2.

15. Graf, O.
"Strength test of thick reinforced concrete slabs supported on all sides under concentrated loads," (In German), Deutscher Ausschuss fur Eisenbeton (Berlin) Heft 88, 1938, 26 pages. Quoted by Reference 2.

16. Richard, F. E. and Kluge, R. W.
"Test of reinforced concrete slabs subjected to concentrated loads," University of Illinois Engineering Experiment Station Bulletin, No. 314, June 1939, 75 pages.

17. Forsell, C. and Holmberg, A.
"Concentrated load on concrete slabs," (In Swedish), Betong (Stockholm), 31, No. 2, 1946, pp. 95-123.

18. Richart, F. E.
"Reinforced concrete wall and column footings," ACI Journal, Proceedings Vol. 45, October-November, 1948, pp. 97-127, and pp. 237-260.

19. Hognestad, E.
"Shearing strength of reinforced concrete column footings," ACI Journal, Proceedings Vol. 50, November 1953, pp. 189-208.

20. Elstner, R. C. and Hognestad, E.
"Shearing strength of reinforced concrete slabs," ACI Journal, Proceedings Vol. 53, July 1956, pp. 29-58.

21. Keefe, R. A.
"An investigation of the effectiveness of diagonal tension reinforcement in flat slabs," Thesis, Massachussetts Institute of Technology, June 1954, 43 pages.

22. Whitney, C. S.
"Ultimate shear strength of reinforced concrete flat slabs, footings, beams and frame members without shear reinforcement," ACI Journal, Proceedings Vol. 54, October 1957, pp. 265-298.

23. Hahn, M. and Chefdeville, J.
"Flat slab without column capitals, tests." (In French) Annales de L'Institut Technique du Batiment et des Travaus Publics (Paris), No. 167, Beton, Beton Arme, No. 16, January 1951, pp. 23-31, Quoted by Reference 2.

24. Scordelis, A. C., Lin, T. Y. and May, H. R.
"Shearing strength of prestressed lift slabs." ACI Journal, Proceedings Vol. 55, October 1958, pp. 485-506.

25. Base, G. D.
"Some tests on the punching shear strength of reinforced concrete slabs." Cement and Concrete Association, London, Technical Report TRA/321, July 1959, 5 pages.

26. Kinnunen, S. and Nylander, H.
"Punching of concrete slabs without shear reinforcement." Transaction of the Royal Institute of Technology, Stockholm, Sweden, No. 158, 1960.

27. Kinnunen, S.
"Punching of concrete slabs with two-way reinforcement with special reference to dowel effect and deviation of reinforcement from polar symmetry." Transactions of the Royal Institute of Technology, Stockholm (Civil Engineering 6), No. 198, 1963, pp. 1-109.

28. Anderson, J. L.
"Punching of concrete slabs with shear reinforcement." Transaction of the Royal Institute of Technology, Stockholm, Sweden, No. 212, 1963.

29. Yitzhaki, D.
"Punching strength of reinforced concrete slabs." ACI Journal, Proceedings Vol. 63, May 1966, pp. 527-542.

30. "The structural use of reinforced concrete in buildings." British Standards, CP 114 (1957).

31. Long, A. E. and Bond, D.
"Punching failure of reinforced concrete slabs." The Institute of Civil Engineers Proceedings Vol. 57, May 1967, pp. 109-135.

32. Long, A. E.
"Punching failure of reinforced concrete slabs under combined loading conditions." The Institute of Civil Engineers, 13th February 1967.

33. Zaldi, S. T., Sabonis, G. J. and Roll, F.
"Shear resistance of perforated reinforced concrete slabs." A progress presented to the ACI Committee 426, Shear and Diagonal Tension, March 31, 1969, Chicago, Illinois.

34. Smith, A. E., and Simmonds, S. H.
"Test of flat plate supported on columns elongated in plan." Structural Engineering Report No. 21, May 1969, Department of Civil Engineering, The University of Alberta, Alberta, Canada, 71 pages.

35. Simmonds, S. H.
"Flat slabs supported on columns elongated in plan." ACI Journal, Proceedings Vol. 67, No. 12, December 1970, pp. 967-975.

36. Hawkins, N. M.
"Effect of column rectangularity on the strength and behaviour of slab-column specimens." University of Washington, Structures and Mechanics Report SM 70-2, September 1970.

37. Rosenthal, I.
"Experimental investigation of flat plate floors." ACI Journal, Proceedings Vol. 56, August 1959, pp. 153-166.

38. Tsuboi, Y. and Kawaguchi, M.
"On earthquake resistant design of flat slabs and concrete shell structures." Proceedings of the Second World Conference on Earthquake Engineering, Vol. III, July 1960, pp. 1693-1708.

39. ACl Committee 318 Report, ACl Standard.
"Building Code Requirement for Reinforced Concrete (ACl 318-56)". American Concrete Institute, July 1956, pp. 913-986.

40. Kreps, R. and Reese, R. Discussion of a paper by Di Stasia and Van Buren.
"Transfer of bending moment between flat plate floor and column." ACl Journal, Proceedings Vol.57, March 1961, pp. 1261-1263.

41. Frederick, G. R. and Pollauf, F. P.
"Experimental determination of the transmission of column moment to flat plate floor and column."
University of Toledo, (Unpublished report, May 1959).

42. Report of the ACl Committee 318, Standard Building Code.
"Commentary on Building Code Requirements for Reinforced Concrete (ACl 318-63)." Publication Sp-10, American Concrete Institute, 1965, 91 pages.

43. Anderson, A. J. L.
"Punching of slabs supported on columns at free edges."
Nordisk Betong, No. 2, 1966, pp.179-200. (English summary is given in Reference 4.)

44. Stamenkovic, A.
"Flat slab construction column head strength under combined vertical load and wind moment." PhD Thesis, University of London, London, UK, 1969.

45. Birkeland, P. W. and Birkeland, H. W.
"Connections in precast concrete construction." ACI Journal, Proceedings Vol. 63, No. 3, March 1966.

46. Mast, P. E.
"Stresses in flat plates near columns." ACI Journal, Proceedings Vol. 67, No. 10, October 1970, pp. 761-768.

47. Mast, P. E.
"Plate stresses at columns near the free edge." ACI Journal, Proceedings Vol. 67, No. 11, November 1970, pp. 898-902.

48. Girkmann, K.
"Flachentragwerke." 5th Edition, Springer Verlag Wien 1959, pp. 188-189.

49. Mast, P. E.
"Influence lines for shear around columns in flat plates." Final Report, Eighth Congress of the International Association for Bridge and Structural Engineering, New York, September 1968, pp. 983-993.

50. Hawkins, N. M. and Corley, W. G.
"Transfer of unbalanced moment and shear from flat plates to columns." Report, PCA R/D ser. 1482, Portland Cement Association, Skokie, Illinois, October, 1970.

51. ACI Standard 318-71. "Building Code Requirements for Reinforced Concrete (ACI 318-71)". American Concrete Institute, 1971.

52. "The Structural Use of Concrete." British Standards, CP 110, Part 1, 1972.

53. Regan, P. E.
"Design for punching shear." The Structural Engineer, June 1974, No. 6. Vol. 52, pp. 197-207.

54. Hatcher, D. S., Sozen, M. A. and Siess, C. P.
"A study of tests on a flat plate and a flat slab." Structural Research Series No. 217, University of Illinois, July 1961.

55. Johansen, K. W.
"Yield line theory." Translated from Danish, Cement and Concrete Association 1962, original copyright by K. W. Johansen, 1943.

56. Hognestad, E.
"Yield line theory for ultimate strength of reinforced concrete slabs." ACI Journal March 1953, Proceedings Vol. 49, pp. 637-656.

57. Wood, R. H.
"Plastic and elastic design of slabs and plates." Thames and Hudson (London), 1961.

58. Jones, L. L. and Wood, R. H.
"Yield line analysis of slabs."
Thames and Hudson, Chatto and Windus (London) 1957.

59. ACI Standard 318-77. "Building Code Requirements for Reinforced Concrete (ACI 317-77)". American Concrete Institute, 1977.

(1) The primary failure mechanism for an edge column-slab connection subjected to moment and shear can be idealised as illustrated in Fig. 4.43. (The term mechanism refers to the last stage of the structure before failure which is capable of undergoing deformation without change in the resistance to external loads).

(2) For these structures, cracks can be expected at loads as low as 50 to 68 percent of the ultimate load.

(3) The failure of the specimen at ultimate load followed the formation of the torsional cracks on the column sides and flexural shear cracks at the inner side of the column.

(4) The flexural capacity of the joint is sensibly constant for the range of column aspect ratios tested. Such variation as can be seen indicates that as r_1 increases relative to r_2 there is a small reduction in flexural capacity of the joint.

CHAPTER V

STRENGTH ANALYSIS

5.1 Shear Strength

5.1.1. General

The effect of the variables on the shear strength of the connection is discussed and their effect on the capacity of the connection in the light of the experimental evidence is pointed out.

5.1.2. Method of analysis

It may be of interest to analyse the results obtained experimentally in the present investigation using the conventional method of analysis

$$v_u = \frac{V}{A_c} + \frac{kMC}{J_c} \qquad (5.1)$$

where

v_u = ultimate shear stress

V = shear force

A_c = Area of concrete in assumed critical section, periphery times effective slab depth d.

k = moment reduction factor

M = unbalanced moment

C = distance from centroidal axis to the most remote part of critical section

J_c = polar moment of inertia

and then compare the ultimate shear stresses obtained from

these results with the allowable ultimate shear stresses given by both ACI 318-77 Building Code and CP110 Code of Practice using both assumed critical sections.

This method (Eq. 5.1) was chosen because of its acceptance by a number of researchers[2,7,11,12] and also by ACI 317-71 and ACI 318-77 codes. This type of approach was used in comparing with the CP110 approach in obtaining the modification factor for interior slab-column connection subjected to shear and moment (see section 3.6.2 CP110 and Eq. 2.27). The differences between this approach and the approach followed by CP110 as mentioned by Regan[53] are as follows.

(1) The ACI code includes torsion in its uneven shear effects.

(2) In the ACI code uneven shear effects are greater if the column dimension parallel to the eccentricity is larger than that perpendicular to it, while in CP110 rectangularity has no effect.

(3) According to CP110 the effect of uneven shear decreases for greater slab spans. There appears to be no evidence either way on this point for flat slabs, but there are cases in bridge decks where the ACI predictions are better.

(4) The biggest difference is in the treatments of moments perpendicular to slab edges, where the ACI code applies the above approach with a suitable

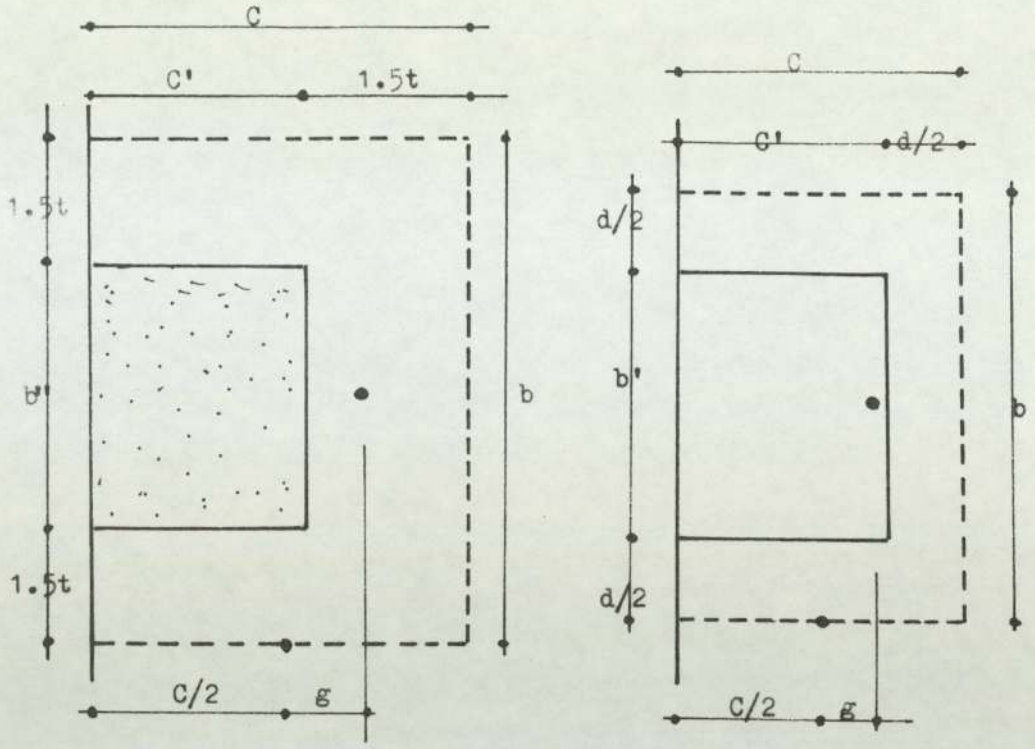

(a) CP110

(b) ACI-77

$C=C'+1.5$ or $C'+d/2$

$b=b'+3t$ or $b'+d$

$a_1=C/2+g$

$a_2=C/2-g$

$A_c=(2C+b)d$

$J_c=2dC^3/12 + 2Cd^3/12 + 2Cdg^2 + bd(C/2-g)^2$

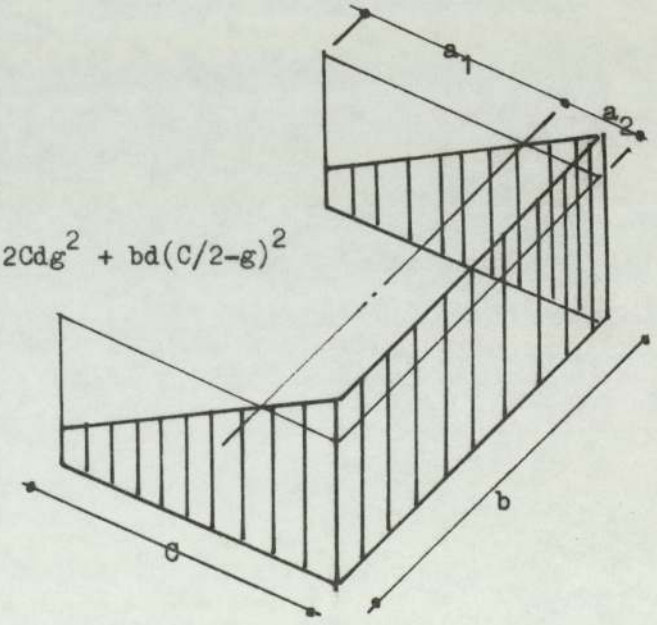

Fig. 5.A Critical sections for shear stress

modification of J_c and predicts a considerable influence on punching resistance, while CP110 totally ignores any such effect.

Eq. 5.1 was used to calculate shear stresses for comparison with CP110 using the critical section assumed by CP110. Three different values of k were used.

(1) k = 0 according to CP110

(2) k = 0.20 according to ACI-ASCE Committee 326.

(3) k = 0.40 according to Hanson and Hanson.

5.1.2.1. Typical calculation of the shear stress using Eq. 5.1

For c' = 140 mm, b' = 260 mm, d = 60 mm from Fig. 5.A we find (for CP110)

$c = 252.5$ mm, $b = 485.0$ mm

$g = 61.85$ mm, $a_2 = 64.4$ mm

$A_c = 59400$ mm^2

$J_c = 406.7 \times 10^6$ mm^4

Substitute these values in Eq. 5.1 using k = 0.2 and then get another value for v_u by using k = 0.4.

Then follow the same approach to calculate v_u according to ACI-77 assumptions (see Fig. 5.A and Table 5.1).

5.1.3. Effect of r_1/r_2 ratio

In Figs. 5.1 to 5.4 the calculated ultimate shear stress (according to CP110 assumptions) is plotted against

		CP110			(N/mm²)	ACI-77	(N/mm²)		
SP.NO	f_c' (N/mm²)	v_c (code)	v_c (k=0)	v_c (k=.2)	v_c (k=.4)	v_c (code)	v_c (k) code value	r_1/r_2	r_1/d
1	27.76	0.893	0.673	1.220	1.760	1.486	3.060	0.54	2.33
2	25.93	0.872	0.421	0.920	1.420	1.436	2.320	"	"
3	29.00	0.902	0.293	0.750	1.214	1.519	2.170	"	"
4	26.00	0.873	0.210	0.618	1.024	1.439	1.850	"	"
5	26.80	0.881	0.547	0.970	1.390	1.461	2.520	0.73	2.67
6	27.30	0.905	0.336	0.720	1.103	1.475	2.050	"	"
7	29.80	0.910	0.295	0.738	1.182	1.540	2.230	"	"
8	29.20	0.904	0.210	0.600	0.999	1.525	1.910	"	"
9	22.50	0.840	0.547	0.950	1.349	1.339	2.590	1.00	3.00
10	29.00	0.902	0.421	0.880	1.337	1.519	2.660	"	"
11	22.90	0.843	0.303	0.740	1.177	1.359	2.390	"	"
12	26.30	0.876	0.185	0.518	0.851	1.448	1.750	"	"
13	30.30	0.915	0.539	0.925	1.311	1.554	2.650	1.43	3.33
14	26.20	0.875	0.387	0.804	1.220	1.444	2.560	"	"
15	28.90	0.901	0.252	0.615	0.976	1.516	2.110	"	"

Table 5.1: Shear stresses

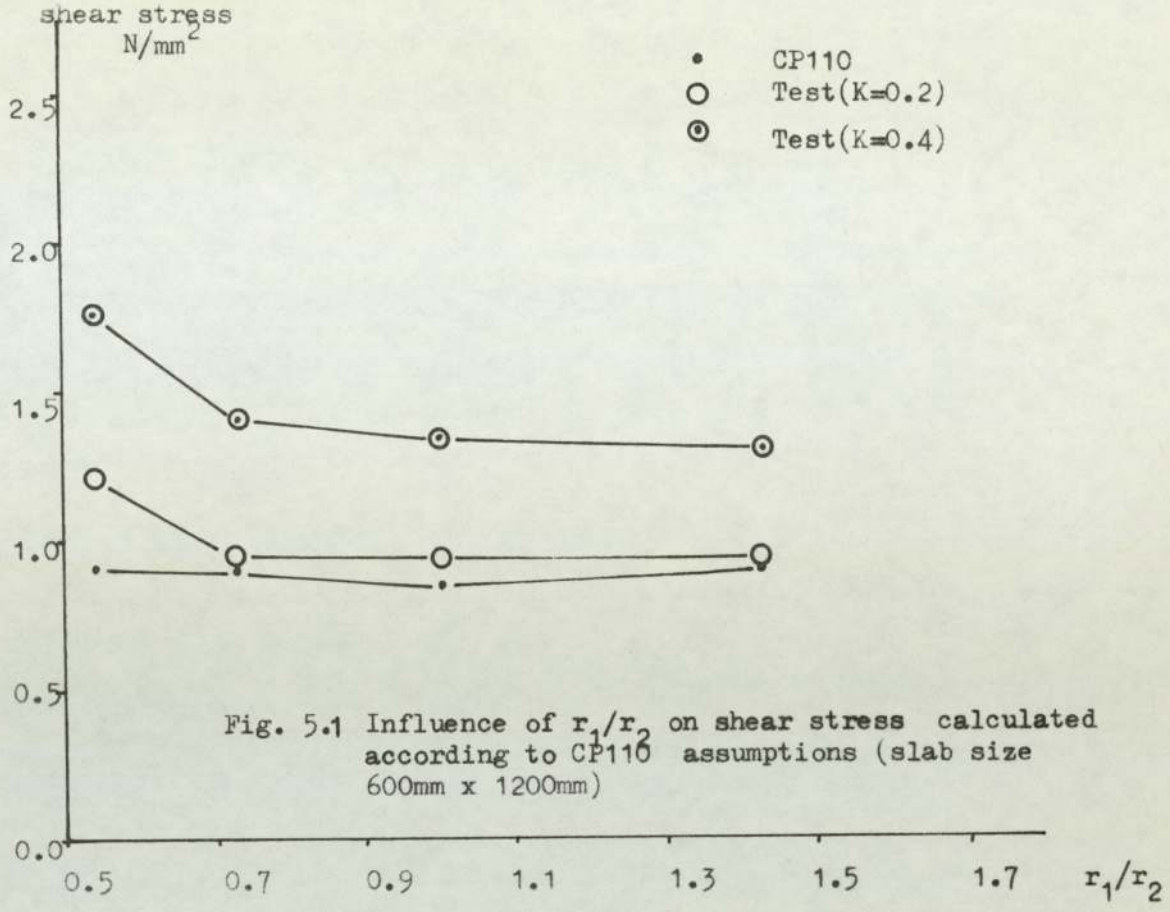

Fig. 5.1 Influence of r_1/r_2 on shear stress calculated according to CP110 assumptions (slab size 600mm x 1200mm)

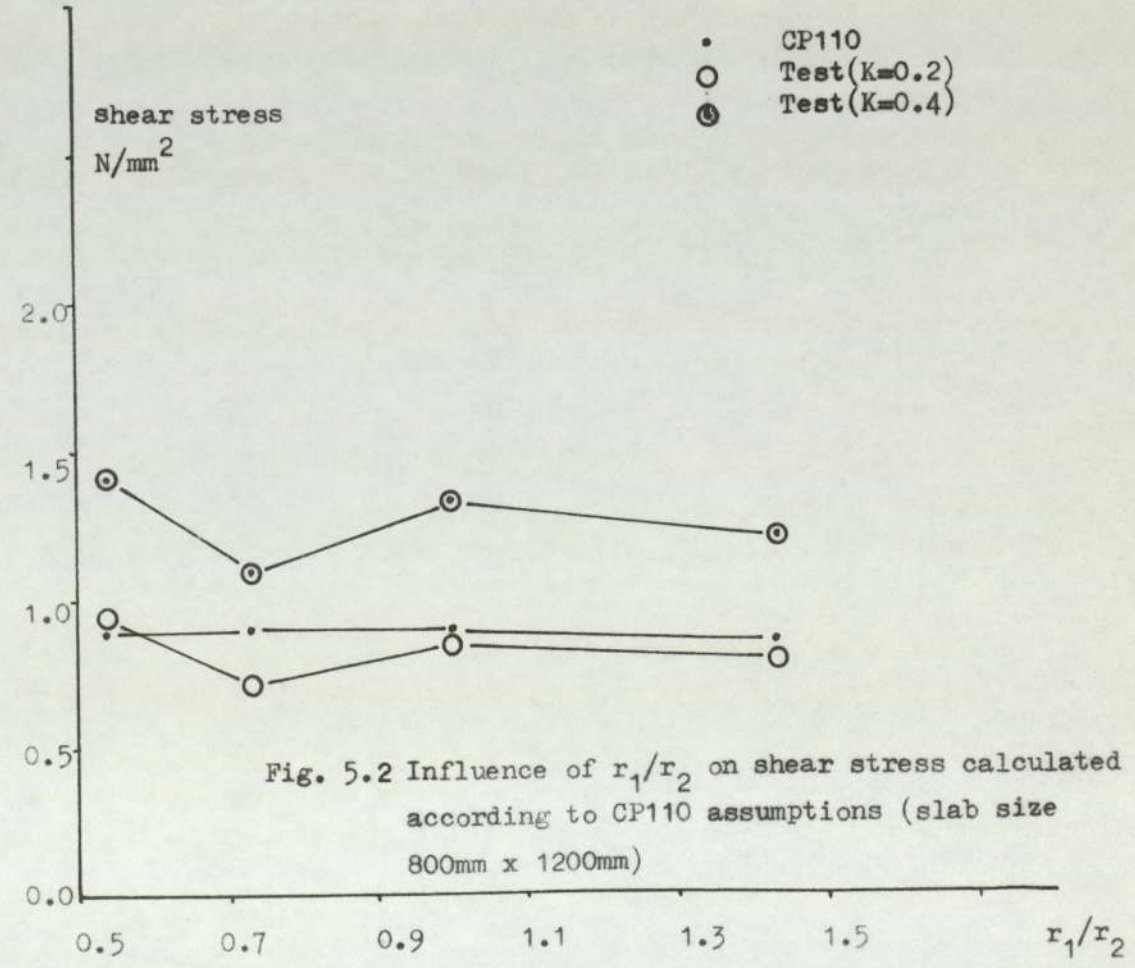

Fig. 5.2 Influence of r_1/r_2 on shear stress calculated according to CP110 assumptions (slab size 800mm x 1200mm)

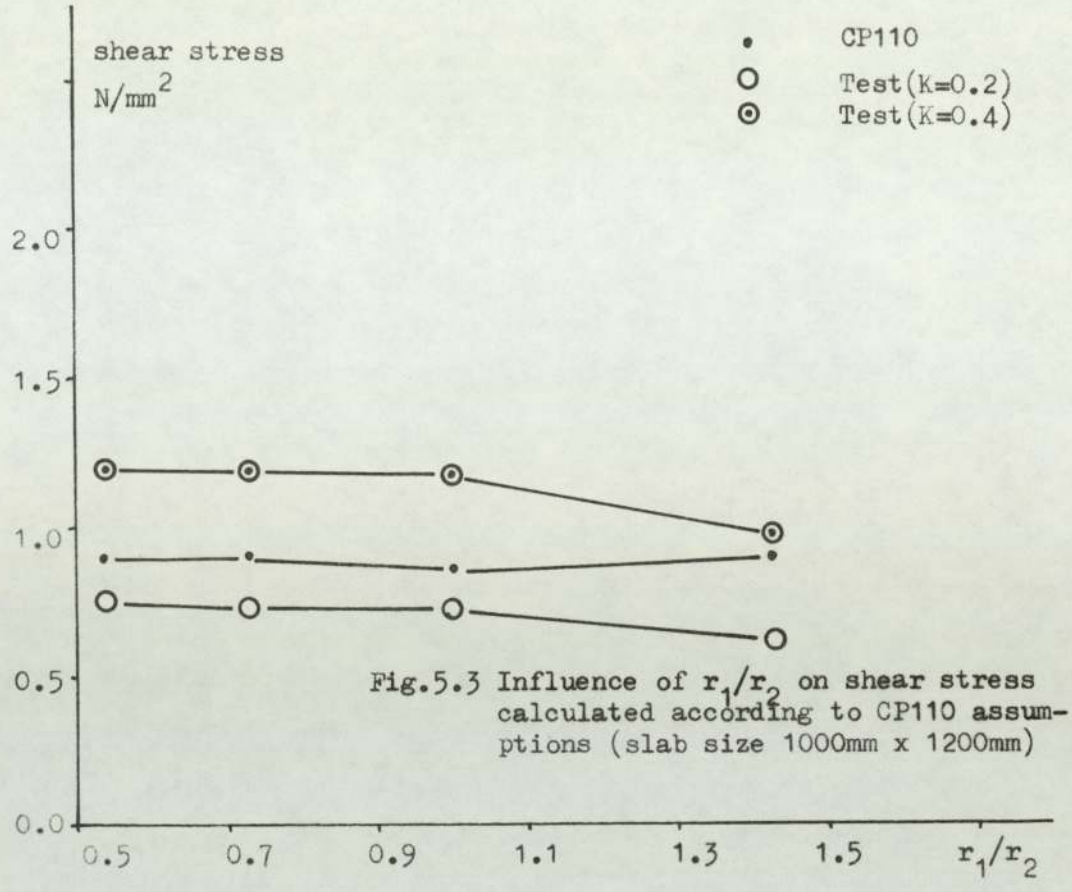

Fig.5.3 Influence of r_1/r_2 on shear stress calculated according to CP110 assumptions (slab size 1000mm x 1200mm)

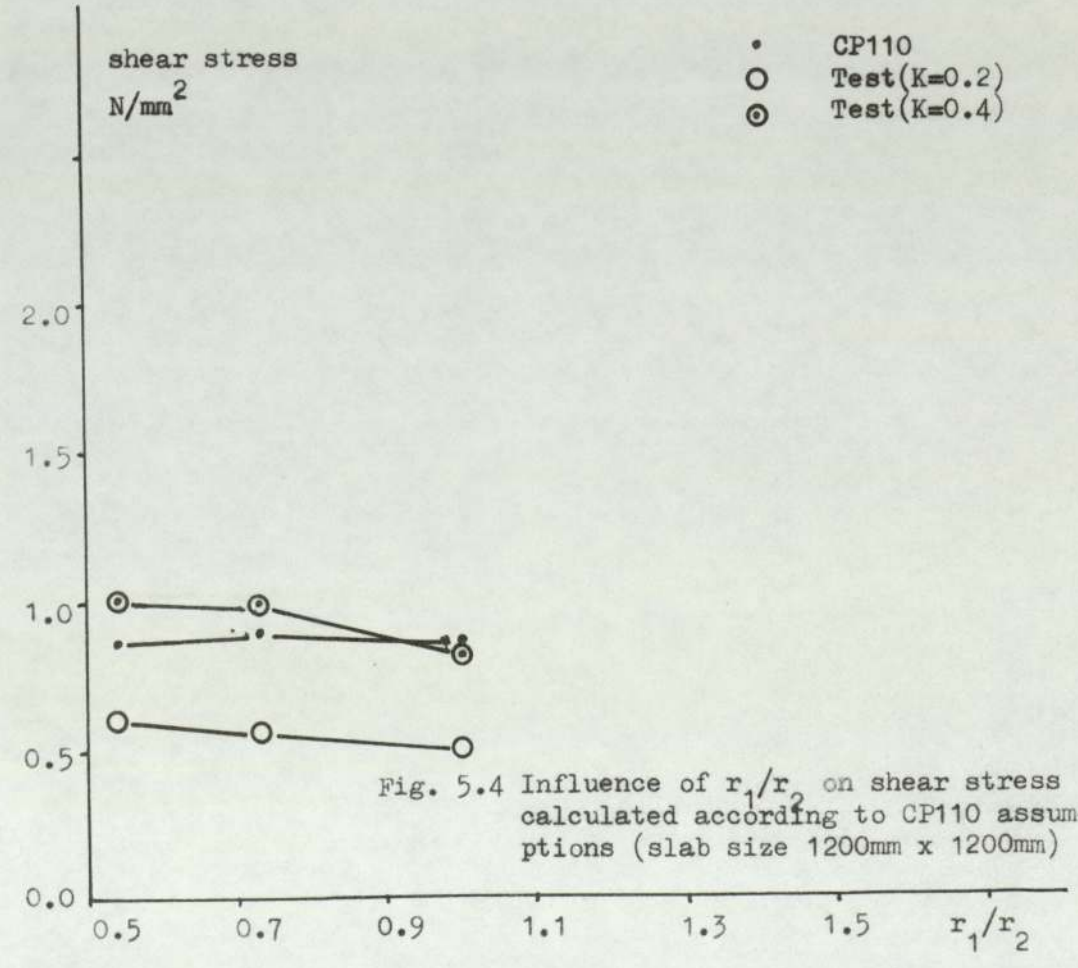

Fig. 5.4 Influence of r_1/r_2 on shear stress calculated according to CP110 assumptions (slab size 1200mm x 1200mm)

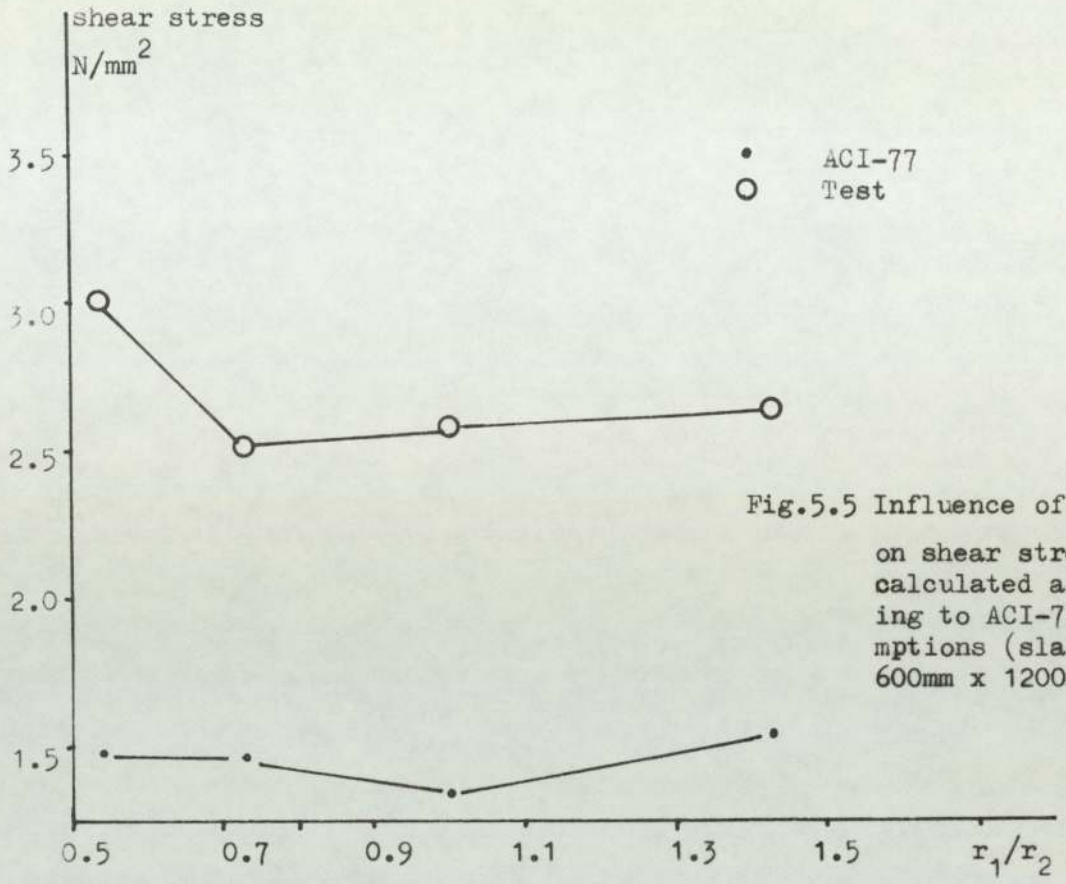

Fig.5.5 Influence of r_1/r_2 on shear stress calculated according to ACI-77 assumptions (slab size 600mm x 1200mm)

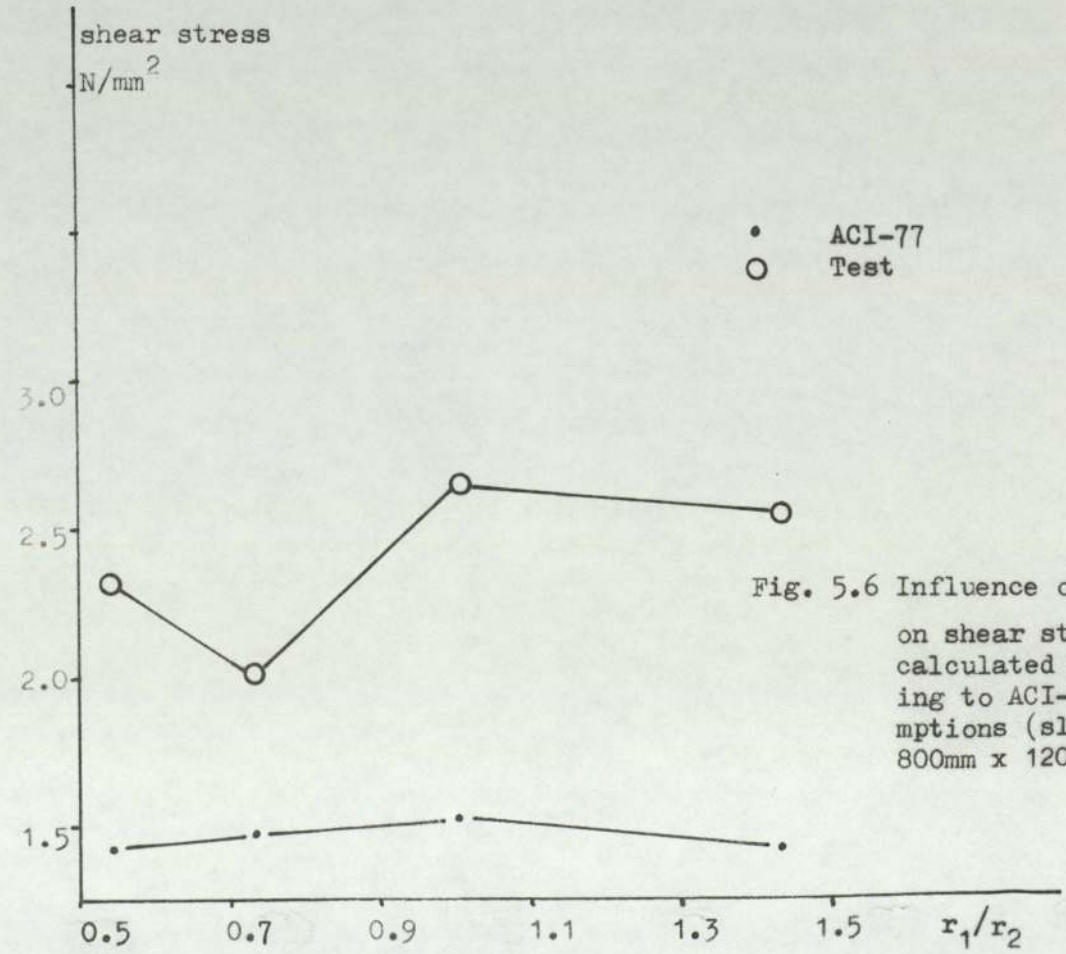

Fig. 5.6 Influence of r_1/r_2 on shear stress calculated according to ACI-77 assumptions (slab size 800mm x 1200mm)

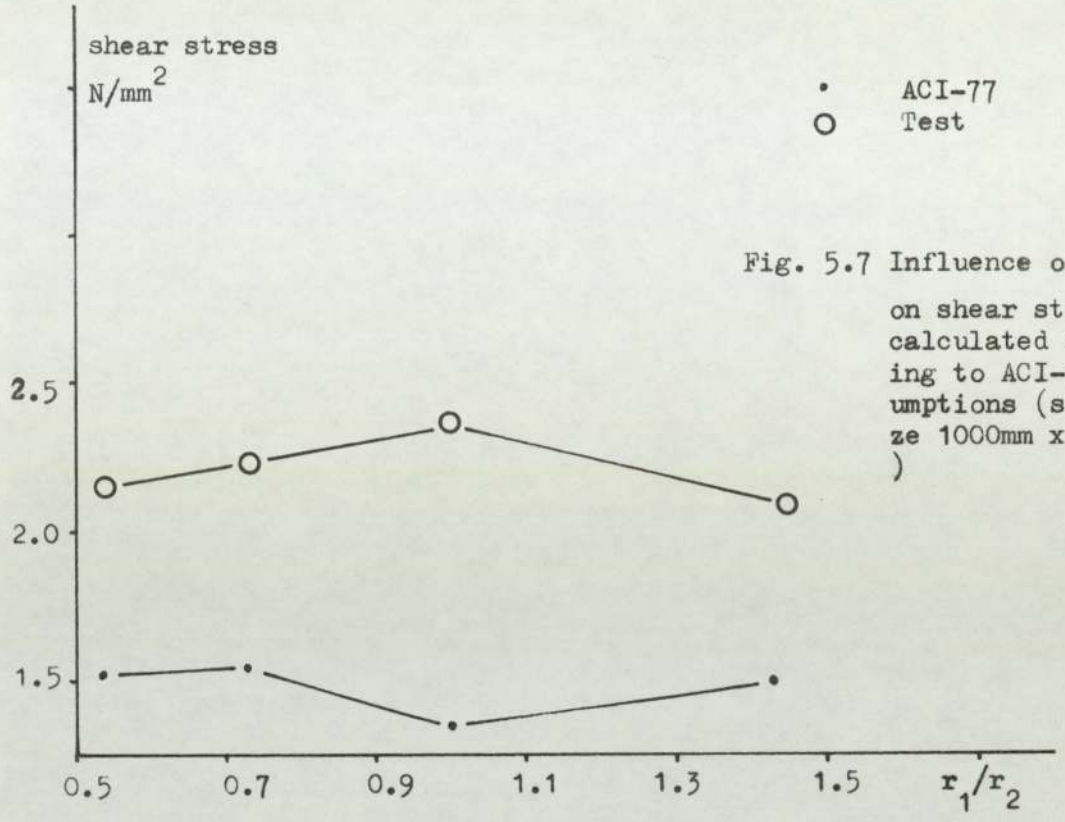

Fig. 5.7 Influence of r_1/r_2 on shear stress calculated according to ACI-77 assumptions (slab size 1000mm x 1200mm)

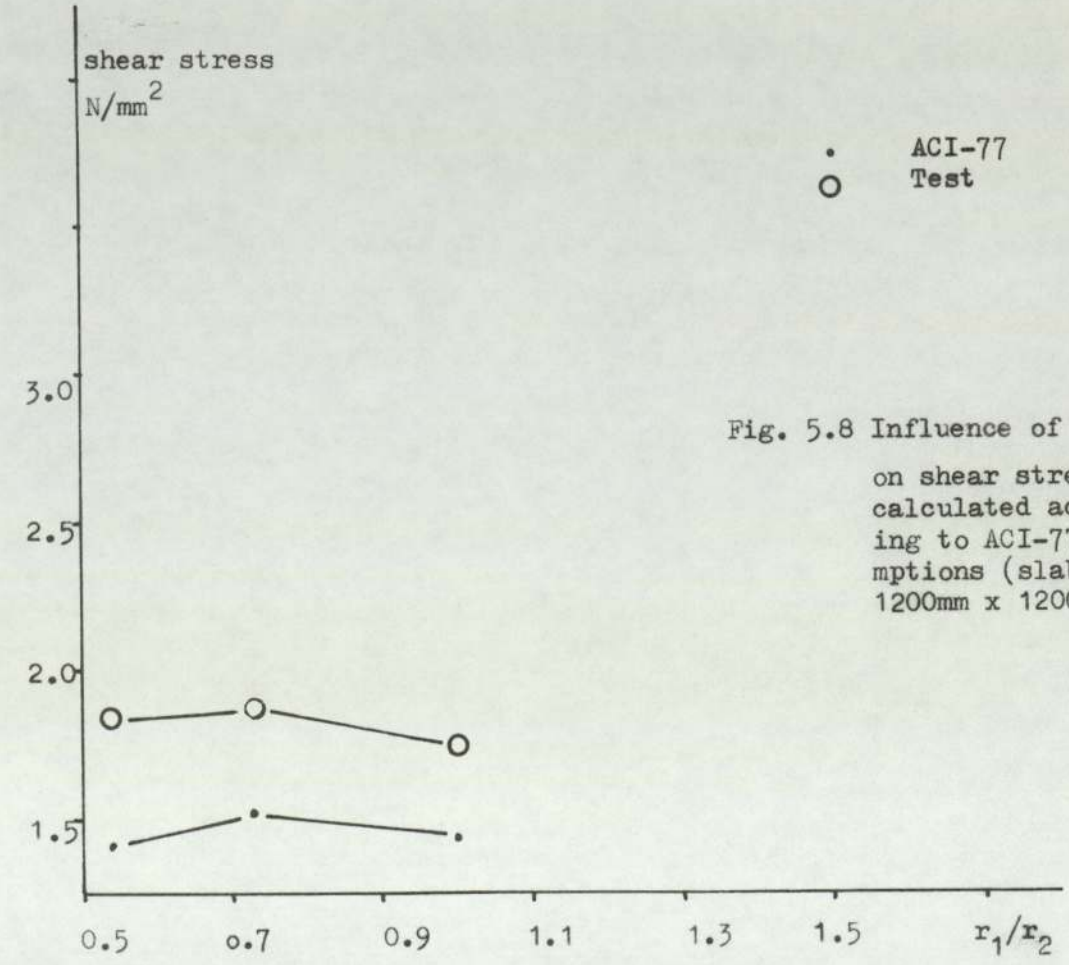

Fig. 5.8 Influence of r_1/r_2 on shear stress calculated according to ACI-77 assumptions (slab size 1200mm x 1200mm)

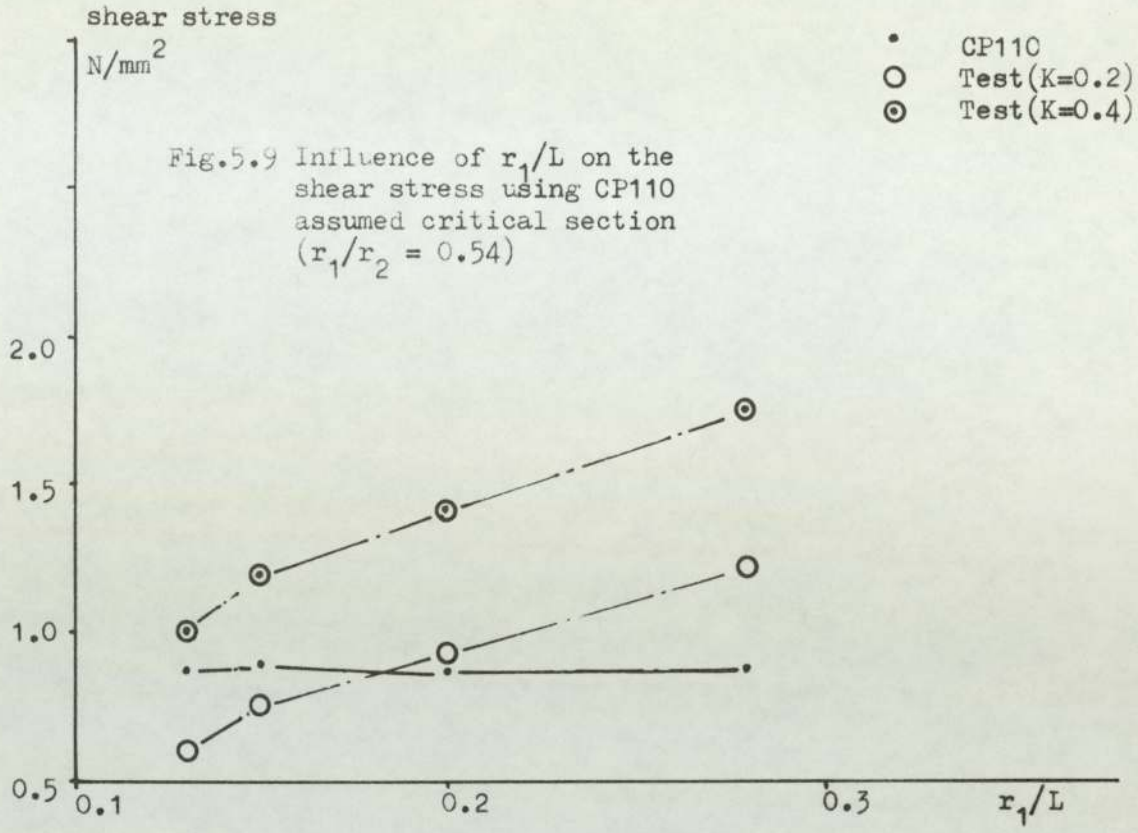

Fig.5.9 Influence of r_1/L on the shear stress using CP110 assumed critical section ($r_1/r_2 = 0.54$)

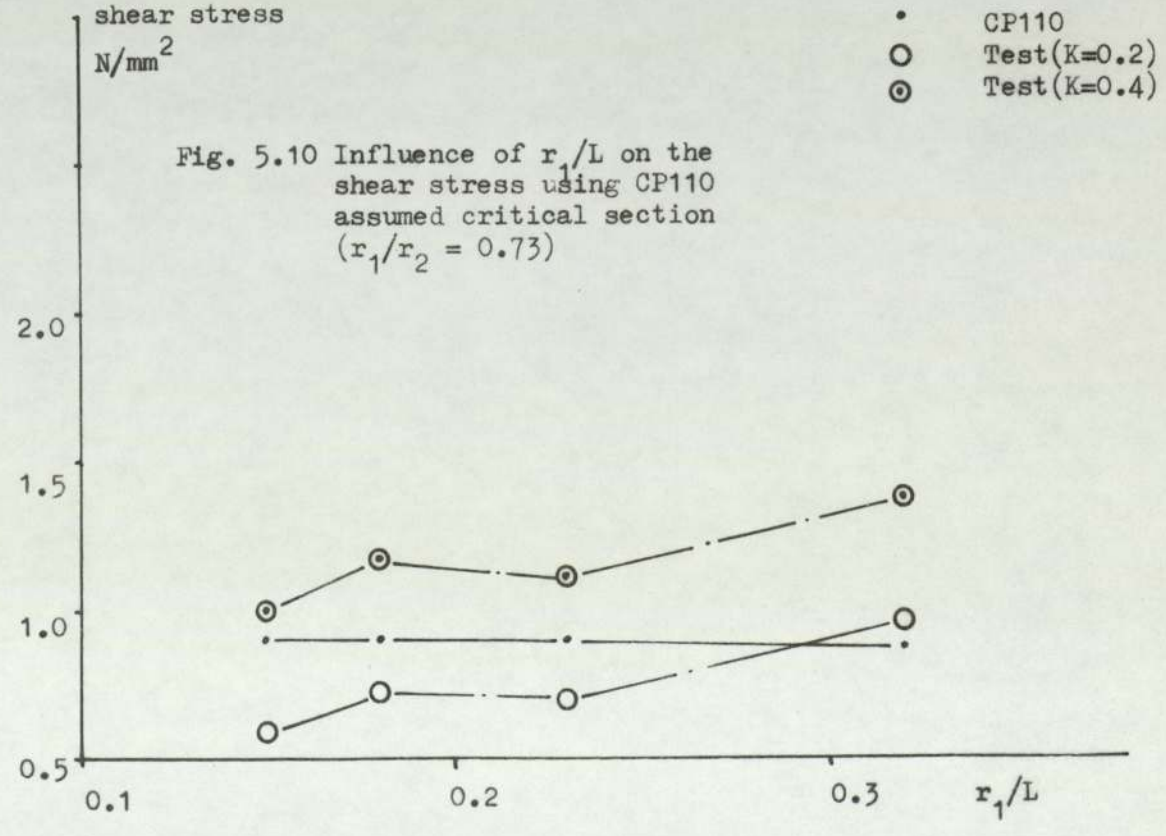

Fig. 5.10 Influence of r_1/L on the shear stress using CP110 assumed critical section ($r_1/r_2 = 0.73$)

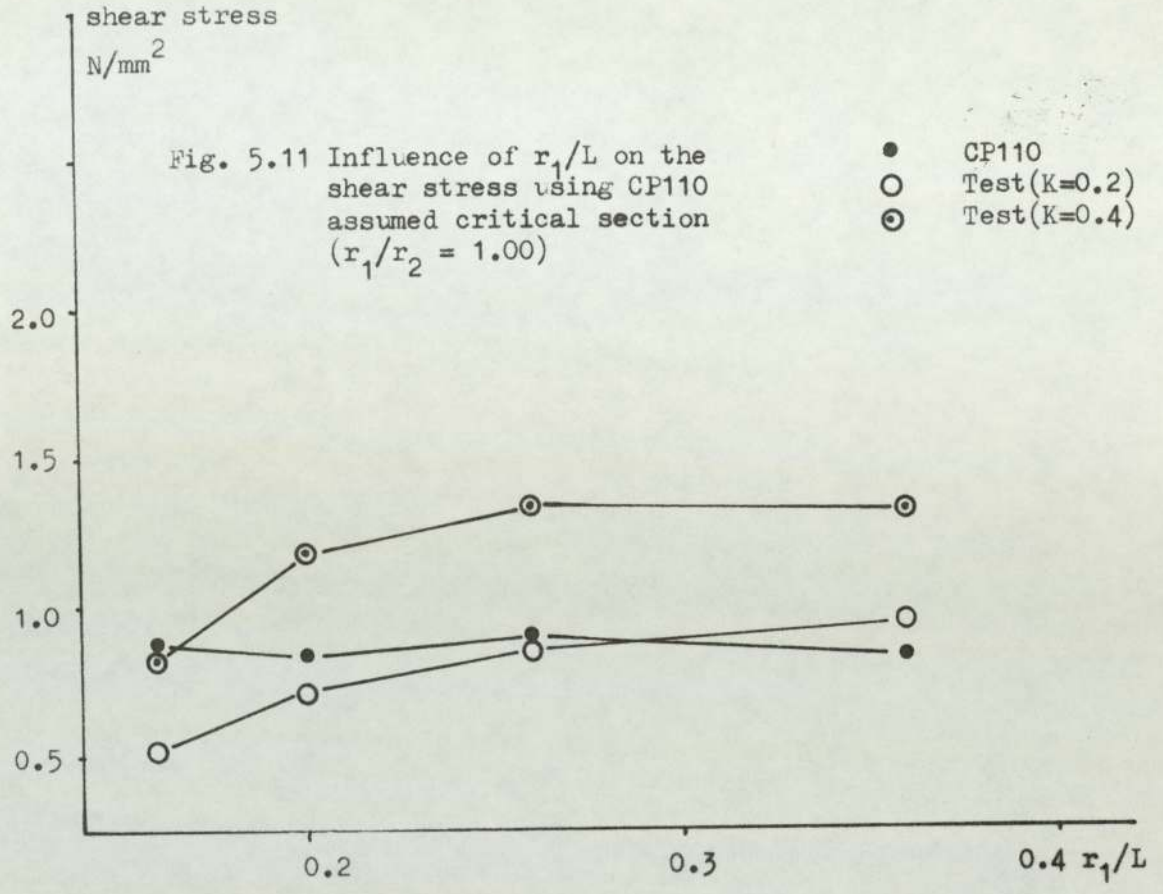

Fig. 5.11 Influence of r_1/L on the shear stress using CP110 assumed critical section (r_1/r_2 = 1.00)

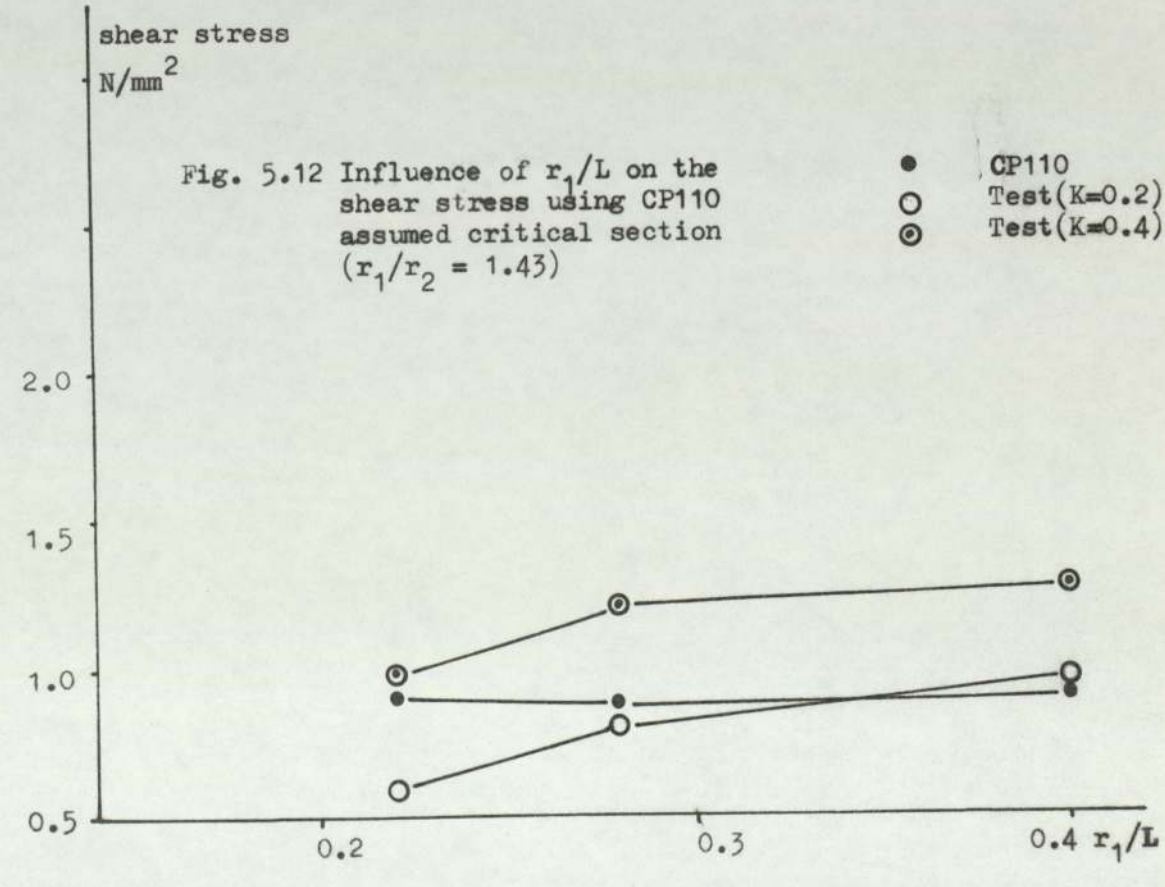

Fig. 5.12 Influence of r_1/L on the shear stress using CP110 assumed critical section (r_1/r_2 = 1.43)

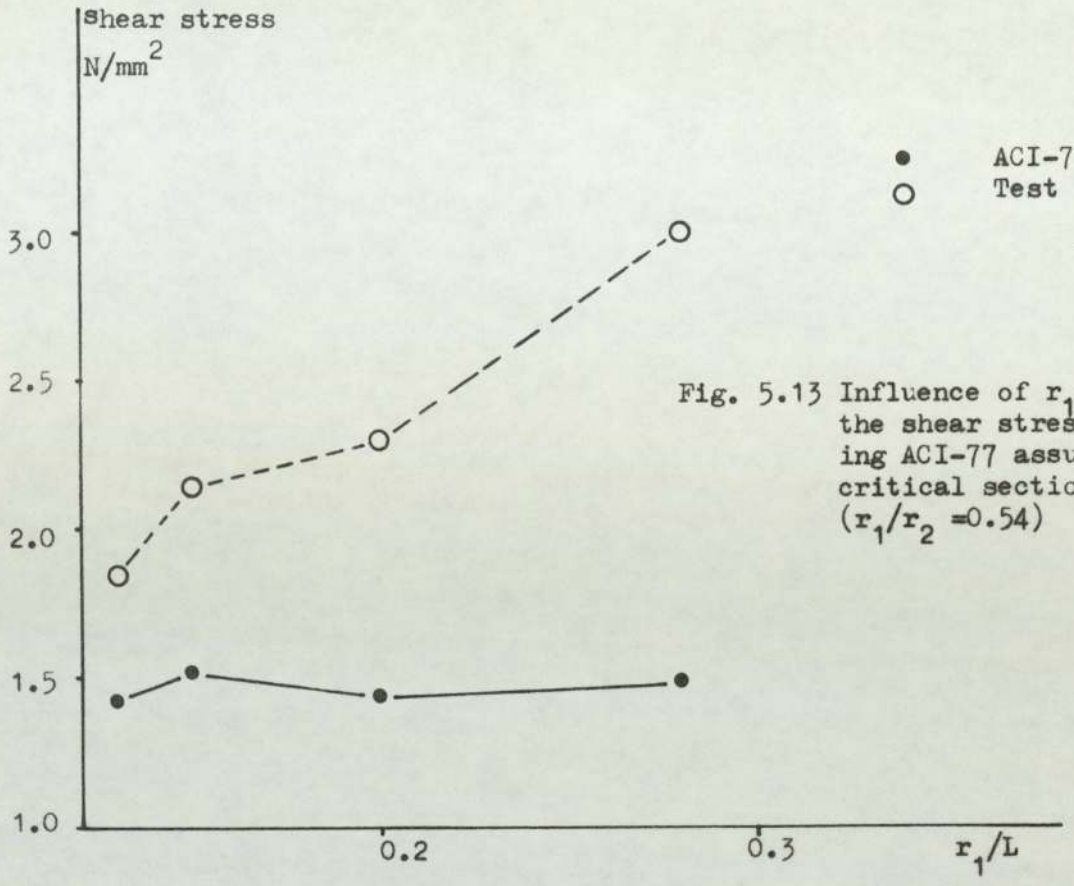

Fig. 5.13 Influence of r_1/L on the shear stress using ACI-77 assumed critical section (r_1/r_2 =0.54)

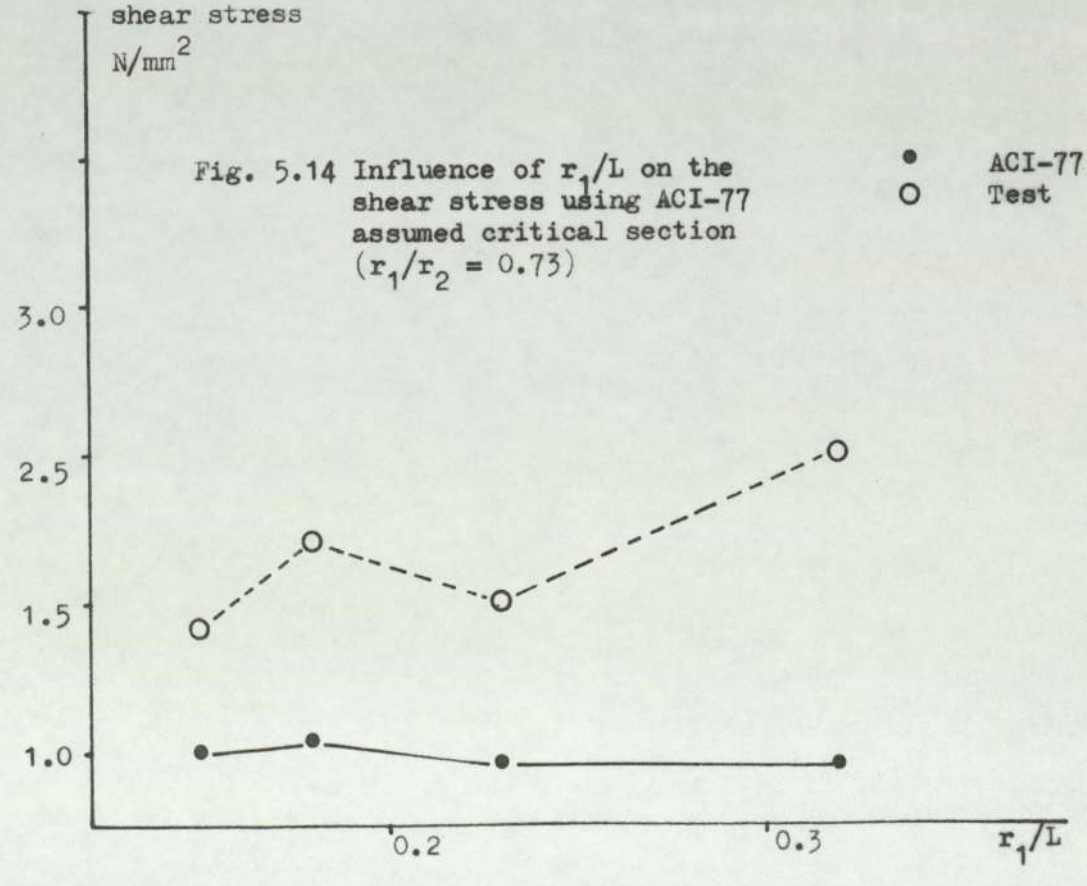

Fig. 5.14 Influence of r_1/L on the shear stress using ACI-77 assumed critical section (r_1/r_2 = 0.73)

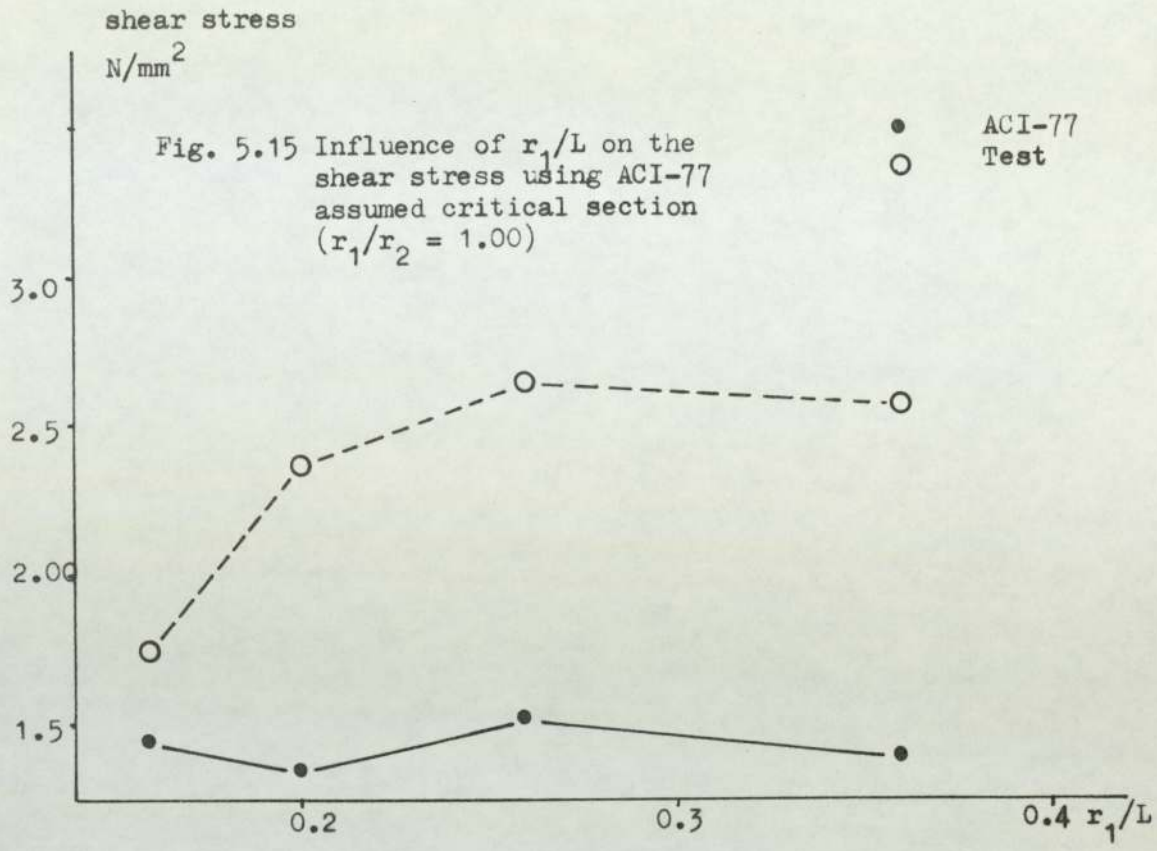

Fig. 5.15 Influence of r_1/L on the shear stress using ACI-77 assumed critical section (r_1/r_2 = 1.00)

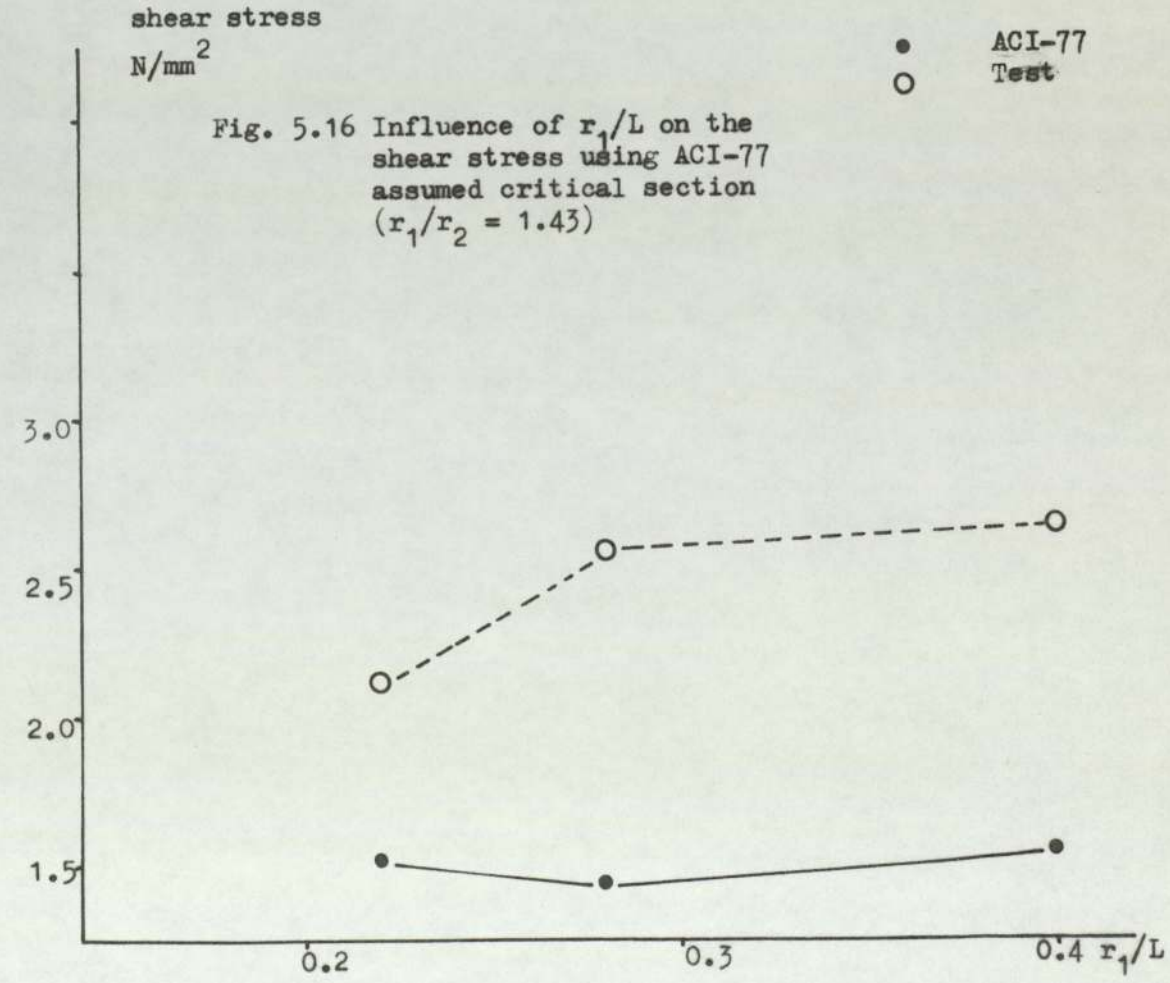

Fig. 5.16 Influence of r_1/L on the shear stress using ACI-77 assumed critical section (r_1/r_2 = 1.43)

r_1/r_2 ratio. Also in Figs. 5.5 to 5.8 the calculated ultimate shear stress (according to ACI-77) is plotted against r_1/r_2 ratio. As shown in these figures, the effect of r_1/r_2 ratio on the ultimate shear stress is small. As r_1/r_2 increases the ultimate shear stress decreases slightly, while the allowable shear stress given by the codes remains practically constant. Also we can notice from those figures that the code values are not on straight line because they are dependent on concrete strength.

The allowable ultimate shear strength under ACI-77 code seems to be highly conservative when the value of k is taken according to the code equation (Eq. 2.26), while the ultimate shear strength under CP110 appears to be unsafe for all tests when k = 0 and unsafe for high values of r_1/r_2 when k = 0.20. If the value of k = 0.40 is used in calculating the shear stress using the CP110 assumptions for critical section, and the results are compared with CP110, it can be seen that all specimens produce safe results except those with high values of r_1/r_2.

5.1.4 Effect of r_1/L ratio

In Figs. 5.9 to 5.12 the calculated ultimate shear stress,using a critical plane at 1.5h from the column as is done in CP110,is plotted against r_1/L ratio. In Figs. 5.13 to 5.16 the calculated ultimate shear stress,using a critical section at d/2 from the column as in ACI-77 code, is plotted against r_1/L ratio.

As shown in these figures the ultimate shear stress calculated using Eq. 5.1 tends to increase with the increase in r_1/L while the allowable shear stress remains practically constant. These figures also demonstrate that the ratio v_{test}/v_{code} increases as r_1/L ratio increases, therefore for high values of r_1/L the allowable ultimate shear strength under the present codes seem to be more conservative than for low values of r_1/L; while it seems to be unsafe for small values of r_1/L (see Fig. 5.17). Fig. 5.18 shows the effect of the ratio P/L (where P is the perimeter of the column for three sides). As shown from this figure, for high values of P/L the allowable shear strength under the present codes is conservative and it is unsafe for small values of P/L.

5.1.5. Effect of r_1/d ratio

In Figs. 5.19 to 5.22 the calculated ultimate shear stress (according to CP110 assumptions) is plotted against r_1/d ratio. In Figs. 5.23 to 5.24 the calculated ultimate shear stress (according to ACI-77) is plotted against r_1/d ratio.

As shown in these figures, the effect of r_1/d ratio seems to be similar to the effect of r_1/r_2 ratio. As r_1/d ratio increased the calculated ultimate shear stress decreased slightly while the allowable shear stress remained constant.

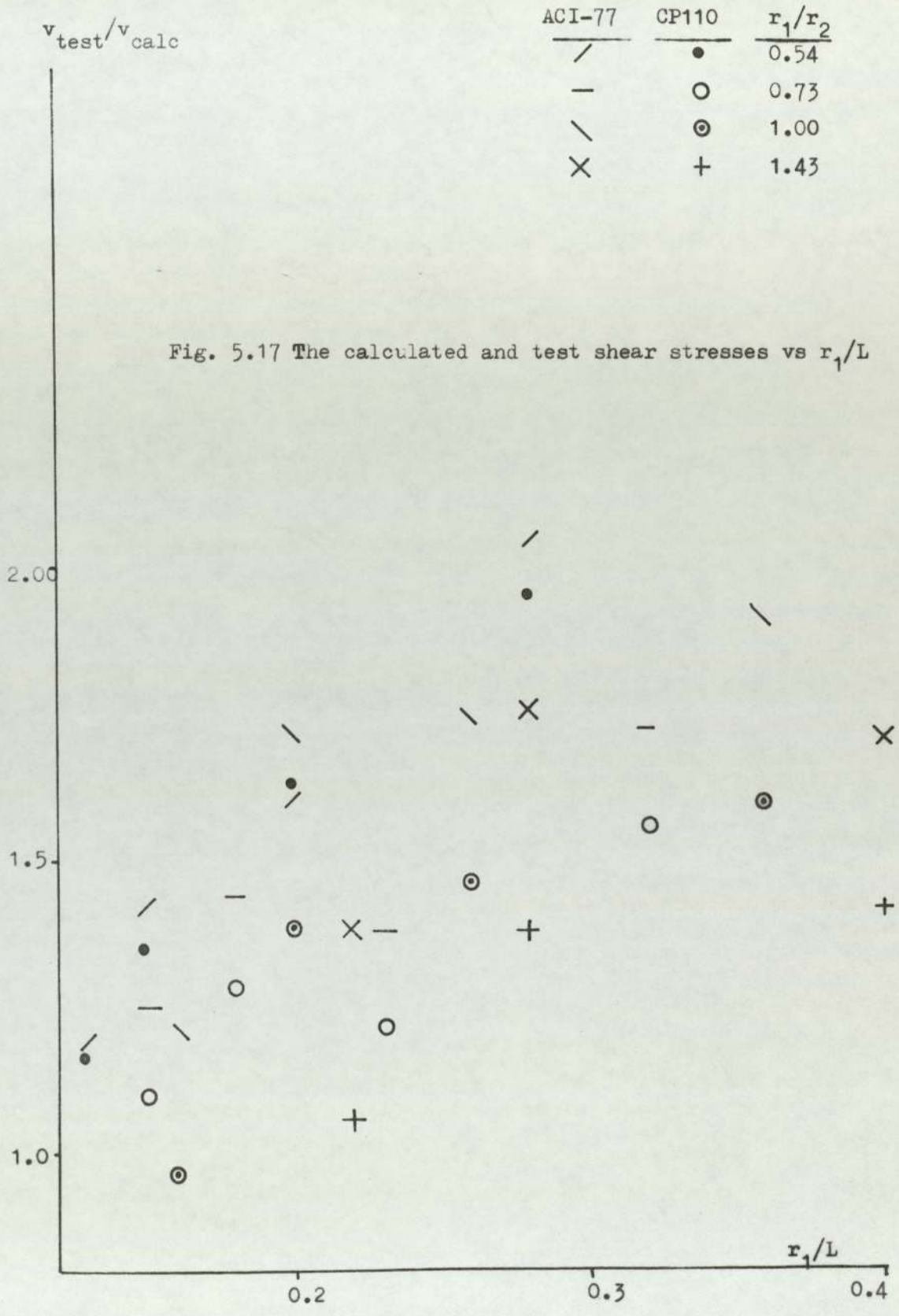

Fig. 5.17 The calculated and test shear stresses vs r_1/L

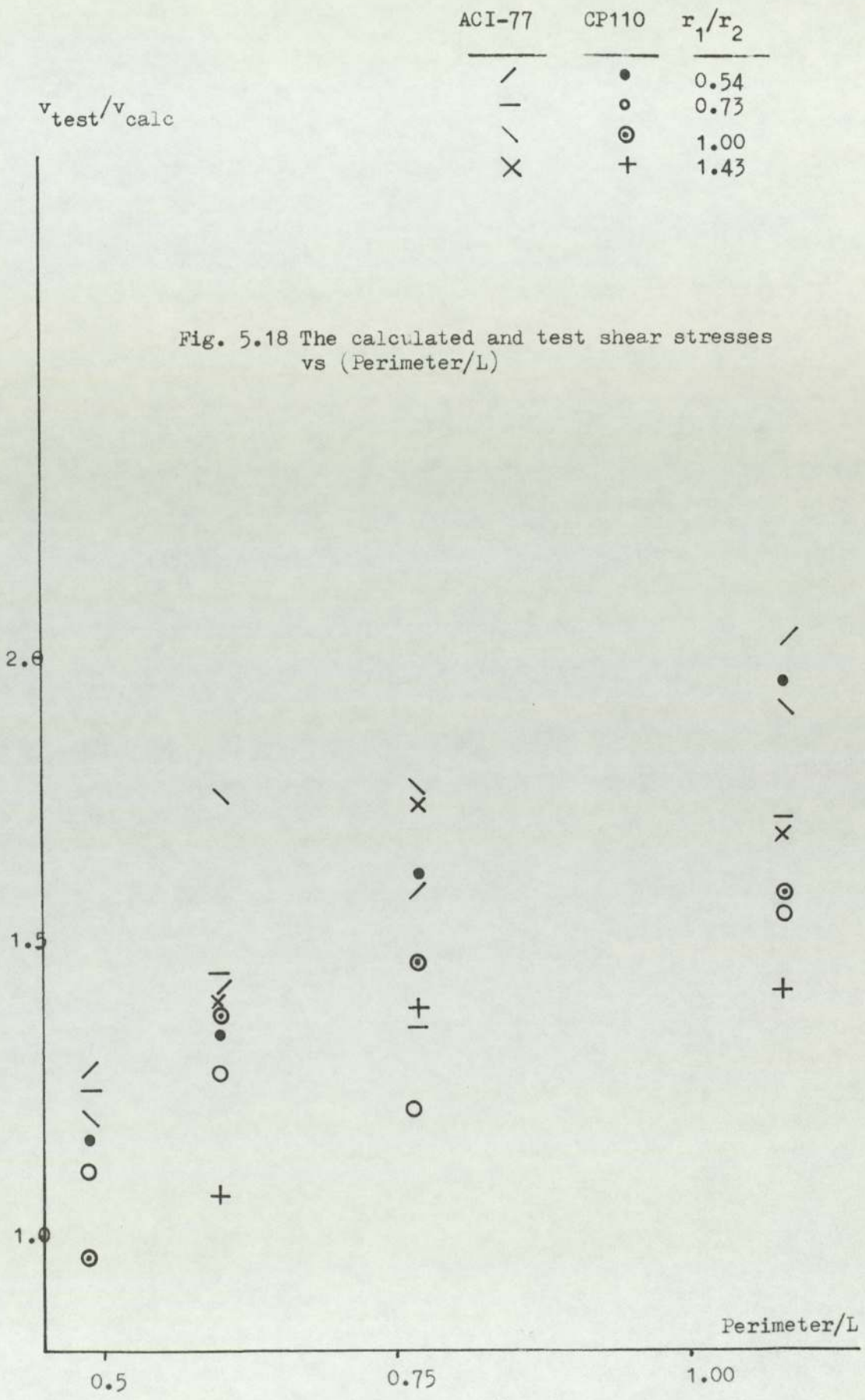

Fig. 5.18 The calculated and test shear stresses vs (Perimeter/L)

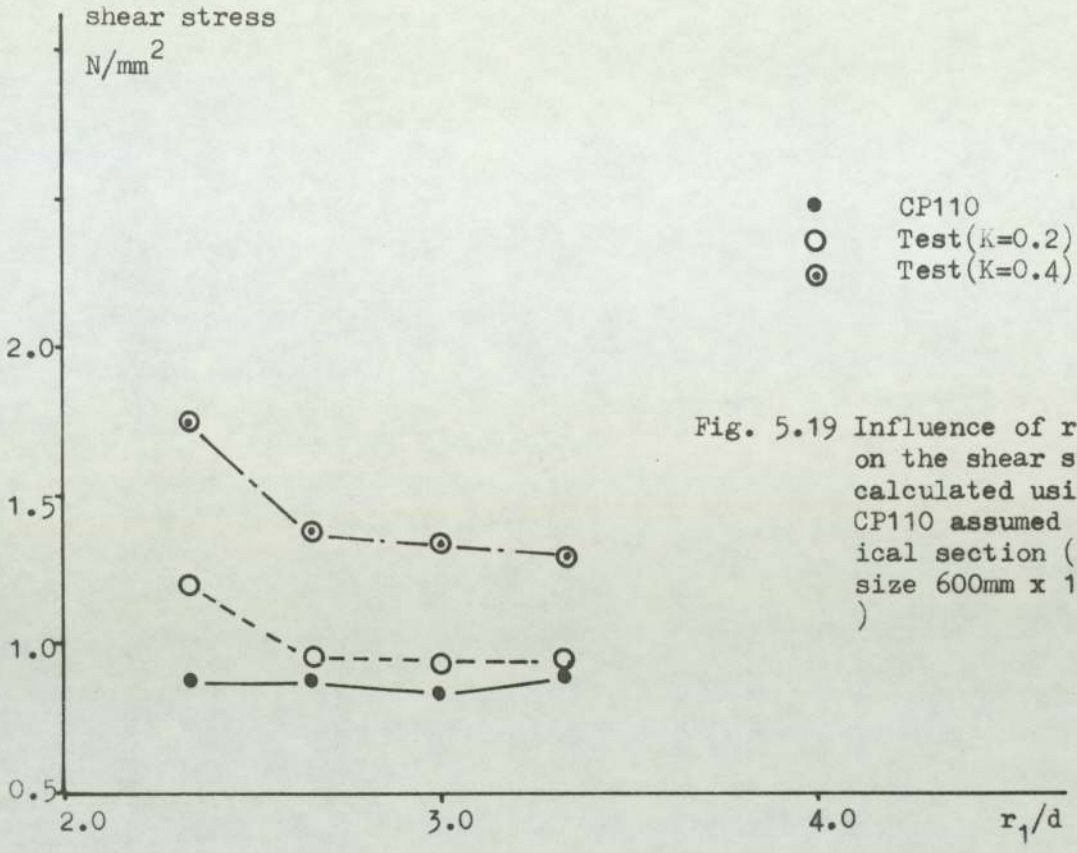

Fig. 5.19 Influence of r_1/d on the shear stress calculated using CP110 assumed critical section (slab size 600mm x 1200mm)

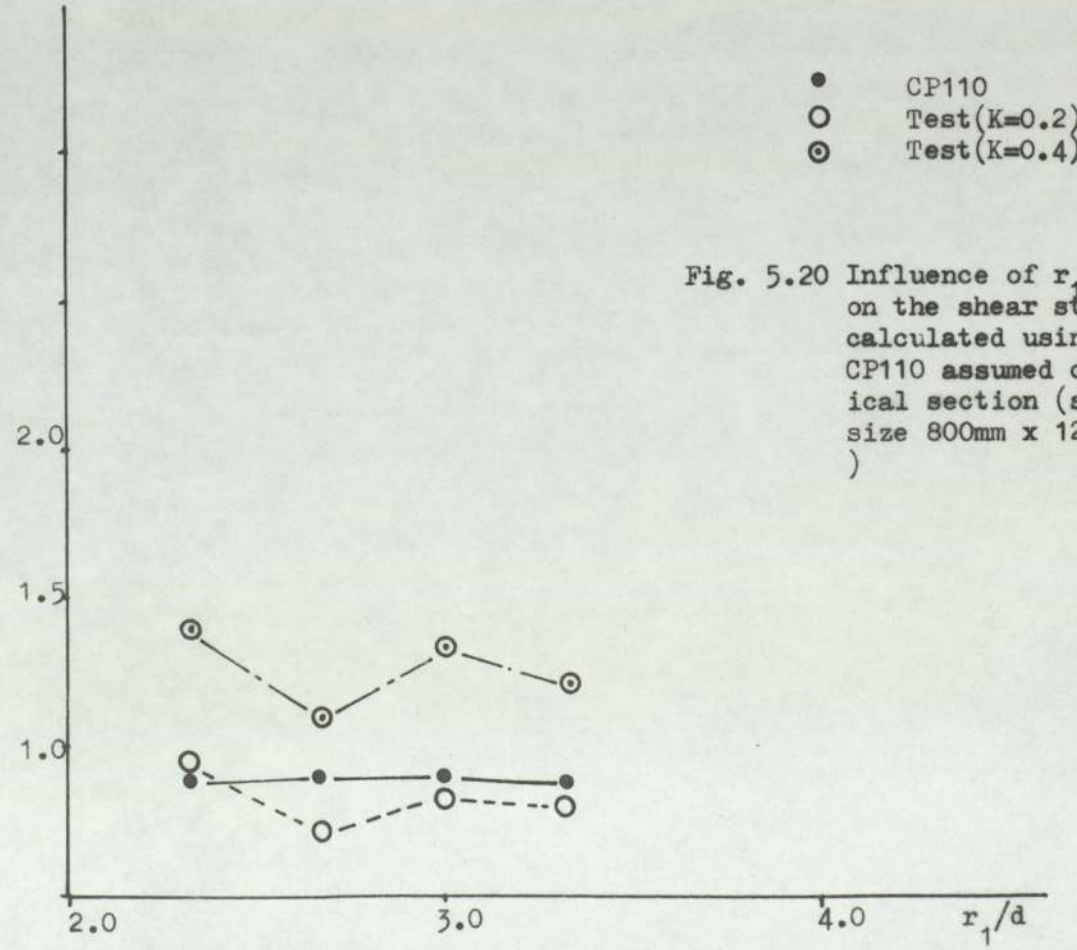

Fig. 5.20 Influence of r_1/d on the shear stress calculated using CP110 assumed critical section (slab size 800mm x 1200mm)

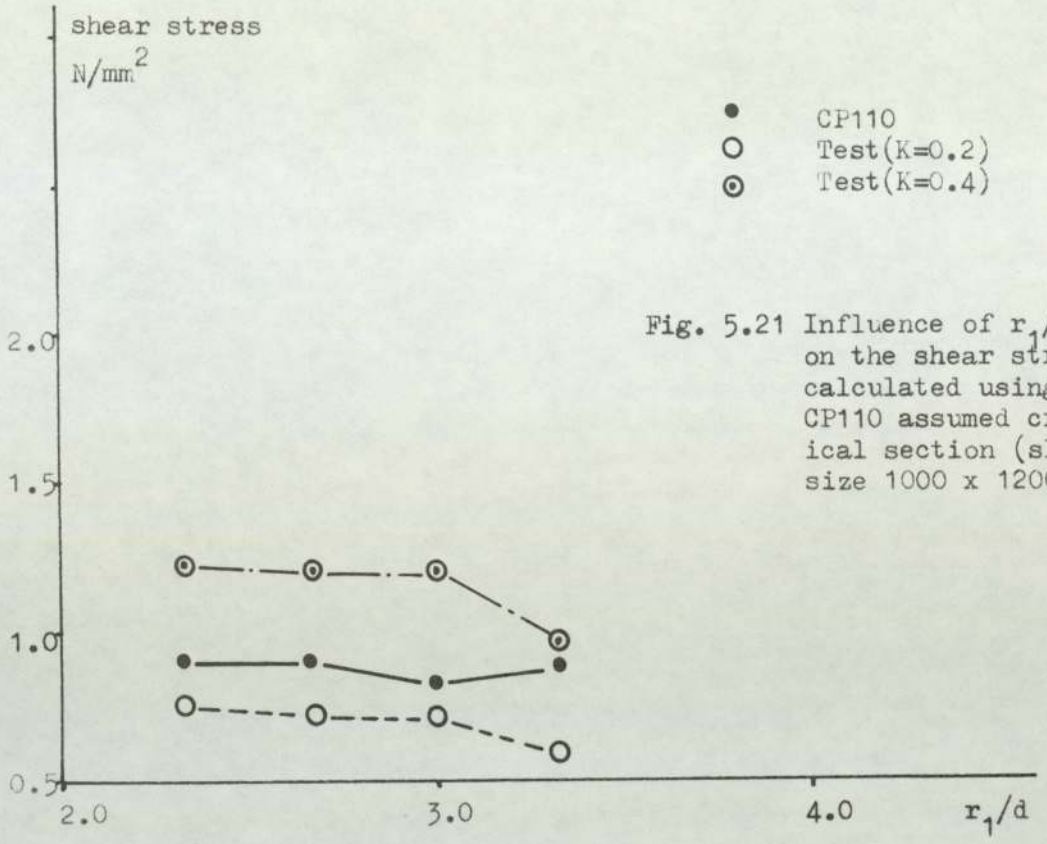

Fig. 5.21 Influence of r_1/d on the shear stress calculated using CP110 assumed critical section (slab size 1000 x 12000mm)

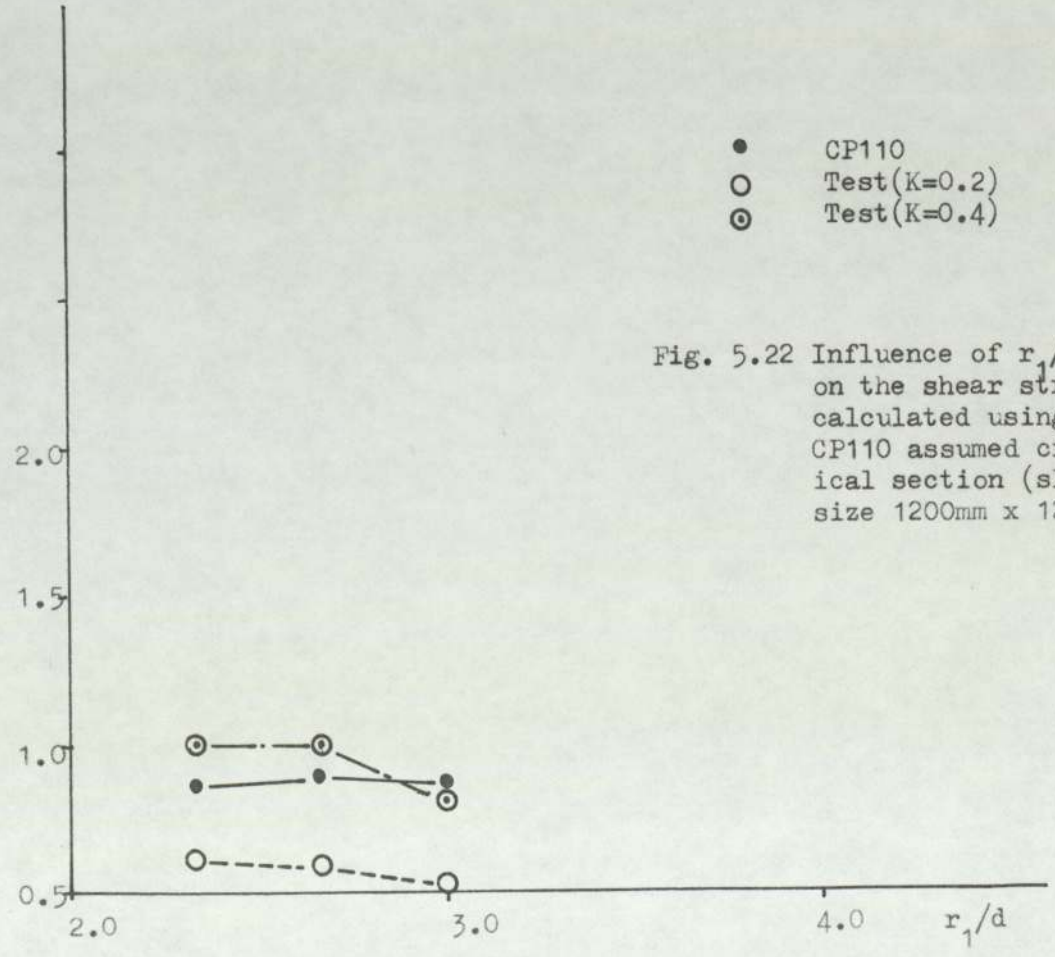

Fig. 5.22 Influence of r_1/d on the shear stress calculated using CP110 assumed critical section (slab size 1200mm x 1200mm)

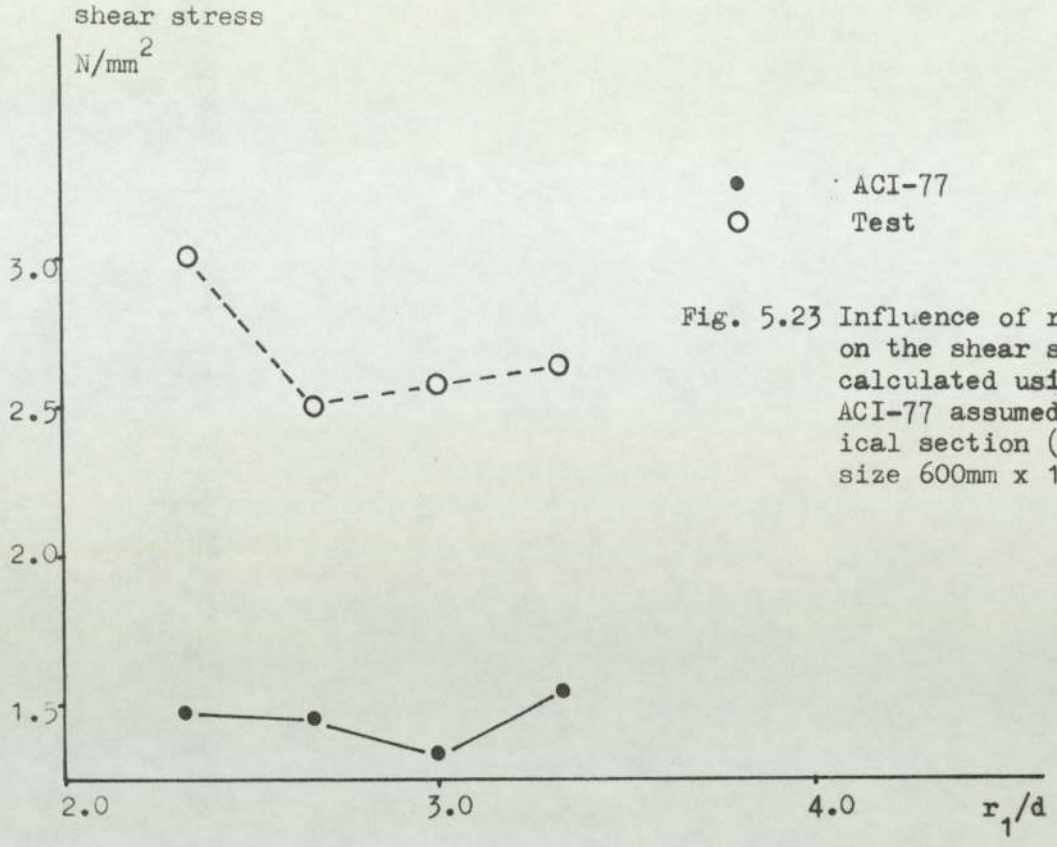

Fig. 5.23 Influence of r_1/d on the shear stress calculated using ACI-77 assumed critical section (slab size 600mm x 1200mm)

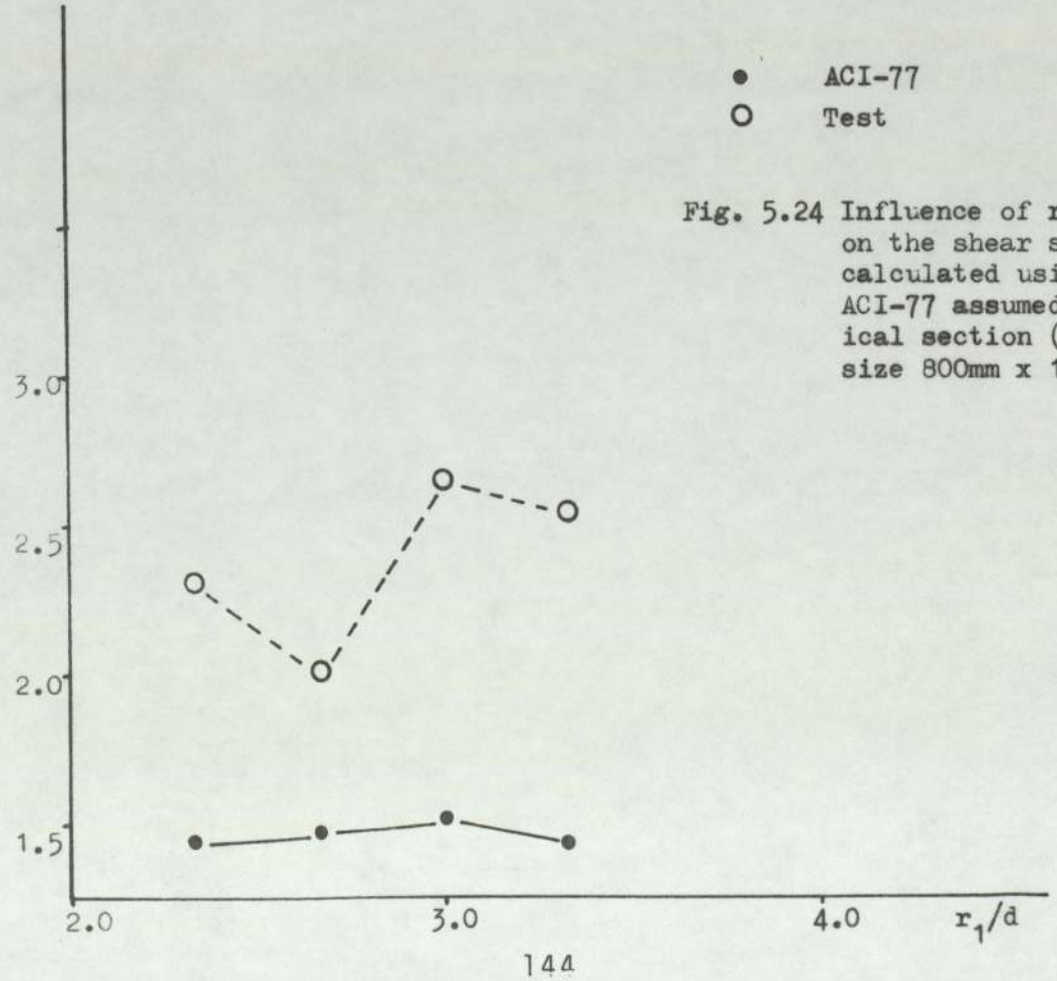

Fig. 5.24 Influence of r_1/d on the shear stress calculated using ACI-77 assumed critical section (slab size 800mm x 1200mm)

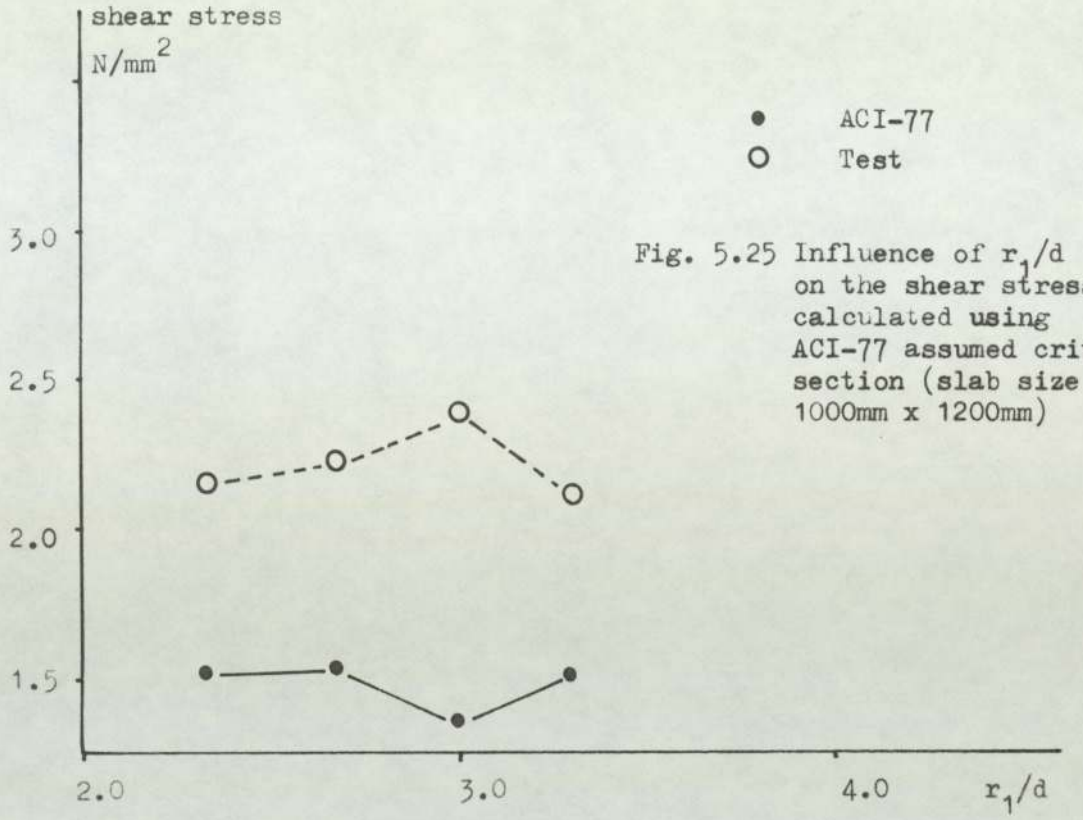

Fig. 5.25 Influence of r_1/d on the shear stress calculated using ACI-77 assumed critical section (slab size 1000mm x 1200mm)

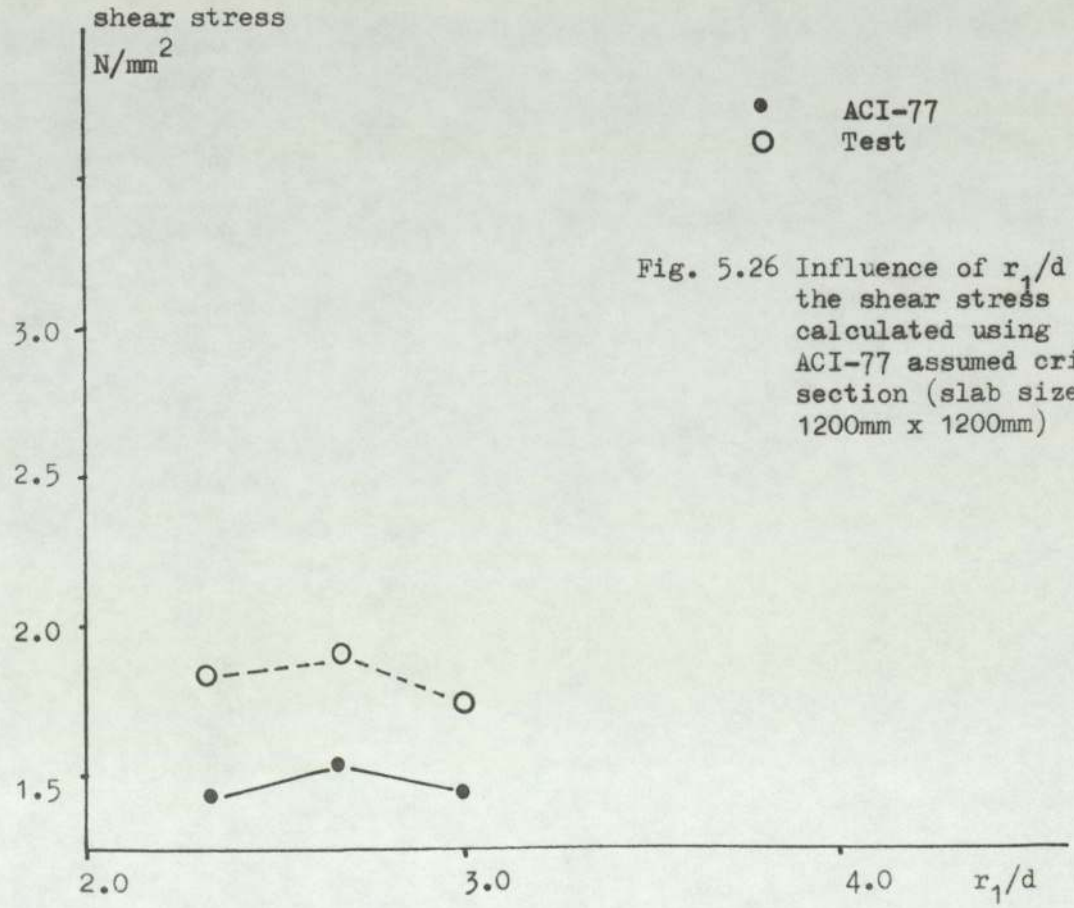

Fig. 5.26 Influence of r_1/d on the shear stress calculated using ACI-77 assumed critical section (slab size 1200mm x 1200mm)

5.1.6. Effect of $\frac{M}{V}$

From Figs. 5.27 to 5.34 the calculated ultimate shear stress decreases slightly as M/V increases. From these results it can be said that the current codes do not recognise the variation in the ultimate shear stress due to the variation in the M/V ratio.

5.1.7. Comparison with Regan's analysis for the edge connection.

To determine the punching resistance of an edge column, Regan used the following equation:

$$V_c' = 0.8\xi_s v_c b_p d \qquad (5.2)$$

where $b_p = b_o + 1.5\pi h$

He assumed that "The three-sides shapes of these perimeters are such as to offer very little bending stiffness, and it can be assumed that, so long as the combined flexural and torsional resistances are not exceeded, the shear distribution remains substantially uniform."

He supported this assumption by some test results from various sources as shown in Fig. 5.35. The moment resistances of this figure were calculated as

$$M_u = m_x b_y + 2\sqrt{m_x m_y}\, b_x$$

where M_u = ultimate bending resistance about an axis through the 'centre of gravity of the column perimeter

m_x, m_y = flexural resistance moments per unit width in x and y directions

$\sqrt{m_x m_y}$ = torsional resistance moments per unit width.

b_x, b_y = column dimensions.

By applying these equations on the present test results we find that these results give low shear strengths similar to the shear strengths obtained for the tests by Stamenkovic and shown in Fig. 5.35. This effect may be due to their small scale as suggested by Regan, h = 75 mm, and this scale is similar to Stamenkovic's scale (h = 76 mm).

5.2 Flexural Strength

5.2.1. General

The calculation of the ultimate flexural strength of the various test structures was made ignoring the possibility of a premature shear failure. The yield line theory as developed by K W Johanson[55] and discussed by others [56, 57, 58] was used for this purpose.

An evaluation of the strength of a test structure is important, not only because the computed or the observed strength of structures have general application to other structures of the same type, but also because a comparison of the computed and observed strength of the test structures is indicative of the reliability of the known methods of analysis in predicting the strength of relatively complex slabs.

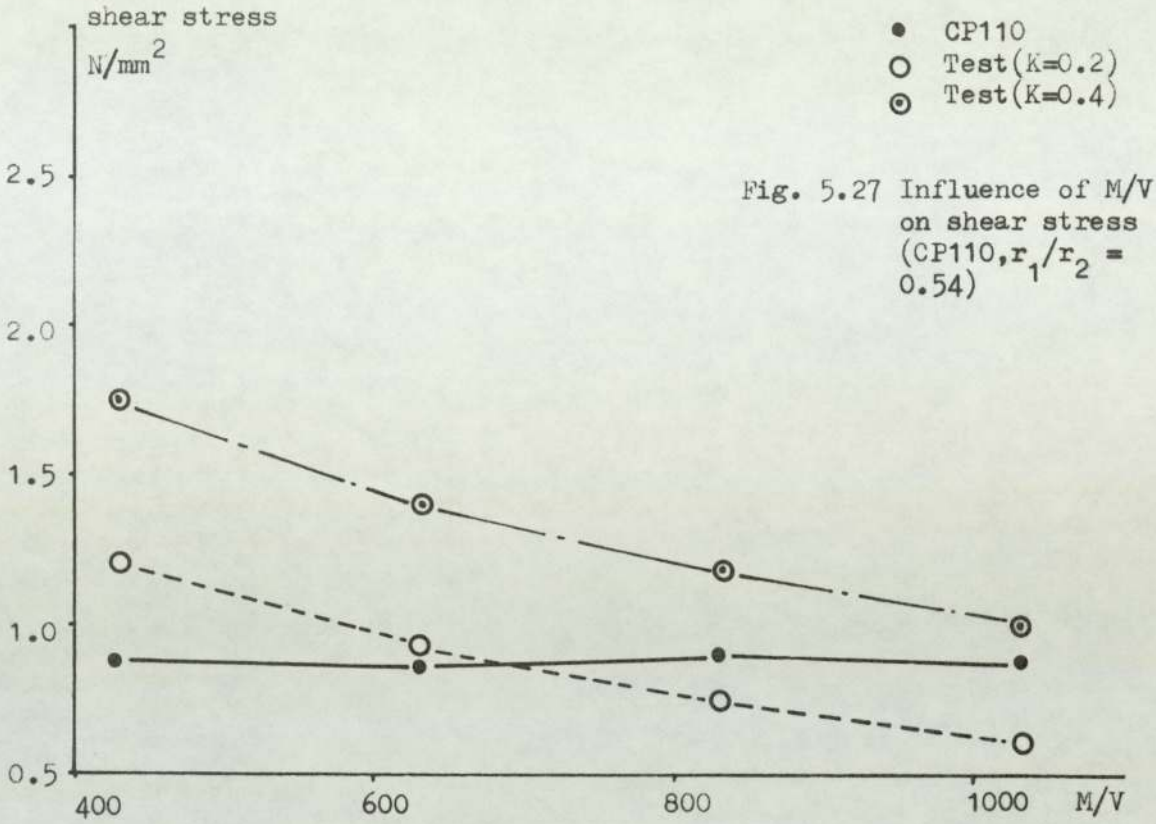

Fig. 5.27 Influence of M/V on shear stress (CP110, r_1/r_2 = 0.54)

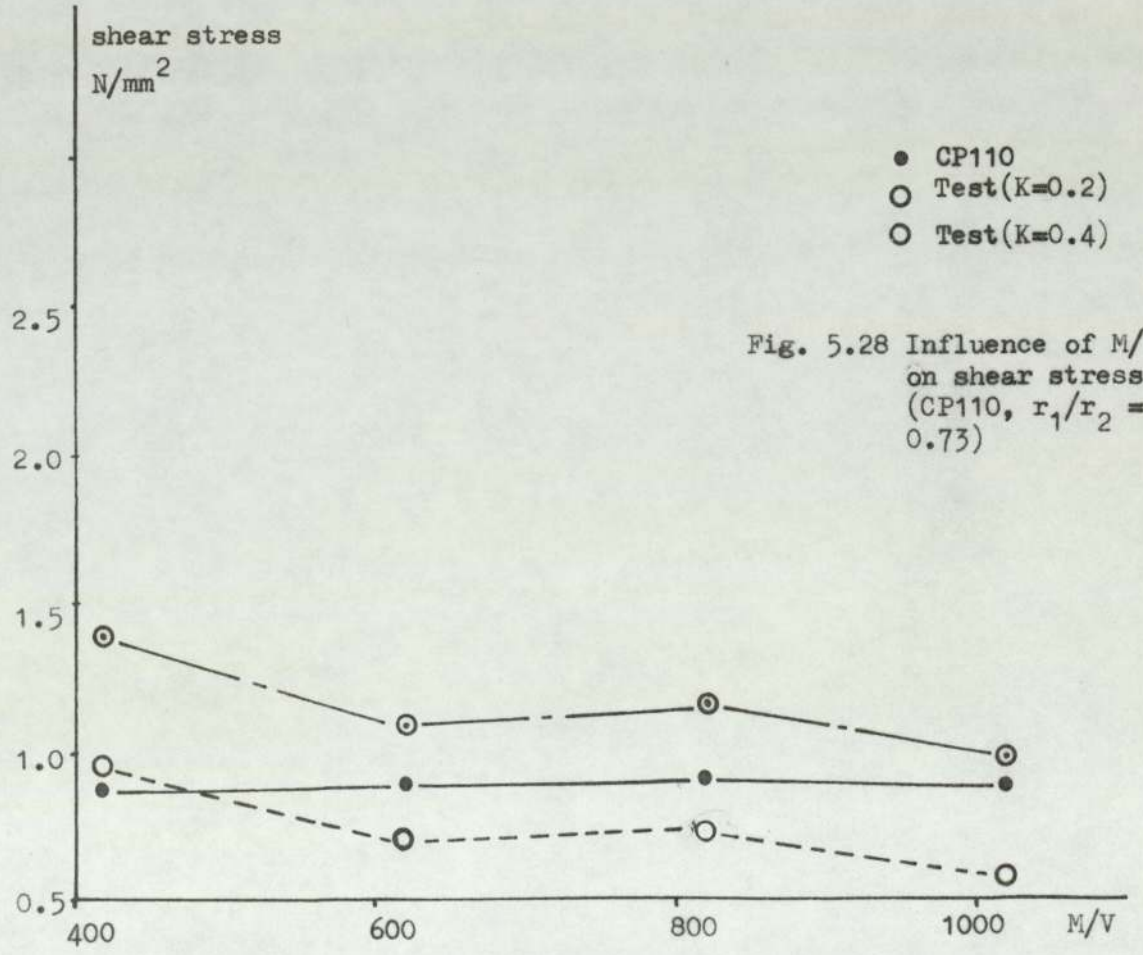

Fig. 5.28 Influence of M/V on shear stress (CP110, r_1/r_2 = 0.73)

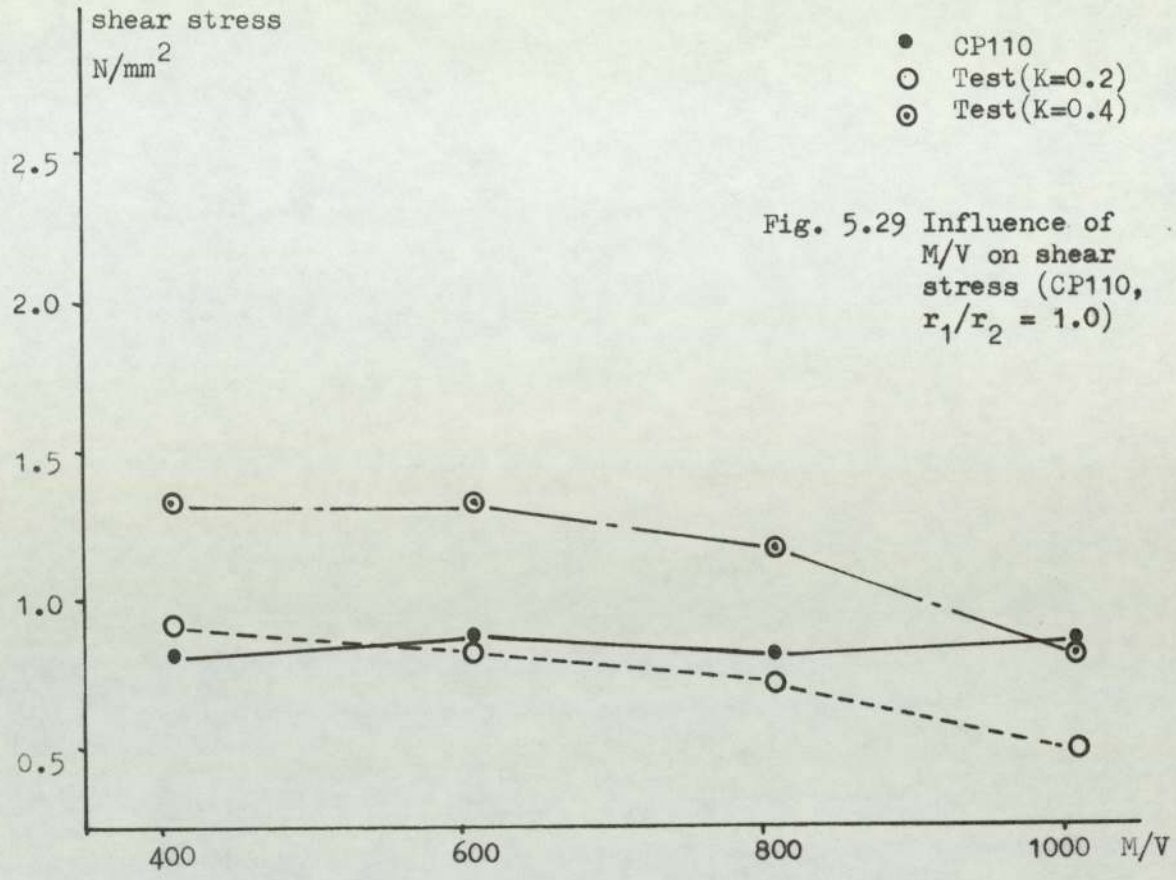

Fig. 5.29 Influence of M/V on shear stress (CP110, $r_1/r_2 = 1.0$)

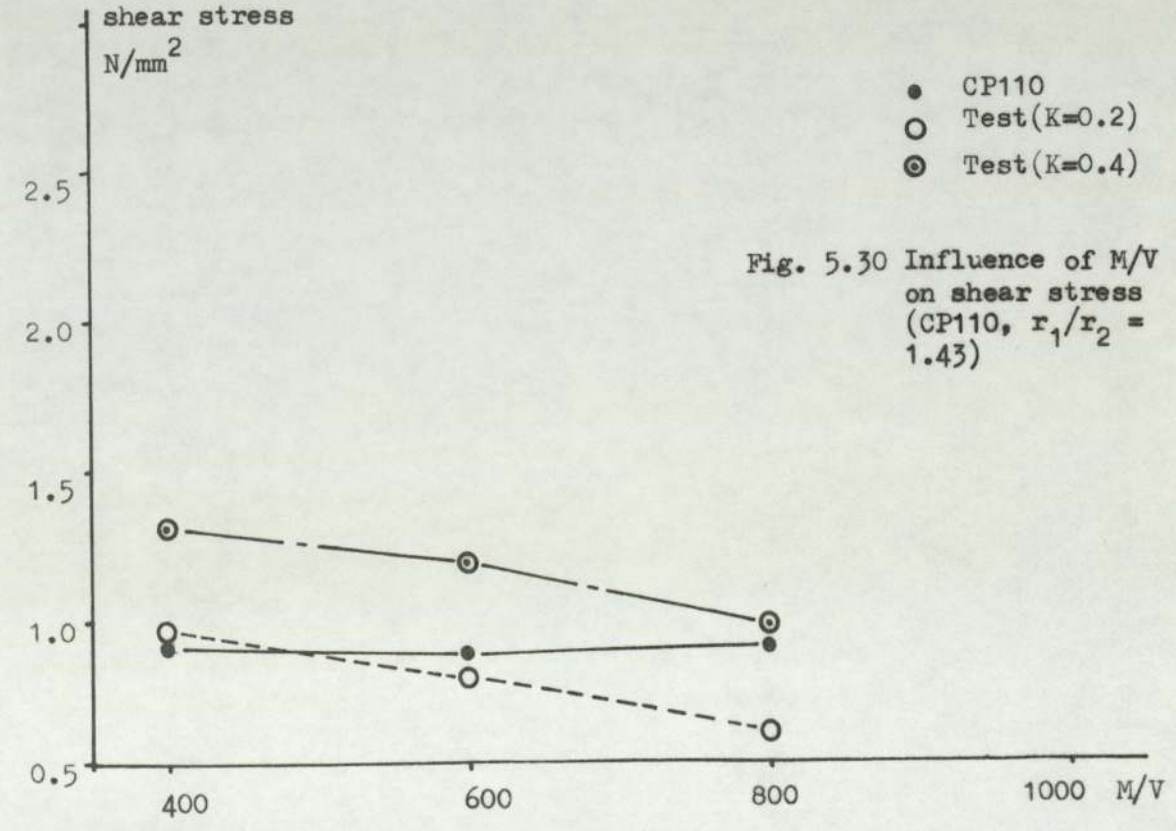

Fig. 5.30 Influence of M/V on shear stress (CP110, $r_1/r_2 = 1.43$)

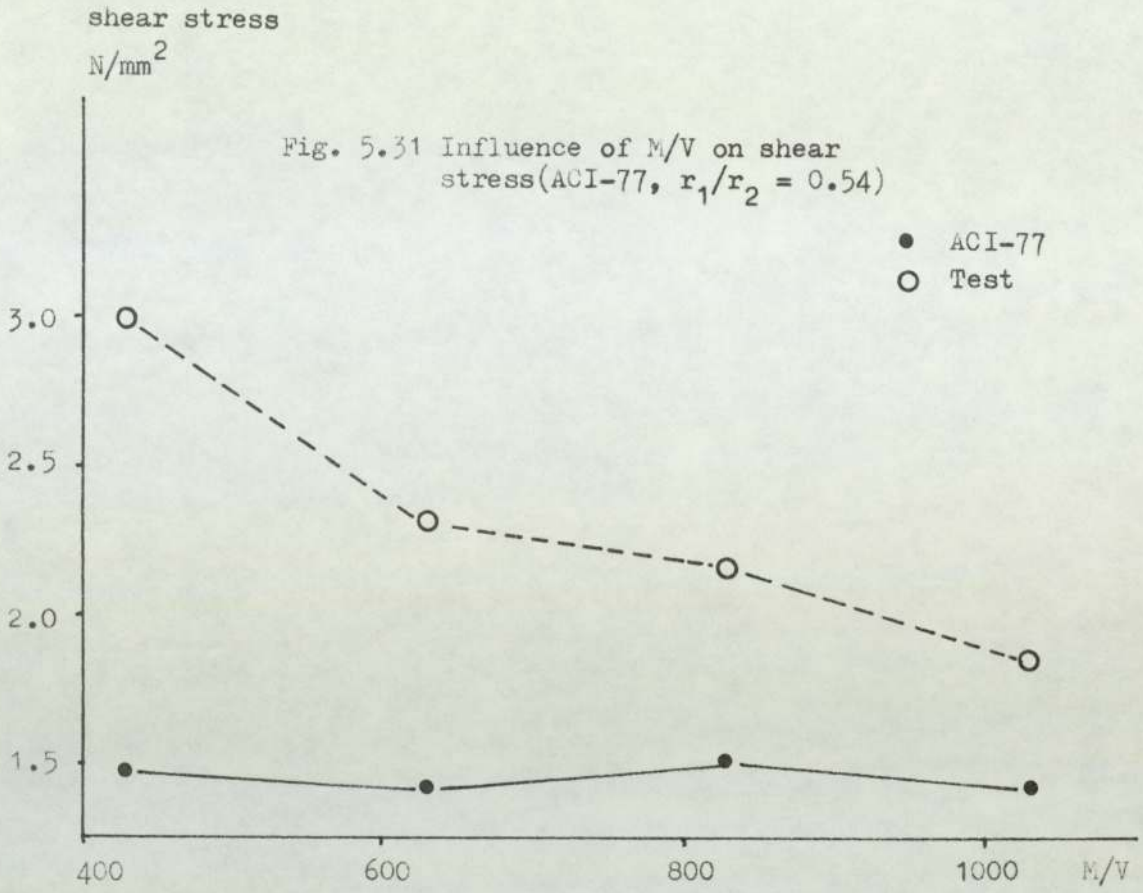

Fig. 5.31 Influence of M/V on shear stress(ACI-77, $r_1/r_2 = 0.54$)

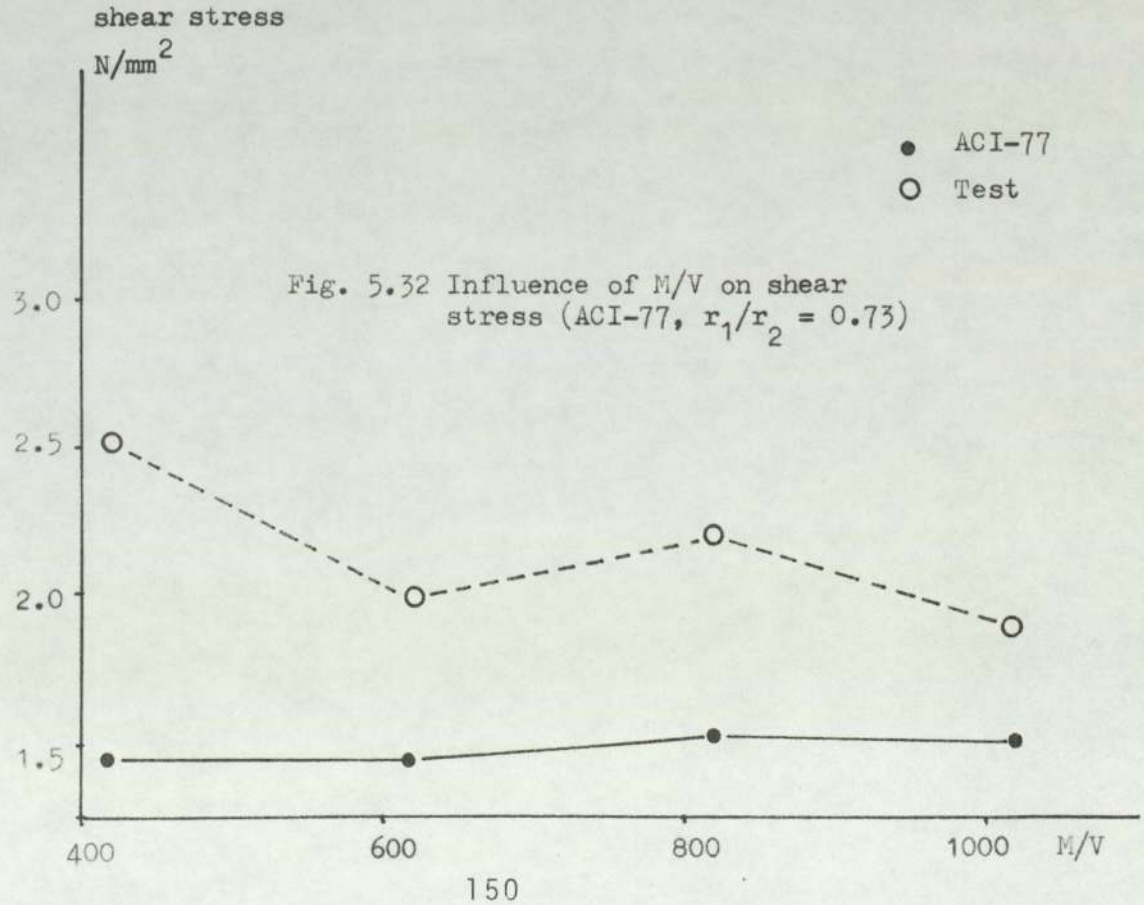

Fig. 5.32 Influence of M/V on shear stress (ACI-77, $r_1/r_2 = 0.73$)

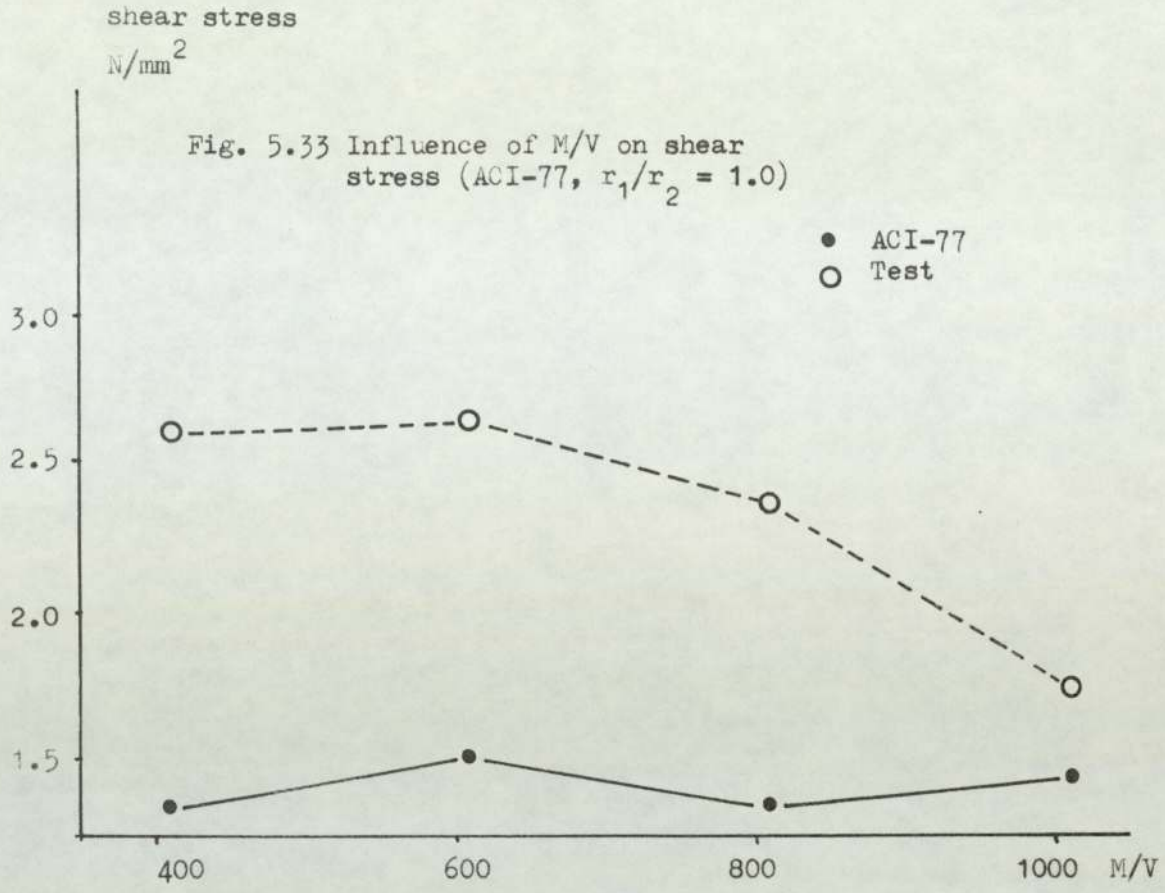

Fig. 5.33 Influence of M/V on shear stress (ACI-77, r_1/r_2 = 1.0)

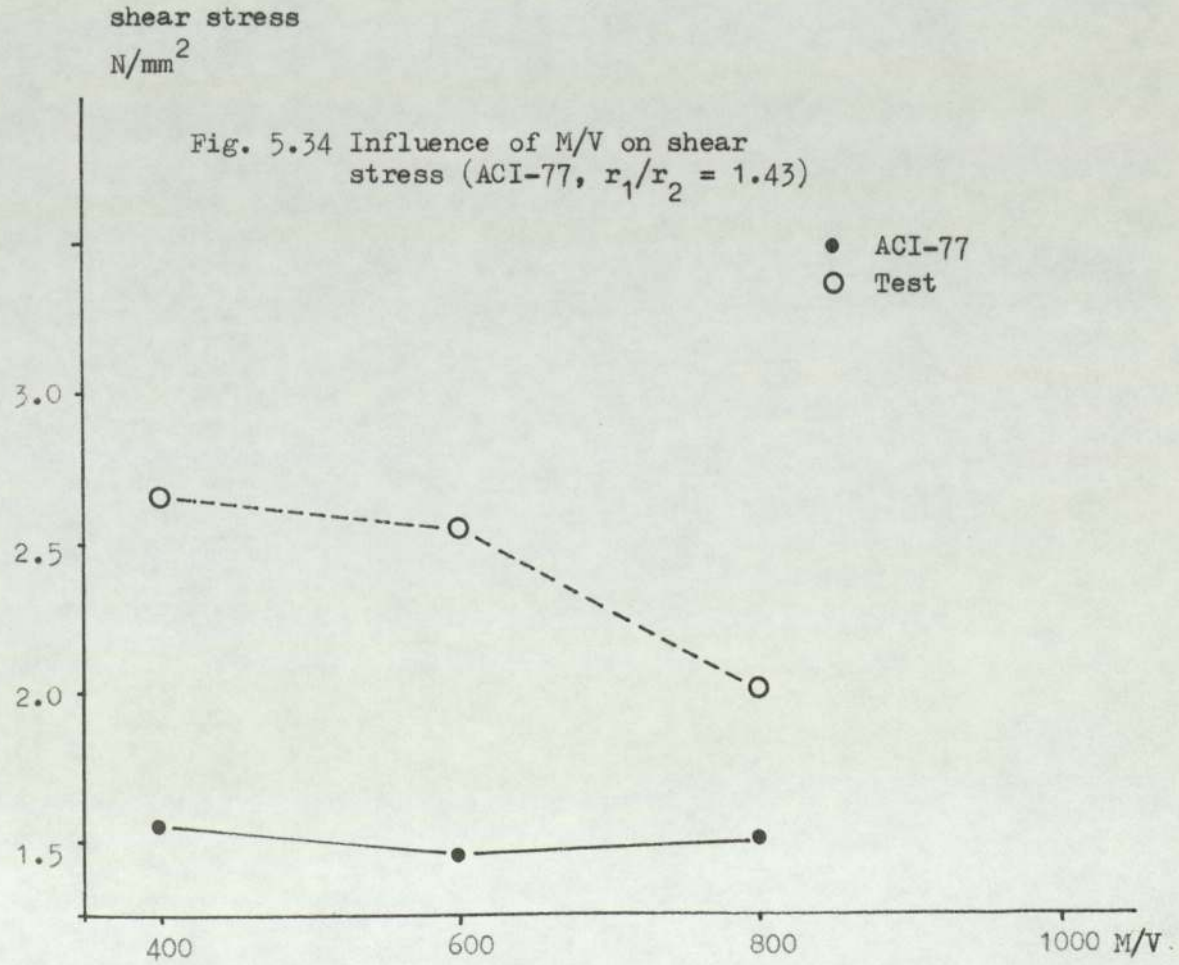

Fig. 5.34 Influence of M/V on shear stress (ACI-77, r_1/r_2 = 1.43)

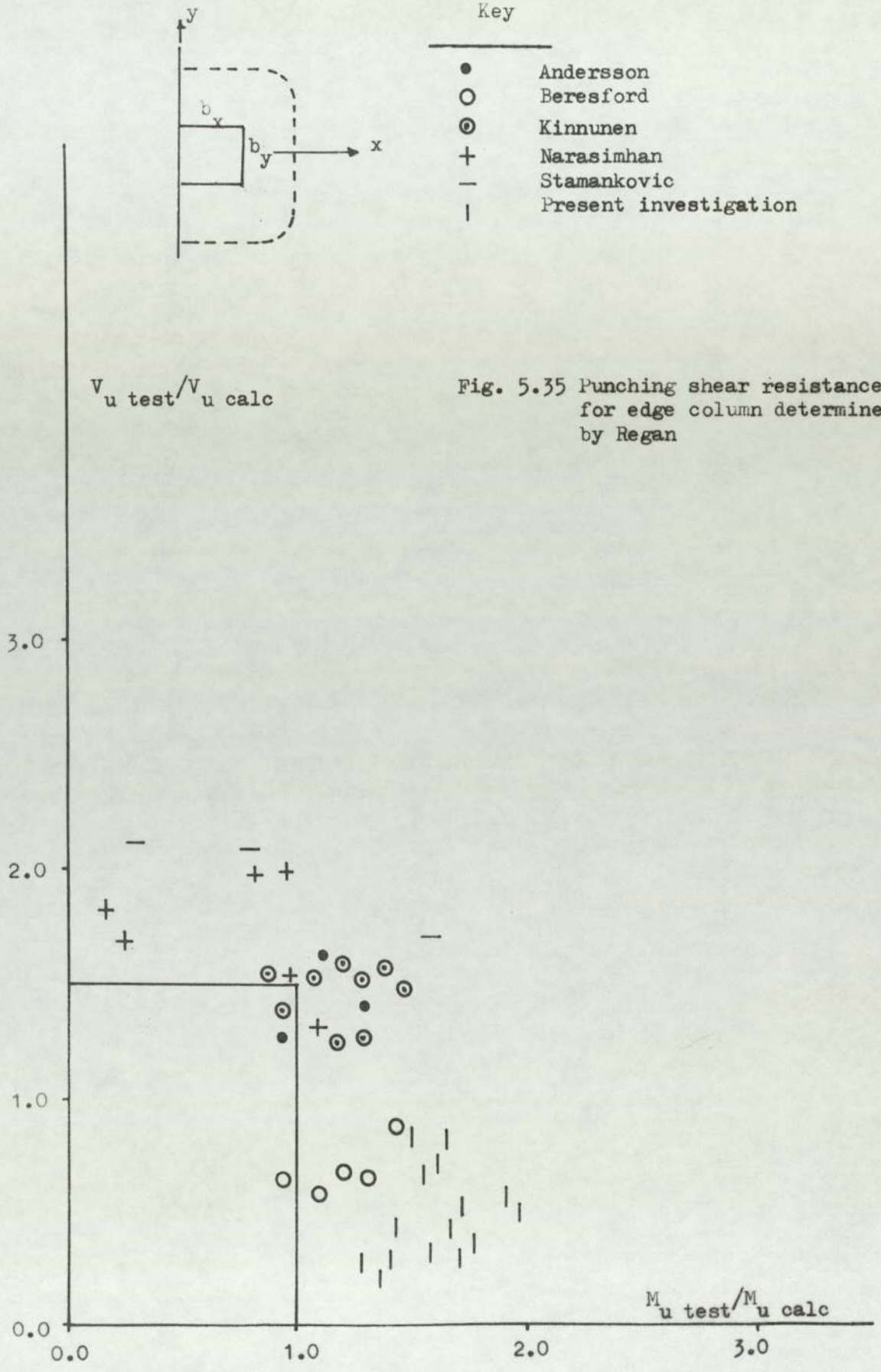

Fig. 5.35 Punching shear resistance for edge column determined by Regan

In applying the yield line theory, the yield moments of the slabs were based on the ultimate strength. Certain assumptions were applied in calculating the ultimate flexural capacities of the test structures.

5.2.2. Application of yield line analysis to the test structures.

To determine the collapse load of a given slab the sequence of the steps may be summarised as follows:

(1) A possible yield line pattern is adopted.

(2) The ultimate moment (m) per unit length is calculated for various yield lines.

(3) The collapse load (Wu) which corresponds to the assumed yield line pattern is calculated by the use of virtual work.

(4) The dimensions of the particular failure pattern are adjusted to minimise (Wu).

(5) Different trial yield line patterns are assumed and steps 2, 3 and 4 are repeated.

(6) Provided all possible collapse mechanisms (yield line patterns) have been investigated, the lowest computed value of (Wu) is theoretically the correct collapse load (because of the approximation in the theory).

The virtual work theorem states that the "external work" U_{ext}, and the "internal work", U_{int}, are equal. The term external work is the summation of the products of

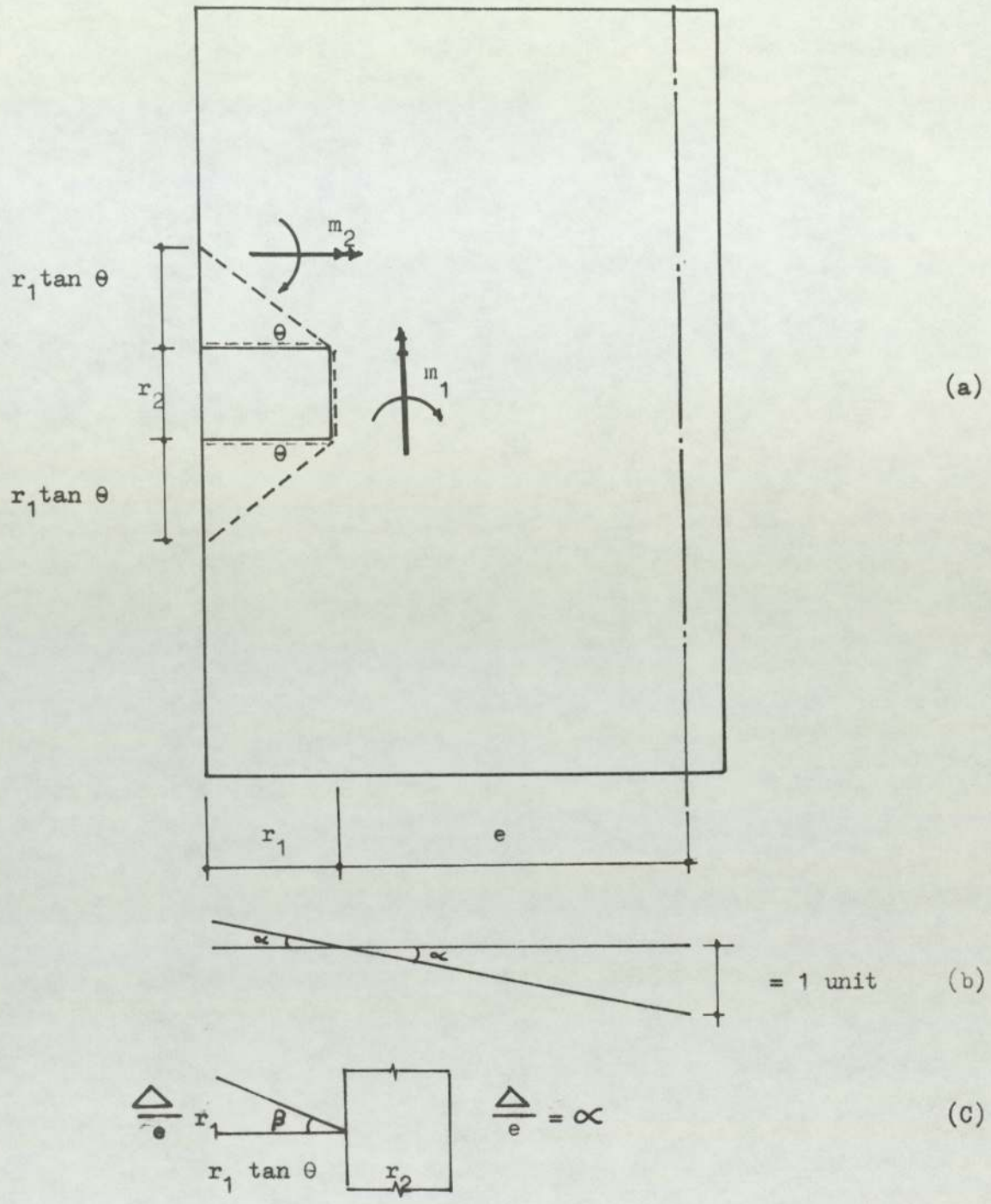

Note: The same layer of reinforcement used at the top and bottom of the slab.

Fig. 5.36 First yield line pattern

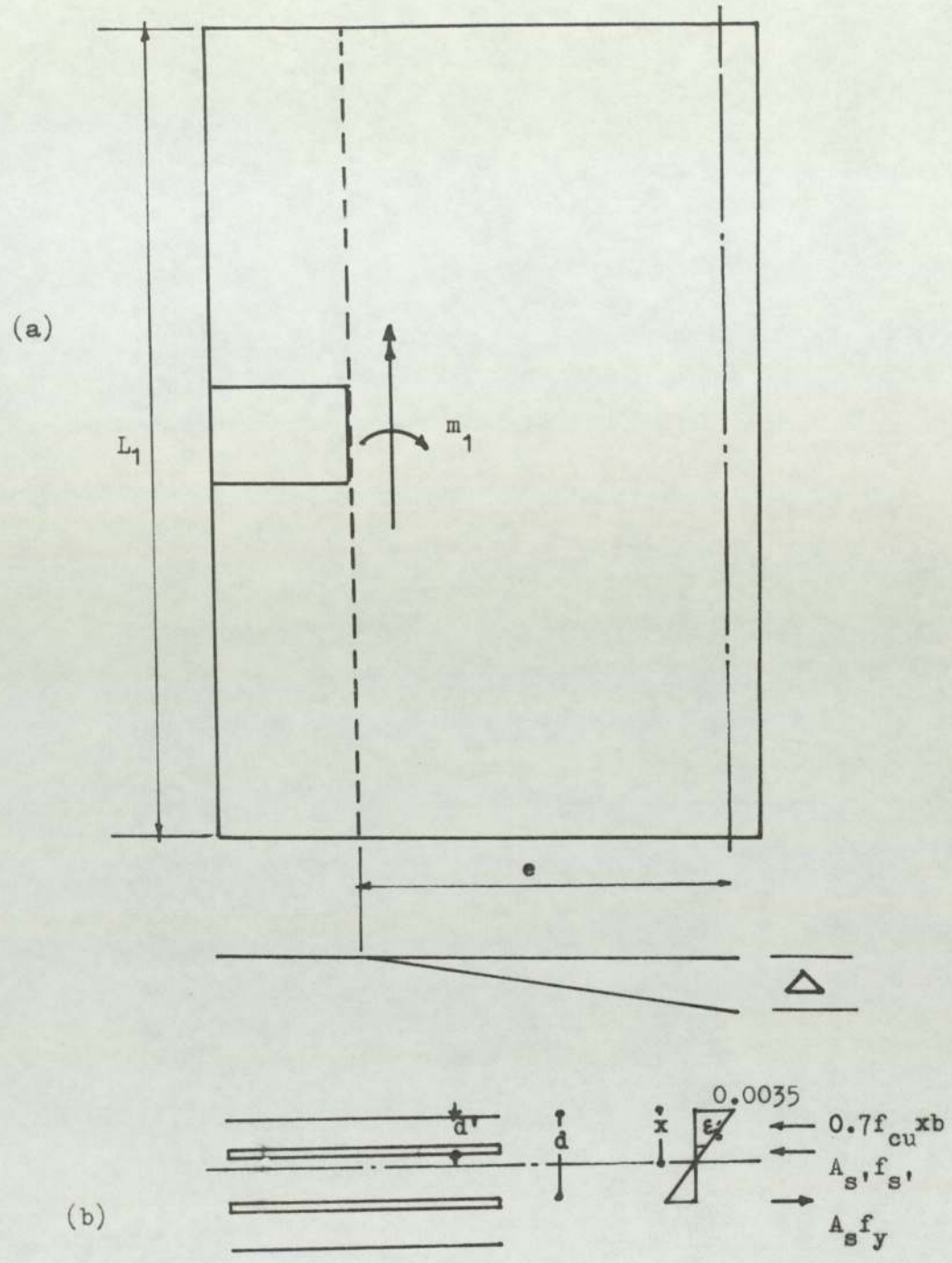

Fig. 5.37 Second yield line pattern

external forces and their conjugate displacements which arise from the virtual displacement system. The term internal work is the summation of the products of the internal stresses and displacements.

If a vertical load is applied on the free edge of a slab, then the possible failure patterns are as follows:

(1) The first yield line pattern is shown in Fig. 5.36 If the load is given a vertical deflection of unity, then the solution for the slab is obtained by following the above six steps.

To calculate the ultimate moment per unit length, the following method was used.

From Fig. 5.37(b) we have

$$\varepsilon'_s = \frac{x - d'}{x} \times 0.0035 \qquad (5.2)$$

$$A'_s f'_s + 0.7 f_{cu}.x.b = A_s f_y \qquad (5.3)$$

$$f'_s = E\varepsilon'_s \quad (\text{where } E = 213333 \text{ N/mm}^2) \qquad (5.4)$$

By solving these equations to find f'_s and x, the ultimate moment can be determined as:

$$M_u = 0.70 f_{cu}.x.b.(d-\frac{x}{2}) + A'_s f'_s (d-d') \qquad (5.5)$$

The external work of the slab is

$$U_{ext} = We\alpha \qquad (5.6)$$

The internal work is

$$U_{int} = m_1 r_2 \alpha + 2m_1 r_1 \tan\theta\alpha + 4m_2 r_2 \beta$$

where $\beta = \frac{\frac{\Delta}{e} r_i}{r_1 \tan\theta} = \frac{e\alpha}{e\tan\theta} = \frac{\alpha}{\tan\theta}$ (see Fig. 5.36(c))

By equating the external work to the internal work we obtain

$$w = \frac{m_1 r_2}{e} + \frac{2m_1 r_1 \tan\theta}{e} + \frac{4m_2 r_1 \cot\theta}{e} \qquad (5.7)$$

The minimum value of w can be found by differentiation

$$\frac{dw}{d\theta} = 0 + \frac{2r_1 m_2}{e} \sec^2\theta - \frac{4m_2 r_1}{e} \operatorname{cosec}^2\theta = 0$$

$$\therefore \quad \tan\theta = \sqrt{\frac{2m_2}{m_1}} \qquad (5.8)$$

Now substitute the values of m_1, m_2, θ, and f_y of each specimen into Eq. 5.7 to get the values of w.

(2) The second possible yield line pattern is shown in Fig. 5.37. By following the same steps as in (1) we obtain:

$$w = \frac{m_1 L_1}{e} \qquad (5.9)$$

5.2.3. Flexural strength of test structures

The two possible modes of failure shown in Figs. 5.36 and 5.37 were studied and the failure load (V_{flex}) and the ultimate capacity M_{flex} have been found. Clearly the smaller value of these two failure loads will be used.

The values of V_{flex}, M_{flex}, V_{test} and M_{test} are tabulated in Table 5.2 where M_{test} represents the maximum moment reached during testing.

SP.NO	F_y (N/mm^2)	M_1 (N-mm)	M_2 (N-mm)	e (mm)	V_{flex} (1) kN)	V_{flex} (2) (kN)	$\phi_0 = \frac{V_{test}}{V_{flex}(1)}$
1	414.42	29971.34	13541.89	360	65.96	99.90	0.61
2	299.60	22226.13	10230.79	560	31.64	47.63	0.79
3	335.46	24869.95	11457.10	760	26.10	39.27	0.67
4	375.60	27285.02	12371.81	960	22.55	34.11	0.55
5	329.22	24253.58	11124.10	340	59.42	85.60	0.55
6	341.63	25150.53	11524.85	540	38.78	55.89	0.52
7	326.36	24332.86	11235.21	740	27.46	39.46	0.64
8	358.60	26422.66	12135.10	940	23.43	33.73	0.53
9	352.20	25392.61	11395.10	320	68.41	95.22	0.48
10	327.98	24359.36	11238.25	520	40.83	56.21	0.61
11	379.84	27285.89	12135.03	720	32.56	45.48	0.55
12	354.38	25886.06	11807.14	920	24.41	33.76	0.45
13	375.60	27644.76	12691.96	300	83.54	110.58	0.38
14	381.96	27720.89	12541.60	500	49.95	66.53	0.46
15	333.16	24706.18	11387.62	700	32.05	42.35	0.47

Table 5.2 A Flexural capacities

SP. NO.	$r_1 \times r_2$	V_{test} (kN)	r_1/r_2	r_1/d	M_{flex} kN - mm	$M_{test}=Ve$ kN - mm	$\frac{M_{test}}{M_{flex}}$
1	140 x 260	40	0.54	2.33	17676.0	15852.0	0.89
2	"	25	"	"	12768.0	14907.5	1.16
3	"	17.5	"	"	14288.0	13935.25	0.97
4	"	12.5	"	"	16032.0	12453.75	0.77
5	160 x 220	32.5	0.73	2.67	14314.0	12590.5	0.88
6	"	20.0	"	"	14310.0	11748.0	0.82
7	"	17.5	"	"	14208.0	13779.5	0.97
8	"	12.5	"	"	15604.0	12342.5	0.79
9	180 x 180	32.5	1.00	3.00	15616.0	12350.0	0.79
10	"	25	"	"	14560.0	14500.0	0.99
11	"	18	"	"	16848.0	14640.0	0.83
12	"	11	"	"	15640.0	10780.0	0.69
13	200 x 140	32	1.43	3.33	16980.0	11971.2	0.71
14	"	23	"	"	17250.0	13204.3	0.76
15	"	15	"	"	15050.0	11611.5	0.77

Table 5.2 B Flexural Capacities

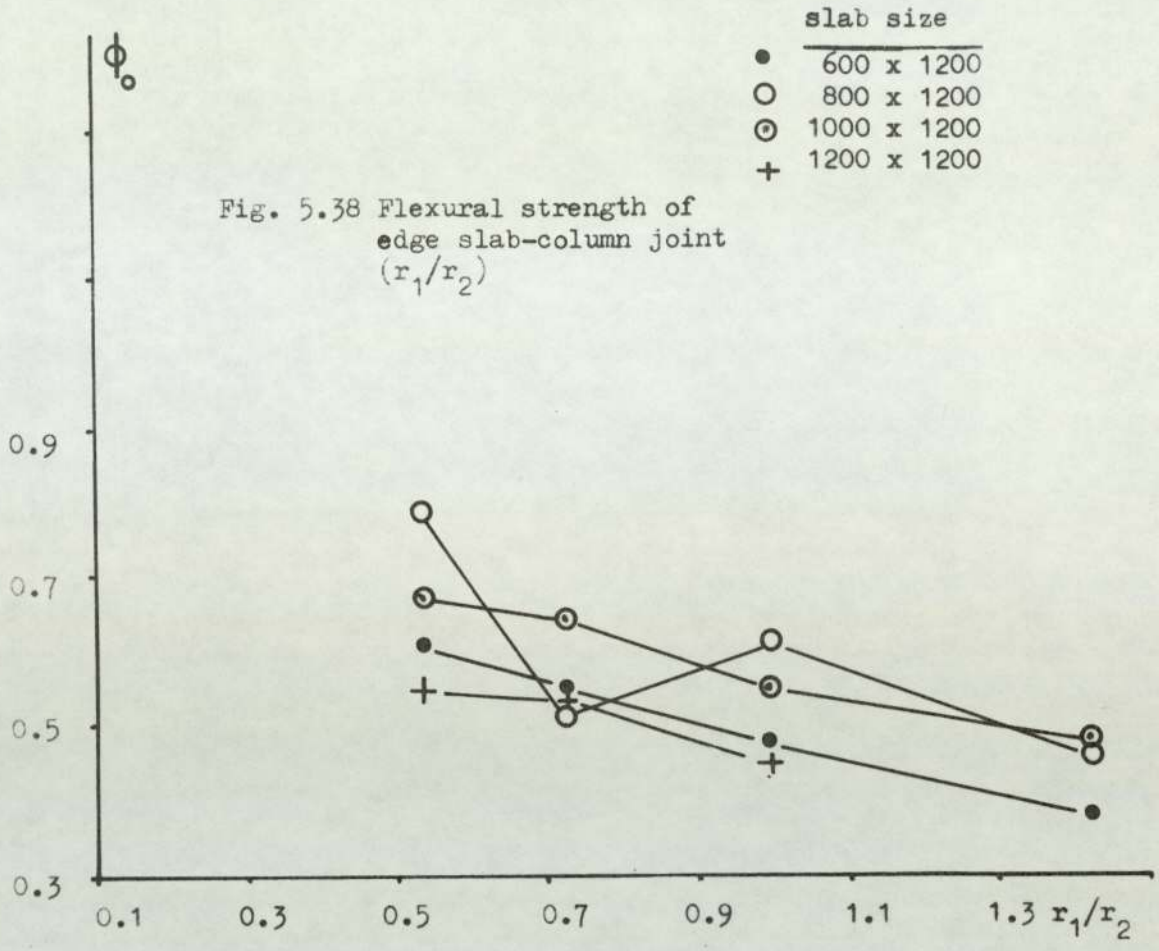

Fig. 5.38 Flexural strength of edge slab-column joint (r_1/r_2)

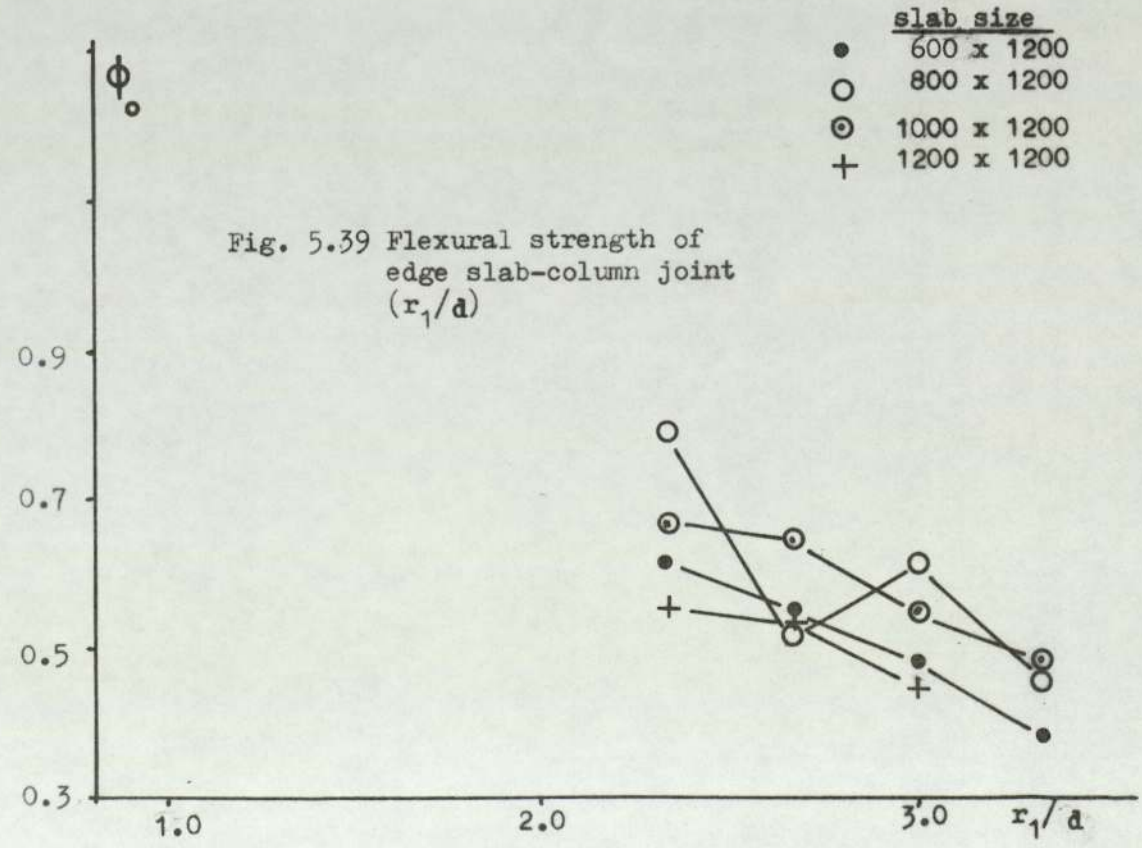

Fig. 5.39 Flexural strength of edge slab-column joint (r_1/d)

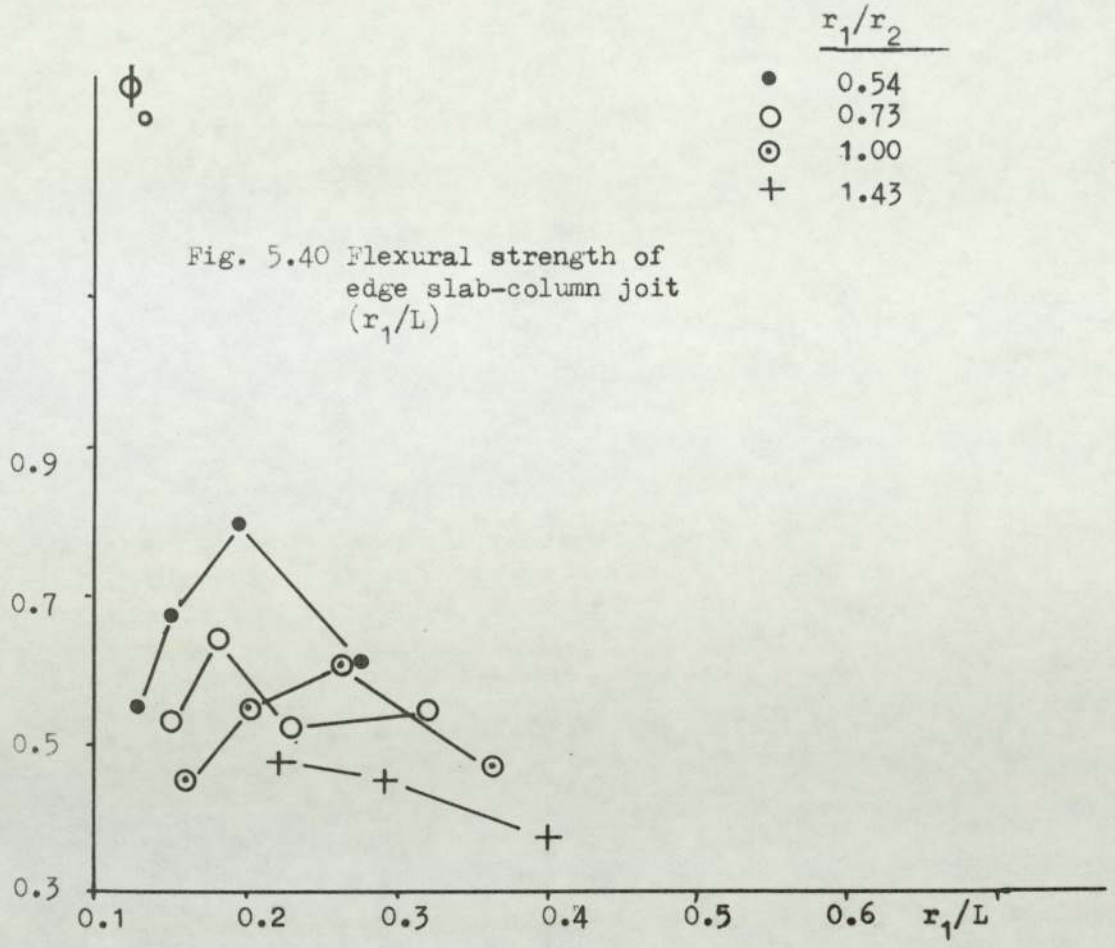

Fig. 5.40 Flexural strength of edge slab-column joit (r_1/L)

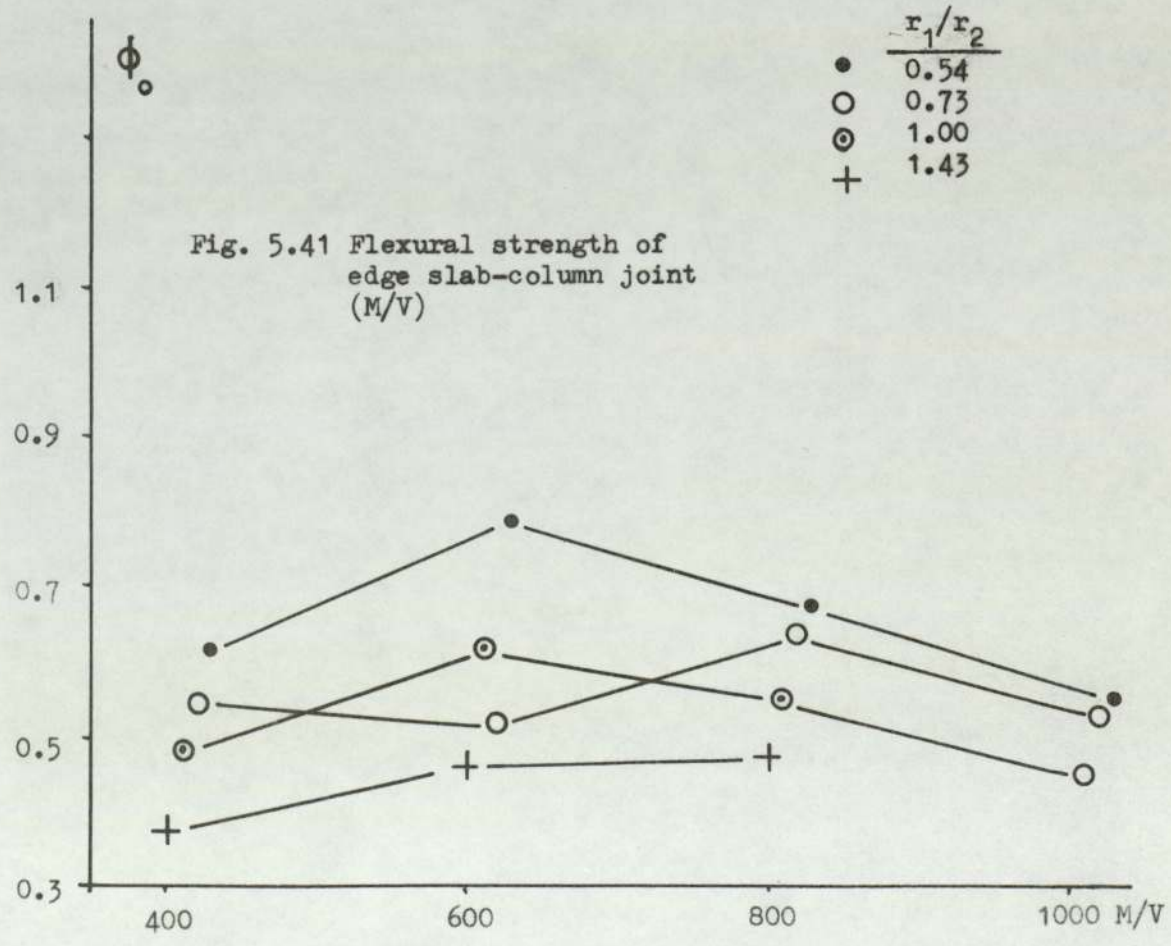

Fig. 5.41 Flexural strength of edge slab-column joint (M/V)

5.2.4. Comparison with test results

In this section the ultimate theoretical load capacity of the slab obtained from the yield line theory as described before is compared with the test ultimate capacity of the connection. ϕ_0 as shown in Table 5.2 is plotted against r_1/r_2, r_1/d, r_1/L and M/V in Figs. 5.38, 5.39, 5.40 and 5.41 respectively; where ϕ_0 is the ratio of test ultimate strength to the theoretical ultimate strength of the slab.

As shown in Fig. 5.38, for all specimens, ϕ_0 decreases as r_1/r_2 ratio increases. It appears that as r_1/r_2 ratio increases the ultimate flexural strength of the connection becomes overestimated by greater amounts. This case is the same for ϕ_0 against r_1/d (see Fig. 5.39).

In Fig. 5.40, where ϕ_0 has been drawn against r_1/L, for both low and high values of r_1/L, ϕ_0 is nearly the same, but for intermediate values of r_1/L, ϕ_0 is relatively high, which indicates that the ultimate flexural strength is overestimated specially for low and high values of r_1/L. The same conclusion can be drawn in the case of ϕ_0 drawn against M/V ratio (see Fig. 5.41).

5.3 Summary

The following conclusions from this chapter can be drawn:

(1) "k" factor was used equal to 0.4 by Hanson and

Hanson[12], in equation no. 5.1. For most specimens this value gives safe results when used with CP110 stresses and failure plane. In only one case does it give a slightly low safety factor (0.97).

(2) Equation 5.1 appears not to fully describe the failure since a constant shear stress is not obtained when using it. The calculated shear stress is higher for small eccentricities than it is for large eccentricities.

(3) The method proposed by Regan and adopted in part by CP110 appears to give safe results, although the margin of safety is very variable.

(4) The values of $\frac{M_{test}}{M_{flex}}$ and the values of ϕ_0 as shown in Table 5.2 for all specimens are less than unity. This indicates that the ultimate flexural strength is overestimated by a considerable margin for all specimens. The yield line method is therefore not suitable for the calculation of the strength of such joints, and some method which takes more account of shear would be better.

CHAPTER VI

ANALYSIS FOR ULTIMATE STRENGTH AND COMPARISON WITH TEST RESULTS

6.1 General

An ultimate strength procedure is derived for determining the shear and unbalanced moment capacity of exterior column-slab junctions. This theory is based on an extension of previous investigations. The strength of such junctions as predicted by the theory is shown to give good agreement with test results.

6.2 Introduction

In most cases the strength of flat plate column junctions without any shear reinforcement is governed by a shear-flexure failure on some critical section surrounding the column before the formation of the complete yield line pattern for the slab. On this critical section the applied shear and unbalanced moment are resisted by three actions within the slab, namely (i) flexure, (ii) shear, and (iii) torsion. The theory for the failure mode is based on the evaluation of these three quantities which are obtained from the results and previous investigations.

Fig. 6.1 shows the portion of a flat plate surrounding an exterior column. Let V be the resultant shear and M the unbalanced moment about the x-x axis acting on the

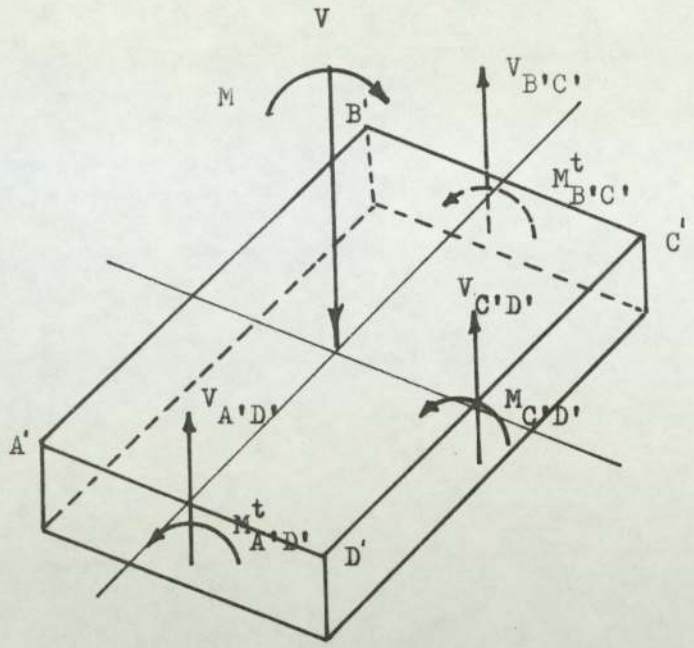

A D C B = column perimeter

A'D'C'B' = the assumed shear plane perimeter

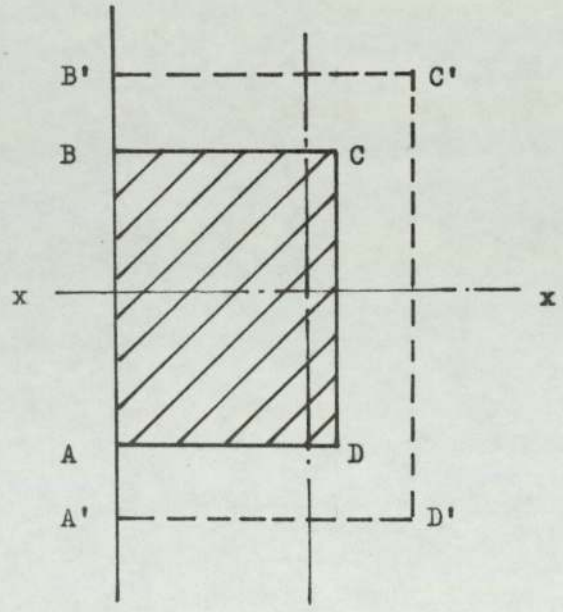

Fig. 6.1 Critical section for the shear stress of an edge slab-column junction

centroid of the slab-column junction at ultimate loading conditions. The forces and moments acting on a critical section A'B'C'D' within the slab and contributing to the transfer of the shear V and the moment M are indicated in the figure.

The unbalanced moment M is transferred by three actions, namely (i) flexure on face C'D', (ii) vertical shear on face C'D', and (iii) torsion on faces A'D' and B'C'.

The individual contributions of these actions will be determined and summed to obtain the total unbalanced moment that can be transferred with shear force at the edge column-slab junction.

The distribution of stresses in the slab around the column at the ultimate load is very complex. Mast[47] has obtained the distribution of stresses in flat plate near columns due to the moment transfer in accordance with the theory of elastic plates. This elastic stress distribution does not apply at the ultimate load because of the effect of inclined cracking in the slab around the column, which has been ignored in the theory, and is likely to alter the stress distribution; additionally the elastic theory does not account for the influence of the slab reinforcement and the concrete does not behave as an elastic homogeneous material at ultimate load. Because of this complex behaviour it is necessary to make some simplifying assumptions in order to derive design equations.

6.3 Assumptions and Prediction of Strength of Edge Column-slab Connection.

In this section a method is proposed for predicting the strength of the edge column-slab connection in flat plate slabs under combined shear and unbalanced moment loadings.

In Moe's method the ultimate strength analysis was developed by assuming that the critical section is directly adjacent to the periphery of the column and that failure takes place when the maximum shear stress reaches a limiting value equal to the shear strength of the same connection under concentric load. For an interior square column and slab connection subjected to combined bending moment M and vertical shear force V the ultimate vertical shear stress is given in Eq. 5.1 as

$$v_u = \frac{V}{A_c} + \frac{kMC}{I_c}$$

in which $A_c = bd$, and $I_c = (2/3)r^3d$, b = the perimeter of the column; r = the column width; C = one half the width of the column, and k = a moment reduction factor which accounts for that part of the shear which is resisted by bending moments and torsional moments acting at the column and slab intersection. Moe determined the constant k experimentally and found that the best correlation with his test results is obtained for $k = {}^1/_3$.

In considering the strength of the edge column-slab

connections under the action of shear and biaxial moment, it is assumed that the critical section is located at a distance equal to half the effective depth of the slab from the periphery of the column, and, as was done by Moe, that failure takes place when the maximum shearing stress reaches a limiting value equal to the shearing strength of the same connection under concentric load. The limiting ultimate shearing stress under concentric load was calculated using the equation

$$v_{(psi)} = \frac{V}{b_0 d} = \frac{15(1-0.075\frac{r}{d})\sqrt{f'_c}}{1+5.25\frac{bd\sqrt{f'_c}}{V_{flex}}} \qquad (6.1)$$

Equation 6.1 was chosen for development because of the following:

(1) This equation was found to give good results.

(2) The shear strength of a flat plate was found, as in Moe's investigations, to be affected by the ratio of column side to slab thickness.

(3) The shear strength of a flat plate is dependent upon the flexural strength.

The value of V_{flex} in equation 6.1 was calculated for the test structures by means of the yield line theory according to the modes of failure discussed in Chapter V. The application of this method, with some developments, to

the test structures will be discussed in the following sections. Note that Equation 6.1 was used after conversion to SI units, therefore it becomes:

$$v_u \text{ N/mm}^2 = \frac{1.244\left(1-0.075\frac{r_1}{d}\right)\sqrt{f'_c}}{1+0.435\frac{b_0 d\sqrt{f'_c}}{V_{flex}}} \qquad (6.1A)$$

v_u in N/mm^2

f'_c in N/mm^2

r_1, b_0, d in mm

V_{flex} in N

6.3.1. Prediction of strength of edge column-slab connection

Referring to Fig. 6.1 which is a plan of an edge column-slab connection in a flat plate floor slab, the connection is subjected, in addition to the axial shear force, to unbalanced moment M. As mentioned before, this moment is balanced by torsional moment, vertical shear stresses and flexural moment of the slab at the critical section. The effective depth of the critical section for shear is equal to the effective depth, d, of the slab at that section.

To obtain a semi-empirical formula by which the ultimate shear strength can be predicted, the balance of the above-mentioned forces has to be achieved as follows.

Equilibrium condition in the x-direction in Fig. 6.1 gives:

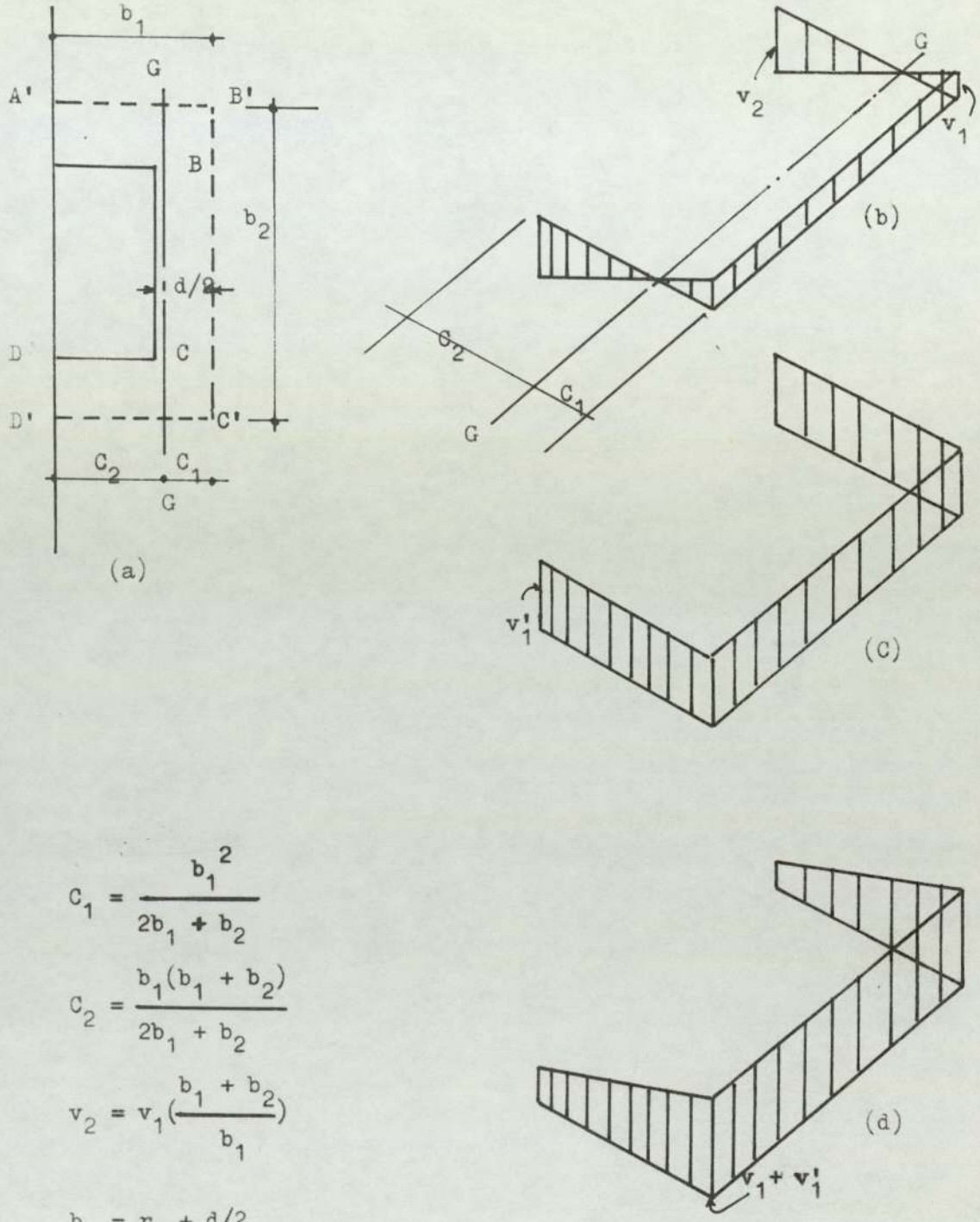

$$C_1 = \frac{b_1^2}{2b_1 + b_2}$$

$$C_2 = \frac{b_1(b_1 + b_2)}{2b_1 + b_2}$$

$$v_2 = v_1\left(\frac{b_1 + b_2}{b_1}\right)$$

$$b_1 = r_1 + d/2$$

$$b_2 = r_2 + d$$

Fig. 6.2 Assumed shear stress distribution

$$M-(M_{CD}'' + M_{BC}^{t}'' + M_{AD}^{t}'' + Vx) = 0 \qquad (6.2)$$

where x is the eccentricity of the resultant V in the x direction, M_{BC}^{t}'' and M_{AD}^{t}'' are torsional moments on section BC'' and AD'' respectively.

From Equation 6.2 we have

$$Vx = M-(M_{CD}'' + M_{BC}^{t}'' + M_{AD}^{t}'') \qquad (6.3)$$

If the part of the total external moment in the x-direction to be taken by the vertical shear stresses is assumed to be proportional to the total moment, M, Equation 6.3 becomes

$$Vx = kM \qquad (6.4)$$

where k is a coefficient which defines the amount of external moment which is carried by vertical shearing stresses between the slab and column. Furthermore, it is assumed that the shear stresses are uniformly distributed across the effective depth of the slab, and,as was assumed by Moe,that the failure takes place when the maximum shear stress reaches a value equal to the shear strength of the same connection concentrically loaded. Also it is assumed that the shear stresses are proportional to the distance from the centre line of the critical section $A''B''C''D''$ (see Fig. 6.2(a)) hence from Fig. 6.2 (b) we have:

(1) The line of zero shear stress G-G is located such that the resultant of vertical forces due to moment only is zero.

(2) The moments of shear stress areas about line G-G equal to the amount of external moment which is carried by vertical shearing stresses is kM.

By taking moments about GG we find:

$$\left[2\left(\frac{1}{2}v_2c_2\right)\left(\frac{2}{3}c_2\right) + 2\left(\frac{1}{2}v_1c_1\right)\left(\frac{2}{3}c_1\right) + v_1b_2c_1\right]d = kM \qquad (6.5)$$

By substituting c_1, c_2 and v_2 (Fig. 6.2) into equation 6.5 we have

$$v_1 = \frac{kM}{\frac{b_1 d}{3b_0^2}\left[4b_1^3+12b_1^2b_2+9b_1b_2^2+2b_2^3\right]} \qquad (6.6)$$

where $b_0 = 2b_1 + b_2$

The vertical shearing stress due to the vertical shearing force (Fig. 6.2(c)) can be expressed as

$$v_1' = \frac{V}{(2b_1+b_2)d} = \frac{V}{b_0 d} \qquad (6.7)$$

Therefore the maximum shearing stress at the inner corners of the section shown in Fig. 6.2 (d) can be expressed as:

$$v_{max} = v_s + v_m$$

$$v_{max} = \frac{V}{b_0 d} + \frac{kM}{\frac{b_1 d}{3b_0^2}\left[4b_1^3+12b_1^2b_2+9b_1b_2^2+2b_2^3\right]} \qquad (6.8)$$

but $v_{max} = \frac{V_0}{b_0 d}$

where $V_0 = v_u(2b_1+b_2)d$ = shearing capacity at zero eccentricity, and v_u is to be determined from Eq. 6.1. (Note: Eq. 6.1 must be multiplied by $\frac{2r_1+r_2}{2b_1+b_2}$ because of the new critical section assumed by the writer where $b_1 = r_1 + \frac{d}{2}$ and $b_2 = r_2 + d$

Therefore

$$V = V_0 - \frac{kM}{\frac{b_1}{3b_0^3}\left[4b_1^3+12b_1^2b_2+9b_1b_2^2+2b_2^3\right]} \qquad (6.9)$$

Substitute $M = V_e$ in Eq. 5.9 and we get

$$V = V_0 - \frac{kVe}{\frac{b_1}{3b_0^3}\left[4b_1^3+12b_1^2b_2+9b_1b_2^2+2b_2^3\right]}$$

or

$$V = \frac{V_0}{1+\frac{ke}{\frac{b_1}{3b_0^3}\left[4b_1^3+12b_1^2b_2+9b_1b_2^2+2b_2^3\right]}} \qquad (6.10)$$

The constant k can now be determined from the test results.

6.3.2. Interaction diagram

The test results may also be evaluated in terms of an interaction diagram after Hanson considering the critical section is assumed to be located at a distance d/2 from the periphery of the column, and the ultimate shear capacity of the connection is then calculated for the case of shear transfer without moment transfer as:

$$V_0 = v_u b_0 d = v_u A_c \qquad (6.11)$$

For the case of moment transfer (M_0) without shear transfer, the ultimate shear capacity of the connection is obtained from Equation (6.6) as

$$v_m = \frac{kM_0}{\frac{b_1 d}{3b_0^2}\left[4b_1^3+12b_1^2b_2+9b_1b_2^2+2b_2^3\right]}$$

therefore

$$M_0 = \frac{v_m b_1 d}{3b_0^2 k}\left[4b_1^3+12b_1^2b_2+9b_1b_2^2+2b_2^3\right] \qquad (6.12)$$

For intermediate case, the connection capacity from Equation 6.8, where the axial shear controls, becomes:

$$v_s = v_{max} - v_m$$

$$V_u = v_u A_c - A_c \frac{kM_u}{\frac{b_1 d}{3b_0^2}\left[4b_1^3+12b_1^2b_2+9b_1b_2^2+2b_2^3\right]}$$

$$V_u = A_c\left(v_u - \frac{kM_u}{\frac{b_1 d}{3b_0^2}\left[4b_1^3+12b_1^2b_2+9b_1b_2^2+2b_2^3\right]}\right) \qquad (6.13)$$

From Equations 6.11, 6.12 and 6.13 we obtain:

$$\frac{V_u}{V_0} = 1 - \frac{M_u}{M_0} \qquad (6.14)$$

6.3.3. Determination of k factor

The factor "k" in Equation 6.9 defines the portion of the column moment which is carried by vertical shear stresses as already mentioned. The results from the test structures are used in determining a value for this factor.

A trial was made to check a similar factor determined experimentally by Moe[2] from his tests for eccentric loads in one direction and Zaglool from his tests for eccentric loads in two directions. Moe found that the ultimate shear strength of all his slabs could be predicted with a standard deviation of 0.103 when k was taken as equal to $\frac{1}{3}$. The ultimate shear strength of Zaglool's slabs could be predicted when k was taken equal to 0.04. In applying these two factors to the test structures it was found that the results were a conservative lower bound when $k = \frac{1}{3}$ and unsafe when k = 0.04, as can be seen from Figs. 6.3 and 6.4 and Table 6.1. Also it is noticed from Fig. 6.3 that as r_1/r_2 increases the "k" factor increases. From this, it can be concluded that the behaviour of edge column-slab connection subjected to axial force and bending moment is nearly similar to the behaviour of the interior column-slab connection subjected to similar loads when the ratio of r_1/r_2 is more than unity, and it is nearly similar to the behaviour of the corner column-slab connection subjected to axial force and biaxial bending moment when the ratio of r_1/r_2 is less than unity.

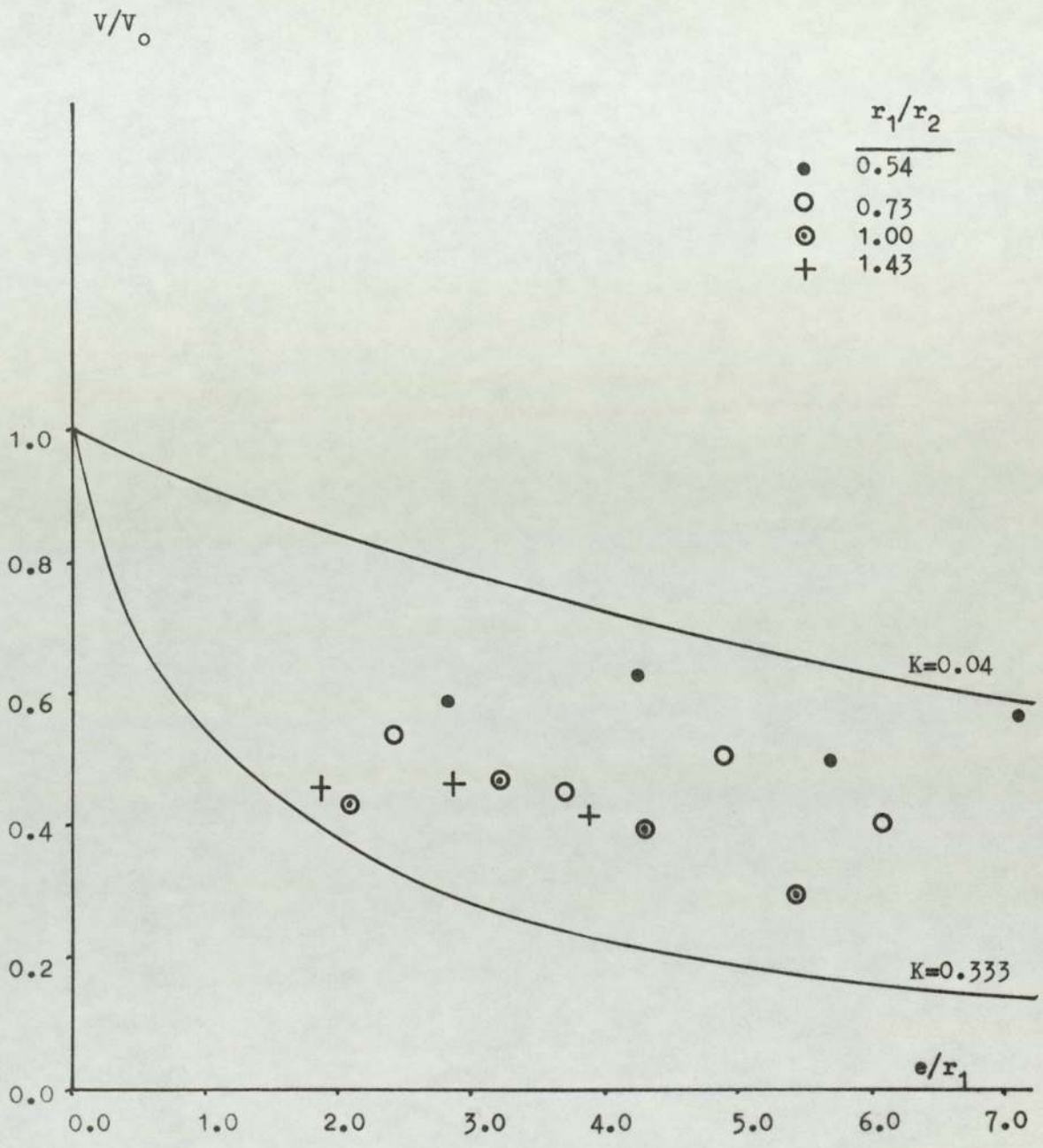

Fig. 6.3 Effect of eccentricity on ultimate shear strength of flat plates

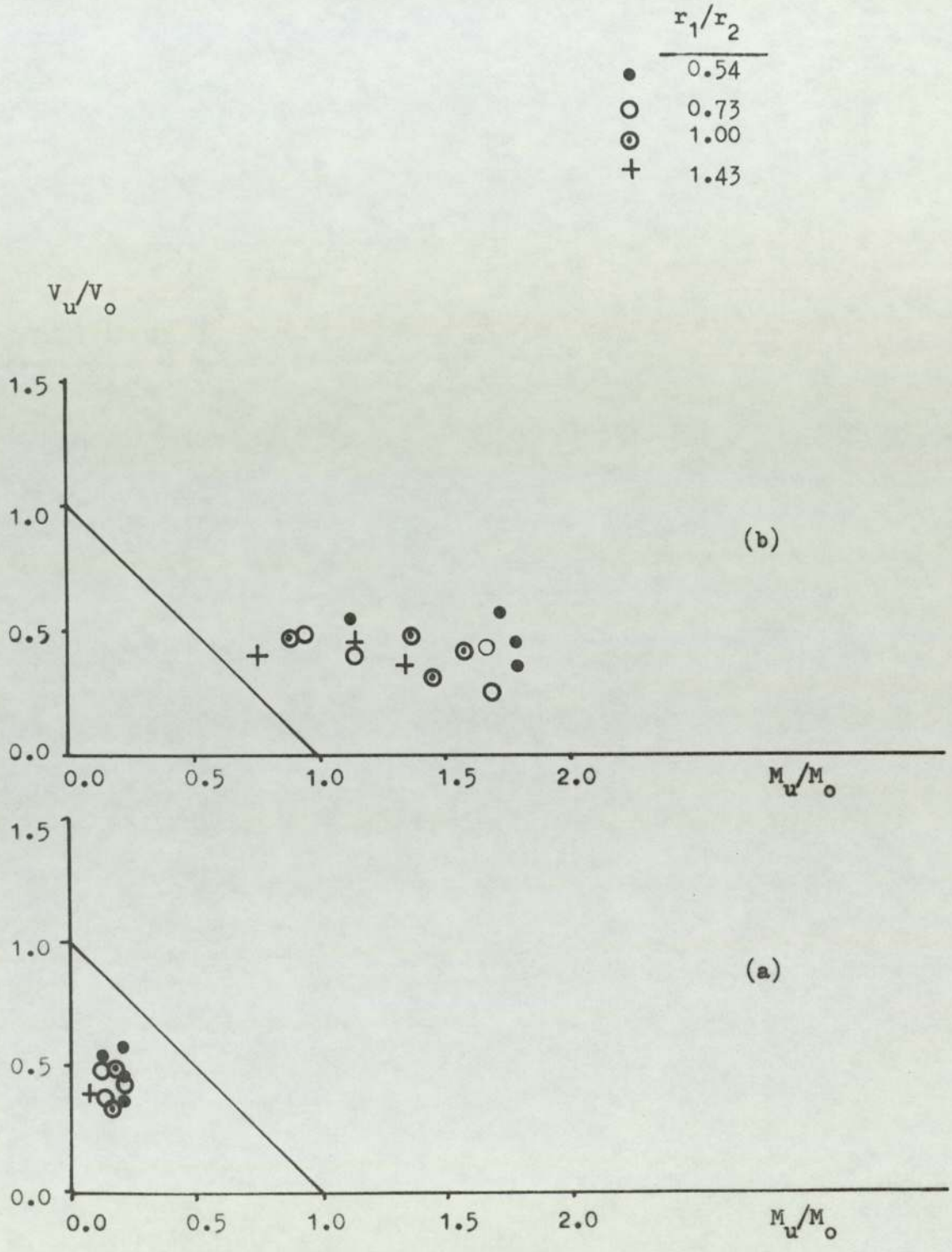

Fig. 6.4 Interaction of shearing force and bending moment of slab-column connection (a) K = 0.04 (b) K = 0.333

The deficiency of Moe's and Zaglool's factors in this case could be related to the difference between the type of specimens used by those investigators and the specimen used in this investigation. Moe's specimens were square slabs with square columns, while Zaglool's specimens were full size, square single panel flat plate structures cast monolithically with a square column at each corner. For a description of the specimens tested by the present author, refer to Section 3.3.

It was therefore felt that a determination of a more suitable moment reduction factor (taking into consideration the effect of r_1/r_2) was desired, rather than using that obtained to fit Moe's and Zaglool's results.

The determination of "k" factor proceeded as follows:

Equation 6.12 can be written in the form

$$k = \frac{v_u b_1 d}{3b_0^2 M_0}\left[4b_1^3+12b_1^2b_2+9b_1b_2^2+2b_2^3\right] \qquad (6.15)$$

Also Equation 6.14 can be written

$$M_0 = \frac{M_u}{1 - \frac{V_u}{V_0}} \qquad (6.16)$$

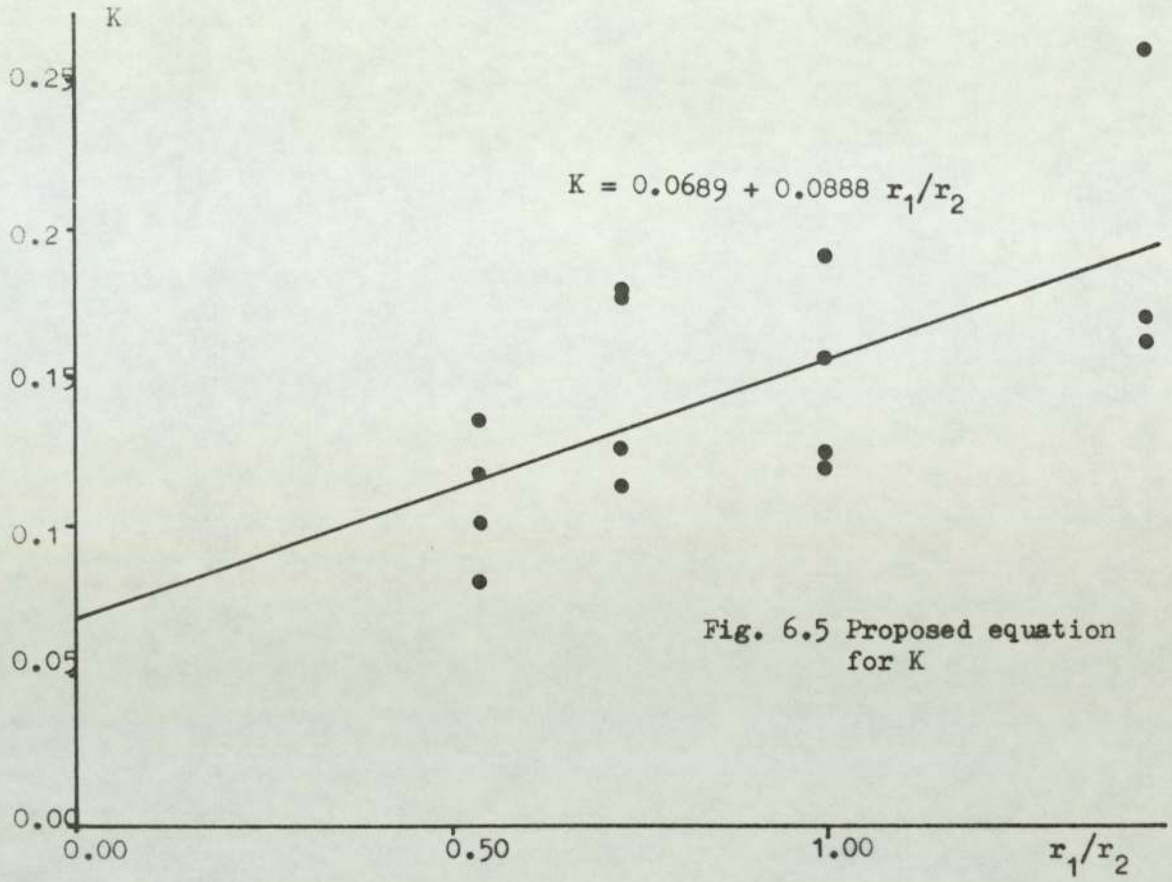

Fig. 6.5 Proposed equation for K

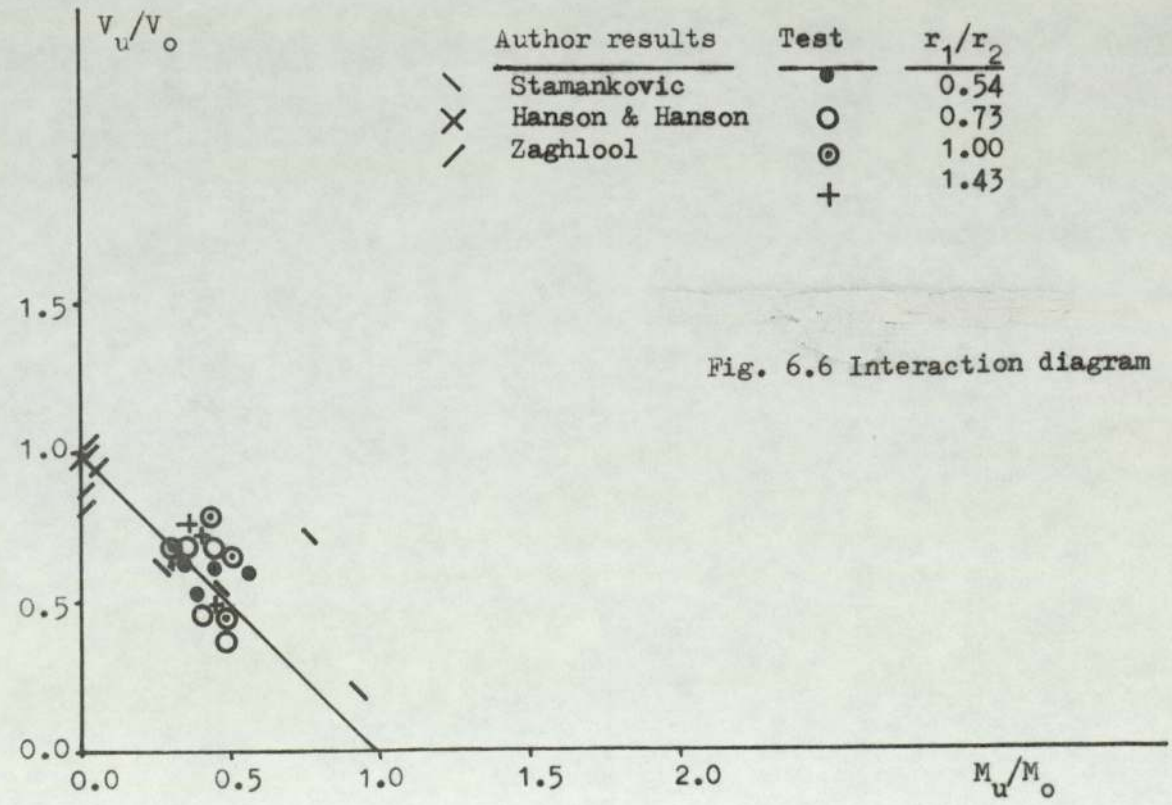

Fig. 6.6 Interaction diagram

SP. No.	v_u N/mm^2 (Eq. 5.1)	V_u kN (Test)	M_u kN-mm (Test)	V_0 kN (Eq. 6.11)	M_0 kN-mm k=0.333	M_0 kN-mm k=0.04	$\frac{V_u}{V_0}$	$\frac{M_u}{M_0}$ k=0.333	$\frac{M_u}{M_0}$ k=0.04
1	1.86	40.00	17200	73.70	15389.85	128120.50	0.543	1.118	0.134
2	1.10	25.00	15750	43.56	9101.53	75770.24	0.574	1.730	0.208
3	0.98	17.50	14525	38.81	8108.63	67504.34	0.451	1.791	0.215
4	0.87	12.50	12875	34.45	7198.48	59927.35	0.363	1.789	0.215
5	1.67	32.50	13650	66.13	14305.92	119096.78	0.491	0.954	0.115
6	1.28	20.00	12400	50.69	10965.01	91283.71	0.395	1.131	0.136
7	1.01	17.50	14350	39.99	8652.08	72028.57	0.438	1.659	0.199
8	0.88	12.50	12750	34.85	7538.45	62757.60	0.359	1.691	0.203
9	1.70	32.50	13325	67.32	14766.83	122933.80	0.483	0.902	0.108
10	1.29	25.00	15250	51.08	11205.42	93285.12	0.489	1.361	0.163
11	1.06	18.00	14580	41.97	9207.55	76652.85	0.429	1.583	0.190
12	0.88	11.00	11110	34.85	7644.01	63636.38	0.316	1.453	0.174
13	1.96	32.00	12800	77.62	17030.69	141780.50	0.413	0.752	0.090
14	1.40	23.00	13800	55.44	12164.78	101271.79	0.415	1.134	0.136
15	1.05	15.00	12000	41.58	9123.56	75953.64	0.361	1.315	0.158

Table 6.1

Bending moments and shear strengths for test specimens

SP. NO.	M_0 kN-mm (Eq. 6.16)	k (Eq. 6.15)	r_1/r_2	k (Eq. 6.17)	M_0 kN-mm (Eq. 6.12)	$\frac{M_u}{M_0}$	$V_{calc.}$ kN (Eq. 6.9)	$\frac{V_{test}}{V_{calc.}}$
1	37636.76	0.136	0.54	0.116	44125.85	0.390	45.02	0.888
2	36971.83	0.082	"	"	26135.25	0.603	17.30	1.445
3	26457.19	0.102	"	"	23264.08	0.624	14.59	1.200
4	20211.93	0.118	"	"	20560.41	0.626	12.98	0.960
5	26817.29	0.178	0.73	0.134	35542.92	0.384	40.74	0.798
6	20495.87	0.178	"	"	27225.86	0.455	27.62	0.724
7	25533.81	0.113	"	"	21494.13	0.668	13.30	1.316
8	19890.79	0.126	"	"	18732.97	0.681	11.13	1.123
9	25773.69	0.191	1.00	0.158	31124.18	0.428	38.50	0.844
10	29843.44	0.125	"	"	23610.32	0.646	18.09	1.382
11	25534.15	0.120	"	"	19393.02	0.752	10.43	1.726
12	16242.69	0.157	"	"	16109.05	0.690	10.82	1.017
13	21805.79	0.260	1.43	0.196	28926.05	0.443	43.28	0.739
14	23589.74	0.172	"	"	20665.09	0.668	18.42	1.249
15	18779.34	0.162	"	"	15502.54	0.774	9.39	1.597

Table 6.2 Calculated and Test Results

Average $\frac{V_{test}}{V_{calc.}} = 1.13$

Standard deviation $\sigma = 0.32$

SP. NO.	f'_c N/mm^2	f_y N/mm^2	P %	Col. size mm	V_{test} kN	M_{test} kN-mm	v_u N/mm^2	V_o kN	M_o kN-mm	$V_{cal.}$ kN	$\frac{V_{test}}{V_o}$	$\frac{M_{test}}{M_o}$	$\frac{V_{test}}{V_{cal.}}$
STAMANKOVIC'S TESTS: SLABS DEPTH 3 in., SLABS ARE 3'-0" SQUARE													
C /E/1	38.47	448.18	1.17	127x127	73.17	5593.50	2.82	77.65	26821.10	61.51	0.942	0.208	1.19
C /E/2	32.41	495.75	"	"	54.71	9175.60	2.60	71.59	24728.60	45.06	0.764	0.731	1.21
C /E/3	33.99	495.75	"	"	24.91	10057.00	1.99	54.80	18926.90	27.72	0.454	0.531	0.97
C /E/4	34.34	495.75	"	"	10.94	8842.25	1.48	40.75	14076.30	15.18	0.268	0.628	0.72
HANSON AND HANSON'S TESTS: SLABS DEPTH 3 in., SLABS ARE 3'-0" SQUARE													
D15	31.10	365.43	1.65	152.4 x 152.4	12.05	9932.70	1.18	38.57	15467.80	13.80	0.312	0.642	0.87
ZAGHLOOL'S TESTS: SLABS DEPTH 6 in., SLABS ARE 3'-2" x 6'-0"													
Z-IV(1)	27.33	475.76	1.23	177.8 x 177.8	122.32	3971.95	1.38	128.99	79848.10	118.96	0.948	0.057	1.03
Z-V(1)	34.34	473.69	"	266.7 x 266.7	277.55	7051.20	1.93	242.49	192500.0	233.61	1.145	0.037	1.19
Z-V(2)	40.40	473.69	1.65	"	306.91	7797.0	2.34	295.21	233334.0	285.39	1.040	0.033	1.08
Z-V(3)	38.75	475.07	1.23	"	339.83	8633.20	3.28	412.57	327067.0	401.79	0.823	0.026	0.85
Z-V(6)	31.30	476.44	"	"	289.12	7345.0	2.60	326.70	259260.0	317.45	0.885	0.028	0.91
Z-VI(1)	25.99	475.76	"	355.6 x 355.6	350.7	8911.18	2.23	352.22	323073.0	348.98	0.996	0.028	1.01

Table 6.3 Comparison with other results

Substitute the values of M_0 from Equation 6.16 into Equation 6.15 and then evaluate the values of "k" for each specimen (see table 6.2).

Now plot "k" against r_1/r_2 ratio and find the relation between "k" and r_1/r_2 (see Fig. 6.5). Therefore the equation of the line passing through the points in Fig. 6.5 is

$$k = 0.0689 + 0.0888 \frac{r_1}{r_2} \qquad (6.17)$$

Also it can be said that when r_1/r_2 is equal to zero, 6.8% of the total moment are assumed to contribute to the shearing stresses,which is negligible; this increases as r_1/r_2 increases, until the ratio reaches unity, where 15.8% of the total moment are assumed to contribute to the shearing stresses with the distribution assumed to be linear, as shown in Fig. 6.2.

6.4 Comparison with test results

The validity of the method for predicting the edge column-slab connection strength presented in Section 6.3 was checked using:

(1) The test results of the writer

(2) Hanson and Hanson's tests[12]

(3) Stamankovic's tests

(4) Zaglool's tests.

The theoretical predictions are tabulated against the test results in Tables 6.2 and 6.3.

In all cases the theoretical predictions were in reasonable agreement with the experimental results. Some of the measured results, however, were somewhat lower than computed. This discrepancy between the measured and computed results may be ascribed to one or more of the following causes:

(1) Variation in the yield strength of the reinforcement.

(2) Variation due to placement of steel at levels other than the assigned ones.

(3) Difficulty in obtaining uniform thickness of the slab.

(4) Local variation in concrete strength throughout the slab which was cast from two batches.

The test results are now evaluated in terms of proposed k values and Equation 6.16, and are plotted in Fig. 6.6.

SP. NO.	V_u kN (Test)	V_o kN Eq. 6.11	M_{flex} kN-mm	LV_o N-mm	V_{calc} kN Eq. 6.14a	$\frac{V_{test}}{V_{calc}}$
1	40.00	73.70	17676.0	26532.0	29.46	1.36
2	25.00	43.56	12768.0	24393.6	14.96	1.67
3	17.50	38.81	14288.0	29495.6	12.66	1.38
4	12.50	34.45	16032.0	33072.0	11.25	1.11
5	32.50	66.13	14314.0	42323.2	19.98	1.63
6	20.00	50.69	14310.0	27372.6	17.40	1.15
7	17.50	39.99	14208.0	29592.6	12.97	1.35
8	12.50	34.85	15604.0	32759.0	11.24	1.11
9	32.50	67.32	15616.0	21542.4	28.29	1.15
10	25.00	51.08	14560.0	26561.6	18.09	1.38
11	18.00	41.97	16848.0	30218.4	15.02	1.20
12	11.00	34.85	15640.0	32062.0	11.43	0.96
13	32.00	77.62	16980.0	23286.0	32.73	0.98
14	23.00	55.44	17250.0	27720.0	21.27	1.08
15	15.00	41.58	15050.0	29106.0	14.17	1.06

Average $\frac{V_{test}}{V_{calc}} = 1.24$

Standard deviation $\sigma = 0.21$

Table 6.4 Calculated and test results

6.5 Modified Interaction Formula

Hanson interaction formula (Eq. 6.14) may be re-written as follows

$$V_{calc} = \frac{V_o M_{flex}}{M_{flex} + LV_o} \qquad (6.14a)$$

where M_{flex} is the flexural capacity of the joint calculated using yield line theory. The results are presented in Table 6.4. As can be seen, the modified form of the interaction formula tends to predict failure loads generally on the safe side except for two values, and the standard deviation is 0.21, which is reasonable.

CHAPTER VII

SUMMARY AND CONCLUSION

7.1 Summary

The purpose of this investigation was to study experimentally the strength and behaviour of the edge column-slab connection of a reinforced concrete flat plate under different loading conditions. The view was to obtain data useful for establishing a method for analysis of this connection.

The experimental study involved tests on 15 reduced scale connections. The test specimens were as shown in Fig. 3.1. The column stubs were cast monolithically with the slabs. The variable parameters were:

(1) The ratio of column sides r_1/r_2.

(2) Ratio of column side to the effective depth r_1/d.

(3) Ratio of column side to the slab length L.

(4) Ratio of bending moment to axial load M/V.

The test results along with the effect of the parameters were discussed in Chapter IV.

A theoretical method for the analysis of an edge connection subjected to the effect of combined axial force and bending moment was developed in Chapter VI. The method was checked against the test results of the writer and the others. Good correlation was found between the test results and the theoretical predictions.

7.2 Conclusions

From the tests conducted and different variables parameters involved in this investigation, it was possible to obtain the following conclusions.

(1) The primary failure mechanism for an edge column-slab connection subjected to moment and shear can be idealised as illustrated in Fig. 4.7.

(2) For these structures, visible cracks can be expected at loads as low as 50% of the ultimate load.

(3) The flexural capacity of the joint is sensibly constant for the range of column aspect ratio tested. Such variation as can be seen indicates that as r_1 increases relative to r_2 there is a small reduction in flexural capacity of the joint.

(4) The critical section governing the ultimate shearing strength of the slab is located at a distance equal to d/2 from the perimeter of the column.

(5) The ultimate shearing strength of plates computed at a section at d/2 distance around the column was found to be predicted with good accuracy by the following equation

$$V = V_0 - \frac{kM_u}{\frac{b_1}{3b_0^3}\left[4b_1^3+12b_1^2b_2+9b_1b_2^2+2b_2^3\right]} \qquad (6.9)$$

(6) The portion of bending moment to be transferred through vertical shear stresses distributed along the critical section as shown in Fig. 6.2, k, was found to be as follows:

$$k = 0.0689 + 0.0888\ r_1/r_2 \qquad (6.17)$$

(7) The interaction between the bending moments and shearing force at the column-slab connection can be expressed by a linear function as follows:

$$\frac{V_u}{V_0} = 1 - \frac{M_u}{M_0} \qquad (6.14)$$

7.3 Suggestions for future research

On the basis of the present investigation the following suggestions for further research concerning shear and moment transfer can be recommended:

(1) A study on plates with different steel ratios in

the vicinity of the columns.

(2) A study of the effect of different slab thicknesses on the ultimate shear strength.

(3) A study of the effect of different types of shear reinforcement on the ultimate shear strength in the case of thick slabs.

(4) A study of the effect of static reversal loading on the ultimate shear strength of column-slab connection is also of great interest.

REFERENCES

1. Talbot, A. N.
"Reinforced concrete wall footings and column footings."
University of Illinois Engineering and Experiment Station, Bulletin No. 67, March 1913, 114 pages.

2. Moe, J.
"Shearing strength of Reinforced concrete slabs and footings under concentrated loads."
Research and Development Department, Bulletin D47, Portland Cement Association, Skokie, Illinois, April 1961.

3. "European Committee of Concrete", (Comite Europeen du Beton), Bulletin D'information No. 50, Paris, 1965 (In French and German).

4. "European Committee of Concrete", (Comite Europeen du Beton) Bulletin D'information No. 58, London, 1966 (In English).

5. Report of ACI-ASCE Committee 326, (Now 426)
"Shear and Diagonal Tension." ACI Journal, Proceedings Vol. 59, January to March 1962, pp1-30, and pp 352-396.

6. ACI Committee 318 Report, ACI Standard, "Building Code Requirements for Reinforced Concrete (ACI.318-63)", American Concrete Institute, June 1963, 144 pages.

7. ACl Committee 318, "Proposed Revision of ACl 318-63: Building Code Requirements for Reinforced Concrete." ACl Journal, Proceedings Vol. 67, No. 2, Febuary 1970, pp 77-186.

8. Corley, W. G. and Hawkins, N. M. "Shearhead Reinforcement for Slabs", ACl Journal, Proceedings Vol. 65, October 1968, pp 811-824.

9. Zaghlool, E. R. F. "Strength and Behaviour of Reinforced Concrete Flat Plate Floor Slabs." MSc Thesis, University of Calgary, Calgary, Alberta, Canada, 1968.

10. Saghlool, E. R. F., de Paiva, H. A. R., and Glockner, P. G. "Test of Reinforced Concrete Flat Plate Floors," Journal of the Structural Division, Proceedings of the American Society of Civil Engineers, Vol. 96, No. ST3, March 1970, pp 487-507.

11. Distasio, J. and Van Buren, M. P. "Transfer of bending moment between flat plate floor and column.", ACl Journal, Proceedings Vol 57, September 1960, pp 299-314.

12. Hanson, N. W. and Hanson, J. M. "Shear and moment transfer between concrete slabs and columns," PCA Journal, Research and Development Laboratories, V.10, No. 1, January 1968.

13. Bach, C. and Graf, O.
"Test of square and rectangular reinforced concrete slabs supported on all sides." (In German), Deutscher Ausschuss fur Eisenbeton (Berlin) Heft 30, 1915, 309 pages. Quoted by Reference 2.

14. Graf, O.
"Test of reinforced concrete slabs under concentrated load applied near one support." (In German) Deutscher Ausschuss fur Eisenbeton (Berlin) Heft 73, 1933, 2 pages. Quoted by Reference 2.

15. Graf, O.
"Strength test of thick reinforced concrete slabs supported on all sides under concentrated loads," (In German), Deutscher Ausschuss fur Eisenbeton (Berlin) Heft 88, 1938, 26 pages. Quoted by Reference 2.

16. Richard, F. E. and Kluge, R. W.
"Test of reinforced concrete slabs subjected to concentrated loads," University of Illinois Engineering Experiment Station Bulletin, No. 314, June 1939, 75 pages.

17. Forsell, C. and Holmberg, A.
"Concentrated load on concrete slabs," (In Swedish), Betong (Stockholm), 31, No. 2, 1946, pp. 95-123.

18. Richart, F. E.
"Reinforced concrete wall and column footings," ACI Journal, Proceedings Vol. 45, October-November, 1948, pp. 97-127, and pp. 237-260.

19. Hognestad, E.
"Shearing strength of reinforced concrete column footings," ACI Journal, Proceedings Vol. 50, November 1953, pp. 189-208.

20. Elstner, R. C. and Hognestad, E.
"Shearing strength of reinforced concrete slabs," ACI Journal, Proceedings Vol. 53, July 1956, pp. 29-58.

21. Keefe, R. A.
"An investigation of the effectiveness of diagonal tension reinforcement in flat slabs," Thesis, Massachussetts Institute of Technology, June 1954, 43 pages.

22. Whitney, C. S.
"Ultimate shear strength of reinforced concrete flat slabs, footings, beams and frame members without shear reinforcement," ACI Journal, Proceedings Vol. 54, October 1957, pp. 265-298.

23. Hahn, M. and Chefdeville, J.
"Flat slab without column capitals, tests." (In French) Annales de L'Institut Technique du Batiment et des Travaus Publics (Paris), No. 167, Beton, Beton Arme, No. 16, January 1951, pp. 23-31, Quoted by Reference 2.

24. Scordelis, A. C., Lin, T. Y. and May, H. R.
"Shearing strength of prestressed lift slabs." ACI Journal, Proceedings Vol. 55, October 1958, pp. 485-506.

25. Base, G. D.
"Some tests on the punching shear strength of reinforced concrete slabs." Cement and Concrete Association, London, Technical Report TRA/321, July 1959, 5 pages.

26. Kinnunen, S. and Nylander, H.
"Punching of concrete slabs without shear reinforcement." Transaction of the Royal Institute of Technology, Stockholm, Sweden, No. 158, 1960.

27. Kinnunen, S.
"Punching of concrete slabs with two-way reinforcement with special reference to dowel effect and deviation of reinforcement from polar symmetry." Transactions of the Royal Institute of Technology, Stockholm (Civil Engineering 6), No. 198, 1963, pp. 1-109.

28. Anderson, J. L.
"Punching of concrete slabs with shear reinforcement." Transaction of the Royal Institute of Technology, Stockholm, Sweden, No. 212, 1963.

29. Yitzhaki, D.
"Punching strength of reinforced concrete slabs." ACI Journal, Proceedings Vol. 63, May 1966, pp. 527-542.

30. "The structural use of reinforced concrete in buildings." British Standards, CP 114 (1957).

31. Long, A. E. and Bond, D.
"Punching failure of reinforced concrete slabs." The Institute of Civil Engineers Proceedings Vol. 57, May 1967, pp. 109-135.

32. Long, A. E.
"Punching failure of reinforced concrete slabs under combined loading conditions." The Institute of Civil Engineers, 13th February 1967.

33. Zaldi, S. T., Sabonis, G. J. and Roll, F.
"Shear resistance of perforated reinforced concrete slabs." A progress presented to the ACI Committee 426, Shear and Diagonal Tension, March 31, 1969, Chicago, Illinois.

34. Smith, A. E., and Simmonds, S. H.
"Test of flat plate supported on columns elongated in plan." Structural Engineering Report No. 21, May 1969, Department of Civil Engineering, The University of Alberta, Alberta, Canada, 71 pages.

35. Simmonds, S. H.
"Flat slabs supported on columns elongated in plan." ACI Journal, Proceedings Vol. 67, No. 12, December 1970, pp. 967-975.

36. Hawkins, N. M.
"Effect of column rectangularity on the strength and behaviour of slab-column specimens." University of Washington, Structures and Mechanics Report SM 70-2, September 1970.

37. Rosenthal, I.
"Experimental investigation of flat plate floors." ACI Journal, Proceedings Vol. 56, August 1959, pp. 153-166.

38. Tsuboi, Y. and Kawaguchi, M.
"On earthquake resistant design of flat slabs and concrete shell structures." Proceedings of the Second World Conference on Earthquake Engineering, Vol. III, July 1960, pp. 1693-1708.

39. ACl Committee 318 Report, ACl Standard.
"Building Code Requirement for Reinforced Concrete (ACl 318-56)". American Concrete Institute, July 1956, pp. 913-986.

40. Kreps, R. and Reese, R. Discussion of a paper by Di Stasia and Van Buren.
"Transfer of bending moment between flat plate floor and column." ACl Journal, Proceedings Vol.57, March 1961, pp. 1261-1263.

41. Frederick, G. R. and Pollauf, F. P.
"Experimental determination of the transmission of column moment to flat plate floor and column."
University of Toledo, (Unpublished report, May 1959).

42. Report of the ACl Committee 318, Standard Building Code.
"Commentary on Building Code Requirements for Reinforced Concrete (ACl 318-63)." Publication Sp-10, American Concrete Institute, 1965, 91 pages.

43. Anderson, A. J. L.
"Punching of slabs supported on columns at free edges."
Nordisk Betong, No. 2, 1966, pp.179-200. (English summary is given in Reference 4.)

44. Stamenkovic, A.
"Flat slab construction column head strength under combined vertical load and wind moment." PhD Thesis, University of London, London, UK, 1969.

45. Birkeland, P. W. and Birkeland, H. W.
"Connections in precast concrete construction." ACI Journal, Proceedings Vol. 63, No. 3, March 1966.

46. Mast, P. E.
"Stresses in flat plates near columns." ACI Journal, Proceedings Vol. 67, No. 10, October 1970, pp. 761-768.

47. Mast, P. E.
"Plate stresses at columns near the free edge." ACI Journal, Proceedings Vol. 67, No. 11, November 1970, pp. 898-902.

48. Girkmann, K.
"Flachentragwerke." 5th Edition, Springer Verlag Wien 1959, pp. 188-189.

49. Mast, P. E.
"Influence lines for shear around columns in flat plates." Final Report, Eighth Congress of the International Association for Bridge and Structural Engineering, New York, September 1968, pp. 983-993.

50. Hawkins, N. M. and Corley, W. G.
"Transfer of unbalanced moment and shear from flat plates to columns." Report, PCA R/D ser. 1482, Portland Cement Association, Skokie, Illinois, October, 1970.

51. ACI Standard 318-71. "Building Code Requirements for Reinforced Concrete (ACI 318-71)". American Concrete Institute, 1971.

52. "The Structural Use of Concrete." British Standards, CP 110, Part 1, 1972.

53. Regan, P. E.
"Design for punching shear." The Structural Engineer, June 1974, No. 6. Vol. 52, pp. 197-207.

54. Hatcher, D. S., Sozen, M. A. and Siess, C. P.
"A study of tests on a flat plate and a flat slab." Structural Research Series No. 217, University of Illinois, July 1961.

55. Johansen, K. W.
"Yield line theory." Translated from Danish, Cement and Concrete Association 1962, original copyright by K. W. Johansen, 1943.

56. Hognestad, E.
"Yield line theory for ultimate strength of reinforced concrete slabs." ACI Journal March 1953, Proceedings Vol. 49, pp. 637-656.

57. Wood, R. H.
"Plastic and elastic design of slabs and plates." Thames and Hudson (London), 1961.

58. Jones, L. L. and Wood, R. H.
"Yield line analysis of slabs."
Thames and Hudson, Chatto and Windus (London) 1957.

59. ACI Standard 318-77. "Building Code Requirements for Reinforced Concrete (ACI 317-77)". American Concrete Institute, 1977.